UNCLASSIFIED

AD NUMBER

AD B020 167

NEW LIMITATION CHANGE

TO Distribution Statement A
Approved for Public Release: Distribution is Unlimited

Limitation Code: 1

FROM Distribution Statement B
Distribution Limited to U.S. Government Agencies Only

Limitation Code: 3

AUTHORITY

USADTC, via ltr., dtd Dec 10, 1979

THIS PAGE IS UNCLASSIFIED

AFATL-TR-76-129

STUDY OF PENETRATION TECHNOLOGY

DEPT OF ENGINEERING SCIENCES
UNIVERSITY OF FLORIDA
GAINESVILLE, FLORIDA 32611

NOVEMBER 1976

FINAL REPORT FOR PERIOD JAN 1975 - SEPT 1976

AIR FORCE ARMAMENT LABORATORY
AIR FORCE SYSTEMS COMMAND • UNITED STATES AIR FORCE
EGLIN AIR FORCE BASE, FLORIDA

UNCLASSIFIED

SECURITY CLASSIFICATION OF THIS PAGE (When Data Entered)

(19) REPORT DOCUMENTATION PAGE

READ INSTRUCTIONS BEFORE COMPLETING FORM

1. REPORT NUMBER (18) AFATL-TR-76-129	2. GOVT ACCESSION NO. N/A	3. RECIPIENT'S CATALOG NUMBER N/A
4. TITLE (and Subtitle) (6) STUDY OF PENETRATION TECHNOLOGY.		5. TYPE OF REPORT & PERIOD COVERED Final Jan 1, 1975 to Sep 29, 1976
		6. PERFORMING ORG. REPORT NUMBER N/A
7. AUTHOR(s) (10) L.E. Malvern, R.L. Sierakowski, C.A. Ross, J.E. Milton, C.S. Ting, J.A. Collins		8. CONTRACT OR GRANT NUMBER(s) (15) F08635-75-C-0054
9. PERFORMING ORGANIZATION NAME AND ADDRESS Dept. of Engineering Sciences, University of Florida, Gainesville, Florida 32611		10. PROGRAM ELEMENT, PROJECT, TASK AREA & WORK UNIT NUMBERS Program Element 62602F (16) JON 2549-04-06 (17) 04
11. CONTROLLING OFFICE NAME AND ADDRESS Air Force Armament Laboratory, Armament Development and Test Center, Eglin AFB, Florida 32542		12. REPORT DATE (11) Nov[redacted] [redacted]76
		13. NUMBER OF PAGES 235
14. MONITORING AGENCY NAME & ADDRESS (if different from Controlling Office) (9) Final rept. 1 Jan 75-29 Sep 76		15. SECURITY CLASS. (of this report) Unclassified
		15a. DECLASSIFICATION/DOWNGRADING SCHEDULE

16. DISTRIBUTION STATEMENT (of this Report)

Distribution limited to U. S. Government agencies only; this report documents test and evaluation; distribution limitation applied November 1976. Other requests for this document must be referred to the Air Force Armament Laboratory (DLYV), Eglin Air Force Base, Florida 32542.

17. DISTRIBUTION STATEMENT (of the abstract entered in Block 20, if different from Report)

(12) 225p.

18. SUPPLEMENTARY NOTES

Available in DDC

19. KEY WORDS (Continue on reverse side if necessary and identify by block number)

Soil penetration, soil impact, seismic wave speed, soil properties, soil trajectories

20. ABSTRACT (Continue on reverse side if necessary and identify by block number)

A study of the performance characteristics of terradynamic impactors is reported on, including the influence of initial input velocity, impactor nose shape, and different soil conditions in Eglin sand. The investigation also included evaluation of various sensing devices for nonintrusive measurement of vehicle motions during the penetration process. The most useful of the experimental tools was found to be flash X-Ray radiography. Additional devices evaluated were magnetic coils, microwaves, capacitive → next page

DD FORM 1473, 1 JAN 73 EDITION OF 1 NOV 65 IS OBSOLETE
S/N 0102-014-6601

UNCLASSIFIED

SECURITY CLASSIFICATION OF THIS PAGE (When Data Entered)

410049

PREFACE

This report represents the results of a study on the soil penetration performance of terradynamic impactors. This study was conducted Jan 1, 1975 to Sept 29, 1976 by the Engineering Sciences Department, University of Florida, Gainesville, Florida, 32611, under Contract No. F08635-75-C-0054 with the Air Force Armament Laboratory, Eglin Air Force Base, Florida. Mr. John Collins served as program manager for the Armament Laboratory.

This technical report has been reviewed and is approved for publication.

FOR THE COMMANDER

J. R. MURRAY
Chief, Weapon Systems Analysis Division

(The reverse of this page is blank)

cont. and other pressure transducers, strain gages on test chamber walls, and breaking-wire sensors. Data analysis was performed by using classical Poncelet predictive techniques, empirical Sandia penetration equations, semi-analytical Cavity Expansion Theory, and a three dimensional code for trajectory analysis developed under this contract for use with an assumed three dimensional force law. To obtain essential input to the aforementioned models, a study of the acoustic wave velocity in a sand medium was made, and results are included in this report.

TABLE OF CONTENTS

TABLE OF CONTENTS (Concluded)

LIST OF FIGURES

LIST OF FIGURES (Continued)

LIST OF FIGURES (Continued)

LIST OF FIGURES (Concluded)

LIST OF TABLES

(The reverse of this page is blank)

SECTION I

INTRODUCTION AND BACKGROUND

This report presents the results of a joint investigation conducted by the Vulnerability Assessment Branch (DLYV) of the Air Force Armament Laboratory and the University of Florida. The University gave analytical support to an experimental program conducted by DLYV/AFATL at Eglin Air Force Base.

The support included reviewing the proposed soil penetration experiments, recommending changes, participating in some of the experiments at Eglin, making independent laboratory investigations at the University of several types of sensors and of ultrasonic wave speeds in sand, extensive data analysis of the Eglin Experiments, study of existing terradynamic penetration models, modification of the models and application of them to the interpretation of the Eglin experiments.

The study of the mechanics of high speed earth penetrators, including predictions of trajectory, depth of penetration, cavity formation, stability, and target interaction has in recent years been given the name of terradynamics. While this area of study has been investigated since the early 18th century, technological barriers have hindered experimental programs in assessing models advanced for characterizing penetrator performance. The principal difficulty encountered has been the unavailability of experimental tools for examining the sequential motion of a vehicle passing through opaque loose and/or semicohesive media.

A recent review of the State of the Art of Earth Penetration Technology by Triandafilidis (Reference 1) has categorized predictive penetration techniques as semi-analytical, analytical, theoretical, and empirical models. The first technique, which includes the classical penetration models based upon Newtonian mechanics, such as Poncelet (Reference 2), requires experimental data for evaluation of the important penetration constants. So-called analytical techniques, which include the Cavity Expansion (References 3 through 7) and Differential Force Law Models (Reference 8), rely upon knowledge of constitutive target material properties. The theoretical models proposed (References 9 through 11) are based upon continuum mechanics formulations describing the penetrator and target, and rely upon finite difference and finite element computer codes as solution techniques. Finally, empirical techniques based upon extensive laboratory and field testing have been introduced with the most extensive work in this area developed at Sandia Laboratories (References 12,13). Additional background on the experimental program is presented in Section II.

The purpose of the experimental program at Eglin was to obtain more complete transient records of the penetration events than previous investigators had obtained in order to provide insight into the actual physical mechanisms involved, which could lead to better terradynamic penetration models for predicting trajectories, penetration depths, and the forces acting on the projectile. In the test program, five consecutively spaced X-ray units have been used to visually record the transient position of several penetrators. Nonspinning projectiles of stable configuration with various nose shapes have been tested in dry and saturated sand at three impact velocities with near zero impact obliquity. This is believed to be the most extensive use ever made of flash radiography in terradynamic research. In addition to the X-ray units, velocity coil sensors have been used as monitoring devices in conjunction with a magnetic tape recording system.

The experimental setup at Eglin and some of the experiments at the University on sensors are described in Section II after a short background account of previous experimental studies. Data from the Eglin tests are described in Section III, with details tabulated in Appendix A. Analysis of the data by classical semi-analytical penetration models and empirical methods is presented in Section IV. The analytical technique based on the spherical cavity expansion technique is discussed in Section V and applied to the Eglin experiments. In Section VI a three-dimensional terradynamic model is developed and applied. Sound speed measurements are reported in Section VII and a summary of the conclusions is given in Section VIII.

SECTION II

EXPERIMENTAL EQUIPMENT AND PROCEDURES

2.1 INTRODUCTION

Penetration experiments were performed by firing projectiles horizontally into sand targets contained in specially designed test chambers. After some preliminary tests with 0.50 caliber and 20mm standard rounds, the major part of the investigation used modelled 20mm projectiles fabricated both at the AFATL and at the University of Florida. These projectiles were cylinders 0.02 meter in diameter by 0.22 to 0.24 meter in length. Three specific nose shapes were investigated: biconic, flat ended, and step-tier. Some of the biconic and step-tier projectiles had a hollow afterbody, but the majority of the results were obtained using solid projectiles.

Various sensing methods were investigated to determine as much as possible about the projectile's position and orientation, the shape of the cavity formed around the projectile, deformation patterns and force distributions in the sand, and shock waves ahead of the projectile. The most successful sensing method was flash radiography. In the primary test program five X-ray heads were fired sequentially with delay times set to record projectile position as it moved through a 1.2-meter-long test chamber. The primary test program was planned to include firings of two projectile types (flat and step-tier projectiles) at three different velocities (approximately 210,320 and 400 m/sec) in dry sand and in saturated sand, with four replications of each type of shot, and five X-ray pictures taken in each shot. This program was completed successfully. Results of these tests are presented in Section III, along with a few examples of other projectile types.

Besides giving a more certain indication of projectile trajectory and attitude than any other sensing method, the X-rays give a good indication of the position on the projectiles where the sand separates to form a cavity, and can show also the reattachment point on the afterbody as the projectile slows down. In the primary test program the X-rays showed that reattachment seldom occurred in the 1.2 meters of the trajectory observed.

The X-rays also revealed a detached bow wave in some cases (notably the higher-speed impacts in dry sand). The bow wave is a density discontinuity moving with the projectile, resembling the detached shock wave ahead of a supersonic aircraft. The X-ray method was emphasized because it was the only method known that could give transient information about separation and about the shock wave shape and density gradients. Other types of sensors envisioned for use in the test program were investigated to complement the X-ray technique or to be used in case the X-ray equipment was not available.

Some of the sensing methods investigated at the University were microwaves, breaking wires, and magnetic sensors. The microwave technique was considered as an alternative to the X-rays for continuous position monitoring, but it was not used in the experiments at Eglin, since the X-ray equipment was available. Various breaking-wire sensors and velocity screens were used at Eglin, and the magnetic sensing method was used extensively both in the primary test program and in the preliminary testing before the X-ray system was fully developed. A pressure transducer in the floor of the test chamber and strain gages on the walls were also used in attempting to build a complete data base.

The general set-up for the primary test program at Eglin and the flash X-ray method are described in paragraph 2.3 after a brief review in paragraph 2.2 of some previous terradynamic experiments. Other sensors used in or examined for the test program are discussed in paragraph 2.4.

2.2 BACKGROUND

Until fairly recently the only experimental data available on ballistic penetration of soils consisted of tabulations of striking velocity V_0 versus final penetration distance S. Comparisons of the plots of S versus V_0 with integration of assumed force laws, e.g., of the form

$$-dV/dt = \alpha V^2 + \beta V + \gamma$$

could in principle determine the coefficients for such laws. The scatter in the data because of variations of <u>in situ</u> soil properties or because of tumbling or other unstable projectile behavior made conclusions from S versus V_0 data difficult to draw.

In 1957 Allen, Mayfield, and Morrison (Reference 14) reported what were apparently the first laboratory investigations to record projectile transient motion. They used a photographic-electronic chronograph to record the successive breaking of copper grid wires located 0.1 meter apart along the trajectory and were able to obtain better determination of force law coefficients than could be obtained from final penetration depths alone.

This brief discussion will not attempt a complete historical account of penetration experiments, but will mention a few of the more recent investigations that have obtained transient data. Some additional historical information is given in References 1 and 14 through 16 and in a 1972 survey of the state of the art by McNeill (Reference 17), which also gives a bibliography. A more extensive bibliography has been prepared by Triandafilidis (Reference 1), and a 1974 annotated bibliography (Reference 18) lists Sandia Laboratories Publications related to Terradynamics.

According to McNeill, significant strides in penetrator system technology began at Sandia in 1961 with penetrators 2.4 to 3 meters in length and 0.23 to 0.46 meter in diameter, with masses on the order of 450 kilograms, delivered by ground-launched rockets or by airplanes. Some of these tests used on-board accelerometers and telemetered data. Since that time, the accelerometer-carrying air-dropped penetrometer has been developed into a practical tool for rapid survey of subsurface soil properties. Wood (Reference 19) has discussed instrumentation and telemetry. Trailing wires have also been used for air gun projectiles at speeds up to 120 m/sec (Reference 19). Murff and Coyle (Reference 20) have obtained deceleration-time records for impact at speeds up to 90 m/sec into three soil types (compacted kaolin clay, dense Ottawa sand and a mixture of kaolin clay and sand). Projectiles varied from 38 to 76 millimeters in diameter and had masses ranging from 1.4 to 52 kilograms.

A microwave monitoring system was developed at the University of New Mexico. Its use was reported in a Ph.D dissertation in 1965 by Hakala (Reference 15). The technique showed considerable promise, although questions of how long a path could be monitored and whether the technique could be used in moist soil were not addressed.

Successful use of flash radiography in soil beginning in 1974 was reported by Culp et al (References 21, 22). Their later work in clay showed the existence of a detached shock wave. Color enhancement techniques of the X-rays revealed density variations. An automatic scanning and image storing and processing technique was used. One significant result of the scanning technique was the discovery that the soil cavity around the projectile seemed to be larger than it had appeared in visual inspection of the radiographs. Flash radiography in soil had been used earlier (Reference 23), but few details about it have been made public.

Although transient trajectory measurements were not made, the shape of the trajectory was revealed by post-test excavation in a 1973 Master's Thesis by Biele (Reference 24), which investigated the stability of scaled model projectiles of various nose types. Initial angles of impact were revealed by yaw cards, and plots of lateral deflection versus penetration distance were made for various initial angles. Even with quite small initial angles (1-2 degrees) lateral deflections of as much as 0.15 meter were observed in a penetration distance of 1.06 meters.

2.3 SETUP OF PENETRATION EXPERIMENTS AT EGLIN

The test setup used in collecting the data base for analysis was developed in an evolutionary manner. Several sensing devices, projectile shapes, and velocity regimes were studied before the basic elements of the primary test matrix were investigated. Details of these techniques are given elsewhere in this section and principal attention is focused upon the test assemblage as used in the March and April 1975 test program. The primary test matrix is shown below with the complete matrix described in paragraph 3.2.

TABLE 1. EXPERIMENTAL TEST MATRIX SHOT NUMBERS

Projectile Type	Target	Velocity		
		210 m/sec	320 m/sec	400 m/sec
Flat Nose	Dry Sand	15,16,17, 18,19	20,22,23,24	14,25,26,27,29
Flat Nose	Wet Sand	70,71,72,73	36,37,38,74,81	76,82,83,84
Step Tier	Dry Sand	52,53,54,55,57	56,58,59,61	62,63,64,65
Step Tier	Wet Sand	42,43,44,45	39,40,41,49	50,51,68,69

The flat-nose projectiles used in these experiments were solid cylinders 0.0198 meter in diameter by 0.225 meter long. For the step-tier projectiles the afterbody was a cylinder of 0.0198 meter diameter amd 0.232 meter length, with a cylindrical nose 0.0095 meter in diameter and 0.0065 meter long. The material used for the projectiles was a high carbon content steel drill rod, supplied in rod form with nominal dimensions of 0.02 meter in diameter and 1 meter long. For specimens made at the University an AISI-W1 water quenched bar stock was used, while for specimens fabricated at the AFATL, AISI-O1 oil quenched bar stock was used. Three of the projectiles used in the Eglin penetration experiments are shown in Figure 1. In addition to the two projectiles described above, the photograph shows a shorter flat-nosed projectile, length 0.152 meter, used for some later tests.

In the Eglin experiments the projectiles were fired horizontally into a test chamber consisting of an open-top box of nominal dimensions 0.15 meter wide by 0.40 meter high and 1.2 meters long. The side walls and floor of the box were made of 0.0023 meter aluminum sheet framed by steel brackets and mounted on a flat wooden table platform as shown in Figure 2. The ends of the test chamber were closed by fiber board that was easily penetrated by the projectiles. The test chamber was backed up by a large open-topped wooden box fitted with vertical slots to accommodate partitions. The partitions were used to fill the box with varying amounts of sand in order to contain the projectiles for re-use in the various velocity regimes tested.

The boxes were filled with Eglin sand that had been sieved with a U.S. Standard Sieve Series No. 25 sieve to remove large debris, but not sieved to a controlled size range. For the dry sand tests the sand was poured slowly into the test chamber from a bucket assembly attached to an overhead crane. The wet sand tests were for the fully saturated condition. For the wet sand tests the sand was first mixed with water in a container and then shoveled into the test chamber. It was maintained in a fully saturated condition by adjusting a flow of water into the open top to compensate for leakage and maintain an essentially constant water level.

Standard triaxial tests were performed on two samples of the Eglin sand. For these tests the sand was first carefully dried following procedures as described in Reference 25. Each sample was tested at three different constant values of the lateral confining pressure σ_3 (0.1962, 0.392, and 0.589 MPa) with axial compressive stress σ_1 increasing until failure occurred (significant increase of axial strain at constant load). The two samples were a loose sand and one compacted by vibration before testing. Table 2 lists the initial density ρ_o and the angle of friction ϕ determined for each sample by analysis of the triaxial data as well as the value $(\sigma_1-\sigma_3)_f$ of the stress difference at failure for each of the confining pressures.

The curve of $\sigma_1-\sigma_3$ versus axial strain ε_1 for the loose sand at the highest confining pressure will be given in Section V, where it is used to determine the deviatoric properties for the penetration analysis by the spherical cavity expansion theory method. Several confined uniaxial strain tests were also performed on dry Eglin sand. These will discussed in Sections V and VII.

Figure 1. Flat-Nosed and Step-Tier Projectiles Used in Eglin Experimental Program

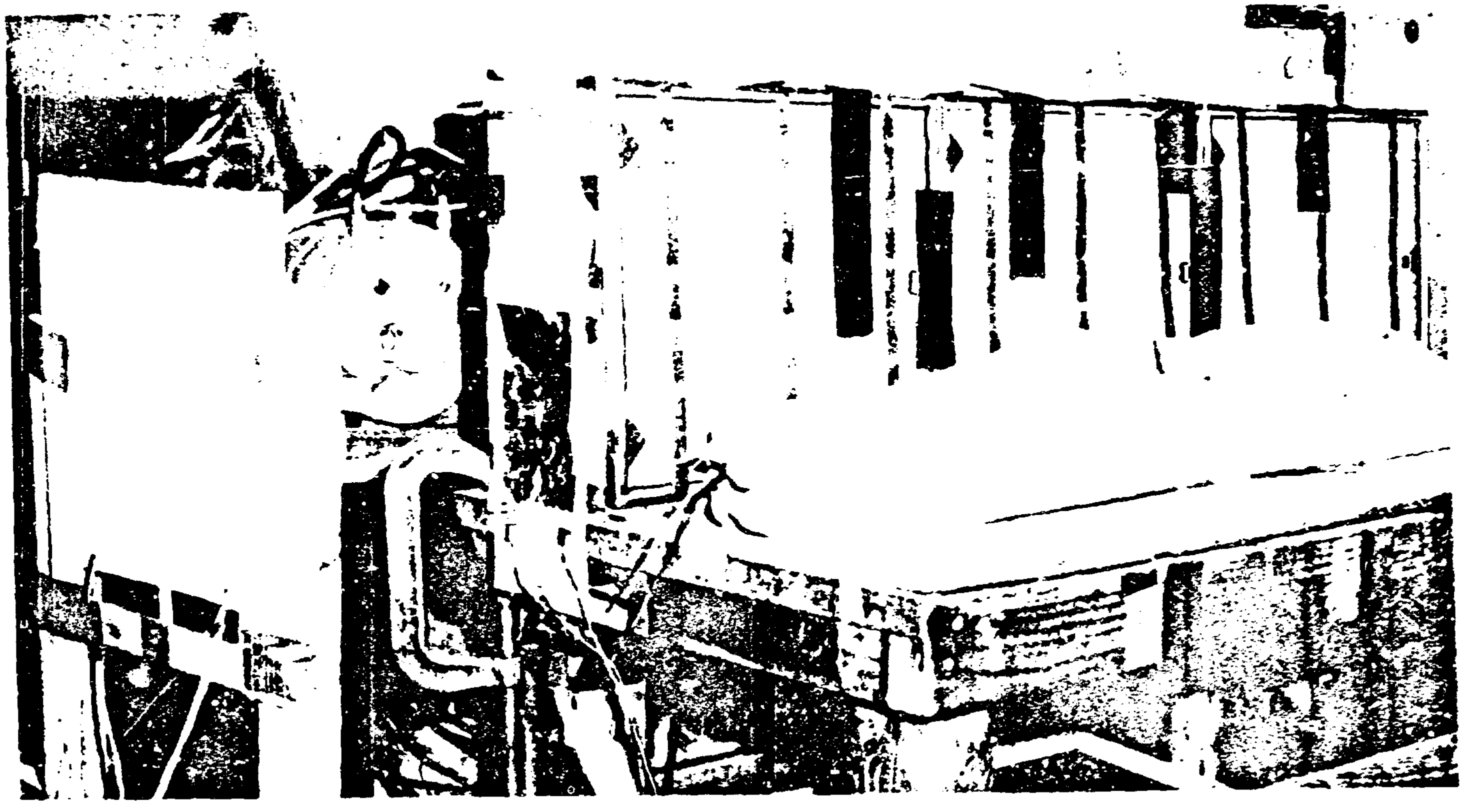

Figure 2. Target Test Chamber Setup for Eglin Experiments

TABLE 2. TRIAXIAL DATA FOR DRY EGLIN SAND

	σ_3	$(\sigma_1-\sigma_3)_f$
Loose Sand	0.1962 MPa	0.538 MPa
ρ_o = 1519 kg/m^3	0.392	0.983
ϕ = 33.4^o	0.589	1.447
Compacted Sand	0.1962	0.763
ρ_o = 1698 kg/m^3	0.392	1.423
ϕ = 39.7^o	0.589	2.02

The projectiles were fired into the test chamber with a 20mm gun. Firing velocity was controlled by varying the powder load in a primed 20mm case. Striking velocity was measured by timing the interval between the breaking of two paper back velocity screens with a Terminal Ballistics Data Acquisition System. The start screen was 1.22 meters from the front of the target, and the stop screen was 0.61 meter from the target. The timing signals were also recorded on a magnetic tape system and later transferred to a paper oscillograph record. Also recorded on the tape was the signal from a break wire on the gun muzzle 3.54 meters from the target.

To monitor the projectile flight path through the sand in the 1.2-meter-long box, five Hewlett-Packard flash X-ray units were used: one 150 KV soft X-ray unit and four 300 KV hard X-ray units. They were spaced sequentially along the horizontal, with the first unit (150 KV) located at 0.038 meter from the front of the box and the four 300 KV units spaced 0.38 meter between centers. Standoff distance for the 300 KV units was nominally 0.55 meter. The front ends of the 150 KV unit (small cylinder) and of one 300 KV unit (large cylinder) are visible in Figure 2.

Several types of X-ray film were evaluated in the course of the test program, with the majority of the data recorded on Dupont Lightning Plus X-ray film. The film cassettes (not shown in Figure 2) were mounted on the outside of the box opposite from the X-ray units. The film plane was positioned at 0.08 meter from the centerline. In the main test program a series of metal letters (A through Q) were taped along the box, separated horizontally by approximately 0.07 meter along a line 0.20 meter from the top of the box, to serve as markers for locating the projectile position in the X-ray pictures. Some of the earlier tests used fewer markers in the form of metal arrows. In some of the tests displacement of the soil medium was observed by suspending 0.0015-meter steel markers that moved with the sand. Preshot and postshot X-ray records were made to locate the initial and final positions of the markers.

Figure 3 is a photograph of the three prints made from the X-ray negatives for Shot No. 26. The two panels on the left show the nose of the flat-ended projectile in four successive positions at the times of the sequential firing of the X-rays. The fifth one in the third panel does not show up well in the reproduction but could be seen in the negative. The separation angles and the cavity around the afterbody are clearly shown in three of the positions illustrated. The aft end of the projectile is not usually visible, since it is out of the main X-ray beam when the firing is correctly timed to show the nose.

A magnetic system was used to furnish supplementary velocity information after preliminary laboratory investigations at the University had established the feasibility of the method. The steel projectiles were magnetized to a strength of about 150 gauss, as measured at the center of the nose with a Hall-effect gaussmeter. When this magnetized projectile passed through a 0.15-meter-diameter coil mounted inside the test chamber a voltage signal was generated. Four such coils were used in most of the Eglin tests, one on the front of the box and three inside at distances of approximately 0.49, 0.80 and 1.09 meters from the front of the box. The positions are recorded in Appendix A for the 26 shots for which the magnetic sensor data were analyzed. The projectile can be seen passing through two of them in the X-ray picture of Figure 3. Each sensing coil was formed with 40 turns of copper wire, forming a rim about 0.004 meter thick. The voltage signals were recorded without any preamplification on the magnetic tape recording system and later transcribed to an oscillograph record. The records indicated voltage peaks of the order of 40 to 80 mv in tests with initial impact velocities around 200 m/sec. Some recovered projectiles showed a residual magnetic strength at the nose of around 20 percent of the value before firing.

Laboratory tests were made at the University on smaller diameter projectiles fired from an air gun. The time when the projectile nose arrived at the plane of the coil was precisely determined with a light beam. Comparison with the time of the peak voltage output showed that in tests with a coil formed by two parallel wires 0.025 meter apart the peak voltage occurred precisely as the nose passed through the loop. With a 0.165-meter-diameter coil a discrepancy was noted, indicating that the nose of the 0.215-meter-long by 0.0095-meter-diameter projectile has advanced approximately 0.021 to 0.027 meter beyond the coil plane when the maximum voltage was observed for the low-speed shots in air (20 to 35 m/sec). Since a comparable direct check could not conveniently be made with the larger diameter projectiles used in the Eglin experiments, an indirect check was made by statically mapping the radial component of the magnetic field.

The mapping was first made for the laboratory projectiles to see if it agreed with the laboratory dynamic measurements. At a radial distance of 0.09 meter from the projectile axis the peak radial magnetic field occurred at a distance of 0.021 meter back of the plane of the nose, in approximate agreement with the discrepancies noted above. Similar mappings of one flat-nosed and one step-tier solid projectile of the type used in the Eglin experiments showed that the maximum radial component of the magnetic field occurred at distances of 0.020 meter and 0.022 meter respectively, back of the nose tip plane when measured at a radial distance of 0.086 meter from the projectile axis. This indicates that the maximum response should occur when the projectiles have penetrated some 0.02 meter through the plane of the sensor coil,

Figure 3. Photograph of Three X-Ray Prints for Shot No. 26

assuming a circular undeformed coil and a straight horizontal flight path through the center of the coil. Possible sources of additional error are imprecise measurement of the coil locations and especially of the time of the peak response, since with coils this large the response curve does not show a very sharp peak.

2.4 OTHER SENSORS USED OR TESTED

2.4.1 Breaking-Wire Sensors

Both wire-grid and coated paper or plastic velocity screens are widely used to time the airborne part of a ballistic test. They have also been used buried in soil targets or sandwiched between slabs of rock or concrete. Because it was believed that the standard wire-grid screens might disturb the deformation patterns and force fields in the target, an attempt was made to develop wire sensors that would interfere less, by using finer wires in parallel arrays, less closely spaced than the screens. A developmental investigation at the University tested single wires impacted by projectiles fired from an air gun. Of particular interest was a method of verifying how much lateral motion of the wires occurred before they broke to give a signal. The 0.0095-meter-diameter projectile was 0.15 meter long. Two pinholes in the air gun barrel near the muzzle transmitted light to a photo-multiplier timing system for measuring projectile velocity. The dual-beam oscilloscope was triggered when the aft end of the projectile passed the first pinhole (farther from the muzzle). The wire sensor was placed 0.15 meter from the second pinhole,so that the projectile nose impacted the first wire just as the aft end passed the second pinhole. The time difference between the two signals (from the second pinhole and from the breaking wire) determined the time delay (or advance) of the breaking-wire signal. With the known projectile velocity, the position error that would be caused by assuming that the wire broke instantaneously in its orginal position could be determined.

Several kinds of wire were tested. The wires were stretched between supports 0.15 meter apart. The first tests were performed in air. Ductile wires of copper and stainless steel stretched so much that the projectile traveled almost 0.05 meter before the wire broke in impacts at 32 m/sec. Brittle wires gave better results. A brittle 0.0001-meter-diameter tungsten wire broke after about 0.0025 meter of travel.

Tests were then performed with the stretched tungsten wires buried in sand. The wires broke before the projectile reached them, because of the sand pushed ahead of the flat-ended projectile. At 39 m/sec the distance was about 0.006 meter and at 65 m/sec about 0.009 meter from the projectile to the initial position of the wire when it broke. In all cases the breaking wire gave a good sharp step on the oscilloscope trace. The last group of tests used 0.0002-meter-diameter steel music wire (static breaking force 89 N as compared to 17.8 N for the tungsten wire). In these last tests the wire sometimes did not break, but was deflected to one side of the projectile. A small perturbation in the voltage trace was noted at about the time the projectile reached the wire's initial position. Such a perturbation may be usable for timing purposes, although it lacks the sharp step that occurs when the wire breaks.

Two of the standard wire grid velocity screens were checked in the test apparatus at the University. With a 12.7 mm-diameter projectile impacting the screen in air at a speed 25.4 m/sec, the screen bent to allow about 0.0025 meter of travel before it broke. When a similar test was performed in sand, the travel appeared to be about 0.0075 meter before the break.

The figures quoted for distances from the initial wire position to the projectile position when the break occurred apply, of course, only for the specific projectiles, wires and configurations tested. Sensors will have to be calibrated in conditions similar to those they are to be used in.

The first test firings at Eglin on 6 June 1975 were planned to test breaking-wire sensors and capacitor sensors prepared at Eglin. Tungsten wires and steel music wires of the types previously tested at the University were strung between supports 0.76 meter apart, and in addition two standard wire grid velocity screens were placed in the sand near the front end of the target. Signals were to be recorded both by counters and on magnetic tape recorders. No signals were obtained from any of the breaking-wire sensors. Post-test checks showed that the velocity screens were broken but the two other wire sensors were not broken by the 0.50 caliber projectiles. Similar wire systems could be used in sand, especially with the larger 20mm projectiles, but it would be necessary to check them out carefully with each projectile and test configuration. The X-ray method could be used as a check. Little further use of breaking-wire sensors in sand was made in the Eglin experiments because the magnetic sensors were so much better, and later the X-ray method gave still better results.

2.4.2 Sensors Responding to Pressure or Deformation: Capacitors, Pressure Transducers, and Strain Gages

Although the major effort in the experimental program was directed toward recording trajectory information and the bow wave formation and cavity formation, several types of sensors were tried that could give some additional information about arrival times and intensities of the stress and deformation waves in the target medium.

A capacitive transducer was developed at AFATL, consisting of two thin metal foils separated by a layer of foam rubber and encased in a flexible electrical insulating material. When the sensor was compressed along with the surrounding sand a voltage change occurred across the charged capacitor. This furnished timing information about the arrival of the pressure wave. With suitable calibration it could also furnish quantitative information about pressure and deformation. It also served as a good antenna for detecting and recording the actual firing times of the flash X-rays.

A pressure cell in the bottom of the test chamber 0.127 meter from the front of the box also gave information about the arrival time and intensity of the pressure waves and furnished a good signal.

One to five strain gages were also mounted on the aluminum plates at the sides of the box. Good strong signals were obtained from the gages. The interpretation of these signals depends on the interaction between the pressure wave in the sand and a flexural wave in the plate.

2.4.3 Microwaves

A microwave monitoring system was reported on in 1965 by Hakala (Reference 15). Its operation gives output depending on the interference between a transmitted signal and a signal reflected from the moving projectile. The transmitter and receiver were at the opposite end of the sand target from the impact point. The interference frequency is a function of the projectile velocity. Since few details about power requirements for penetrating various distances in dry and moist sand were available, an experimental program to determine some of this information was undertaken at the University early in 1975.

A microwave oscillator of maximum power 1 mw fed a variable gain amplifier at a frequency of about 10 GHz through a coupler in a microwave horn into the sand contained in a 1.2-meter-long box. For these static experiments the signal generator carrier frequency was modulated by a 1 kHz square wave. The signal was reflected from the target, which was the end of a metal rod inserted into the opposite end of the box from the horn. Portions of the mixed incident and reflected signals were detected by a crystal detector. The detector output (DC with amplitude varying at the modulation frequency) was fed to a Standing-Wave Ratio Meter (which contained an internal amplifier with a narrow pass band around 1 kHz).

When the rod was moved axially by one quarter wave length the round trip path from coupler to rod was shortened by one half wave length. The reflected and incident waves interfered and a half wave length reduction in path was required for the detected mixed signal to go from a maximum to a minimum.

Preliminary tests showed a strong signal response at a distance of 0.30 meter with 3 mw power output from the microwave amplifier. At 0.60 meter the difference between the maximum and minimum response was down about 5 dB from the difference at 0.30 meter indicating a power transmission drop by about a factor of one-third, but the signal was still clearly distinguishable. In fact it was still clear at 1.0 meter. Precise attenuation factors could not be obtained with the preliminary test set-up, because of reflections from the sides of the box containing the sand.

Additional microwave studies attempted to repeat with naturally moist Eglin sand (approximately 5 percent by weight moisture content) the kind of measurements previously made in dry sand. With the target at a distance of only 0.15 meter however, the attenuation was so great that the alternate constructive and destructive interference by the reflected signal as the target advanced a quarter wave length was barely perceptible.

Some additional measurements with a tuned microwave horn pickup replacing the target were made verifying that detectable microwave signals were transmitted through 0.30 meter of the moist sand even with the low power signal source.

It may be possible to increase the transmitted power and to obtain a coupler that will pick up a smaller fraction of the transmitted signal to mix with the reflected signal from the target in order to enhance the interference.

For projectile velocity monitoring, the carrier wave would not be modulated by the 1 kHz square wave. A projectile advancing at constant speed at 300 m/sec will produce an interference frequency of approximately 20 kHz without any modulation of the original signal. This frequency will decrease as the projectile slows. The amplified signal could be recorded both on an oscilloscope and on one or two channels of a Biomation transient recorder. It would be recorded as a quasi-sinusoidal signal of decreasing frequency. The time between a maximum and a minimum of this signal is the time for the projectile to advance one quarter wave length (of the order of 0.0075 meter although precise values would have to be established by calibration). At a projectile velocity of 300 m/sec the time between maximum and minimum is about 25 x 10^{-6} sec, increasing as the projectile slows.

The microwave system was not actually used in the Eglin experiments since the X-ray equipment was available, but it is a possible option for future use if the power requirements can be met.

In Section III the data collected in the Eglin experiments will be described.

SECTION III

RESULTS OF EGLIN PENETRATION EXPERIMENTS

3.1 INTRODUCTION

During the period from 22 January to 24 May 1976 the Eglin penetration experiments included a total of 91 shots in 17 missions. X-ray data from two or more stations were obtained in 74 shots (No's 14 to 91 except for Shots 21, 28, 60, and 75). Appendix A lists data obtained in Shots 14 through 91, except for the four shots for which X-ray data were not obtained. One page is used for each shot, and they are listed in order. A description of the various kinds of data in Appendix A, both the experimentally measured data and several kinds of information calculated in the data analysis, is given in paragraph 3.3 after an overview of the primary and secondary test programs in paragraph 3.2.

3.2 TEST PROGRAM MATRICES

3.2.1 Primary Test Program Matrix

The primary test program at Eglin was planned to test two projectile configurations at three impact speeds and two target moisture conditions (dry Eglin sand and saturated Eglin sand). With four replications of each test the plan called for 48 shots. Four extra replications brought the total to 52 shots as summarized in Table 3. The two projectile configurations were both solid cylinders of nominal diameter 0.0198 meter, one with a flat nose and the other with a step-tier nose, as described in paragraph 2.3. The wet sand was fully saturated. The letters after the shot numbers indicate that special analysis was made of those shots. The letter V indicates that velocity data from the X-rays were fitted to a Poncelet force law as described in paragraph 4.4, with information about the fitting tabulated in Appendix A. The letter M indicates that the velocity results were compared with the magnetic sensor data obtained with the velocity coils, with results of the comparison listed at the end of each tabulation in Appendix A. The letter B indicates that a bow wave was observed in front of the projectile in one or more of the X-rays (see paragraph 3.5.1).

3.2.2 Secondary Test Program Matrix

Shot numbers not included in the primary test program are listed in Table 4.

3.3 DESCRIPTION OF EXPERIMENTAL DATA

For each of the 74 shots listed in Appendix A the position and cavity separation angle information obtained from the X-ray records is given in the first data group. An example is shown in Table 5.

TABLE 3. SHOT NUMBERS OF EXPERIMENTAL MATRIX FOR PRIMARY TEST PROGRAM

Projectile Type and Sand Condition	Velocity Range 210 m/sec	320 m/sec	400 m/sec
			14 B
	15	20 VB	25 VB
Solid	16	22 VB	26 VMB
Flat Nose	17 V	23 VB	27 VB
Dry Sand	18 V	24 VMB	29 VM
	19 V		
	70 VM	36	
Solid	71 VM	37 VM	76 VM
Flat Nose	72 VM	38 V	82 V
Wet Sand	73 VM	74 V	83 VM
		81 VM	84 VM
	52 V	56 VM	62 VB
Solid	53	58 VM	63 VB
Step-Tier Nose	54 VM	59 VM	64 VMB
Dry Sand	55 VM	61 VM	65 VB
	57 V		
	42	39 V	50 M
Solid	43	40	51
Step-Tier Nose	44	41	68 VM
Wet Sand	45 V	49 VM	69 VM

(V indicates that calculated velocities of nose and center of gravity are Tabulated in Appendix A; M indicates that the tabulation also includes comparison with the magnetic sensor data; B indicates bow waves were observed.)

TABLE 4. SHOT NUMBERS OF EXPERIMENTAL MATRIX OF SECONDARY TEST PROGRAM

Projectile Type	Target Medium	Impact Velocity Ranges Shot Numbers	
Solid Biconic	Dry Sand	320 m/sec 30 V, 31 V, 32 V	
Hollow Biconic	Dry Sand	350 m/sec 35 V	400 m/sec 33, 34
Solid Flat Nose 0.152 meter long	Dry Sand	240 m/sec 77, 78 V, 79 VM	
Hollow Step-Tier	Dry Sand	230 m/sec 88, 89 V	
Hollow Step-Tier	Wet Sand		440 m/sec 90
Hollow Step-Tier	Water	230 m/sec 85, 86 VM, 87 VM, 91 V	
Special	Wet Sand	250 m/sec 46	550 m/sec 47, 48
Model	Dry Sand		66, 67

(V indicates that calculated velocities of nose and center of gravity are listed in Appendix A; M indicates that the tabulation also includes comparison with the magnetic sensor data.)

TABLE 5. EXAMPLE OF FIRST DATA GROUP

SHOT 26 (12 MARCH, 1976, NO. 3)

SAND: DRY, DENSITY:1538. KG/M**3; APPRUACHING VELUCITY: 406. M/S
PRUJECTILE: SOLID FLAT NOSE MASS:0.5443 KG, D=0.02 M, L=0.225 M

X-RAY STATION	NO.1	NO.2	NO.3	NO.4	NO.5
TIME (SECOND)	.000108	.000675	.001687	.003003	.004582
CENTER OF GRAVITY POSITION (M)					
HORIZONTAL	-0.086	0.119	0.420	0.730	1.035
VERTICAL	0.134	0.140	0.146	0.153	0.160
INCLINATION ANGLE(DEG).	0.0	1.0	0.5	-1.5	-6.0
SEPARATION ANGLE(DEGREE)					
ABOVE	****	5.0	3.5	2.5	0.5
BELOW	****	4.5	4.5	5.5	8.5
NOSE WIDTH (M ON FILM).	0.0250	0.0228	0.0230	0.0230	0.0225
NOSE POSITION (M)					
HORIZONTAL	0.027	0.232	0.533	0.843	1.147
VERTICAL	0.134	0.142	0.147	0.150	0.148
INPUT NOSE POSITION (M)					
HORIZONTAL	0.024	0.232	0.533	0.844	1.148
VERTICAL	-0.081	-0.074	-0.068	-0.064	-0.067

The first line below the shot number and date gives the target medium: dry sand, wet sand or H-OH (meaning H_2O for shots into water), the density in kg/m^3, the projectile's approaching velocity in meters per second as measured by the counter start and stop velocity screens as described in paragraph 2.3 and/or by the time from the break-wire on the gun muzzle to the X-ray trigger foil switch located on the front of the box as recorded on the oscillograph strip chart. The second line gives the projectile type, mass in kg, nominal diameter and length in meters. Below each X-ray station number is listed the time in seconds from the foil switch trigger to the firing of that X-ray. The firing times were determined from the delay settings and also by noting signals appearing on the strip chart records for various sensors. The next two lines give the calculated center of gravity position coordinates in meters measured from the front and bottom of the target box. Note that the first horizontal coordinate is negative, since the projectile is still outside the box.

The projectile's angle of inclination to the horizontal and the cavity separation angles at the nose, measured with respect to the projectile axis, are listed in the next two lines of data. A row of asterisks (****) indicates missing data. These angles were measured on the X-ray negatives, as was the measured nose width in meters. The next two lines are calculated nose position coordinates, corrected for X-ray beam divergence. The last two lines give the raw data on the nose position in the X-ray picture, with the vertical position measured from the row of letter markers on the wall of the box, so that a negative coordinate indicates distance below the letters.

For 22 shots (those not marked with a V or M in the experimental matrices of paragraph 3.2, no further data are tabulated in Appendix A. The other 52 shots have additional groups of calculated data to be discussed in paragraph 4.3, and the 26 marked with an M in the experimental matrices of paragraph 3.2 include magnetic sensor data in the last data group, as shown in Table 6.

TABLE 6. EXAMPLE OF LAST DATA GROUP (SHOT NO. 26)

RECORDED TIME OF MAXIMUM/MINIMUM COIL VOLTAGE (S)				
MAX	.000099	.001594	.002864	.004427
MIN	.000625	.002307	.003947	.005650
COMPUTED NOSE POSITION AT MAX/MIN COIL VOLTAGE (M)				
AT MAX	0.024	0.509	0.813	1.118
AT MIN	0.214	0.689	1.029	1.349
RECORDED COIL POSITION (M)				
	0.0	0.486	0.778	1.076
DIFFERENCE BETWEEN COIL AND NOSE AT MAX/MIN VOLTAGE (M)				
AT MAX	0.024	0.023	0.035	0.042
AT MIN	0.214	0.203	0.251	0.273

The first line of data in this last data group (see Table 6) lists the time in seconds from the X-ray trigger coil switch time to the maximum voltage from the four magnetic sensor velocity coils. The second line lists the times of the minimum voltage at each of the coils. These times were transcribed from the strip chart. The next two lines are computed nose positions, as will be described in paragraph 4.4. The next line lists the actual positions of the four coils as recorded in the log book, and the last two lines record the differences between the two computed nose positions and the actual positions. The significance of these differences will be discussed in paragraph 4.4.

3.4 PRELIMINARY ANALYSIS OF TABULATED DATA

3.4.1 Nose Positions

Nose positions as measured on the X-ray photos were recorded as INPUT NOSE POSITION in the first data group of the tabulations of Appendix A (see Table 5) and also the apparent nose width. This apparent nose width as compared to the known actual nose width provides a first-order correction for the divergence of the X-ray beams. A simple computer program, based on similar triangles with apex at the X-ray source, was used to correct all apparent horizontal and vertical distances in proportion to the known correction for nose width. The corrected nose positions are tabulated immediately above the raw data input nose positions.

3.4.2 Center of Gravity Position

The center of gravity position was calculated from the corrected nose position and the (uncorrected) inclination angle by using the known distance from the nose of the projectile to its center of gravity. This correction did not account for projectile yaw. Yaw was believed negligible because of the straightness and lateral stability of the trajectory. Further data analysis is given in Section IV.

3.5 DATA NOT ANALYZED

3.5.1 Bow Waves

Several of the X-rays showed a detached shock wave ahead of the projectile, revealed by a density discontinuity. This occurred notably in the higher speed impacts in dry sand. In the primary test matrix of Table 3 shot numbers marked with a B showed well defined shock waves. Thus the flat-nosed projectiles showed shock waves in the intermediate velocity range also.

The bow shock wave appeared as a roughly parabolic curve (almost a circular arc near the vertex) with vertex at a distance ahead of the projectile nose of the order of magnitude of the projectile diameter. The X-ray pictures have been retained for possible use in future theoretical analysis of the deformation. Figure 4 shows tracings of two of the bow waves ahead of the projectile nose in two positions in Shot 26. The distance between the two positions is not to scale in the figure, but the position of each bow wave is shown relative to the nose.

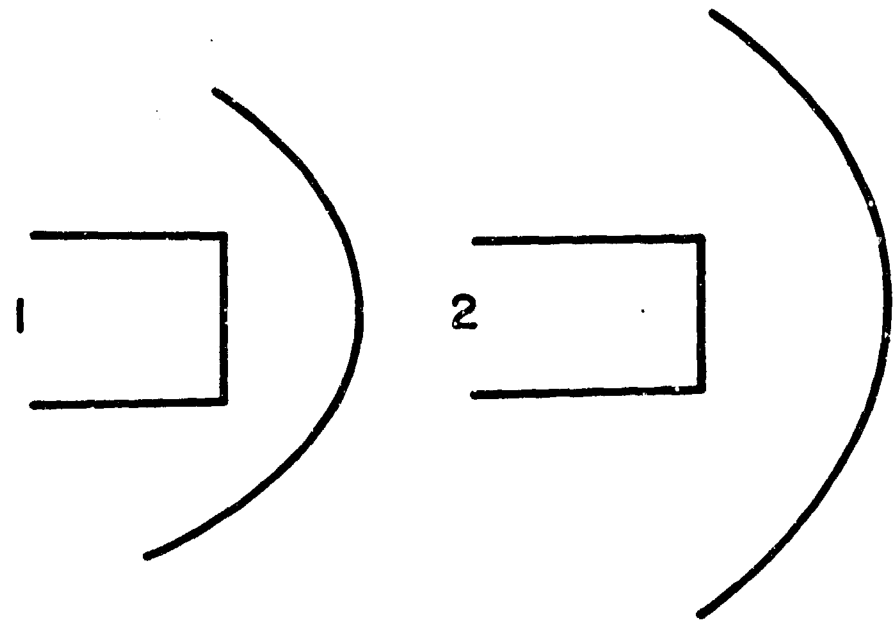

Figure 4. Tracing of a Bow Wave for Shot No. 26

Similar shock waves were also observed in some of the preliminary shots with 0.50 caliber projectiles.

3.5.2 Separation Angles

In some shots the separation angles above and below appeared to be approximately symmetric with respect to the nose velocity vector, which was slightly different from the projectile heading as given by the recorded inclination angle. In almost all of the cases recorded in the primary test program only the nose was in contact with the sand. In future analyses it may be possible to relate the separation angles to the shape of the false nose of sand formed in front of the flat-nose projectiles and/or to the lift forces exerted on the nose.

3.5.3 Marker Movements

The preshot and postshot X-rays showing movement of the small steel markers have not been analyzed. This information may be useful for evaluating future theoretical analyses of target medium deformation.

3.5.4 Pressure and Strain-Gage Measurements

The pressure transducer strip chart records may furnish useful data to compare with the observed bow waves and/or with future theoretical analyses of stress and deformation wave propagation in the target. The strain gage measurements on the aluminum test chamber walls were also recorded on the strip chart. These strain pulses are also related to the pressure wave in the sand, but are strongly influenced by the response of the aluminum plate to a traveling and varying dynamic load.

SECTION IV

CLASSICAL AND EMPIRICAL ANALYSIS OF EXPERIMENTAL DATA

4.1 INTRODUCTION

Trajectory plots for the 52 shots of the primary test program are given in paragraph 4.2. Since these trajectories are very nearly straight and horizontal throughout the 1.2-meters-long region of observation, analysis by one-dimensional penetration models is feasible. In paragraph 4.3.1 computer plots of horizontal positon versus time and of velocity versus position are given for 21 of the shots. These were obtained by first fitting a cubic polynominal interpolation formula to the position data and then fitting a Poncelet force law to each shot, as described in paragraph 4.3.2, which also contains a comparison of the values obtained for the Poncelet drag coefficients of the 41 shots of the primary matrix that have been analyzed by this method. Results of magnetic sensing are compared with the X-ray data in paragraph 4.4. This data analysis was performed at the University.

Results of a different method of determing the Poncelet coefficient for each shot and also results of empirical analysis by methods similar to those developed at Sandia Laboratories (References 12,13) are given in paragraph 4.5. Variation of the drag coefficient within a shot is discussed in paragraph 4.6 by considering separately different segments of several trajectories. These last two data analyses were performed at the AFATL.

4.2 TRAJECTORIES OF PRIMARY TEST PROGRAM

Computer-plotted trajectories for the 52 shots of the primary test program matrix listed in Table 3 are shown in Figures 5 through 10 based on the X-ray data for the positions and inclination angles. In each plot the circles mark center of gravity positions and the other end of the line from the circle is the nose positon. Shot number is shown at the left end of each trajectory. The horizontal and vertical scales are the same, but each successively numbered trajectory in a figure is plotted displaced upward one square (12.5 cm) from the preceding one. The plots give a pictorial summary of the trajectory data. Precise positions are given in the tabulations of Appendix A.

The most remarkable feature of the trajectories is their straightness, following in most cases a nearly horizontal straight line through the 1.2-meters-long target box. All but one of trajectories have a slight upward trend. The greatest rise, 6.2 cm, occurred for Shot 19 in Figure 5(a). Shots 16 to 19 of this group for the solid flat-nose projectile impacting dry sand at about 210 m/sec all show a continuously increasing angle of inclination, reaching 16.5 degrees in Shot 19. This was the largest inclination angle recorded. Positive final inclination angles were recorded for 31 shots, negative for 19 shots and zero for one, Shot 76 in Figure 7(b). In dry sand the flat-nose projectiles showed 9 positive and 4 negative final inclination angles while the step-tier

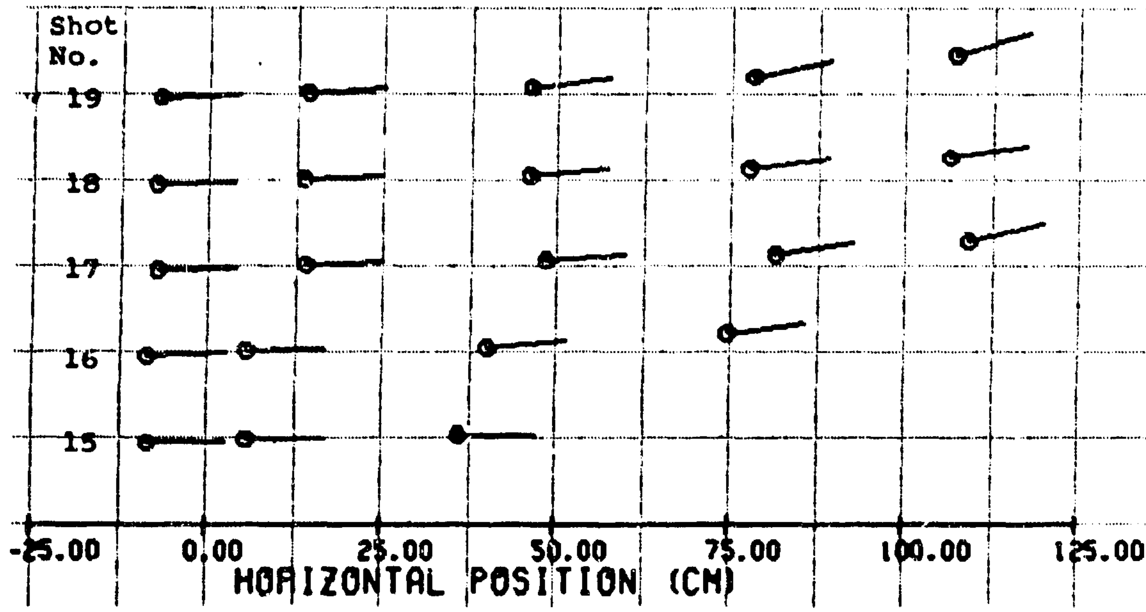

(a) Dry Sand

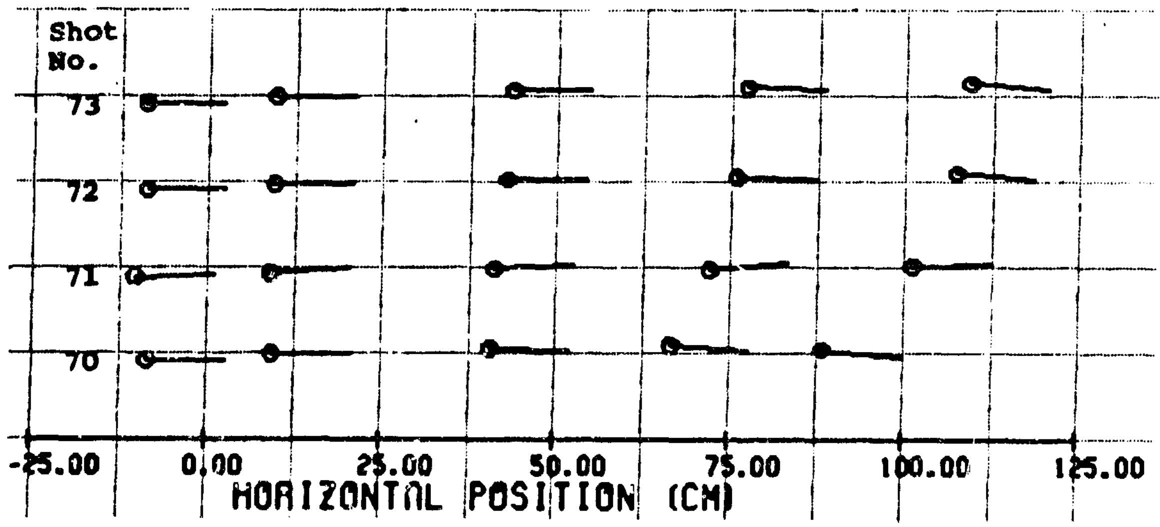

(b) Wet Sand

Figure 5. Trajectories of Solid Flat-Nosed Projectiles for Impact Velocities in the 210 m/sec Range

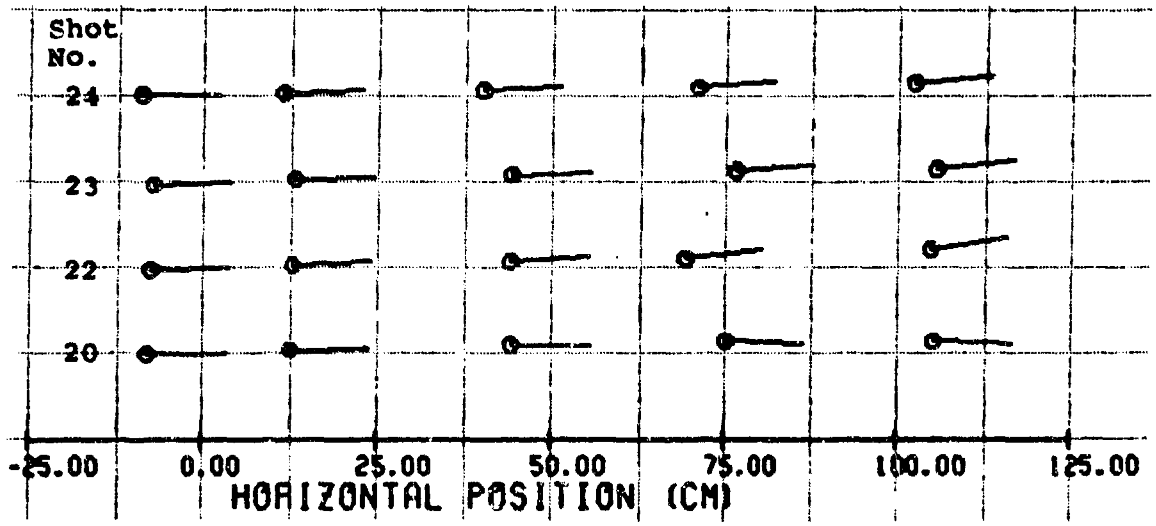

(a) Dry Sand

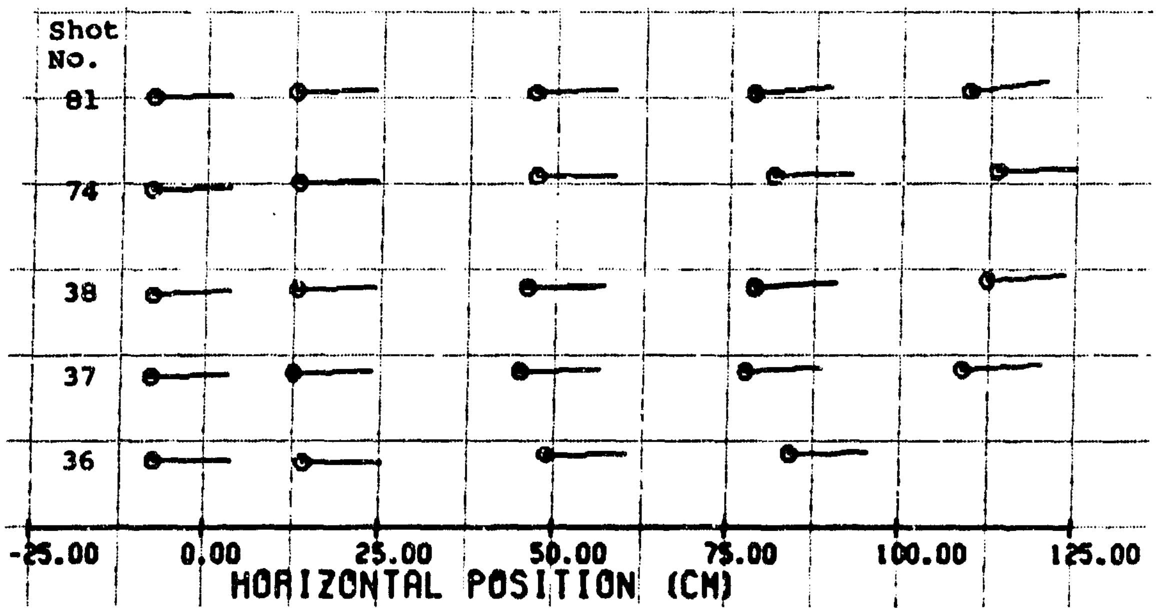

(b) Wet Sand

Figure 6. Trajectories of Solid Flat-Nosed Projectiles for Impact Velocities in the 320 m/sec Range

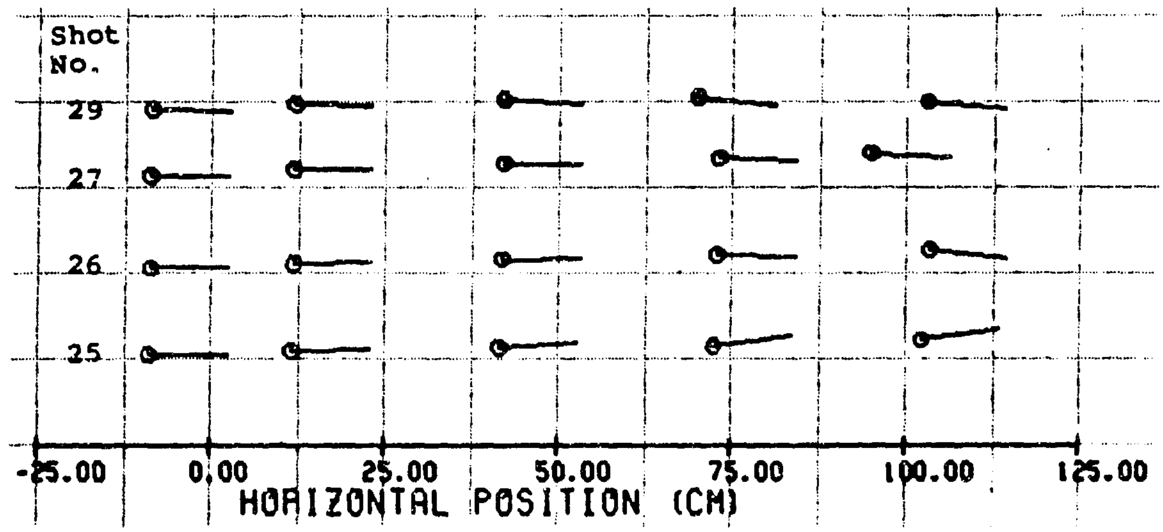

(a) Dry Sand

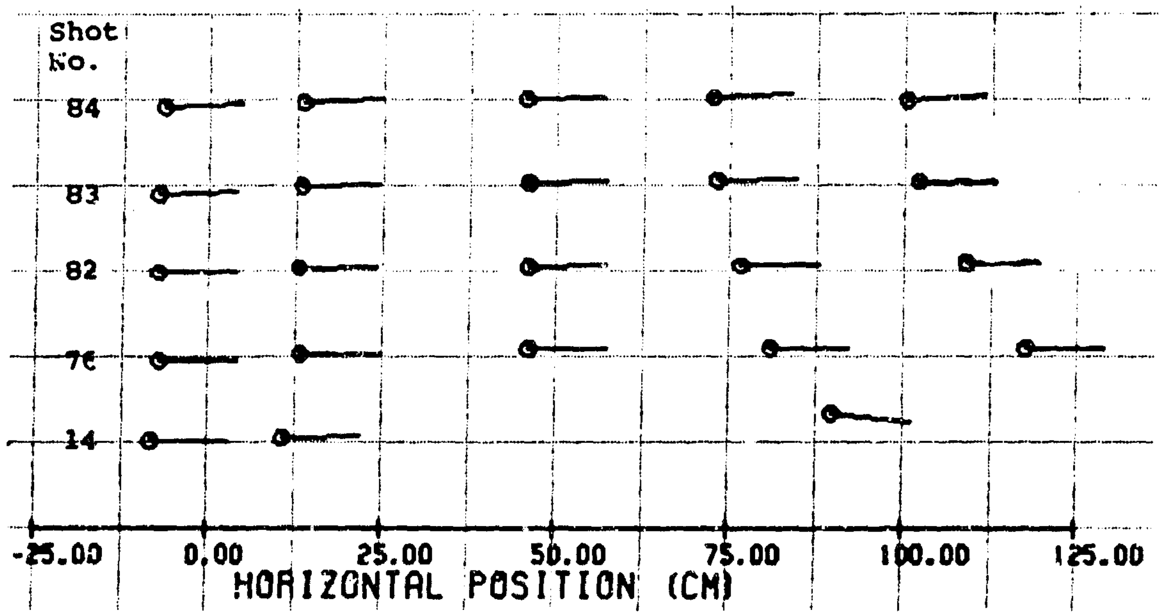

(b) Wet Sand

Figure 7. Trajectories of Solid Flat-Nosed Projectiles for Impact Velocities in the 400 m/sec Range

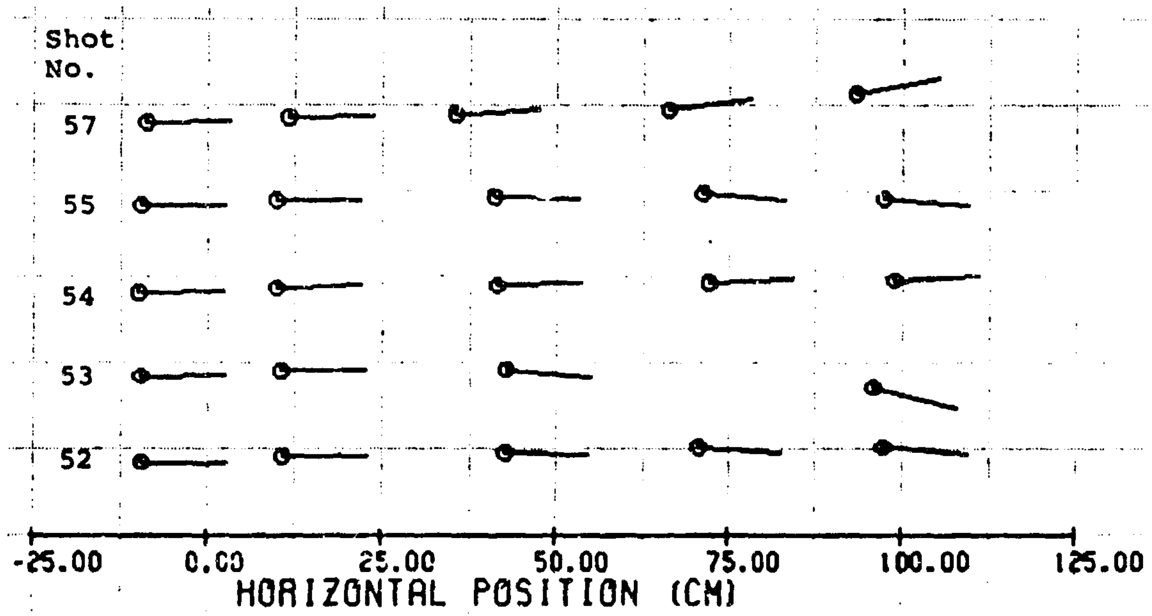

(a) Dry Sand

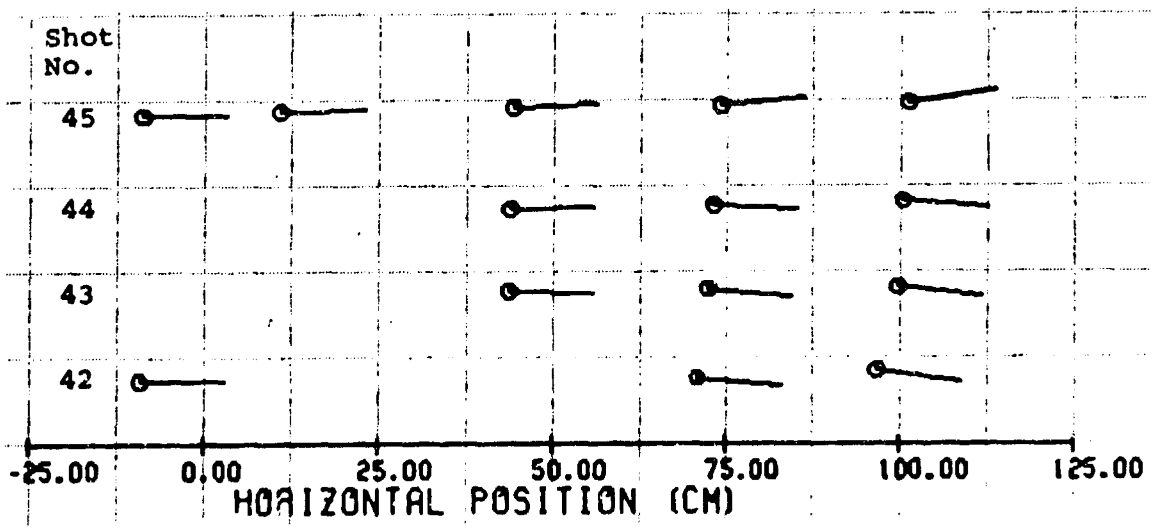

(b) Wet Sand

Figure 8. Trajectories of Solid Step-Tier Projectiles for Impact Velocities in the 210 m/sec Range

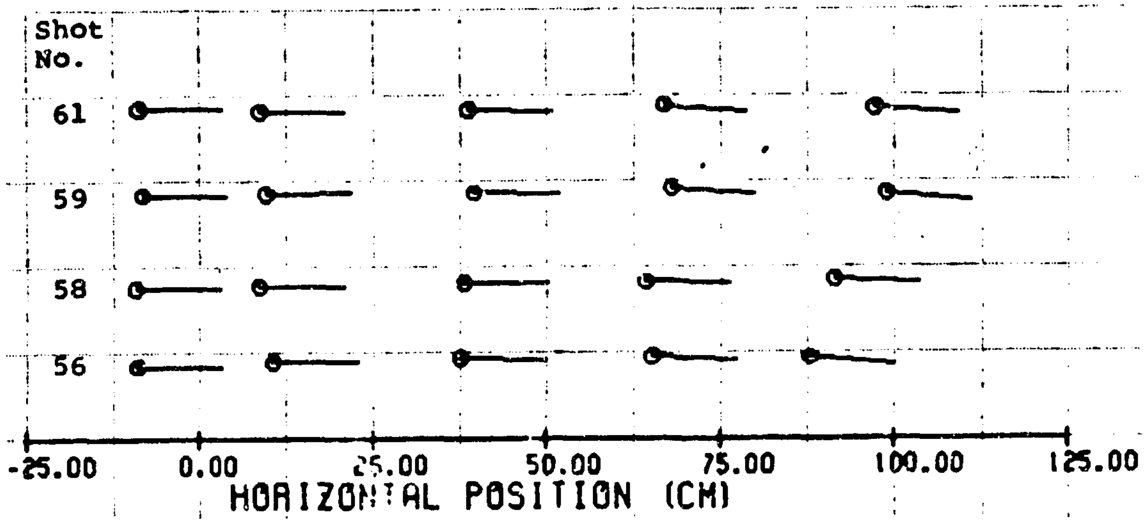

(a) Dry Sand

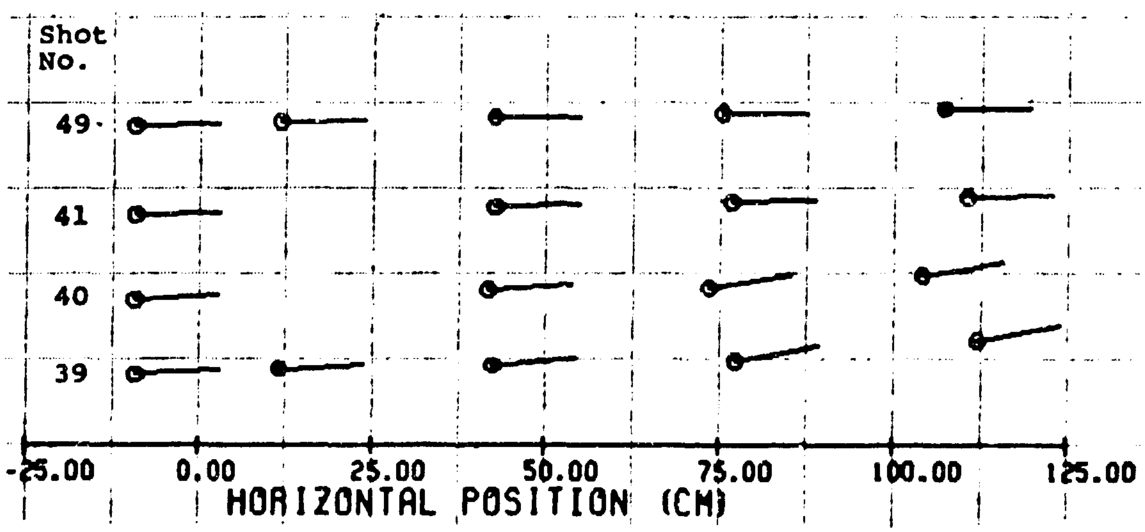

(b) Wet Sand

Figure 9. Trajectories of Solid Step-Tier Projectiles for Impact Velocities in the 320 m/sec Range

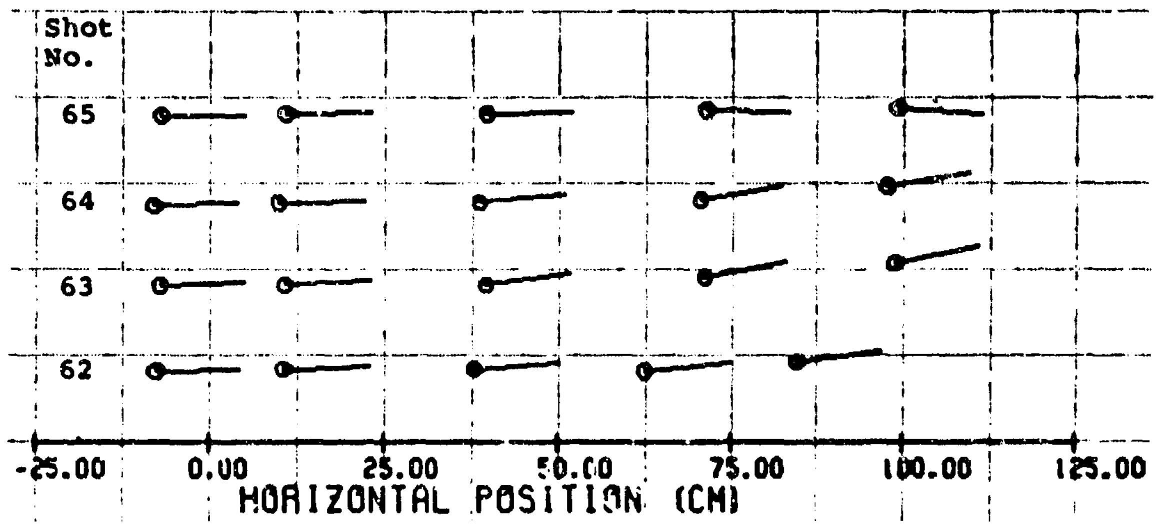

(a) Dry Sand

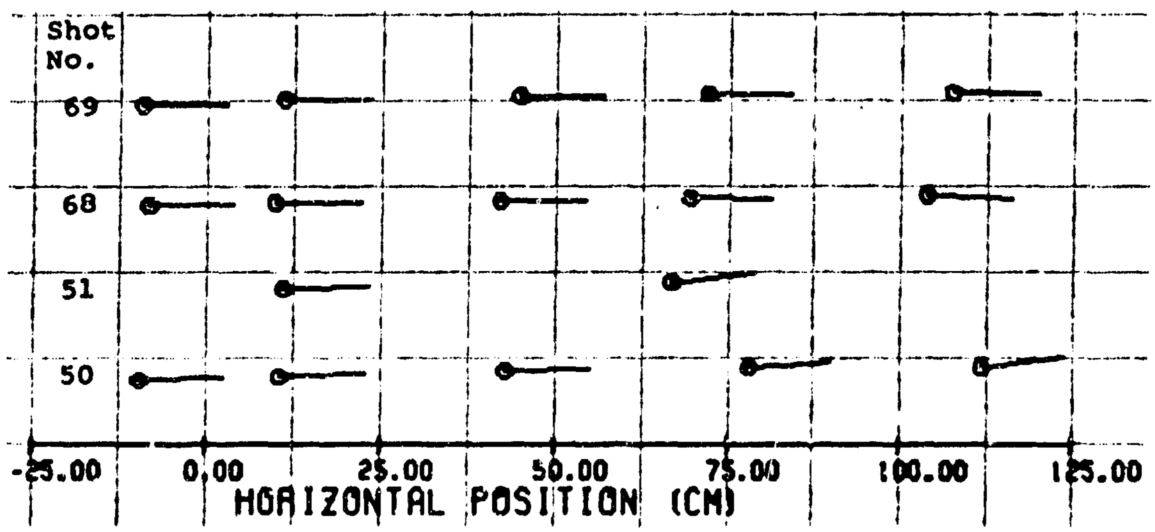

(b) Wet Sand

Figure 10. Trajectories of Solid Step-Tier Projectiles for Impact Velocities in the 400 m/sec Range

projectiles showed 5 positive and 4 negative. In saturated sand the flat-noses showed 11 positive and 2 negative final inclination angles while the step-tier noses showed 7 positive and 5 negative. The largest negative angle was -14.5 degrees in Shot 53 of Figure 8(a). This was also the only trajectory that did not rise.

Some of the trajectories show a continued rise, even with a negative angle. This is most evident in Shots 27 and 29 of Figure 7(a) for the flat nose impacting dry sand at 400 m/sec. The X-ray pictures show that during the part of the trajectory observed only the flat nose was in contact with the sand, so that no forces were acting on the afterbody surface.

Since the trajectories are so straight in the region of observation, analysis by one-dimensional penetration models is reasonable, for example the Poncelet force law to be discussed in paragraphs 4.3 and 4.5 and the Cavity Expansion Theory penetration model in Section V.

4.3 ANALYSIS AND DISCUSSION OF TABULATED POSITION-TIME RESULTS BASED ON X-RAY DATA

4.3.1 Cubic Interpolation, X, t-plots and V, x-plots

Velocity analysis has been carried out for 52 shots for which complete X-ray data (5 stations) were available. This includes 41 shots from the primary test program and 11 from the secondary program (those marked with a V in Tables 3 and 4.) In the data reduction at the University of Florida, the velocity analysis was performed first by fitting a cubic interpolation formula to the data, and later improved results for the x-component of the center of gravity velocity were obtained by fitting the data to a formula derived from the Poncelet force-law penetration model. The Poncelet law fittings will be discussed in paragraph 4.3.2.

The coefficients of each cubic polynomial are listed in the tabulations of Appendix A.

For example, for Shot 26, the tabulated coefficients for C.G. VELOCITY X-COMP. imply the polynomial

$$x = -0.1277 + 393.3t - 46,190t^2 + 3,432,000t^3 \qquad (1)$$

for x in meters and t in seconds. The coefficients were determined by a least-squares fit. At the end of each set of tabulated coefficients is listed the standard deviation in meters [square root of the sum of the squares of the differences between the measured x-positions and those calculated by the cubic at the times of firing of the X-rays]. For Shot 26 the standard deviation is 0.0014 meter for the x-component, indicating a very good fit.

Velocities were calculated from the fitted cubics. For example, for Shot 26 the center of gravity x-component velocity is given by

$$V = \frac{dx}{dt} = 393.3 - 92,380t + 10,296,000t^2 \text{ m/sec} \qquad (2)$$

This should give a good approximation to the velocity near the center of the interval, but larger errors would be expected at the ends. Computer plots of: (a) the calculated x,t-curve and (b) the calculated V,x-curve for 21 shots of the primary test program are shown in Figures 11 through 52. On each x,t-plot the five experimental data points are marked by squares. The solid curve is the fitted cubic, and the curve marked with vertical strokes is a curve based on the Poncelet force law, to be discussed in paragraph 4.3.2. It is seen that the fitted cubic x,t-curves agree very well with the experimental data. The cubic and Poncelet x,t-curves are also close to each other through the whole interval. Their slopes begin to differ at the ends of the intervals of observation. The V,x-plots by the two methods therefore show considerable differences at the ends. The cubic interpolation would give completely unreasonable results outside the interval of observation (0 to 1.2 meters).

4.3.2 One-Dimensional Analysis of Velocities by Fitted Poncelet Force Law

The Poncelet force law (Reference 2) takes the following form, after dividing through by the mass m of the projectile,

$$-\frac{dV}{dt} = A + BV^2 \tag{3}$$

where A and B are parameters depending on the target material as well as on m. For the high velocities in the interval of observation in the present program, the contribution of A is negligible, and the V,x-curves have been fitted by taking A equal to zero and determining a best fit for B by a nonlinear regression procedure that minimizes the standard deviation from the experimental data of the x,t-curve obtained by integrating Equation (3).

Equation (3) can be integrated explictly for given initial data (V_o, x_o, t_o) to obtain

$$V = \left[\left(\frac{A}{B} + V_o^2\right)e^{-2B(x-x_o)} - \frac{A}{B}\right]^{1/2} \tag{4}$$

or, with A = 0

$$V = V_o e^{-B(x-x_o)} \tag{5}$$

With V = dx/dt a second integration of Equation (5) gives then

$$x - x_o = \frac{1}{B}\ln\left[1 + BV_o(t-t_o)\right] \tag{6}$$

The more complicated case, with $A \neq 0$, is discussed in Section V on the Cavity Expansion Theory.

Equation (6) was fitted to the experimental x,t-data. A nonlinear regression is required. The procedure followed in this section was to take initial conditions x_o, V_o, and t_o from the experimental data and the cubic

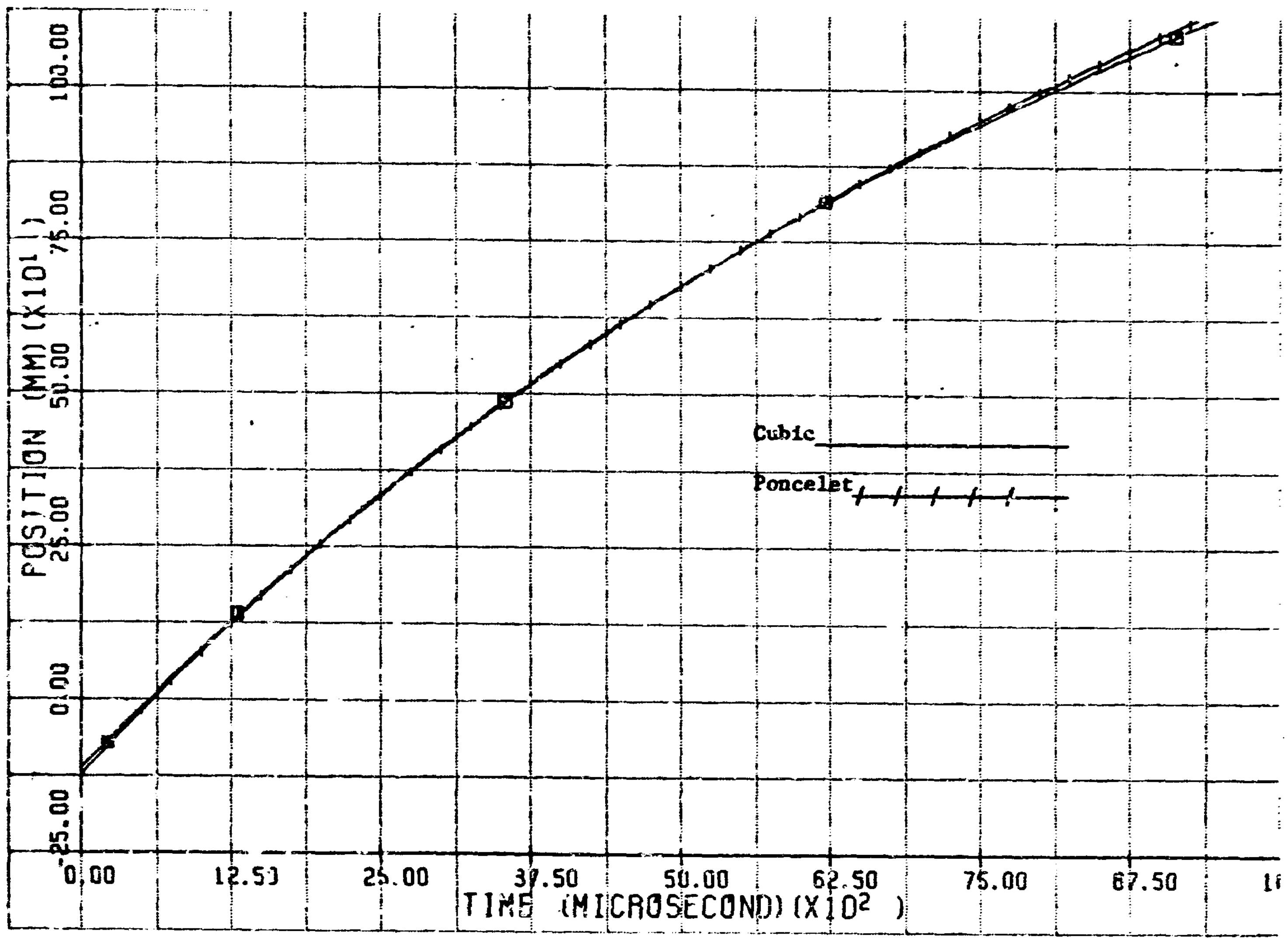

Figure 11. Position-Time Plot for Shot No. 17 (V_o=V_3)

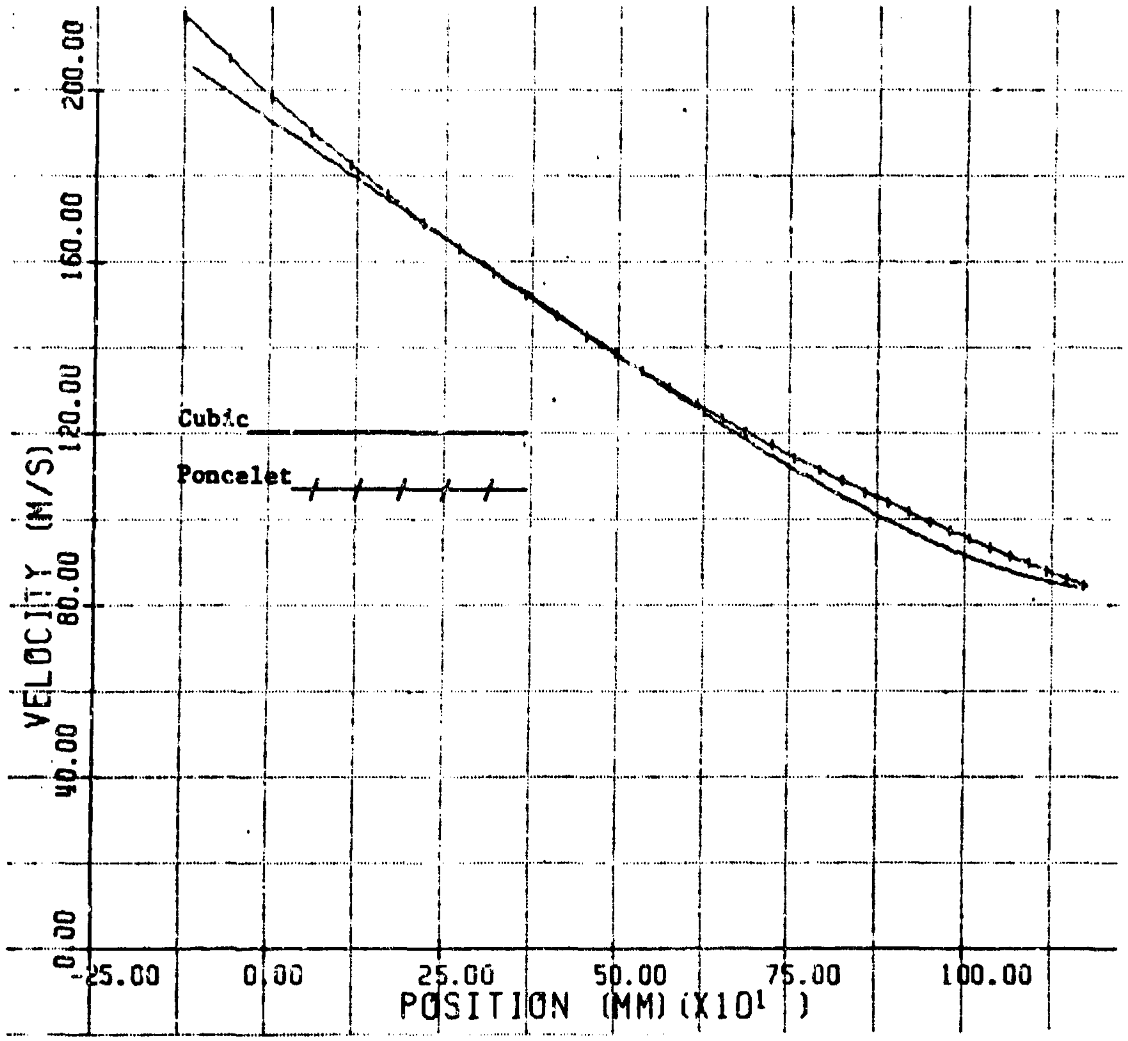

Figure 12. Velocity Versus Position for Shot No. 17 (V_o-V_3)

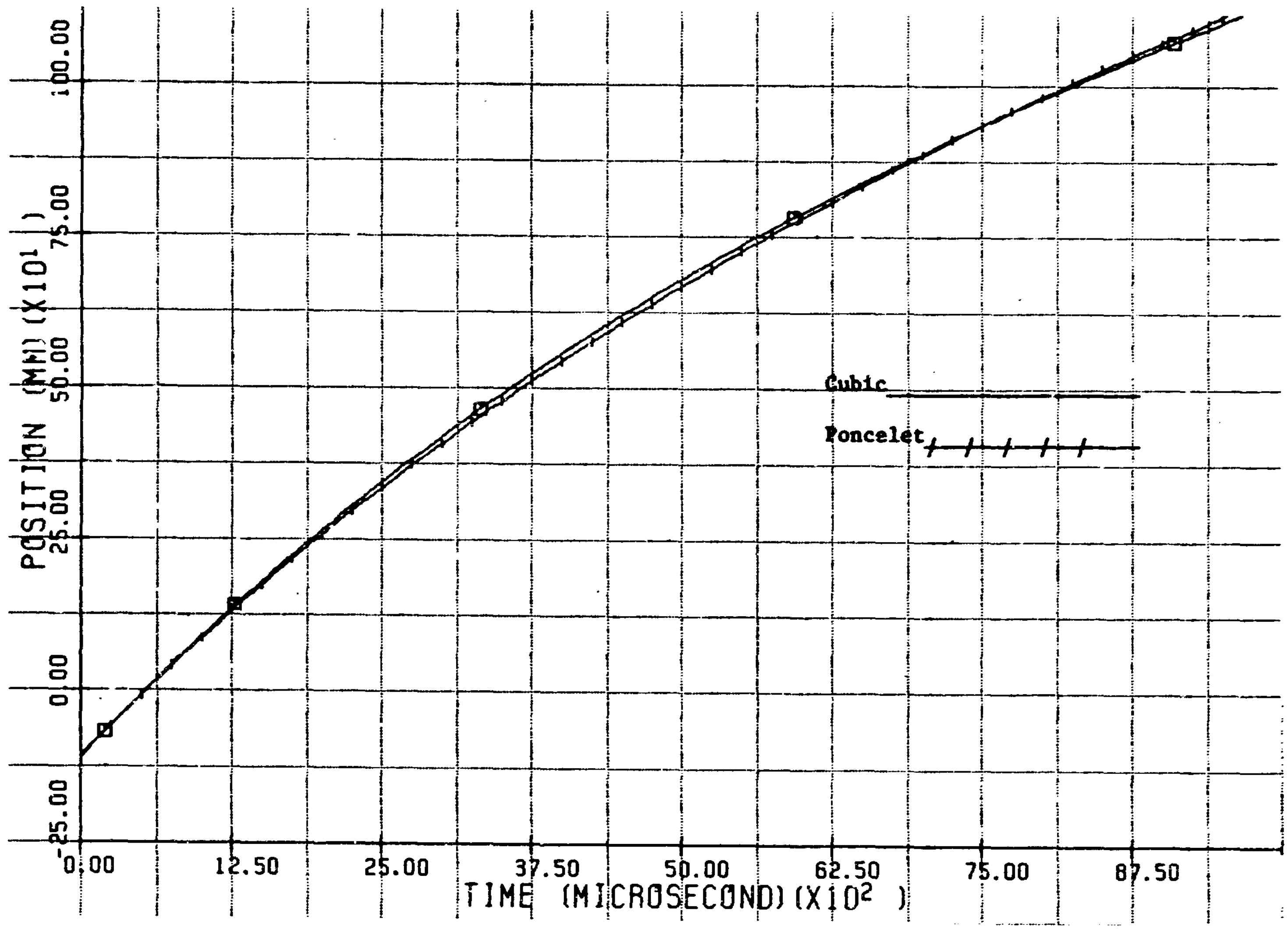

Figure 13. Position-Time Plot for Shot No. 19 ($V_o = V_1$)

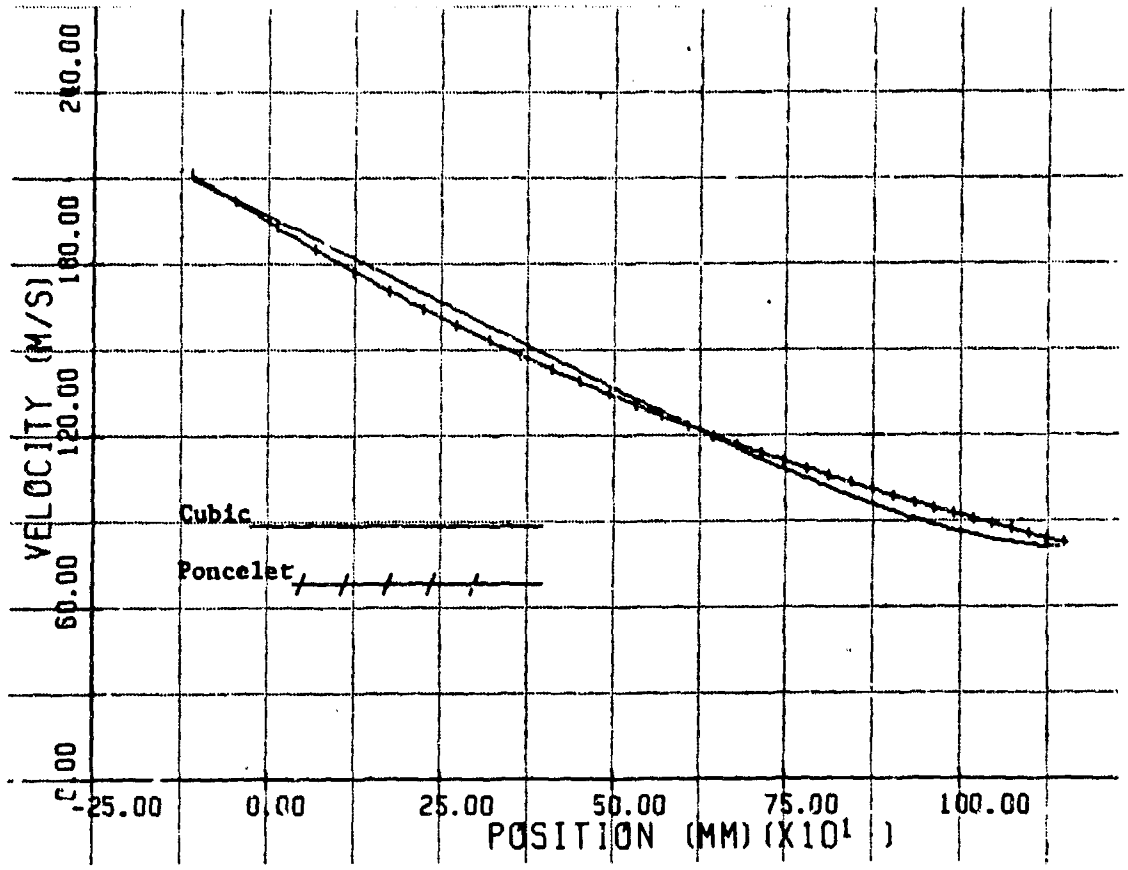

Figure 14. Velocity Versus Position for Shot No. 19 (V_o=V_1)

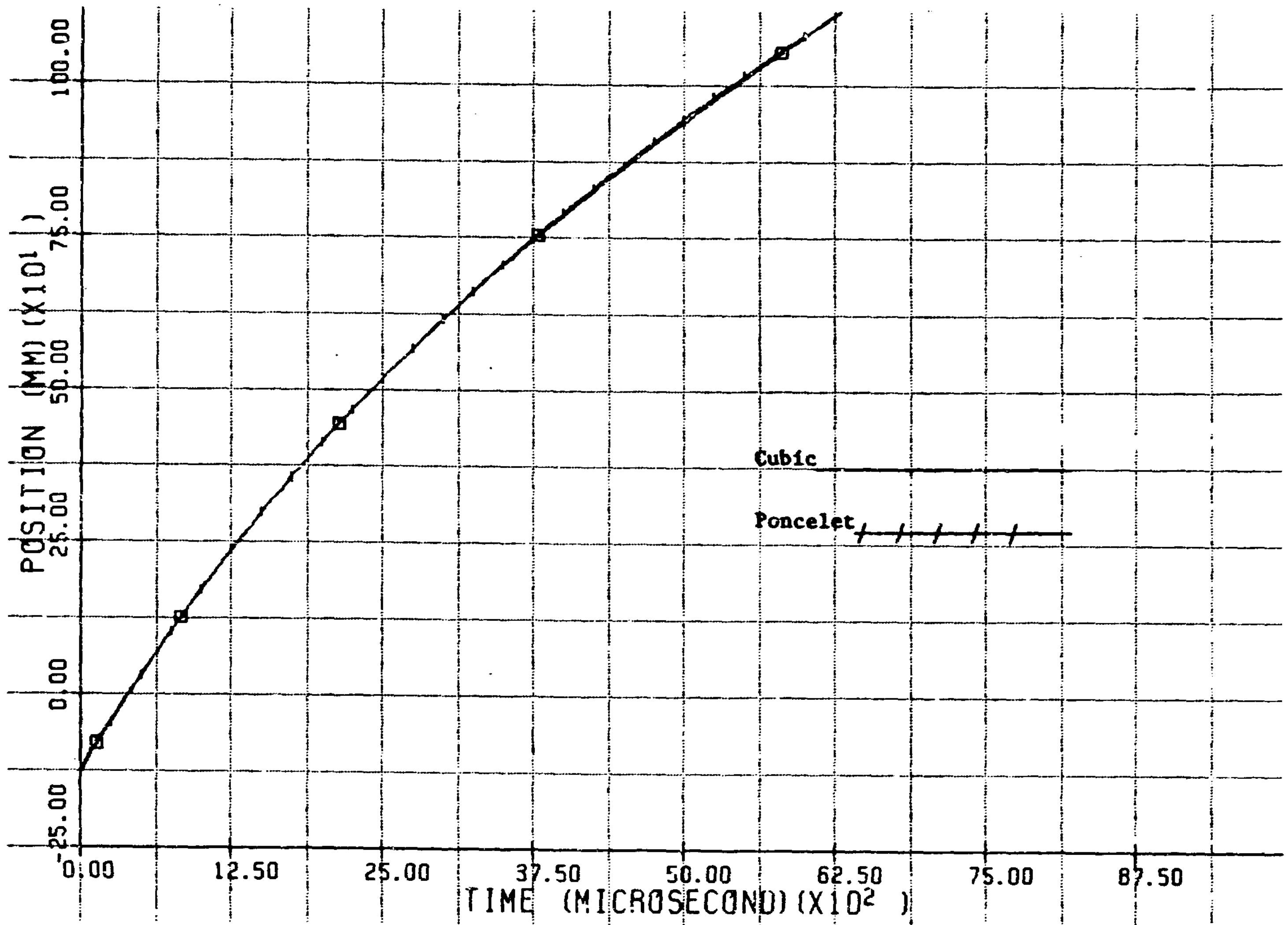

Figure 15. Position-Time Plot for Shot No. 20 ($V_o = V_3$)

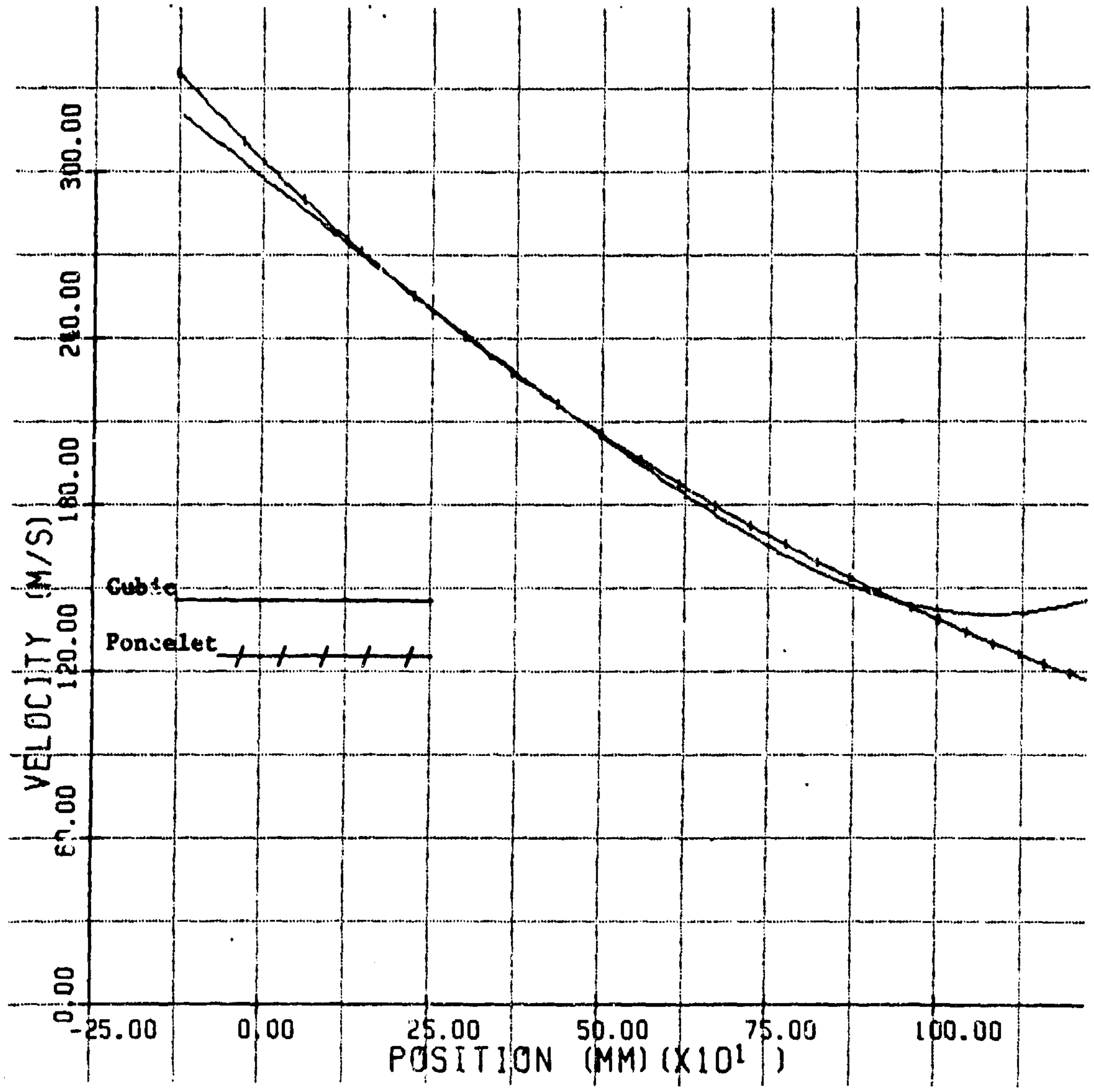

Figure 16. Velocity Versus Position for Shot No.20 (V_o=V_3)

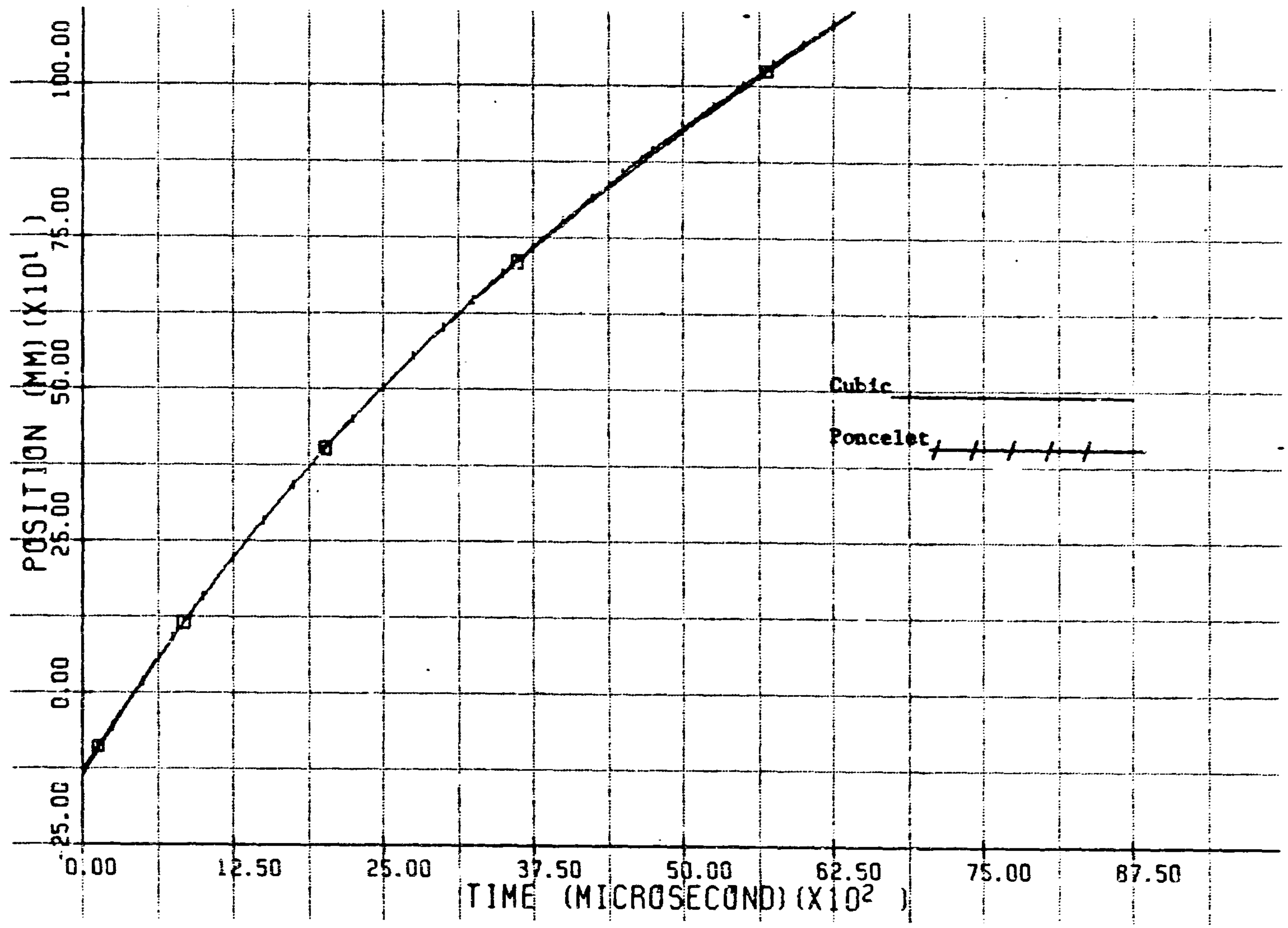

Figure 17. Position-Time Plot for Shot No. 24 ($V_o = V_3$)

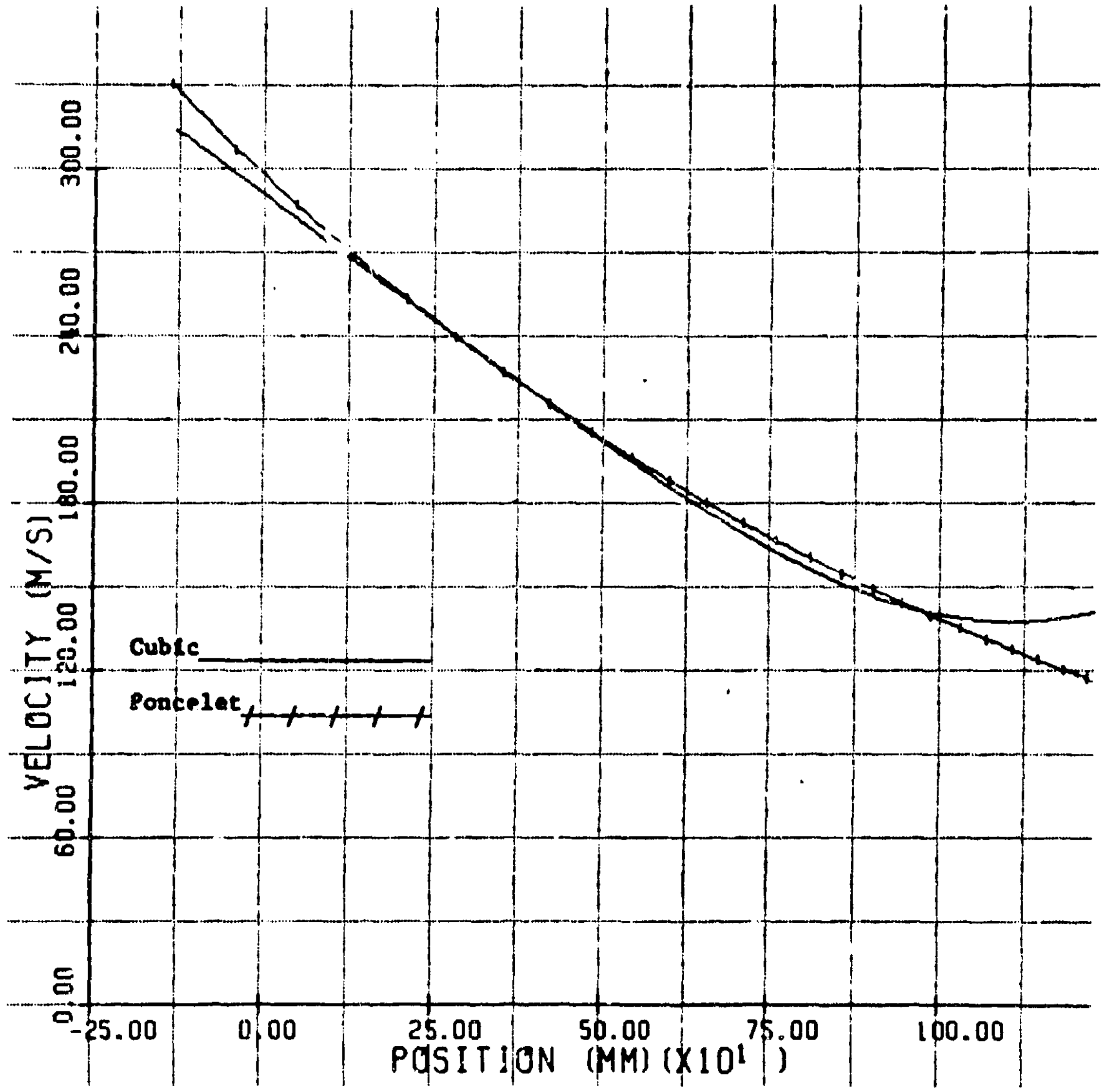

Figure 18. Velocity Versus Position for Shot No. 24 (V_o=V_3)

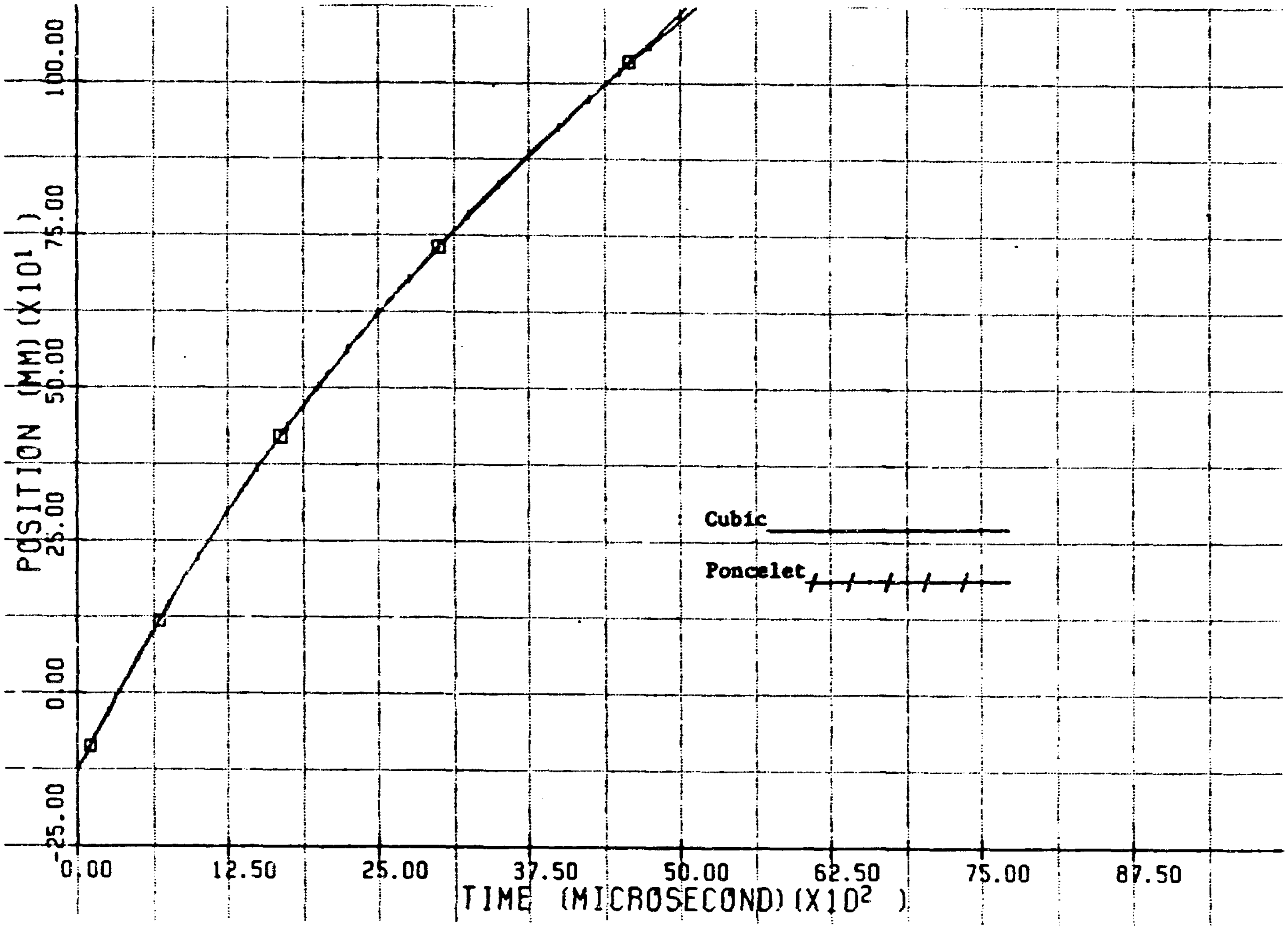

Figure 19. Position-Time Plot for Shot No. 26 (V_o=V_3)

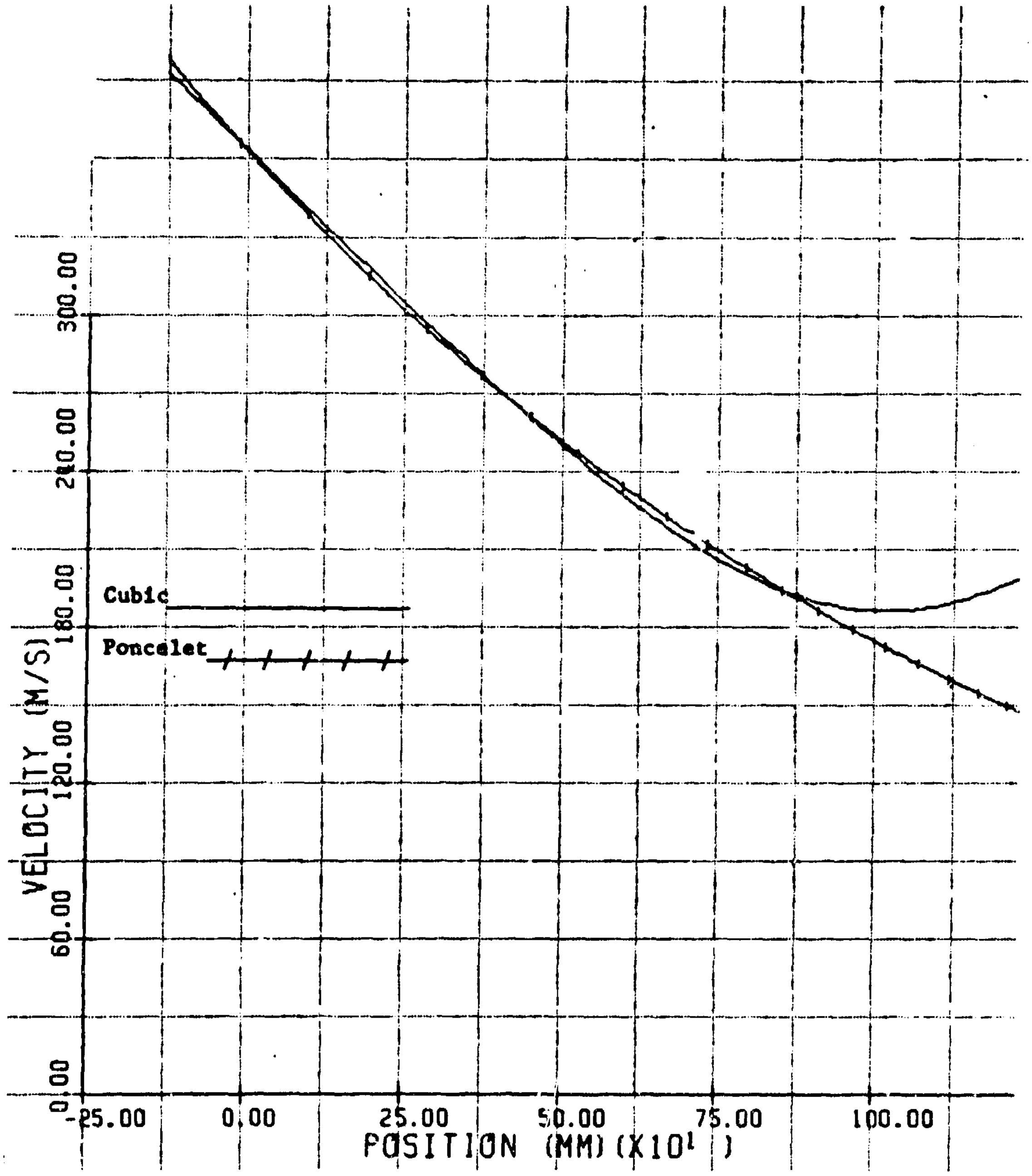

Figure 20. Velocity Versus Position for Shot No. 26 (V_o-V_3)

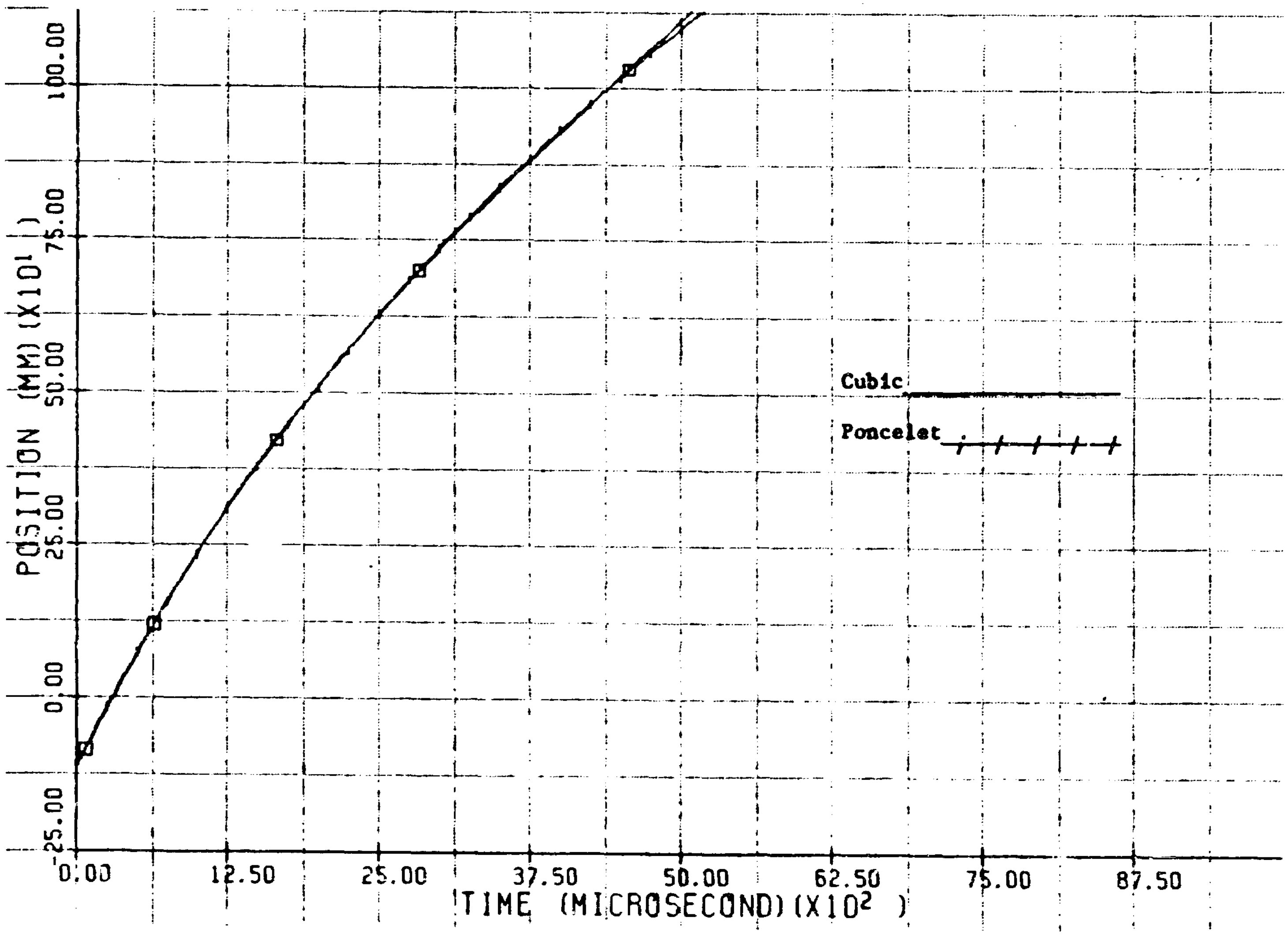

Figure 21. Position-Time Plot for Shot No. 29 ($V_o = V_3$)

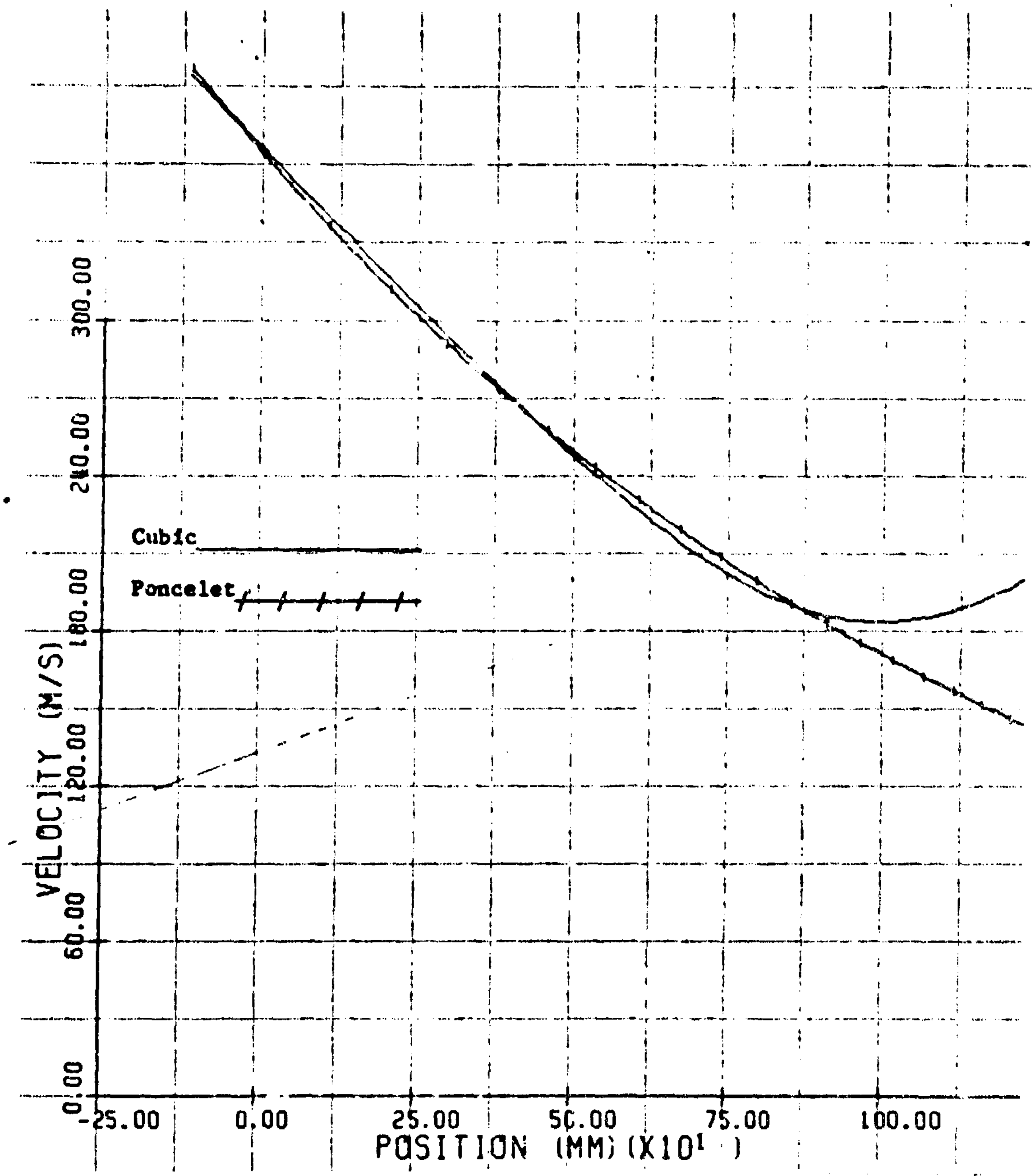

Figure 22. Velocity Versus Position for Shot No. 29 (V_o=V_3)

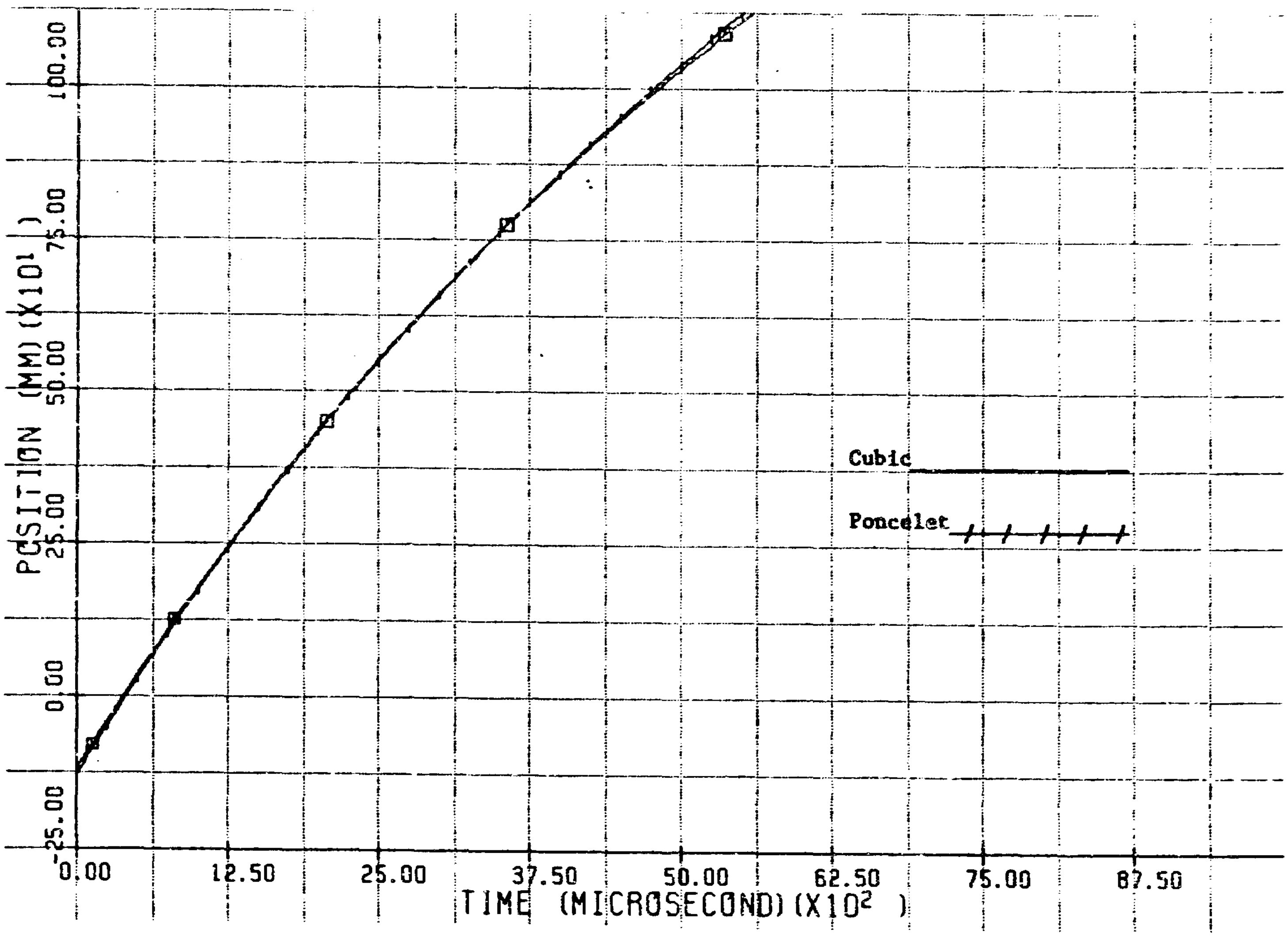

Figure 23. Position-Time Plot for Shot No. 37 ($V_o = V_3$)

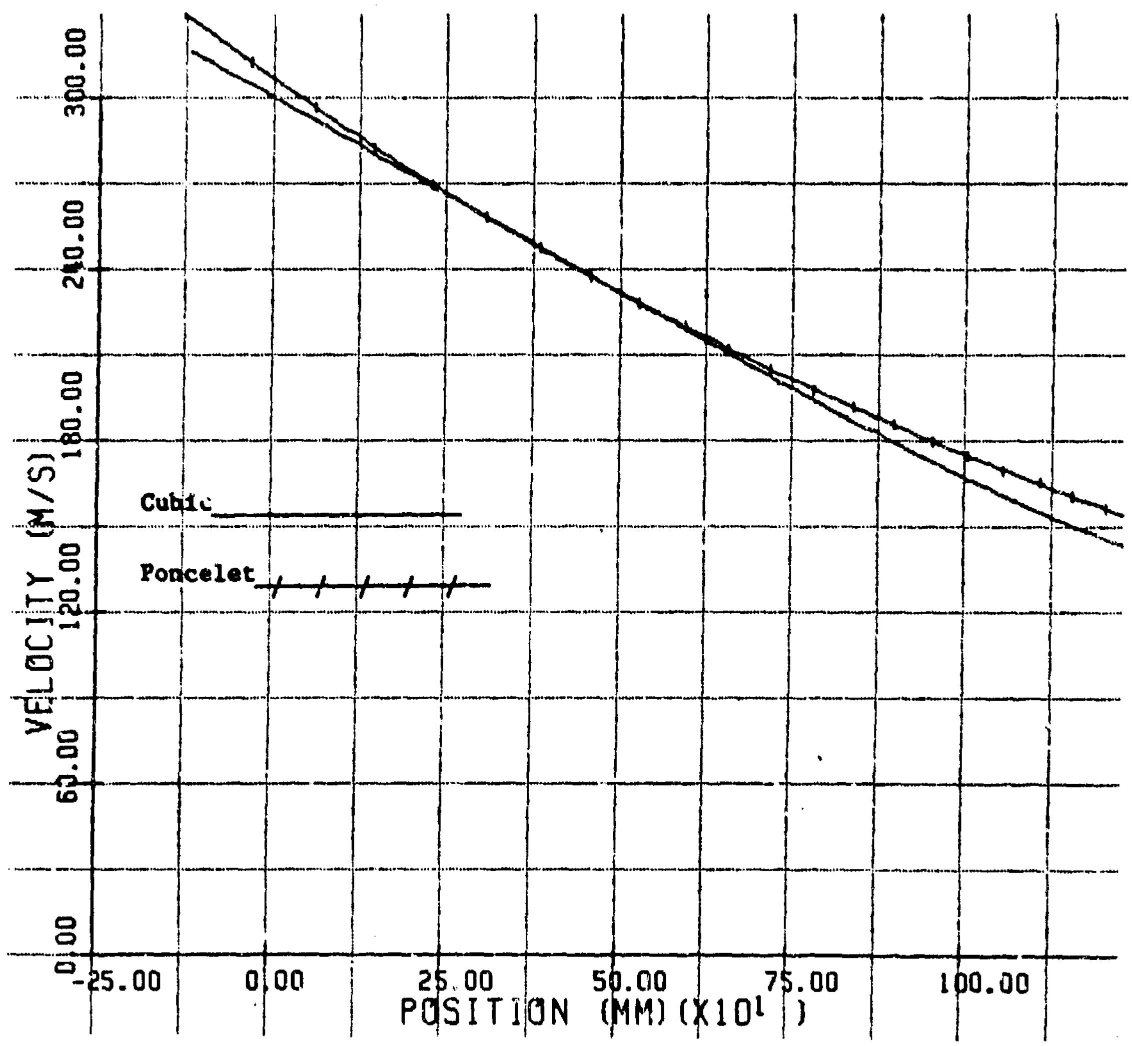

Figure 24. Velocity Versus Position for Shot No. 37 (V_o=V_3)

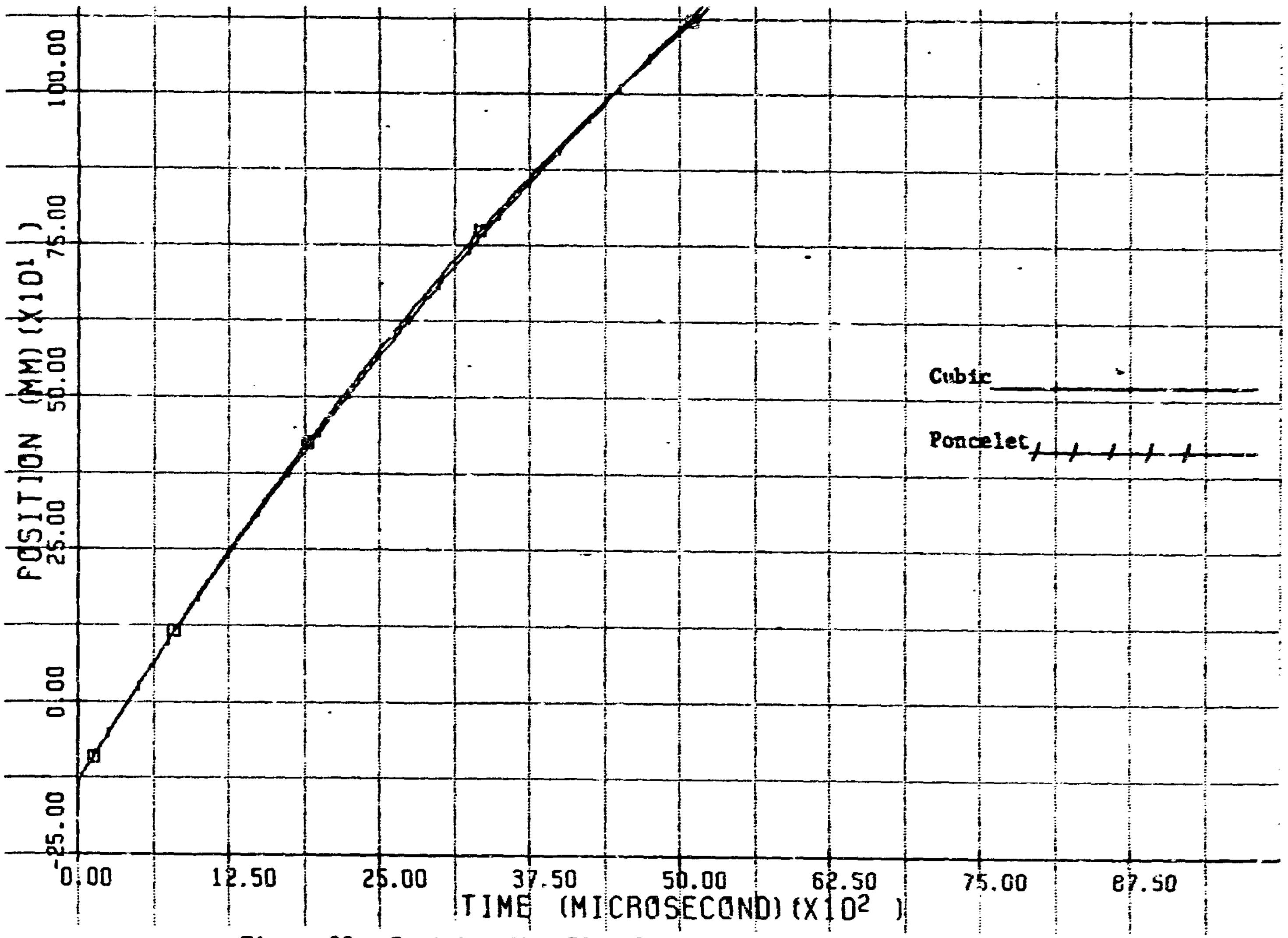

Figure 25. Position-Time Plot for Shot No. 39 ($V_o = V_1$)

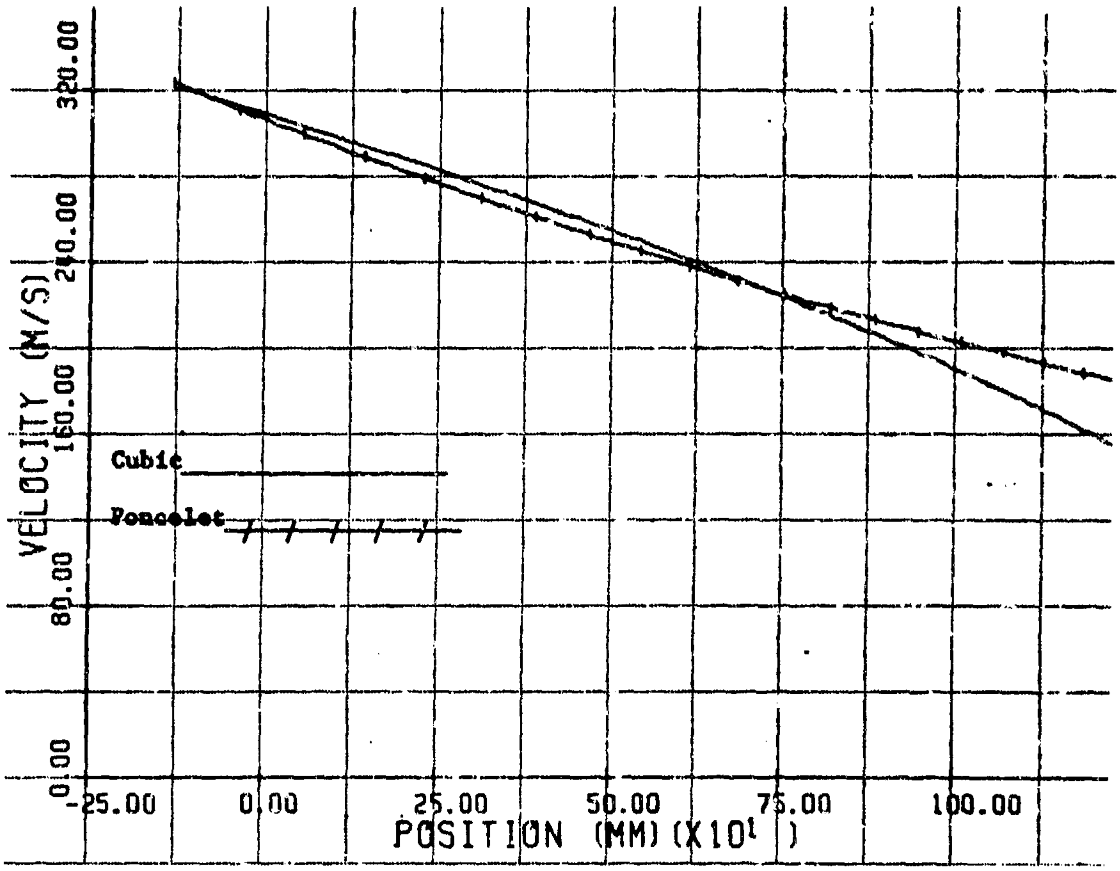

Figure 26. Velocity Versus Position for Shot No. 39 ($V_o = V_1$)

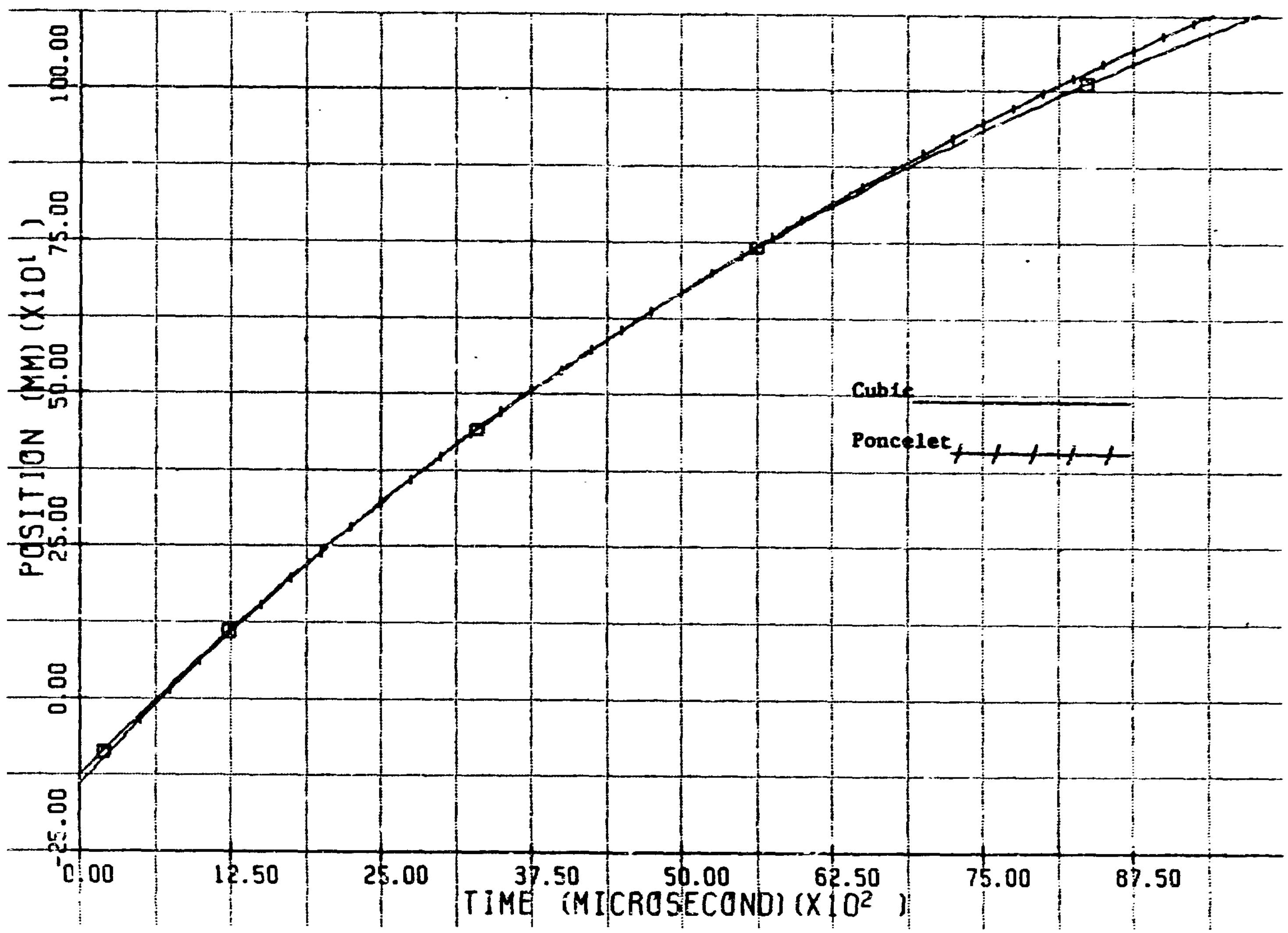

Figure 27. Position-Time Plot for Shot No. 45 (V_o=V_3)

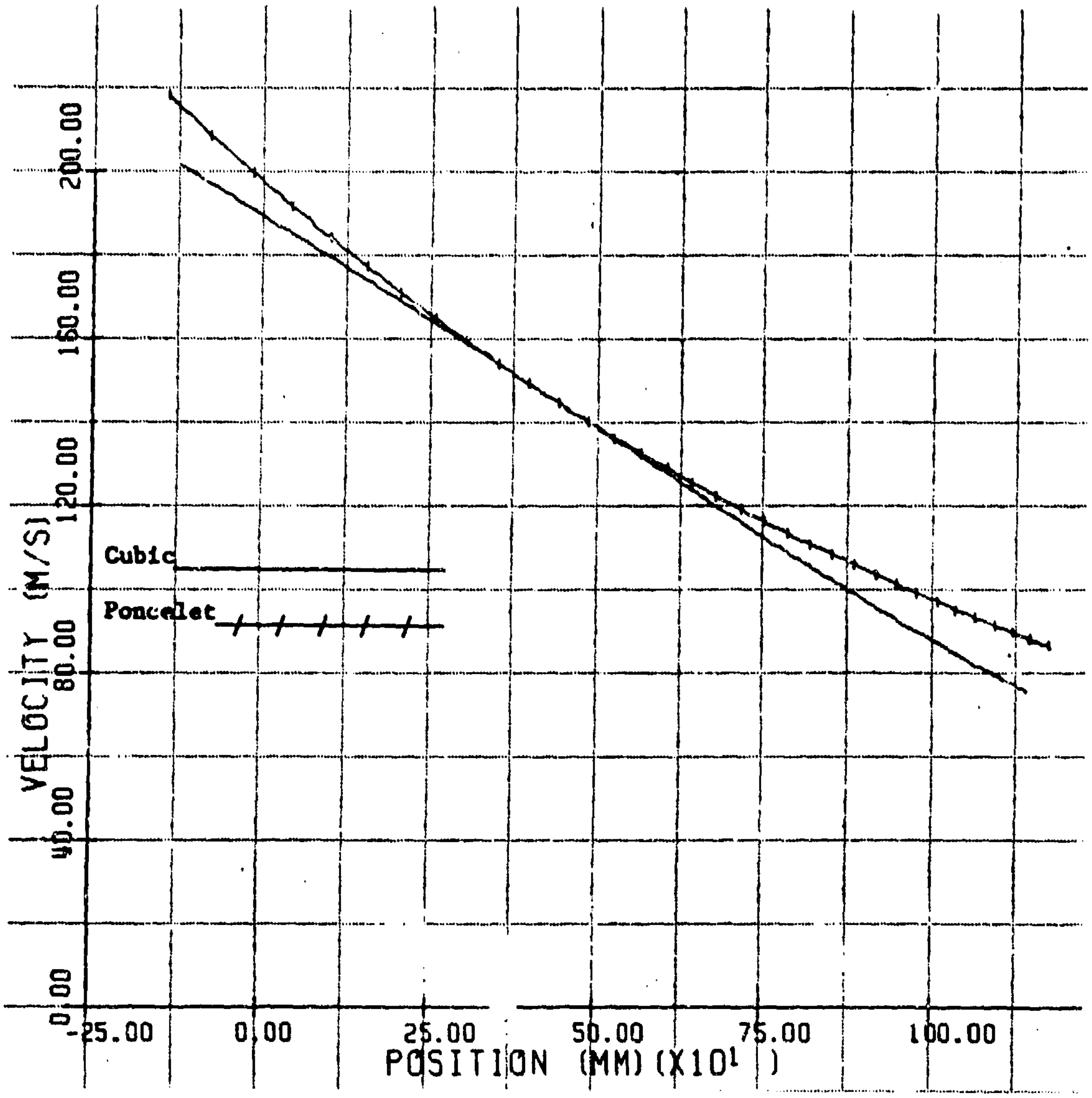

Figure 28. Velocity Versus Position for Shot No. 45 (V_o=V_3)

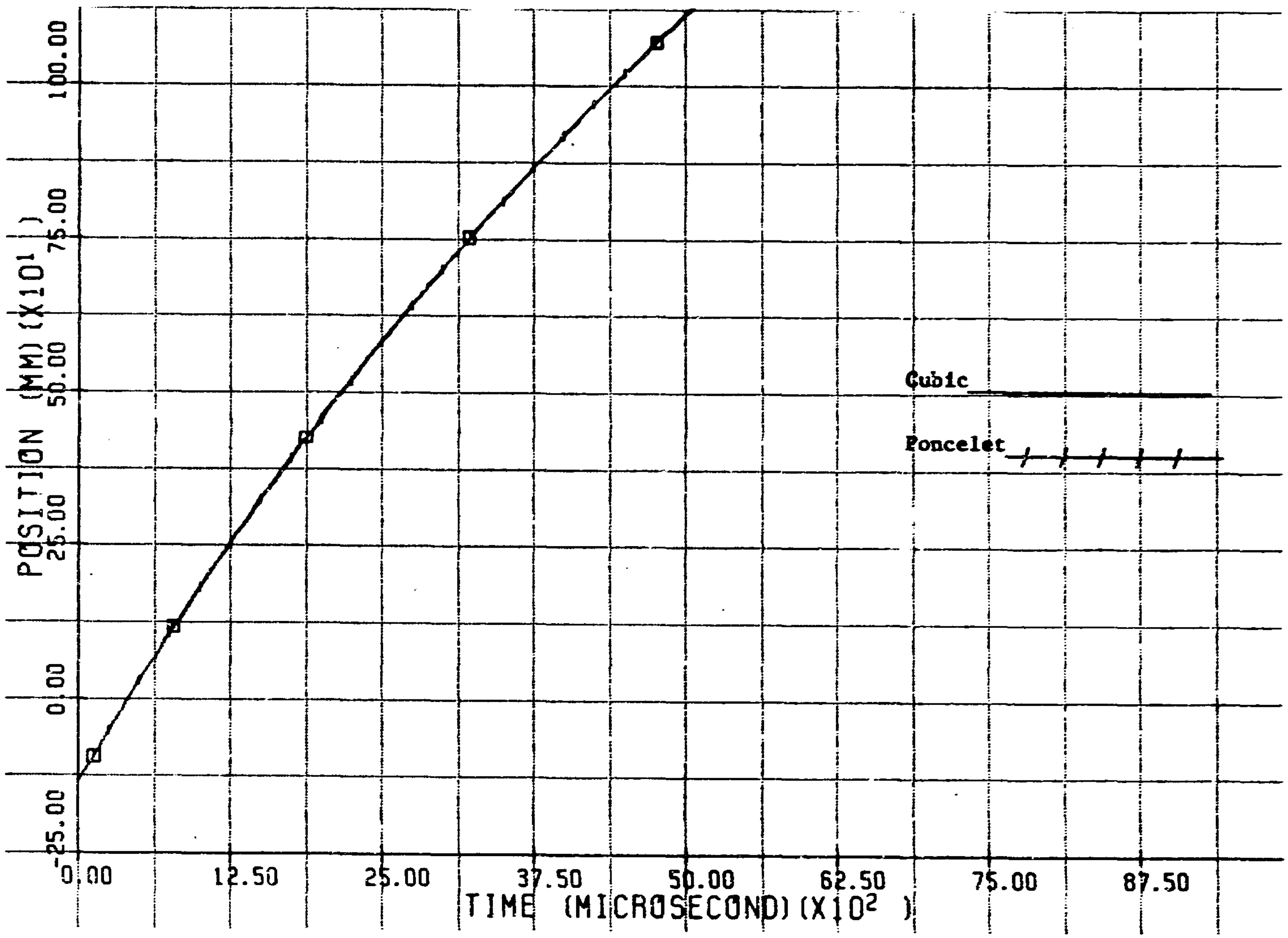

Figure 29. Position-Time Plot for Shot No. 49 ($V_o = V_1$)

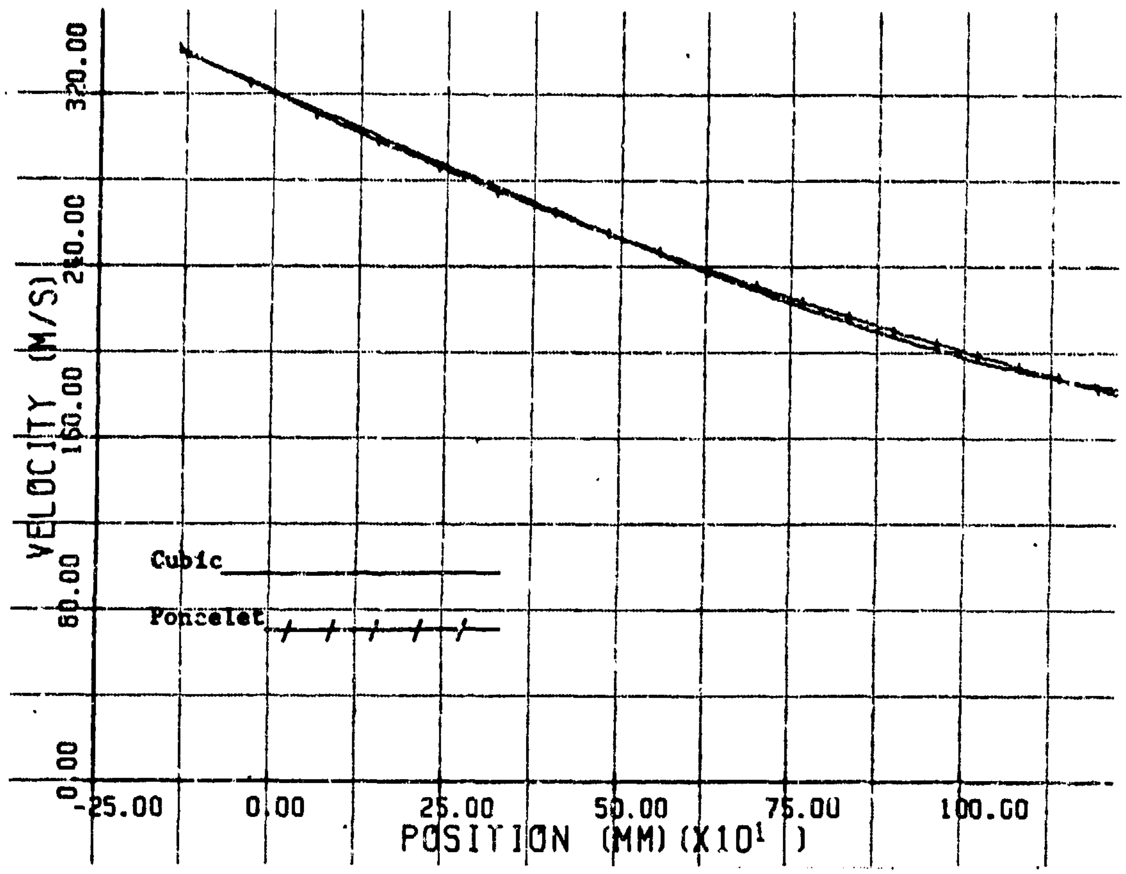

Figure 30. Velocity Versus Position for Shot No. 49 (V_o=V_1)

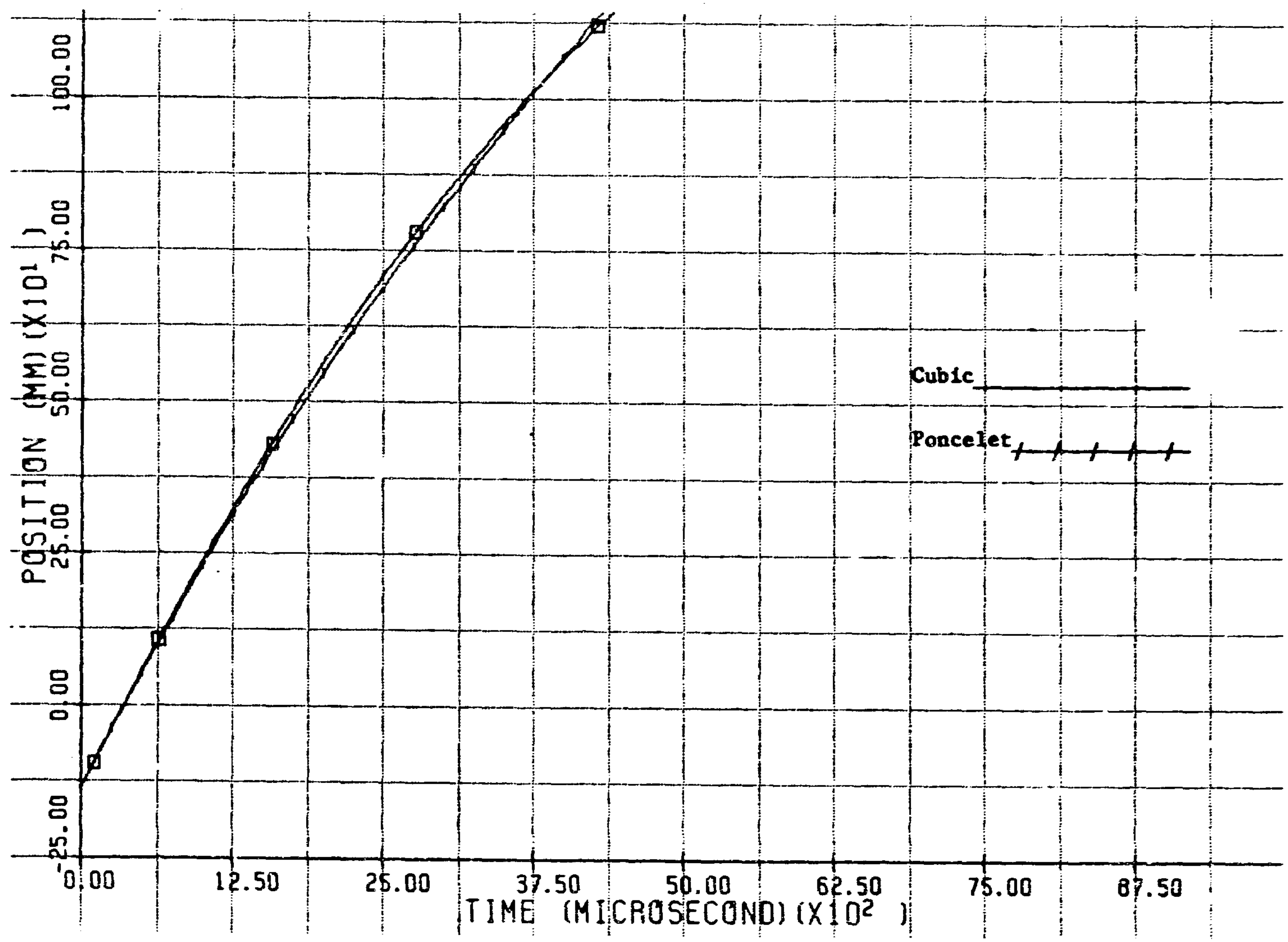

Figure 31. Position-Time Plot for Shot No. 50 (V_o=V_1)

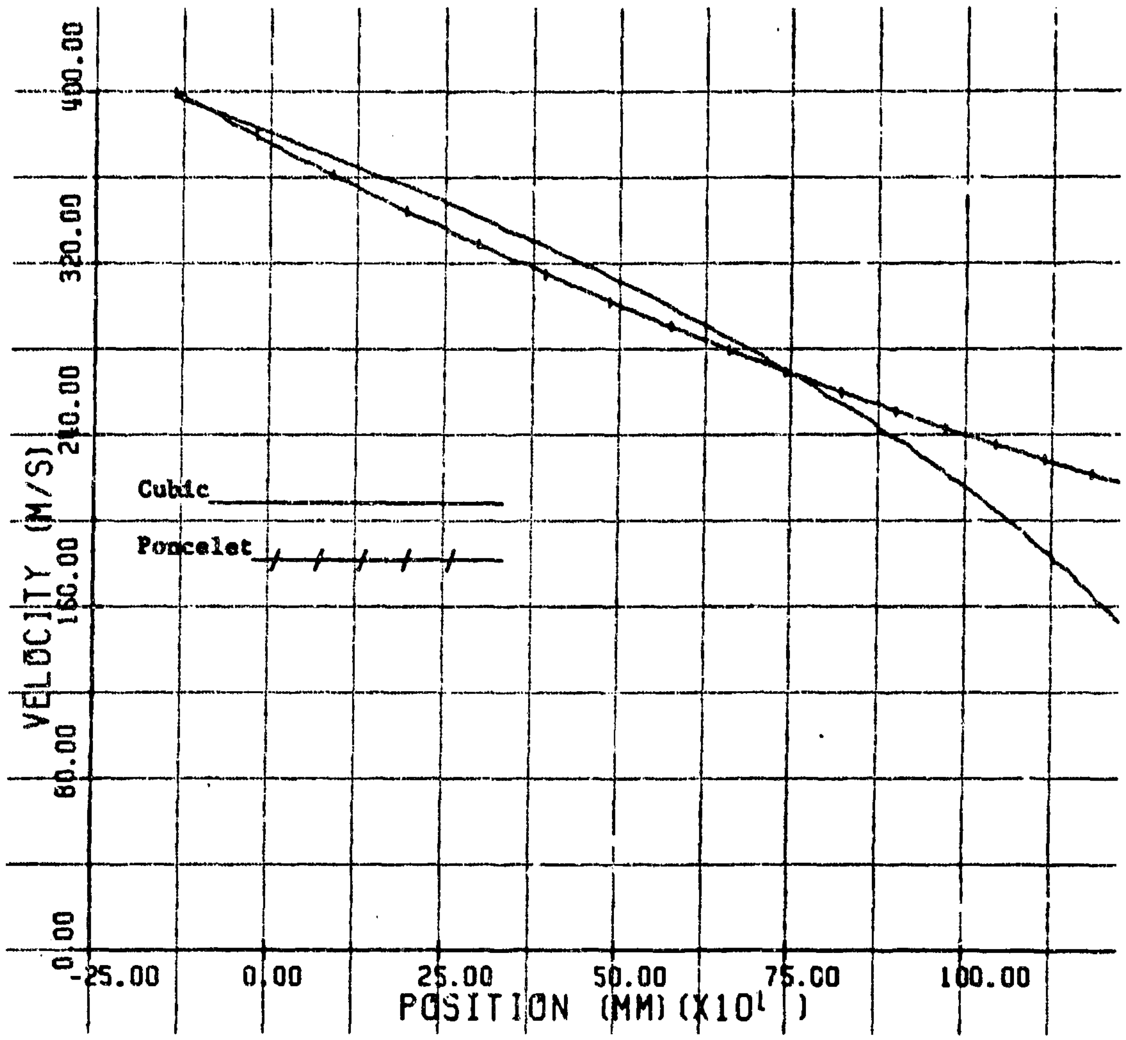

Figure 32. Velocity Versus Position for Shot No. 50 (V_o=V_1)

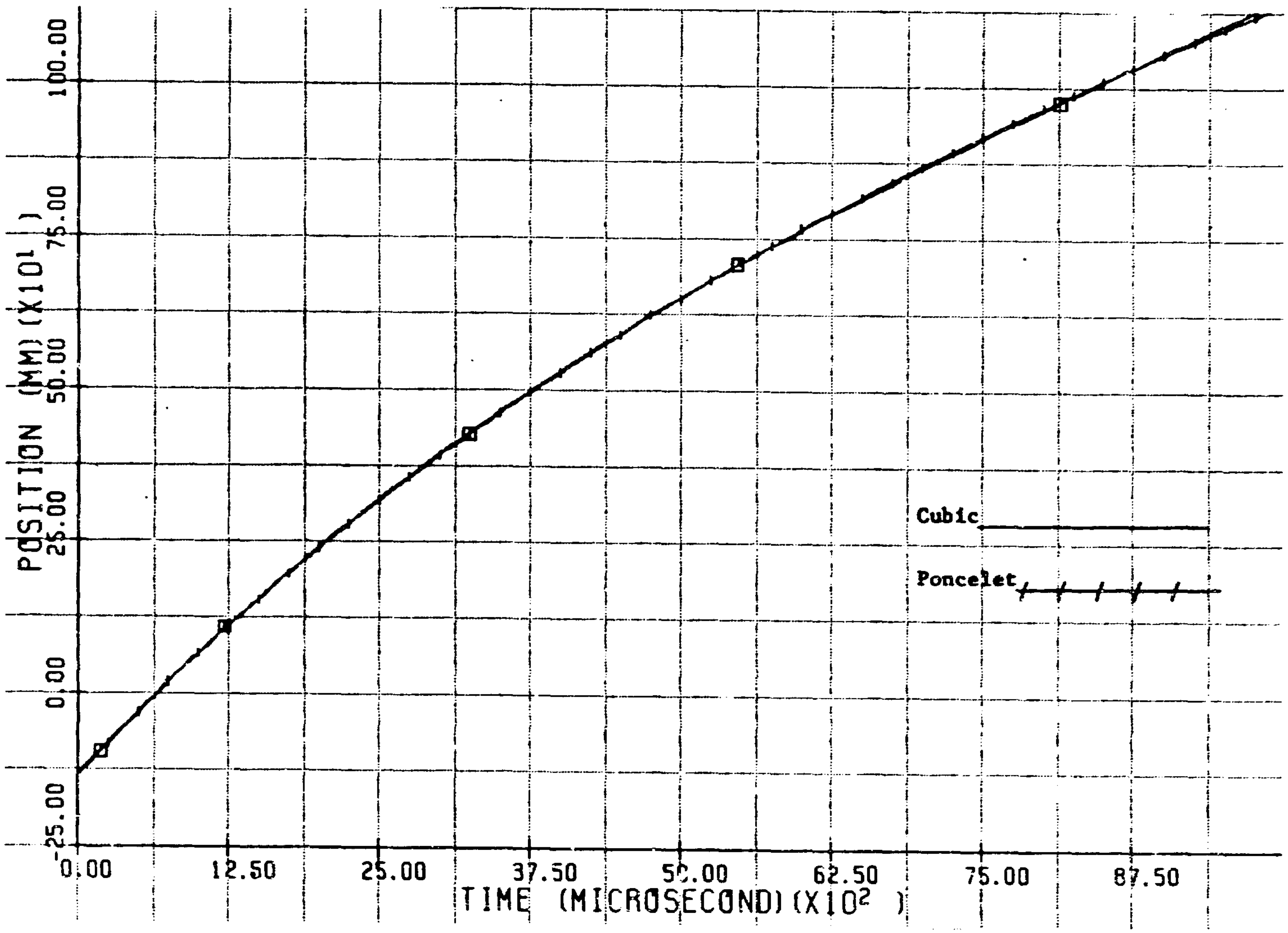

Figure 33. Position-Time Plot for Shot No. 52 (V_o=V_3)

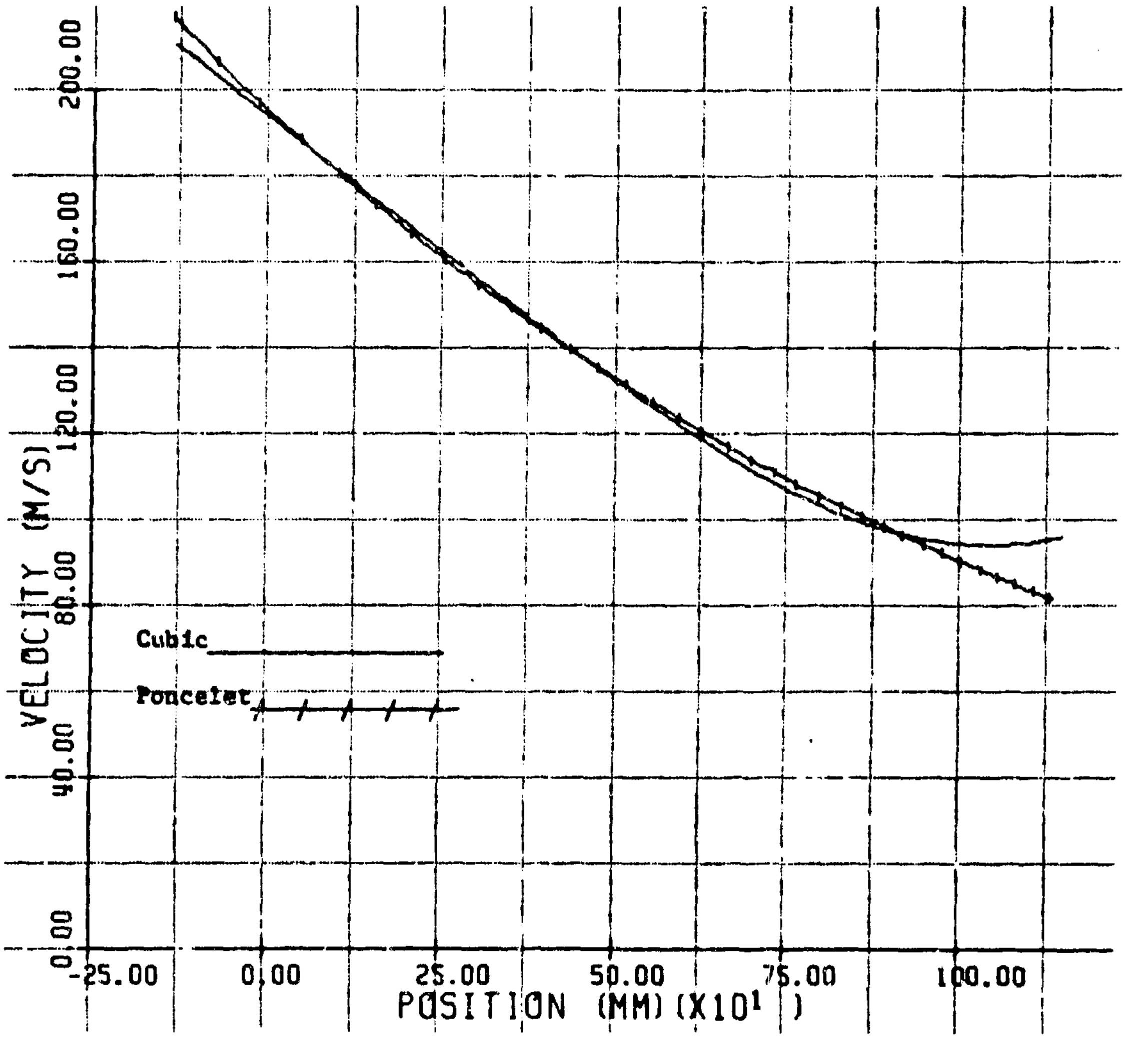

Figure 34. Velocity Versus Position for Shot No. 52 (V_o-V_3)

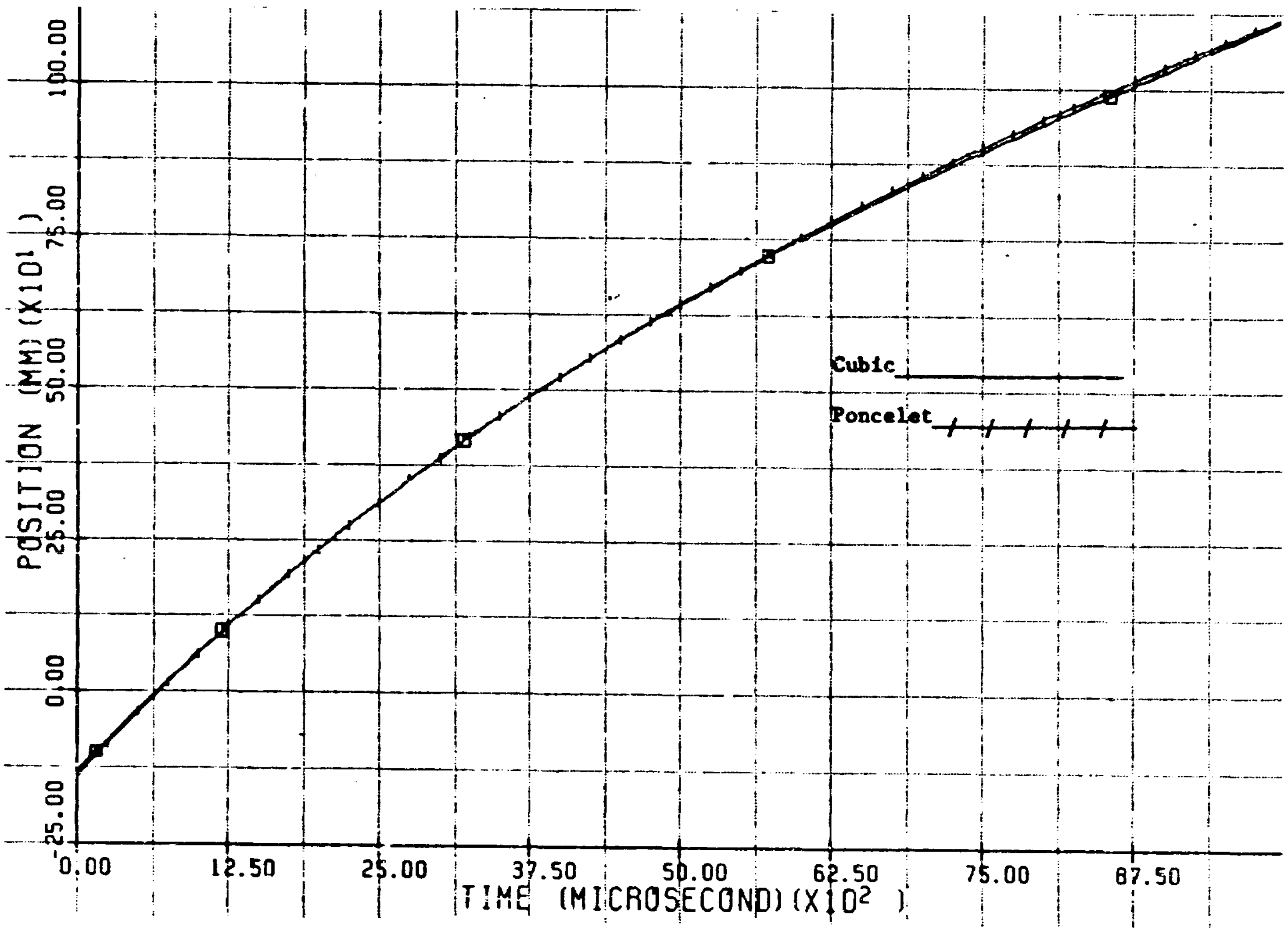

Figure 35. Position-Time Plot for Shot No. 54 (V_o=V_3)

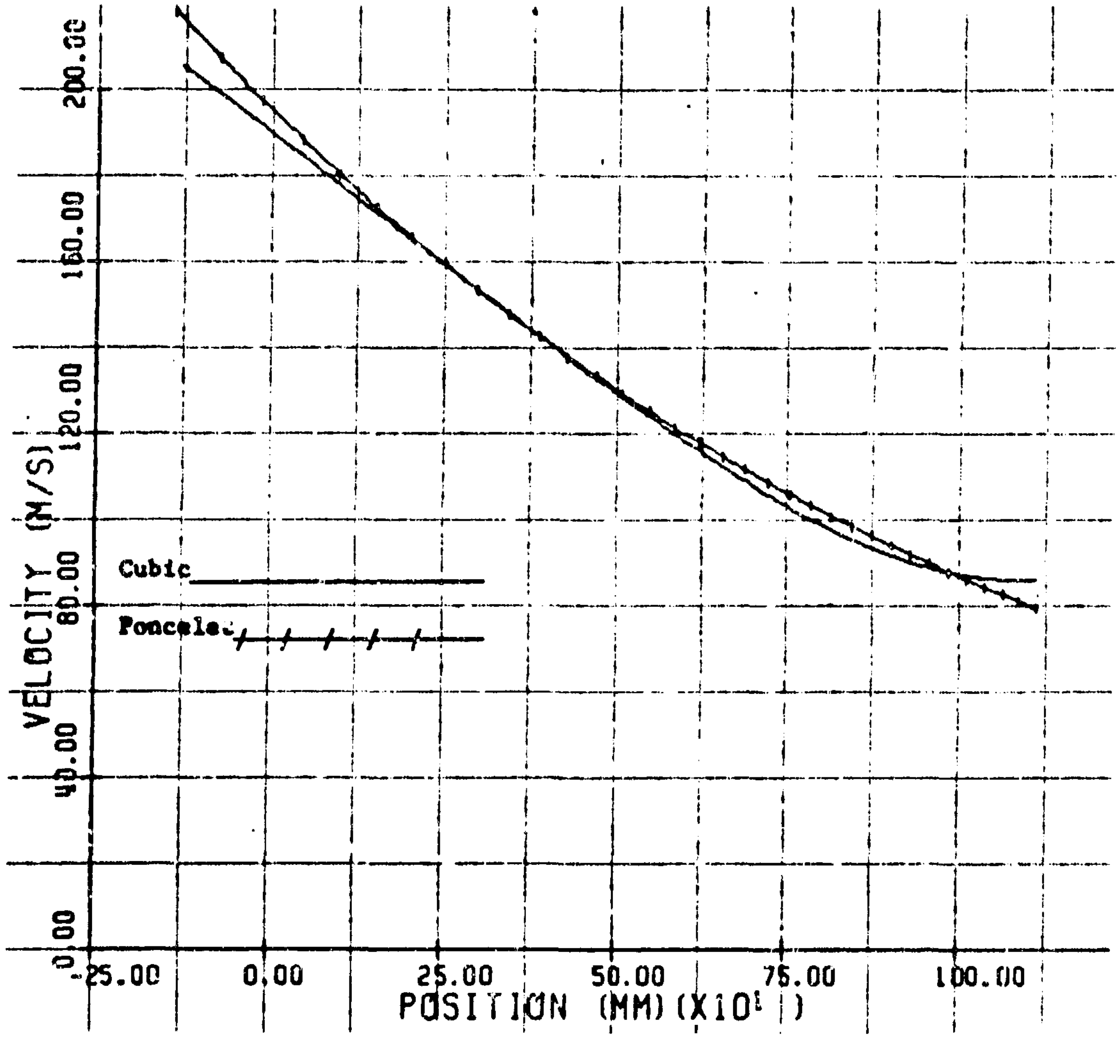

Figure 36. Velocity Versus Position for Shot No. 54 (V_o=V_3)

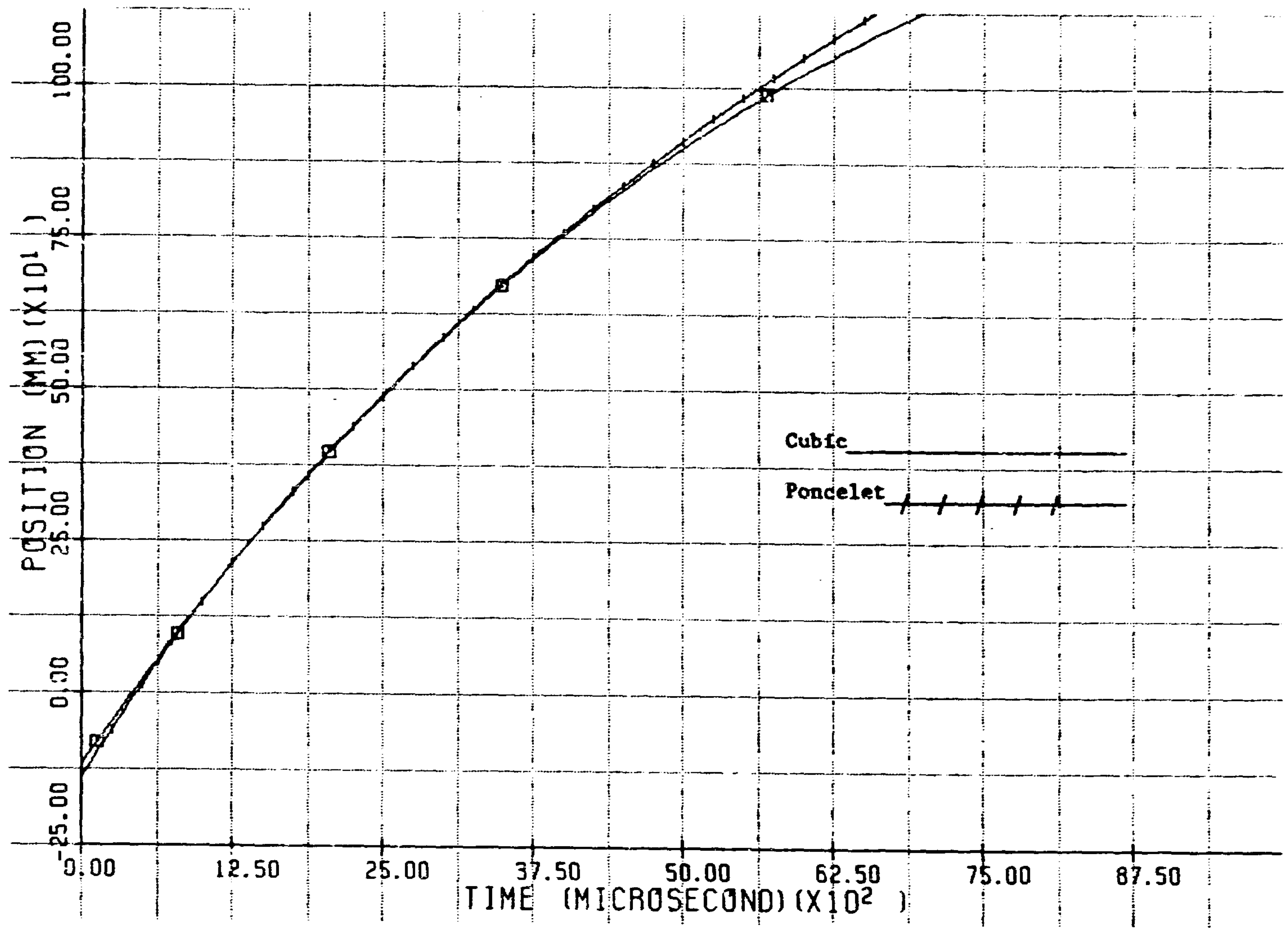

Figure 37. Position-Time Plot for Shot No. 59 ($V_o = V_3$)

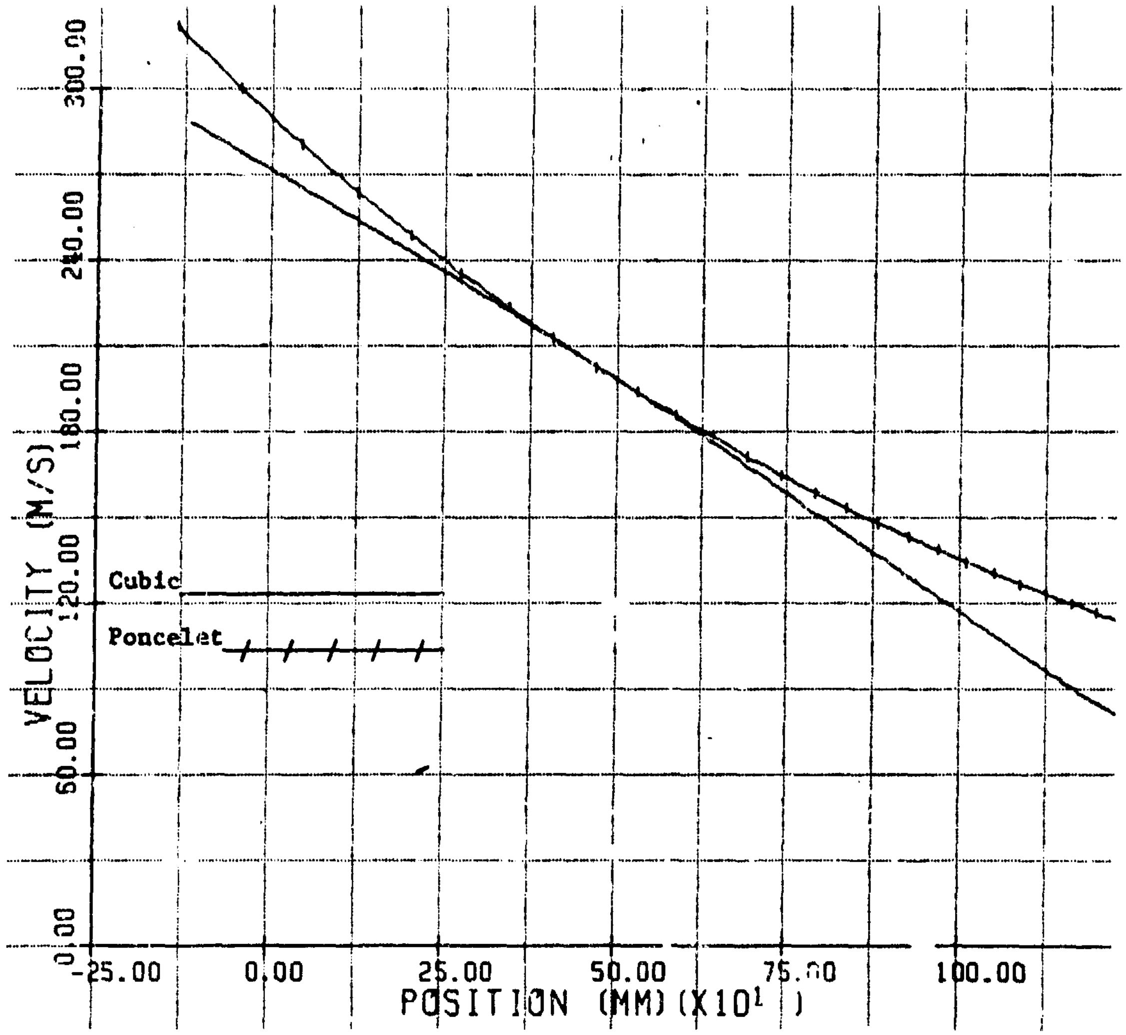

Figure 38. Velocity Versus Position for Shot No. 59 (V_o=V_3)

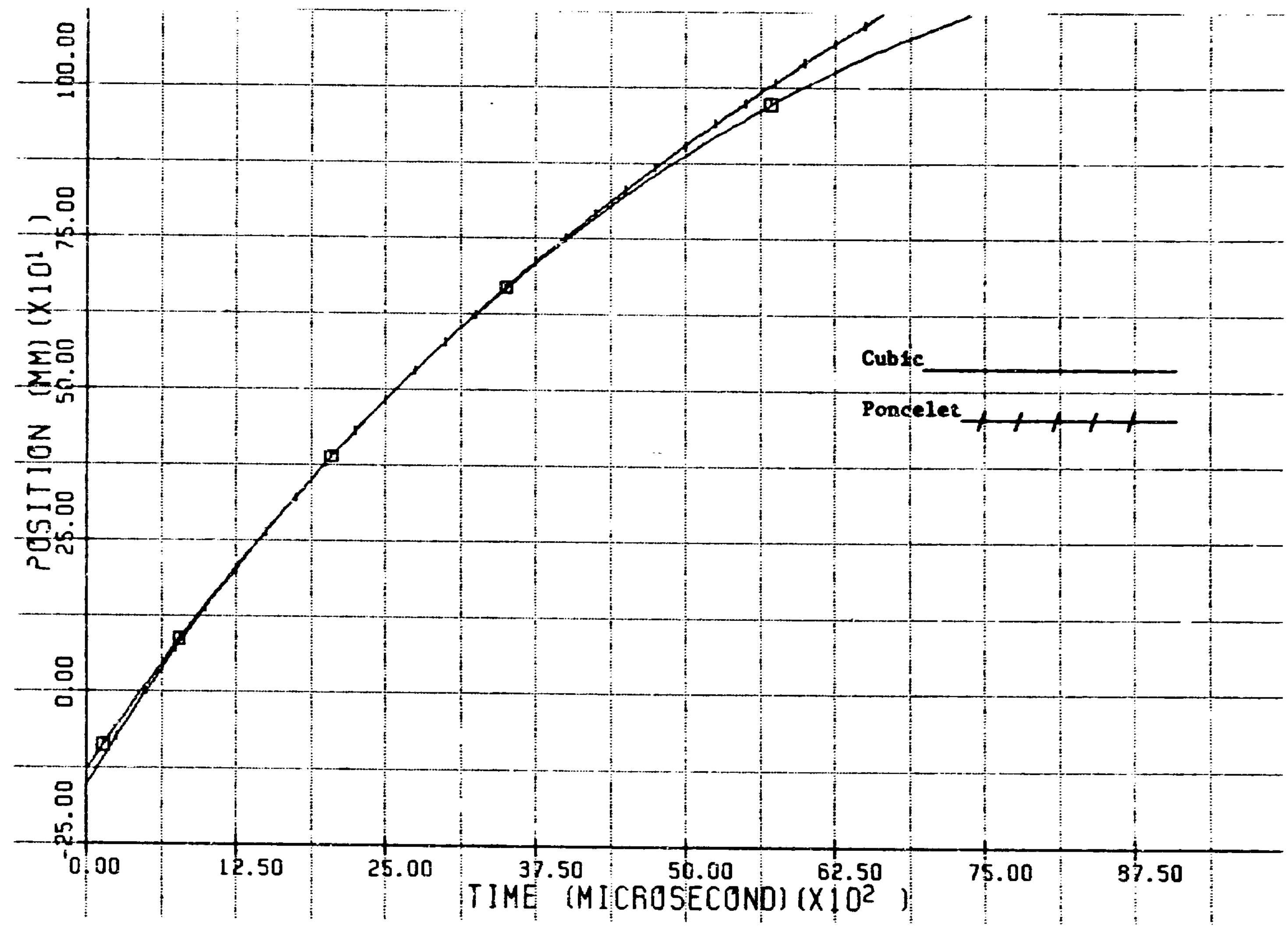

Figure 39. Position-Time Plot for Shot No. 61 (V_o=V_3)

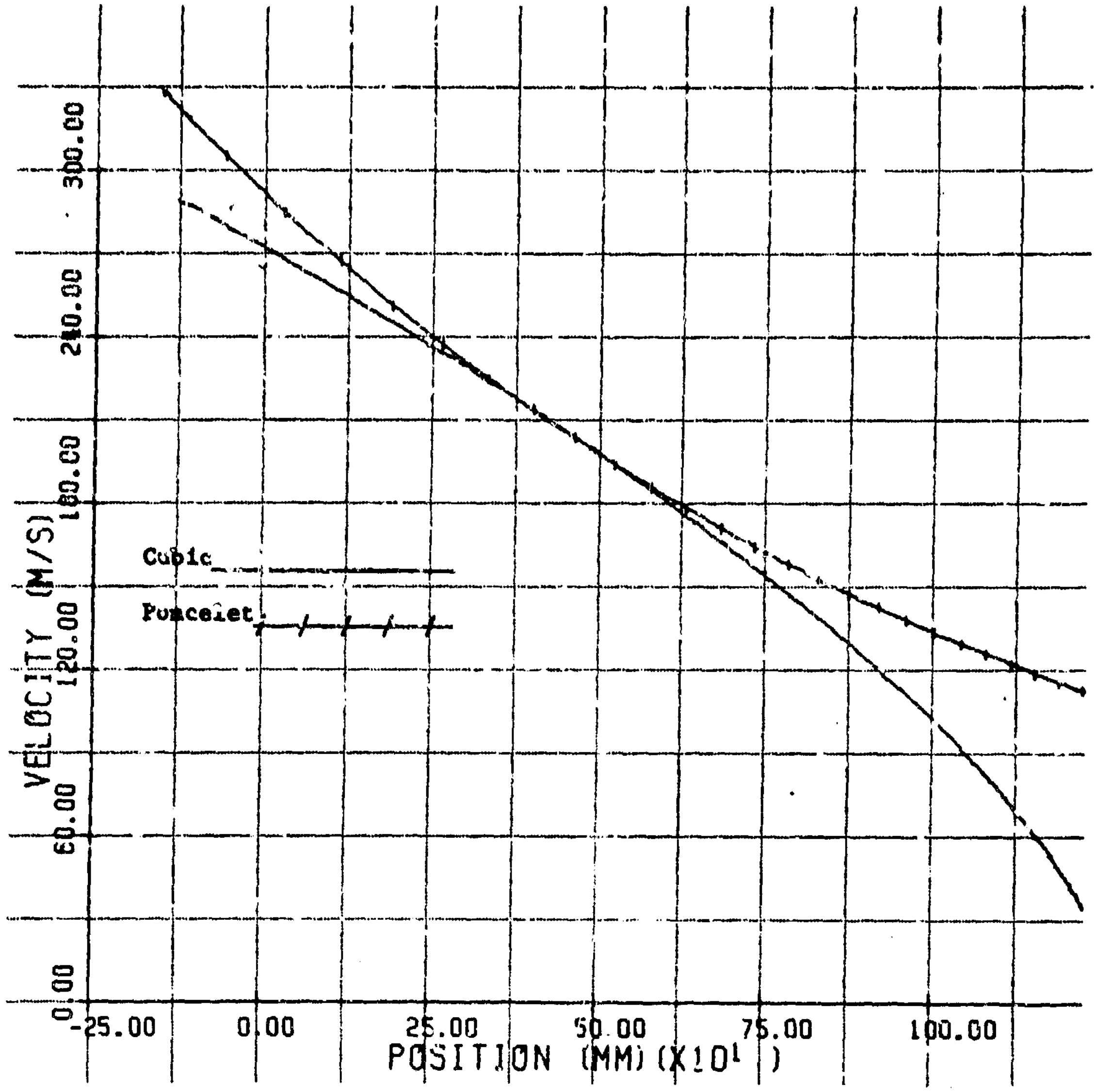

Figure 40. Velocity Versus Position for Shot No. 61 (V_0-V_3)

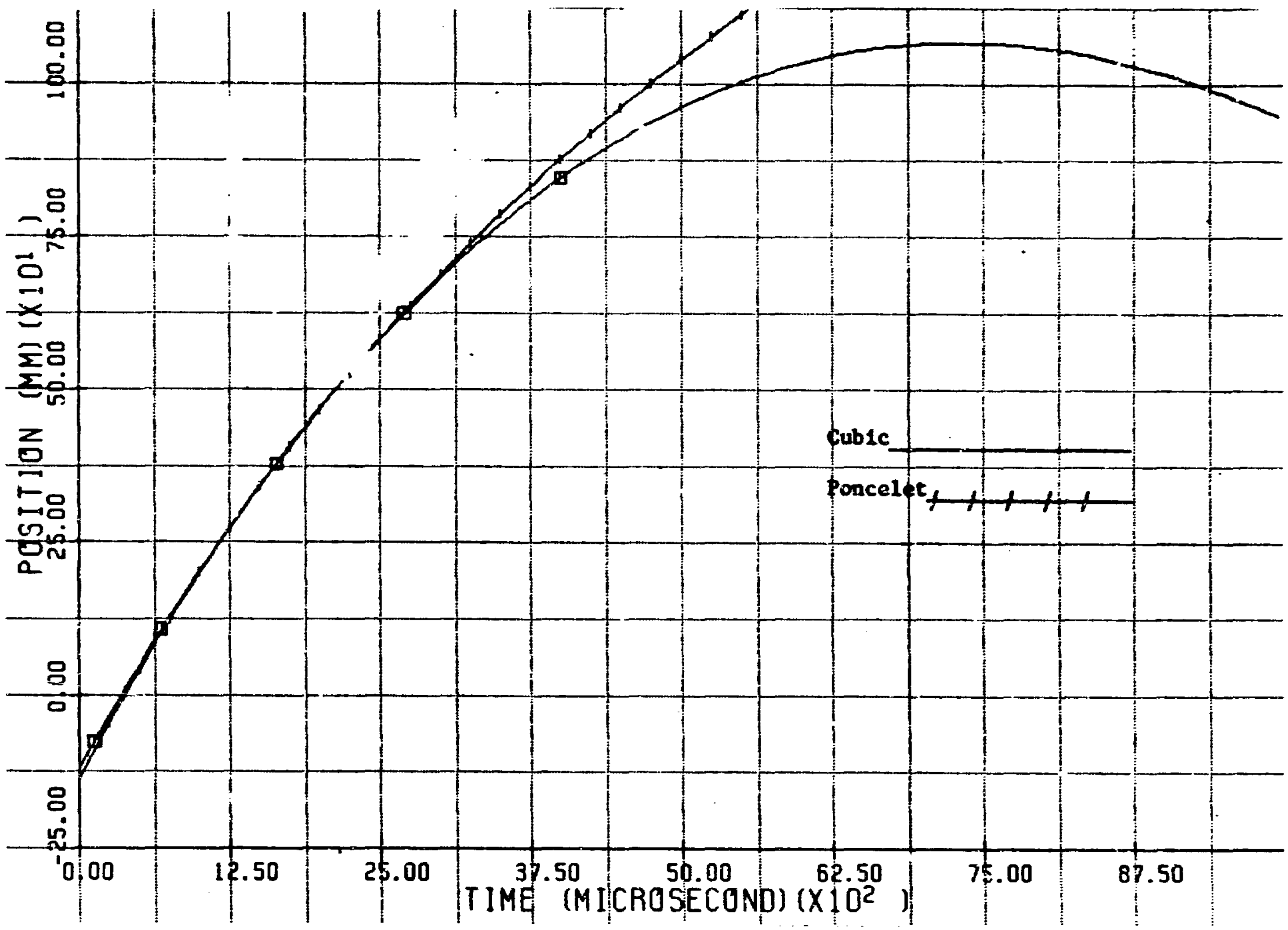

Figure 41. Position-Time Plot for Shot No. 62 (V_o=V_3)

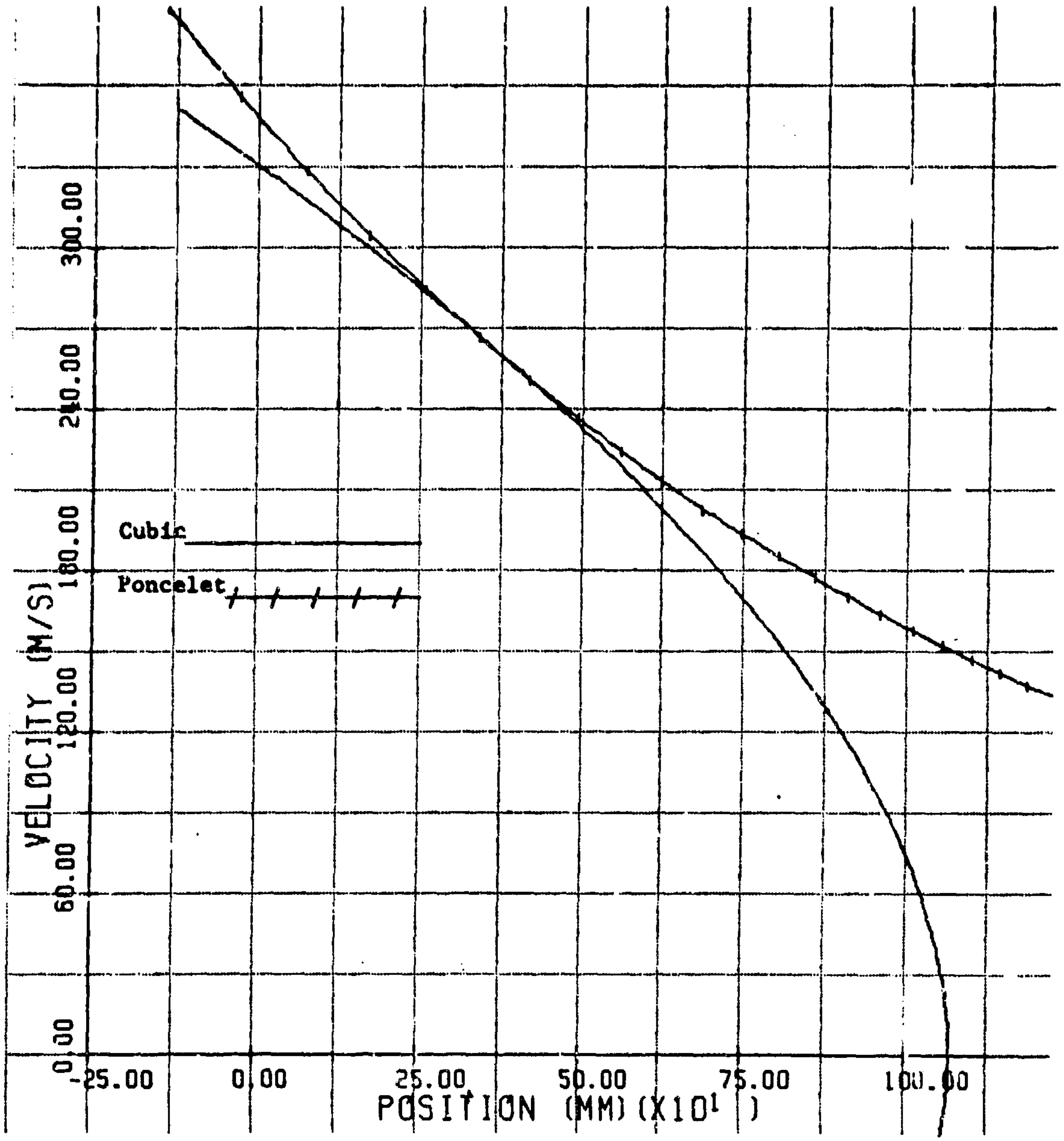

Figure 42. Velocity Versus Position for Shot No. 62 (V_o=V_3)

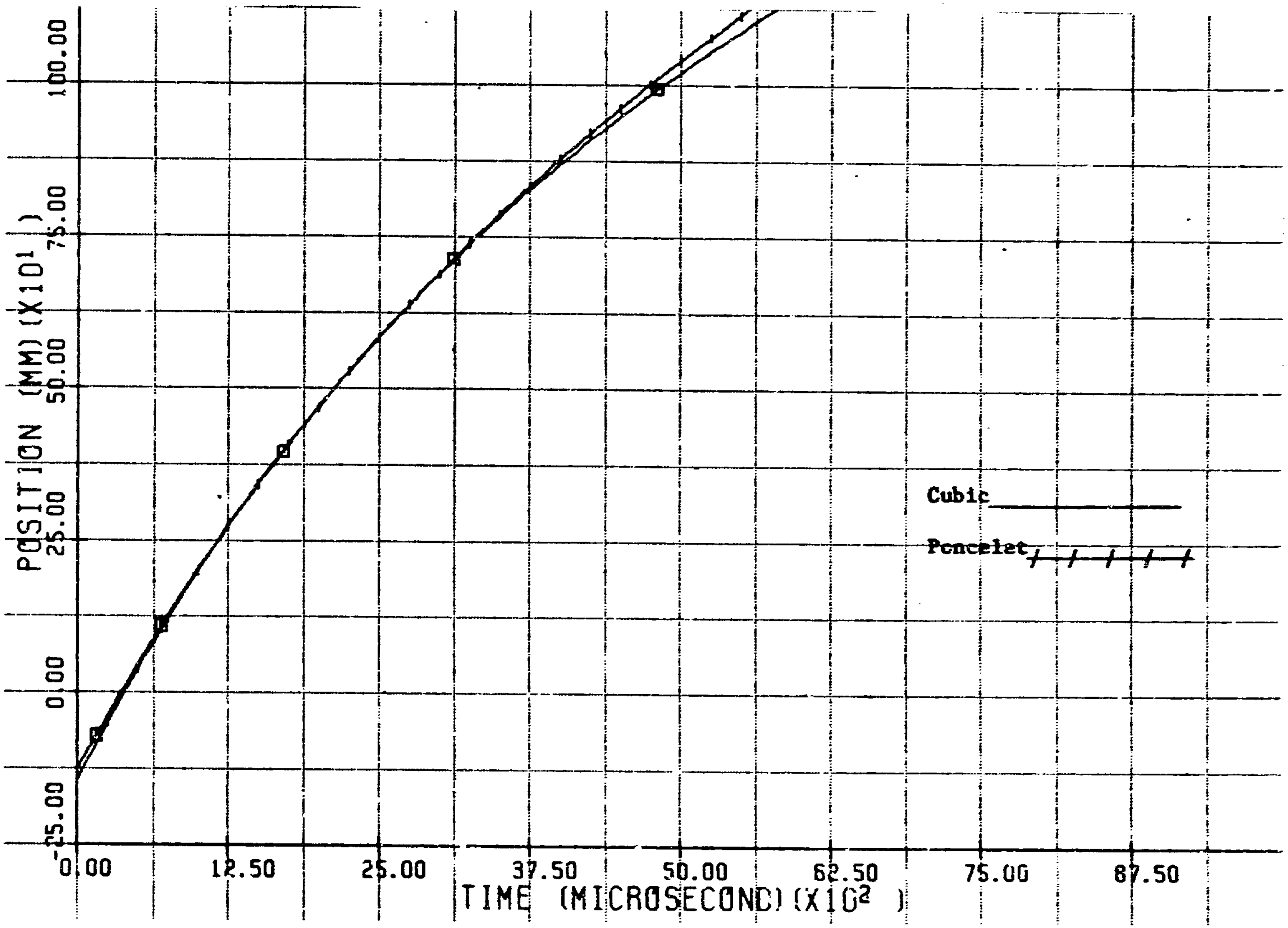

Figure 43. Position-Time Plot for Shot No. 65 (V_o-V_3)

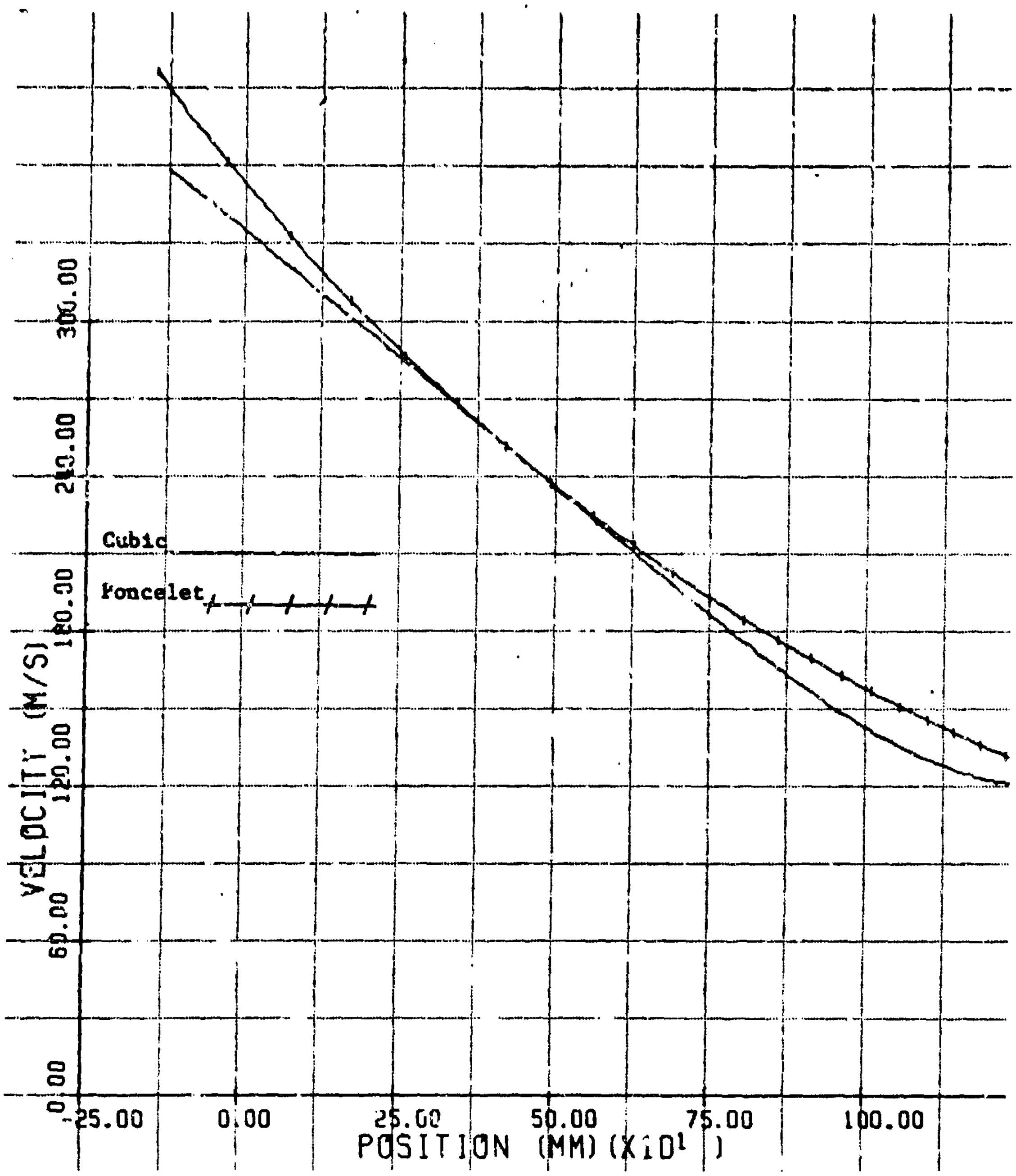

Figure 44. Velocity Versus Position for Shot No. 65 (V_o=V_3)

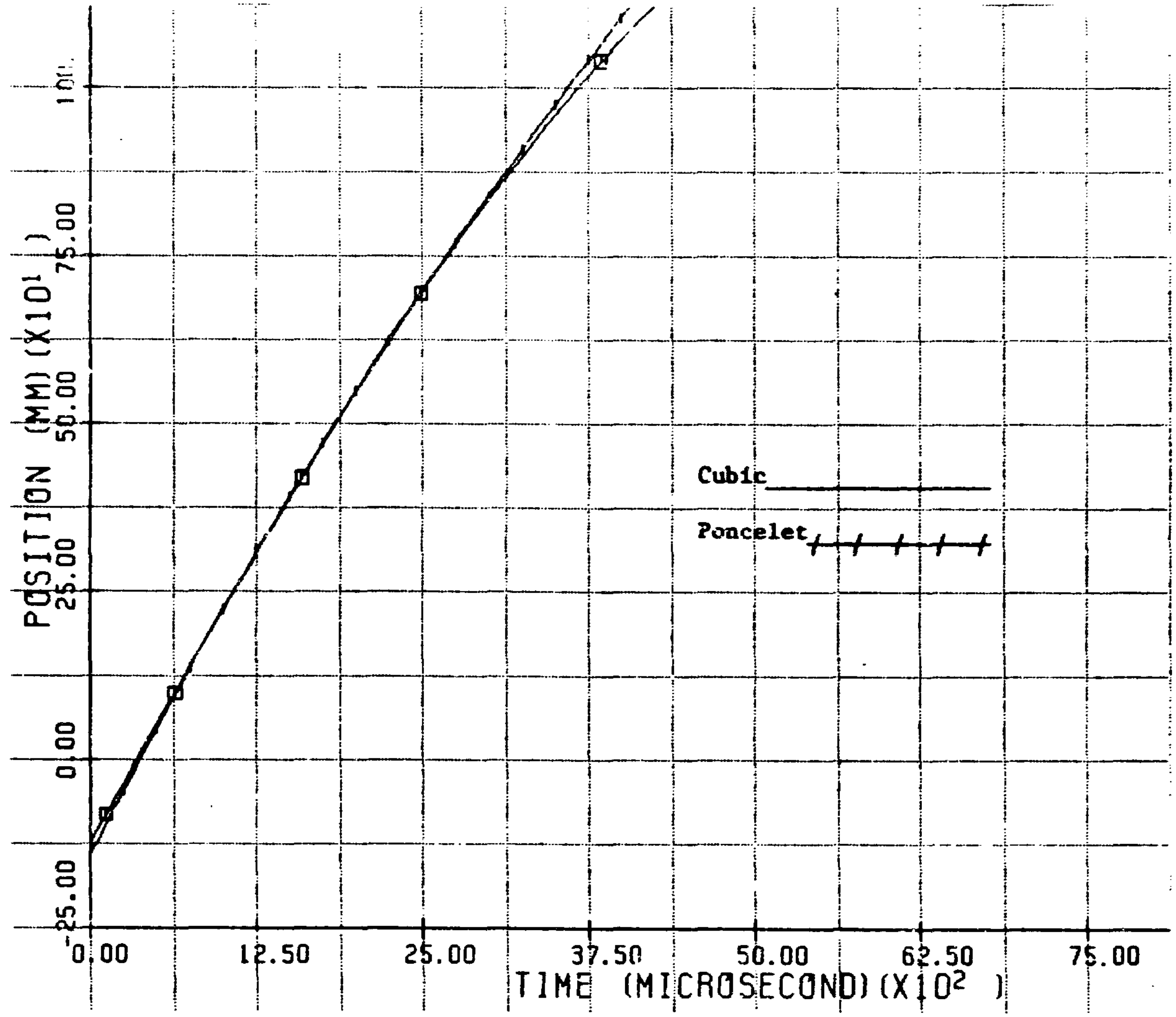

Figure 45. Position-Time Plot for Shot No. 68 ($V_o = V_3$)

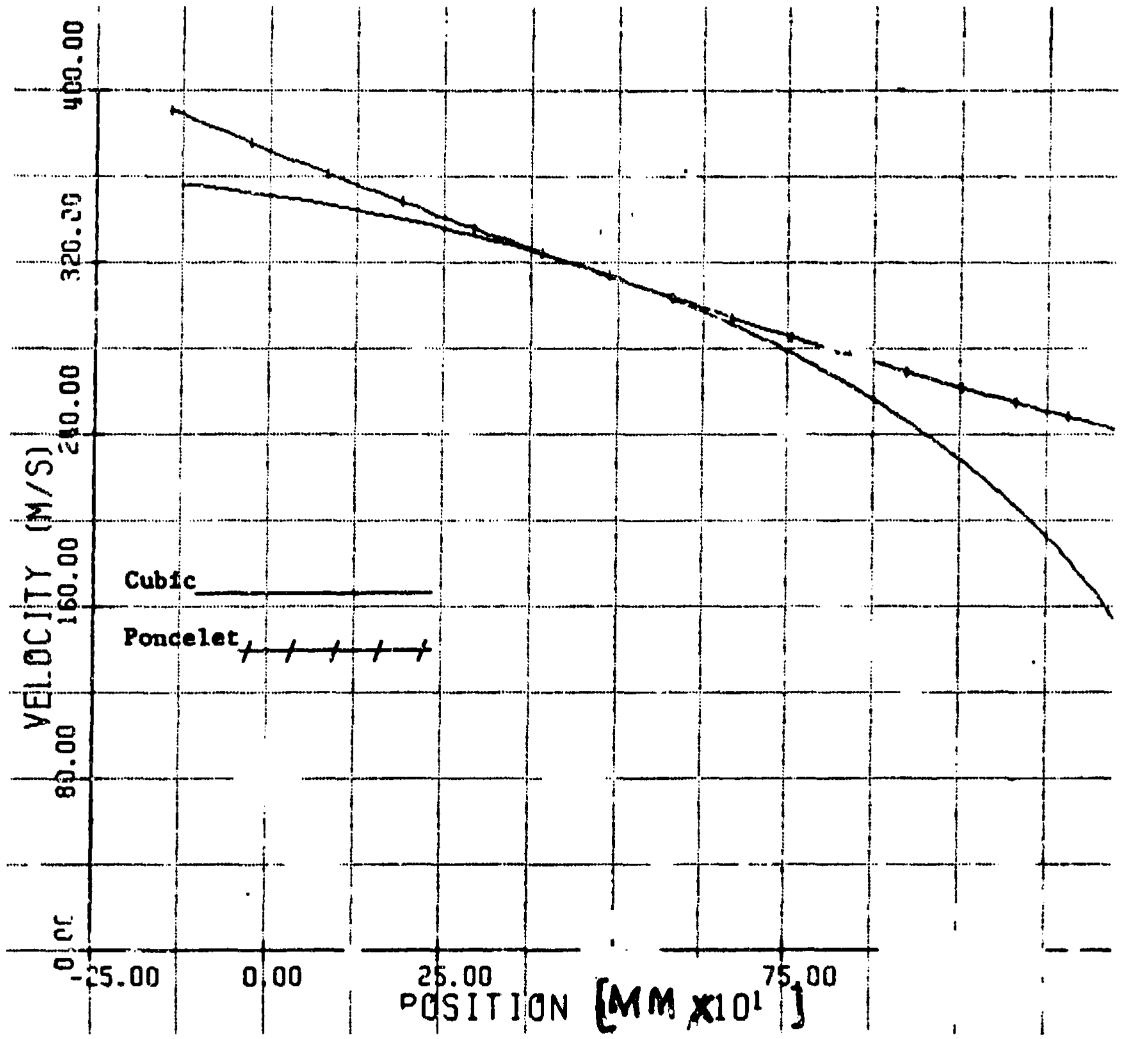

Figure 46. Velocity Versus Position for Shot No. 68 (V_0=V_3)

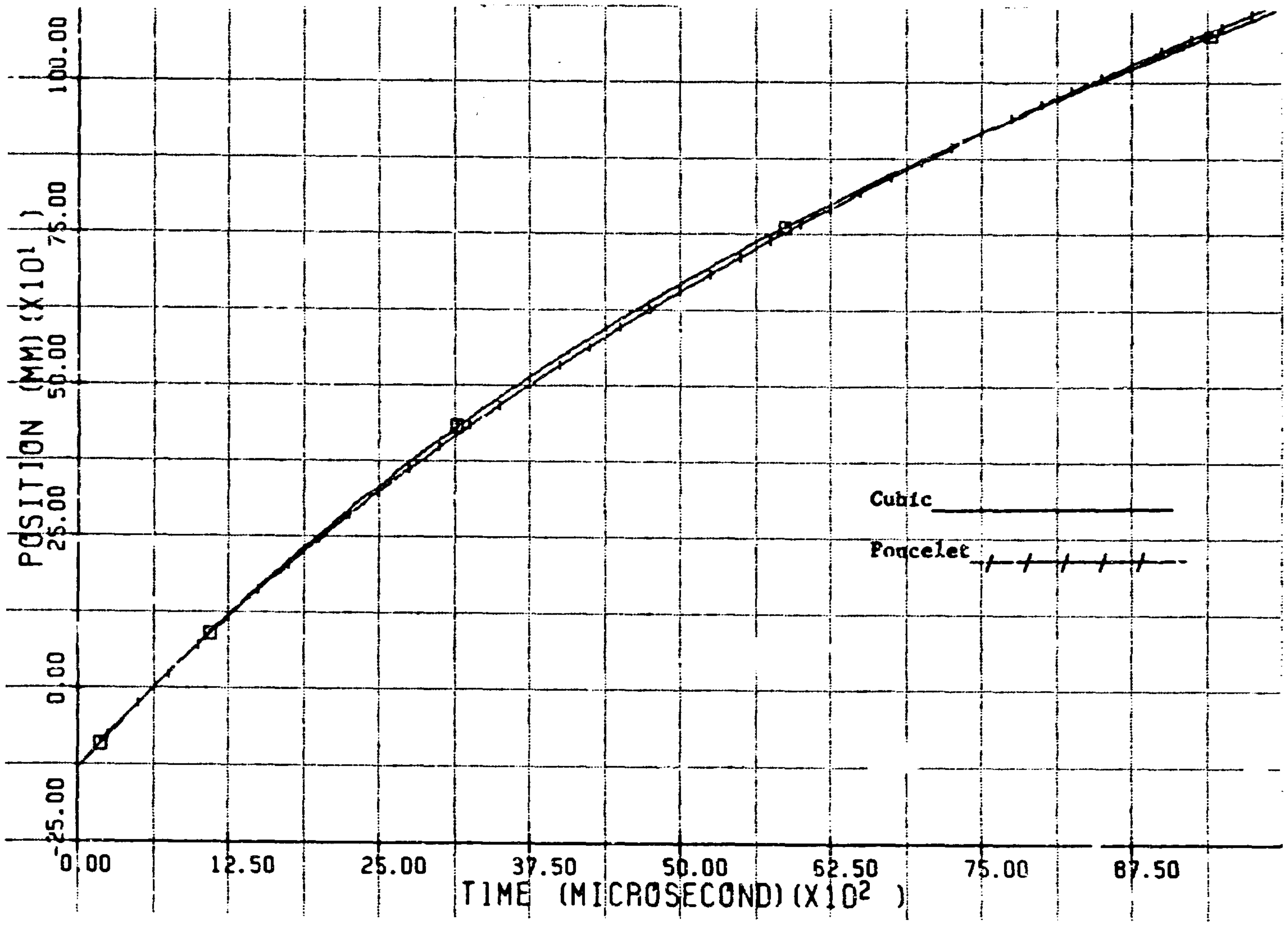

Figure 47. Position-Time Plot for Shot No. 72 ($V_o = V_1$)

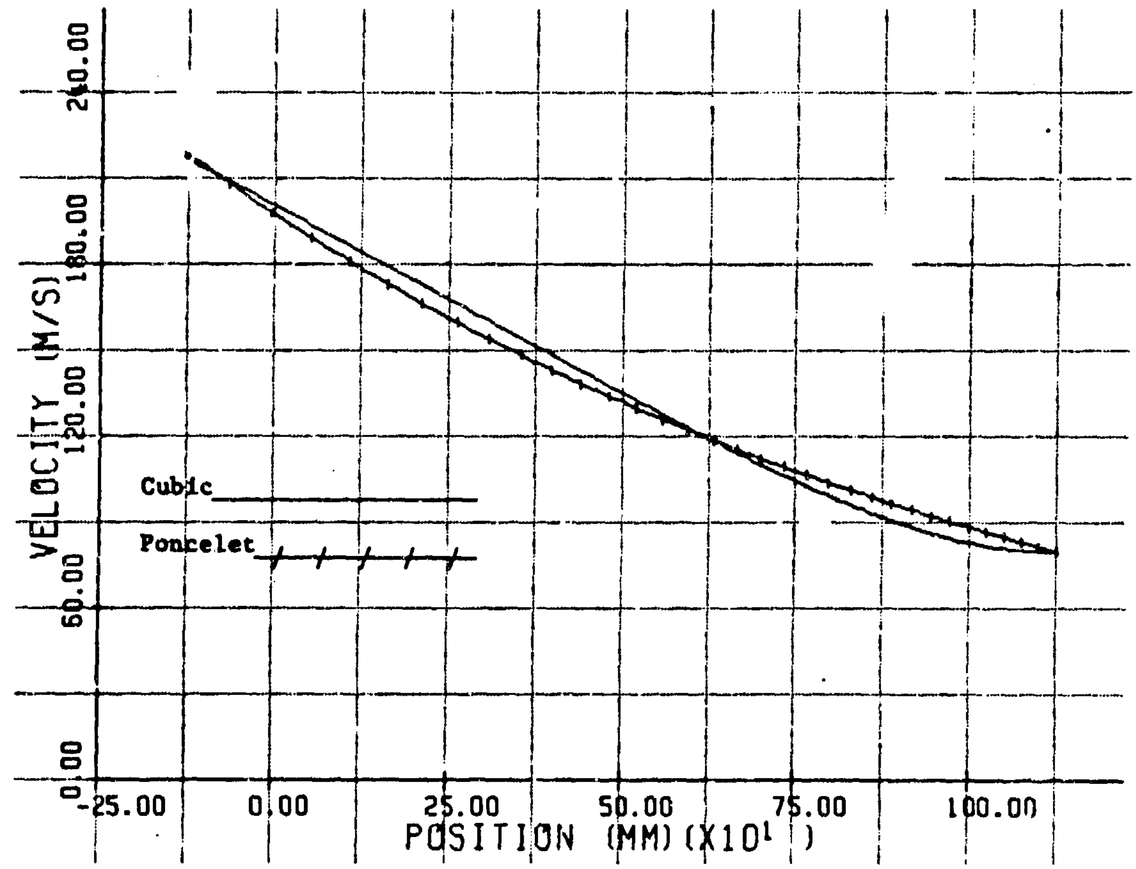

Figure 48. Velocity Versus Position for Shot No. 72 (V_o=V_1)

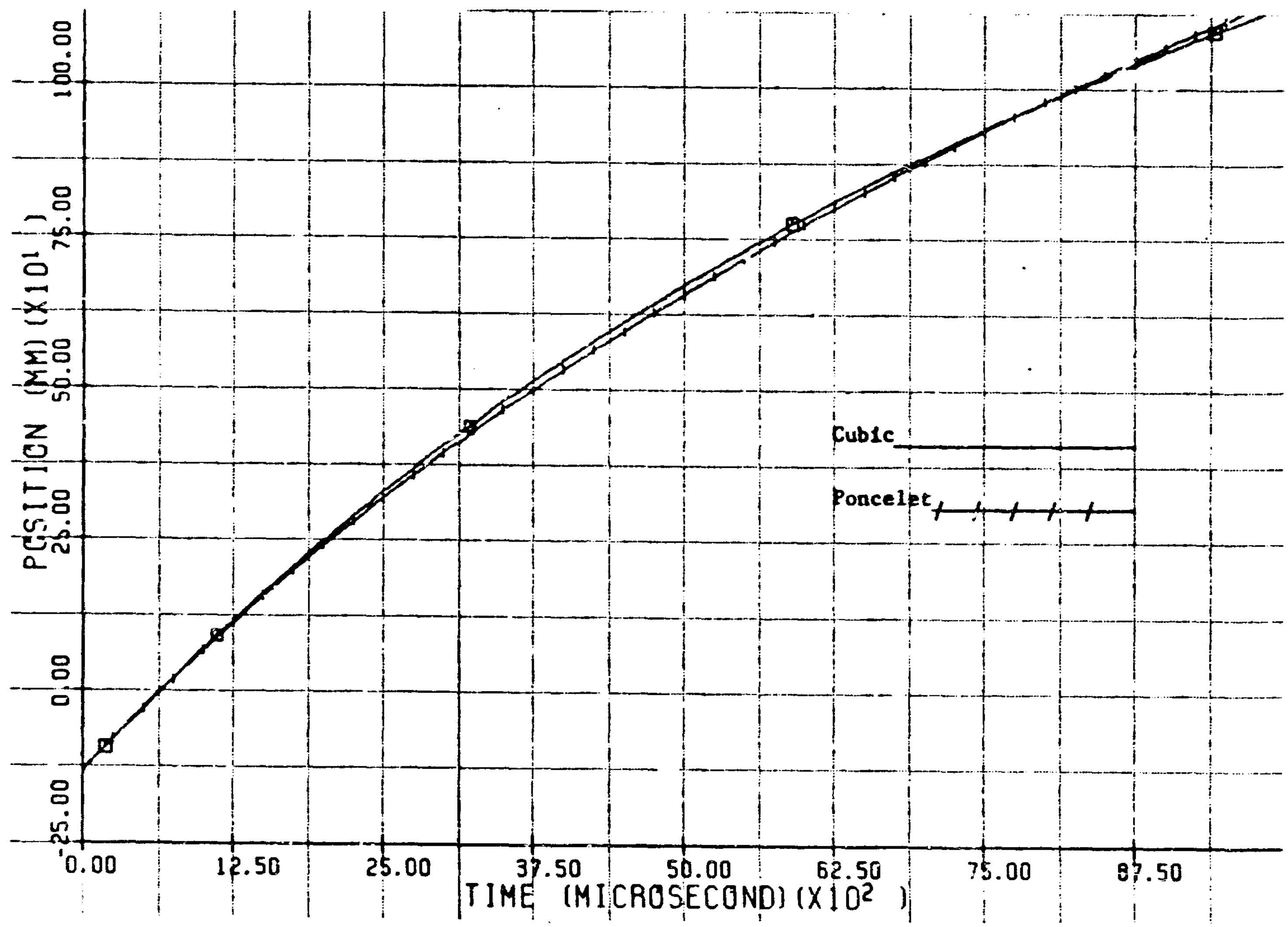

Figure 49. Position-Time Plot for Shot No. 73 ($V_o = V_1$)

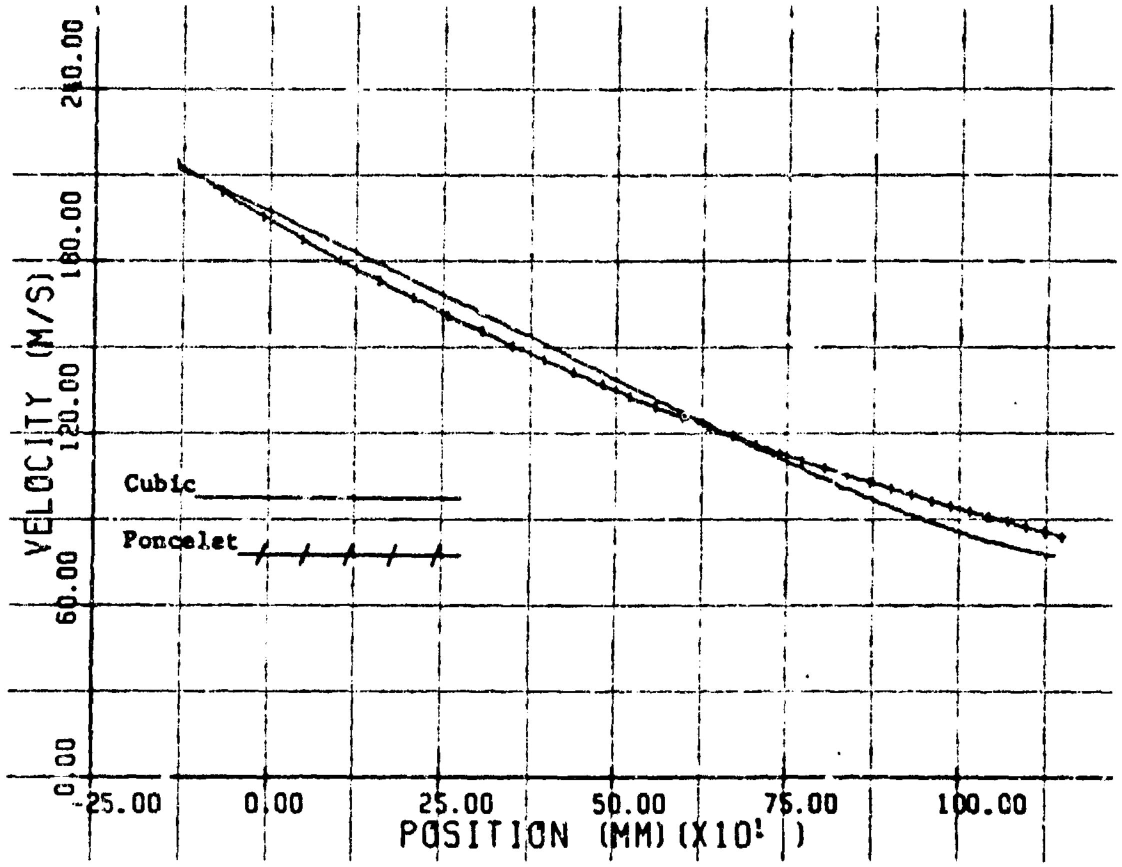

Figure 50. Velocity Versus Position for Shot No. 73 (V_o=V_1)

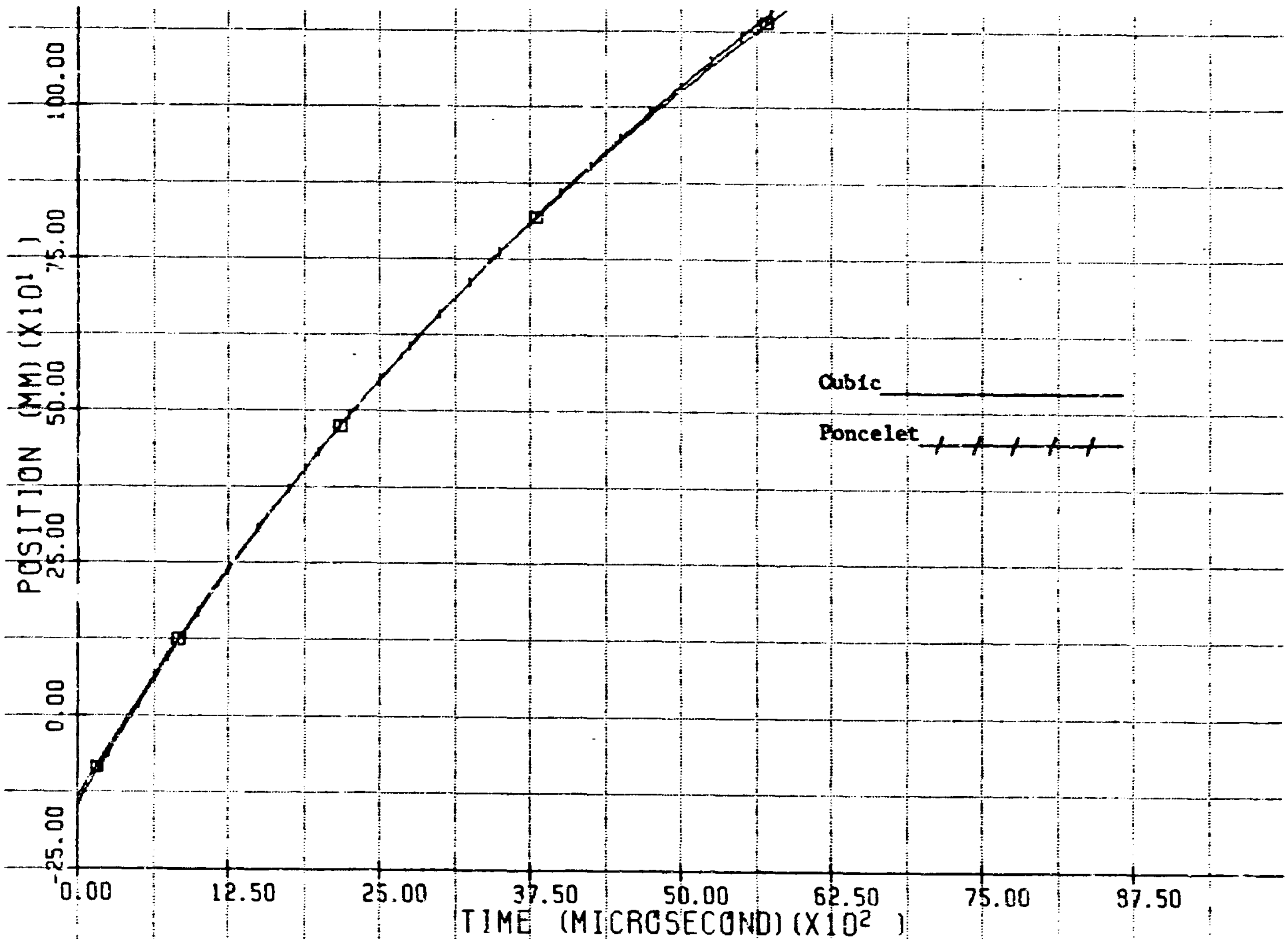

Figure 51. Position-Time Plot for Shot No. 74 ($V_o = V_3$)

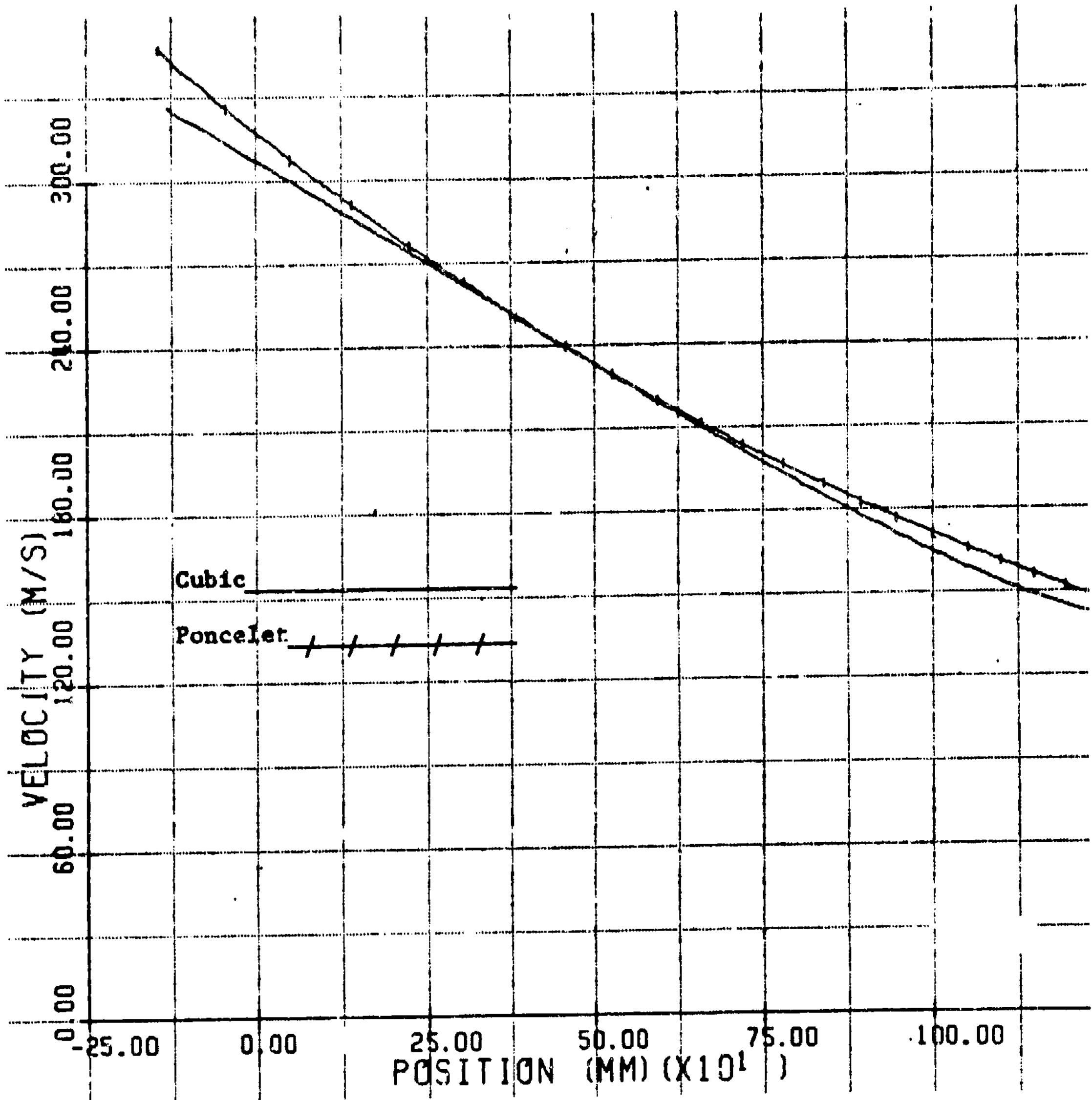

Figure 52. Velocity Versus Position for Shot No. 74 ($V_o = V_3$)

interpolation results of paragraph 4.3.1. A different procedure will be used in paragraphs 4.5 and 4.6. Measured approach velocities were available but there was some uncertainty about the exact time the nose of the projectile first impacted the target. Positions at the times of the X-ray firings were more precisely known. The majority of the analyses (33 shots) were therefore made with Station 3 as initial-value point, with $V_o = V_3$ as given by the cubic interpolation, since that point is near the middle of the interval where differentiation of the cubic interpolation formula should be most accurate. Calculated velocities at Stations 1 and 2 were then obtained for negative values of $t-t_o$ and $x-x_o$. For 19 shots that procedure led to unreasonably large calculated values for V at x = -0.115 meter where V should be equal to the approach velocity. For these cases the analysis was therefore made with Station 1 selected as initial point.

In the tabulations of Appendix A the value of V_o is tabulated as VO on the line below the tabulated Poncelet drag coefficient. For example, for Shot 26 the value VO = 267 is listed. Comparision with C.G.Vel.X-Comp. values four lines above this entry shows that in this case $V_o = V_3$. For the 21 cases plotted in paragraph 4.3.1, the captions include either the statement $V_o = V_1$ or $V_o = V_3$, and it is also easy to tell from the V, x-plots where they were made to agree.

All the fitted Poncelet curves (those marked by vertical strokes) now give a reasonable agreement at x = -11.5 cm with the measured approach velocity.

The standard deviation of the x-positions calculated by Equation (6) from the experimental values is tabulated for each case in Appendix A immediately following the tabulated V_o.

The Poncelet drag coefficient tabulated on the same line is related to the coefficient B of Equation (1) as follows. In aerodynamics a dimensionless drag coefficient C_D is defined such that the drag force on an object of projected area A_1 on a plane perpendicular to the velocity is given by

$$\text{Inertial Drag Force} = \rho A_1 C_D V^2/2 \qquad (7)$$

where ρ is the density of the medium being traversed. Comparison with Equation (3), neglecting A, shows

$$B = \rho A_1 C_D/2m \quad \text{or} \quad C_D = 2mB/\rho A_1 \qquad (8)$$

The projectile mass in kilograms and the target sand density in kg/m^3 are tabulated for each shot in Appendix A.

Table 7 lists the Poncelet drag coefficients C_D for each of the 41 shots of the primary test program whose velocities were analyzed. In dry sand there is little variation with impact velocity of the value of C_D required to fit the X-ray position time data in the region observed. These dry sand results are well characterized by the Poncelet force law with a

TABLE 7 . PONCELET/DRAG COEFFICIENTS CALCULATED FOR PRIMARY TEST PROGRAM

Projectile Type and Sand Condition	Impact Velocity Range					
	210 m/sec		320 m/sec		400 m/sec	
	Shot	C_D	Shot	C_D	Shot	C_D
Solid Flat Nose Dry Sand	17	1.64	20	1.77	25	1.68
	18	1.62	22	2.50[a]	26	1.65
	19	1.69	23	1.72	27	1.77
			24	1.72	29	1.71
	Avg	1.65	Avg	1.74	Avg	1.70
Solid Flat Nose Wet Sand	70	1.59	37	0.95	76	0.96
	71	1.55	38	0.94	82	0.73
	72	1.36	74	1.02	83	0.82
	73	1.23	81	0.96	84	0.78
	Avg	1.43	Avg	0.97	Avg	0.82
Solid Step-Tier Dry Sand	52	1.81	56	1.78	62	1.83
	54	1.90	58	1.91	63	1.81
	55	1.89	59	1.67	64	1.92
	57	1.62	61	1.82	65	0.54[a]
	Avg	1.80	Avg	1.80	Avg	1.85
Solid Step-Tier Wet Sand	45	1.24	39	0.72	50	0.79
			49	0.82	68	0.61
					69	0.71
	Avg	1.24	Avg	0.77	Avg	0.70
(Values marked with[a] excluded from average)						

value of C_D = 1.7 for the flat-nose projectile and C_D = 1.8 for the step-tier projectile. In paragraph 4.6, a different method of determining C_D is presented, however, which shows up variations in C_D along a trajectory.

In the wet sand (fully saturated) there is a downward trend of C_D as the impact velocity increases, indicating that the penetration is not well characterized by a Poncelet force law with coefficients independent of velocity. There is also more scatter in the C_D values obtained for some of the velocity regimes in the wet sand.

The saturated sand C_D values are all lower than any of the dry sand values (except for Shot 65, which is believed to be in error). Shot No. 87 into a water target at 241 m/sec was fitted by C_D = 0.51. Apparently the fully saturated sand tends to respond somewhat like a water target.

Magnetic sensor response is compared with X-ray data in the following paragraph.

4.4 COMPARISON OF MAGNETIC SENSOR RESULTS WITH X-RAY DATA

For the 26 shots marked with an M in Tables 3 and 4 the cubic interpolation formula described in paragraph 4.3.1 was used to compute the nose position of the projectile at the time of maximum and minimum coil voltage from each magnetic sensing coil. These are compared to the coil position in the last data group tabulated from each of these shots in Appendix A. The differences between these two positions (tabulated in two last lines) give the apparent distance back from the nose to where the maximum outward radial component of the projectile's magnetic field cut the sensing coil (or the maximum inward component for the minimum voltage case).

In Shot 26, for example, the distances were 0.024, 0.023, 0.035, 0.042 back to the apparent maxima. The first two of these agree quite closely with the laboratory mapping of the magnetic field of the projectile reported in paragraph 2.3, which indicated that the maximum should occur about 0.02 meter back from the nose of the flat-nosed projectile if the magnetized projectile passed through the center of the coil. There was some discrepancy at the last two stations, but an error of 0.02 meter is quite small compared to the position coordinate of 1.076 meters at the last station. Shot 26 had one of the straightest trajectories.

Larger discrepancies are recorded for several shots. The largest positive difference noted is for Station 2 of Shot 50 where the apparent maximum was 0.063 meter back of the nose as compared with the laboratory measurement of 0.022 meter for a solid step-tier projectile. Since this occurred at Station 2 (position 0.486 meter) it would represent about an 8 percent error in position indication.

For several stations a negative difference was noted. The largest was -0.027 meter for Station 3 in Shot 58, also a solid step-tier projectile, indicating an apparent maximum 0.027 meter ahead of the nose or 0.049 meter ahead of the maximum position according to the laboratory measurement of the field, leading to a 6 percent position error at Station 3.

In the majority of the cases the apparent errors were smaller than these. No laboratory measurement was made for the hollow step-tier projectiles, but differences between computed nose positions and coil positions for them in Shots 79, 86, and 87 were in the range of the differences for the solid projectiles.

A possible source of the errors could be off-center projectile paths, although both Shots 50 and 58 had quite straight trajectories according to the X-ray records. Other possible sources of error are imprecise measurement of coil positions and/or maximum time on the strip chart and possibly distortions of the magnetic field of the projectile caused by the impact.

It is believed that the X-ray data are generally more precise than the magnetic sensor data. Nevertheless the investigation has indicated that the magnetic sensing method can give quite good results, and it is certainly an economical method.

A different procedure for determining the Poncelet drag coefficients will be presented in paragraph 4.5, which also considers application of the empirical penetration formula developed at Sandia Laboratories (References 12,13).

4.5 COMPARISON OF PONCELET AND SANDIA EMPIRICAL FORMULA RESULTS

The Sandia empirical formulas (References 12,13) are rewritten here in SI units. Thus, according to Young (Reference 13) the total depth of penetration D is given in terms of the initial impact velocity V_o by an equation of the form

$$D = 0.0117\ KSN(W/A_1)^{1/2}(V_o - 31.5) \quad \text{for } V_o > 61 \text{ m/sec} \tag{9}$$

or by

$$D = 2KSN(W/A_1)\ln[1 + 2V_o^2(10^{-4})] \quad \text{for } V_o < 61 \text{ m/sec} \tag{10}$$

W is projectile weight
A_1 is cross sectional area

Since all impacts in the present study had $V_o > 61$ m/sec, a procedure based on a method used by Young (Reference 13) to modify Equation (9) for use with layered media was used to analyze the Eglin experiments. In Equation (9), N is a nose coefficient, S is a soil coefficient, and K is an independently determined parameter. Since K, S, and N appear only as the product KSN, the procedure followed was to determine the best value of KSN to fit the experimental velocity versus position data. The projectiles for the present experiments were considerably smaller and lighter than those for which the empirical formulations and scaling laws had been shown to give good results.

According to Young (Reference 13), for $V_o > 61$ m/sec the constant A in the Poncelet Equation (3) of paragraph 4.3.2 is negligible, so that

Equation (5) is the appropriate form of Poncelet law to relate velocity to position, namely (with $x_o = 0$)

$$V = V_o e^{-Bx} \tag{11}$$

In the procedure of this section both the Poncelet parameter B and the initial velocity V_o at $x = 0$ are considered as unknowns to be determined from the experimental data of Appendix A as follows. The velocity V_i at four positions x_i, each located midway between the positions of the projectile in two successive X-ray pictures, is calculated as $V_i = \Delta x_i/\Delta t_i$, where Δx_i is the distance traveled during the time between the firings of the two x-rays. Then the regression procedure gives

$$B = [(\Sigma x_i)(\tfrac{1}{4}\Sigma \ell n V_i) - \Sigma x_i \ell n V_i]/[\Sigma x_i^{\,2} - \tfrac{1}{4}(\Sigma x_i)(\Sigma x_i)] \tag{12}$$

and

$$V_o = \text{Exp}\ [\Sigma \ell n V_i + \tfrac{1}{4}B(\Sigma x_i)] \tag{13}$$

where $i = 1$ to 4.

The Poncelet drag coefficient C_D is then given by $C_D = 2mB/\rho A_1$ as in Equation (8).

The basis for the application of the Sandia empirical formula to layered media (Reference 13) was the assumption of constant deceleration through each layer. Thus if a_n is the acceleration magnitude nondimensionalized with respect to g, the acceleration of gravity (so that $a_n g$ is the dimensional deceleration), then the velocities V_{n+1} at the beginning and the end of a layer were related (Reference 13) by

$$V_{n+1}^2 = V_n^2 - 2g[(a_{n-1} + a_n)\frac{L}{2} + a_n(t_n - L)] \tag{14}$$

where t_n is the thickness of the layer and it is assumed that $t_n >> L$. For the flat-nosed projectile, with $L = 0$, Equation (14) reduces to

$$V_{n+1}^2 = V_n^2 - 2a_n g t_n \tag{15}$$

which is the basis for the following regression procedure to determine the Sandia parameter KSN. Let

$$G_i = V_1^2/[0.0117(V_1 - 30.5)(V_1^2 - V_i^2)\ (W/A)^{1/2}] \tag{16}$$

Then

$$KSN = \frac{\Sigma(x_i - x_1)(\frac{1}{3}\Sigma G_i) - \Sigma(x_i - x_1)(G_i)}{\Sigma(x_i - x_1)^2 - \frac{1}{3}[\Sigma(x_i - x_1)]\,[\Sigma(x_i - x_1)]} \tag{17}$$

$i = 2$ to 4

The different regression analyses presented in this paragraph and in paragraph 4.3.2 gave for the classical Poncelet equations in most cases almost the same results for C_D. The results for C_D as a function of initial velocity for the solid flat-nosed projectiles in dry sand and in wet sand are summarized in Figure 53. When the two regression results differed significantly the result of paragraph 4.3.2 was used. As shown by the solid triangles the value of C_D is almost independent of the initial velocity in dry sand, while the values for saturated sand (marked by the solid circles) are lower than for dry sand and show a downward trend with increasing initial velocity.

A similar plot of the fitted value of the Sandia parameter KSN for the same shots is shown in Figure 54. The greater scatter in the fitted values of KSN than in those of C_D indicated that these penetration events are not well characterized by a single value of KSN for each shot. The greater discrepancies with the Sandia equation can be explained in part by the assumption of a constant deceleration magnitude in each segment, in contrast with the Poncelet prediction which does fit the dry sand experimental data very well.

In paragraph 4.6 the possible variation of the Poncelet coefficient with position along a trajectory is examined by fitting separate values for different portions of the trajectory for each shot. Some of the values of C_D and KSN for the shots analyzed by the regression methods described in this section will also be given in Table 8 for dry sand and Table 9 for wet sand.

4.6 DRAG COEFFICIENT VARIATION WITH POSITION ALONG A TRAJECTORY

The favorable agreement with the experimental data of the position-time and velocity-position curves calculated by the Poncelet force law suggested further analysis by this model. The variation in the drag coefficient along a trajectory was examined for some of the solid flat-nose projectile trajectories, for 9 shots in dry sand and 10 in wet sand, including examples from each of the three impact velocity regimes of the primary test program. These calculations were made by separately evaluating the Poncelet parameter B for three different segments of each trajectory by the following equation.

$$B = \rho C_D A_1/2m = [\ell n(V_n/V_{n+1})]/(x_{n+1} - x_n) \qquad (18)$$

where subscripts n and n + 1 identify values at the beginning and the end of a segment.

Tables 8 and 9, for dry sand and wet sand, respectively, exhibit in the third column the resulting drag coefficients calculated by Equation (18) for three segments of the trajectory for each shot. The tables also list in the last two columns some of the values of C_D and the Sandia parameter KSN fitted to the whole trajectory by the methods of paragraphs 4.3.2 and 4.5. When two values of C_D were listed for a shot, the first was calculated by the method of paragraph 4.3.2 and the second by the method of paragraph 4.5.

As was pointed out at the end of paragraph 4.3 the C_D values fitted to the dry sand shots are consistently higher than those for saturated sand. Moreover the wet sand values show a downward trend with increasing impact

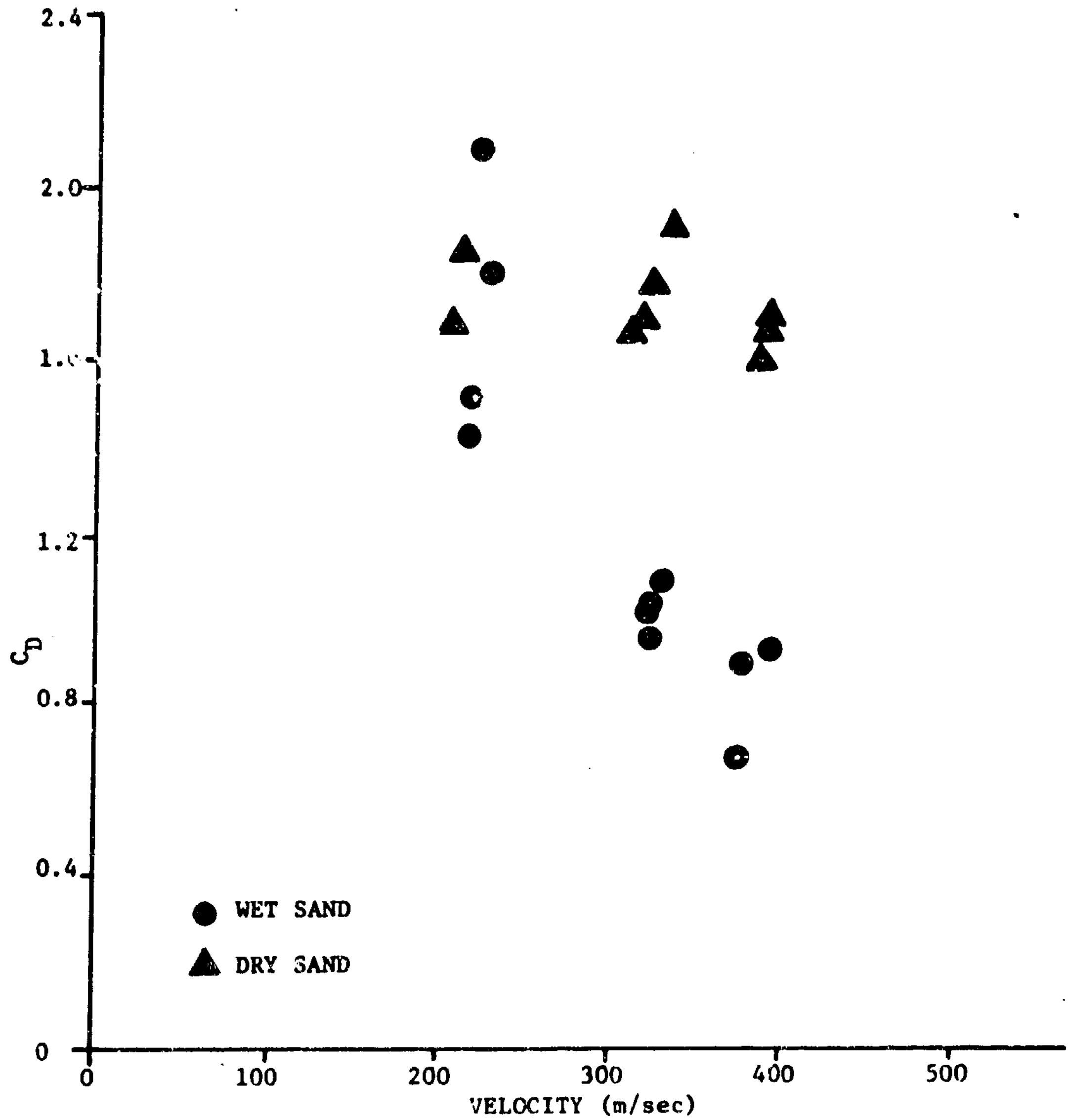

Figure 53. Poncelet Drag Coefficient C_D versus Initial Velocity for Flat-Nosed Projectile Tests in Dry Sand and Wet Sand

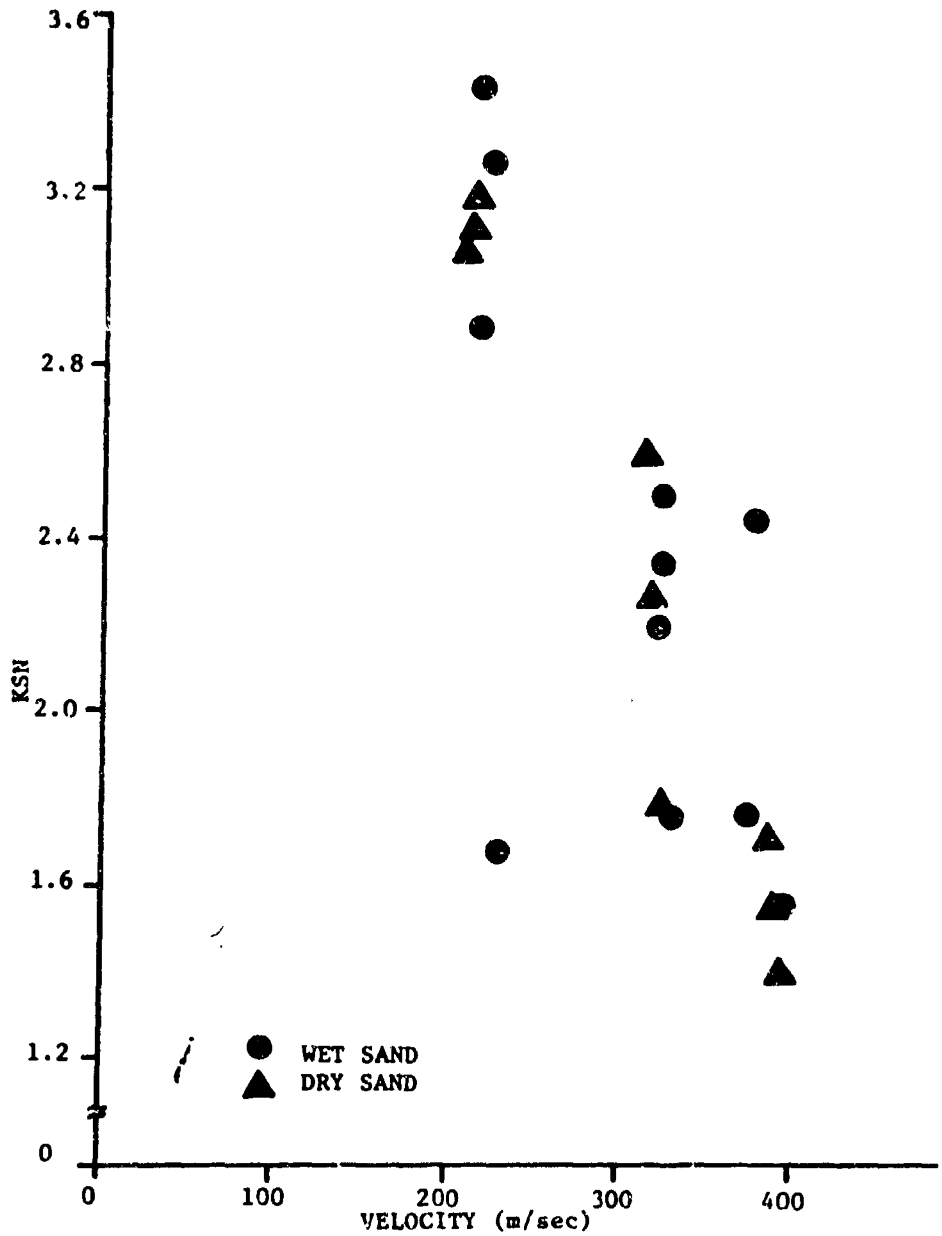

Figure 54. Sandia Penetration Coefficient KSN versus Initial Velocity for Flat-Nosed Projectile Tests in Dry Sand and Wet Sand

TABLE 8. DRAG COEFFICIENTS C_D AND KSN VALUES FOR SELECTED SHOTS IN DRY SAND (SOLID FLAT-NOSE PROJECTILES)

Shot No.	Striking Velocity (m/sec)	Segment C_D	Distance (m)	Average Velocity (m/sec)	Shot C_D*	Shot KSN
17	212.1	1.779 1.590 2.049	0.320 0.590 0.901	174.1 139.3 108.6	1.643 1.779	3.05
18	213.4	1.887 1.673 2.413	0.307 0.570 0.826	174.6 139.3 106.5	1.624 2.230	3.20
19	210.6	1.849 1.880 2.149	0.311 0.573 0.880	176.5 139.6 106.5	1.692 1.973	3.17
20	329.2	1.678 1.910 1.687	0.295 0.552 0.862	268.1 214.8 168.3	1.769 1.786	2.26
23	328.2	2.014 1.578 2.152	0.300 0.562 0.863	269.5 216.0 168.7	1.723 1.867	1.77
24	327.4	1.643 1.774 1.814	0.269 0.525 0.826	265.9 217.8 172.0	1.723 1.765	2.59
25	406.0	1.842 1.400 1.615	0.277 0.534 0.832	329.1 264.2 211.3	1.685 1.561	1.38
26	406.3	1.783 1.760 1.515	0.280 0.538 0.810	329.6 266.5 214.0	1.649 1.670	1.70
29	405.0	1.933 1.761 1.625	0.281 0.522 0.839	330.8 266.3 214.0	1.706 1.735	1.54

*First listed value of C_D calculated by method of paragraph 4.3.2

TABLE 9. DRAG COEFFICIENTS C_D AND KSN VALUES FOR SELECTED SHOTS IN WET SAND (SOLID FLAT-NOSE PROJECTILES)

Shot No.	Striking Velocity (m/sec)	Segment C_D	Distance (m)	Average Velocity (m/sec)	Shot C_D*	Shot KSN
71	207.9	2.167 1.560 1.921	0.268 0.519 0.826	182.3 134.2 98.8	1.545 1.802	1.614
72	214.0	1.302 1.561 1.673	0.285 0.541 0.865	181.1 142.3 104.9	1.359 1.564	3.40
73	212.8	1.410 1.288 1.697	0.287 0.549 0.878	180.9 143.6 108.3	1.233 1.474	2.92
37	336.5	1.134 0.824 1.218	0.298 0.559 0.883	279.6 237.0 196.6	0.947 1.023	2.214
38	333.1	1.032 0.924 0.997	0.300 0.587 0.917	284.0 240.2 200.1	0.937 0.969	2.36
74	334.0	1.240 0.923 1.230	0.309 0.580 0.917	282.7 233.4 189.7	1.016	
81	333.6	1.023 0.885 1.308	0.309 0.570 0.896	278.7 236.3 193.6	0.963	
82	404.8	0.985 0.645 0.499	0.308 0.562 0.889	343.2 299.3 269.2	0.728	
83	419.4	1.228 0.697 1.148	0.307 0.547 0.854	347.0 298.5 258.7	0.819	
84	405.7	0.978 0.584 1.322	0.308 0.545 0.843	333.3 294.0 253.0	0.777	

*First listed value of Shot C_D calculated by method of paragraph 4.3.2

velocity, while for dry sand the values were essentially independent of striking velocity.

Of particular interest here is the change in C_D along a trajectory as shown by the two or three different values listed in the third column for each shot. In many cases the first segment C_D is higher than the second and then the trend is reversed to give a third segment C_D higher than the second. This pattern is followed in 8 of the 10 wet sand cases and in 4 of the 9 dry sand cases, for which three segments were calculated.

The dry sand coefficients show less variation along the trajectory than the wet sand coefficients, a variation of the order of 30 percent between the maximum and minimum values in dry sand and two or three times this much variation in wet sand.

This variation might imply that C_D is velocity dependent instead of being a constant. It seems that in some cases the drag coefficient variation can be fitted to a power law in the velocity. An example of this is given in Section VI.

The apparent variation in the coefficient may, however, actually be a result of assuming an incorrect form for the force law. If the force law contains a term linearly dependent on velocity in addition to the term depending on the square of the velocity, both with constant coefficients, this would lead to an apparent variation in the C_D determined by Equation (18), which is based on a law where the force is proportional to the square of the velocity.

The high drag at the beginning of the trajectory may also be related to shock effects involving not only the velocity but also the impulse duration and the acoustic impedance of the target medium. The minimum C_D appears to be related to momentum transfer to the target medium, where the predominant drag is proportional to the square of the velocity. Finally, as the projectile slows and the cavity collapses onto it, friction and shear resistance in the target medium become important, giving rise to an increase in the apparent drag coefficient.

SECTION V

CAVITY EXPANSION THEORY PENETRATION CALCULATION

In 1975 Bernard and Hanagud (Reference 6) published a report extending the approximate penetration calculation method for projectiles with a hemispherical nose, based on the theory of expansion of a spherical cavity (CET), to projectiles with conical and ogival noses and showing how it could be extended to an arbitrary axially symmetric projectile. The first use of CET methods for dynamic penetration was by Goodier (Reference 26) for a spherical projectile impacting an incompressible strain hardening target. Hanagud and Ross (Reference 3) modified the method to account approximately for target compressibility by treating the target material as a locking medium. The method has been applied to penetration calculations for flat-nose projectiles by Rohani (Reference 4), with the implicit assumption that a false hemispherical nose of target material is formed and carried by the projectile along a stable straight path.

It should be remembered that several quite important assumptions are made in applying the cavity expansion method to penetration calculations, so that extensive experimental verification is necessary to check on the range of approximate validity of predictions by the method. Nevertheless it has achieved some remarkable success in predicting penetration depths from measured soil properties (References 4,6,7). Bernard and Hanagud (Reference 6) defined a dimensionless parameter R_s, which they call the solid Reynolds number

$$R_s = \frac{\rho V^2}{Y} \tag{19}$$

where ρ is target density, Y is target yield strength in a uniaxial strain test, and V is projectile velocity. It was concluded that final penetration depth was reasonably well predicted for R_s between zero and about 100. They considered the upper bound of 100 as a conservative one, since results of experiments at high values of R_s are needed in order to establish a more realistic range. They remarked that accurate prediction of details of the complete deceleration history might demand a much stronger limitation on R_s.

According to the spherical cavity expansion theory for an infinite locking compressible medium the compressive normal stress p at the cavity surface is

$$p = p_s + p_I = p_s + \rho_p \; (B_1 a\ddot{a} + B_2 \dot{a}^2) \tag{20}$$

where p_s and p_I are the separate contributions of the material deformation (shear) and inertia, which Bernard and Hanagud (Reference 6) call the shear resistance and the dynamic pressure, respectively. In this equation ρ_p is the locked plastic density in the region behind the expanding spherical plastic locking shock wave, a is the instantaneous cavity radius, $\dot{a}$, and $\ddot{a}$ are the radial velocity and acceleration of the cavity surface and p_s, B_1, and B_2 are parameters related to properties of the material. The way these parameters are calculated will be indicated later in this section.

In applying this theory to penetration by a projectile with a hemispherical nose two very important assumptions are made (References 3,4) in order to get a simple theory.

(1). The parts p_s and p_I of the normal pressure at the tip of a hemispherical nose of radius a on a projectile traveling at speed V and acceleration $\dot{V}$ are assumed to be equal to the values of p_s and p_I on a spherical cavity surface of the same instantaneous radius a, but expanding with $\dot{a} = V$ and $\ddot{a} = \dot{V}$.

(2). The entire hemispherical nose is assumed to be in contact with the target material, and the dynamic pressure on the projectile's hemispherical nose is assumed to vary from the stagnation point value at the nose tip to zero at the shoulder as the cosine of the polar angle measured from tip (colatitude), while p_s is uniform over the nose.

If friction on the nose and all afterbody forces are neglected this leads in a straightforward manner to the following equation of motion for the projectile of mass M

$$(M + \frac{2}{3}\pi a^3 \rho_p B_1)\frac{dV}{dt} = -\pi a^2 (p_s + \frac{2}{3}\rho_p B_2 V^2) \qquad (21)$$

The term $\frac{2}{3}\pi a^3 \rho_p B_1$ is an added mass term resulting from the acceleration term $\rho_p B_1 a\ddot{a}$ in the expression for the dynamic pressure in Equation (20). In most cases that have been treated the added-mass term was negligible in comparison to the projectile mass M.

In modifying the method to other axisymmetric nose shapes, Bernard and Hanagud replaced the assumption on the variation of p_I over the nose surface by an assumption on the variation along the nose of the tangential component V_t of the target absolute velocity. For a fully embedded nose, the material was assumed to be in contact all along the nose surface (no separation before the base of the nose), an assumption which they recognized was not generally strictly correct. The normal component V_n of target material velocity was therefore required to be equal to the normal component of the velocity of the projectile nose surface. For a conical nose of half apex angle ϕ, it was assumed that the tangential component of target velocity varies from V cos ϕ at the nose tip to zero at the base of the cone, according to the law

$$V_t = [1 - (z/L)^2]^{1/2} V \cos\phi \qquad 0 \le z \le L \qquad (22)$$

where L is the nose length and z is the axial coordinate measured back from the tip of the nose. The velocity dependent part of the dynamic pressure p_I was then assumed to depend on the local resultant particle velocity magnitude $V_p = [V_n^2 + V_t^2]^{1/2}$ in the same way that p_I depends on $\dot{a}$ in the spherical cavity expansion theory. Similar assumptions could be made about the dependence on the local particle acceleration on the nose surface, but because that term is usually much smaller than the velocity-dependent term, Bernard and Hanagud (Reference 6) chose to use the nose tip acceleration $\dot{V}$, so that p_I is given by

$$p_I = \rho_p B_1 a\dot{V} + \rho_p B_2 V_p^2 \qquad (23)$$

where V_p varies over the nose while $\dot{V}$ does not. Integration of the axial force component over the nose then gives the following equation of motion, replacing Equation (21)

$$(M + \pi a^3 \rho_p B_1)\frac{dV}{dt} = - \pi a^2 (p_s + \rho_p B_2 f_n V^2) \quad (24)$$

where the dimensionless nose-shape factor f_n is given for a conical nose of length-to-diameter ratio L/D by

$$f_n = 1 - \frac{2}{3}\frac{4(L/D)^2}{4(L/D)^2 + 1} \quad (25)$$

Besides containing the factor f_n in place of the factor 3/2, Equation (24) differs from Equation (21) by lacking the factor 3/2 in the term containing B_1.

Bernard and Hanagud (Reference 6) observed that with the assumption listed above the variation in f_n as L/D varies from zero (flat nose) to infinity (long pointed nose) produces a variation in predicted final penetration depth by a factor of three. For L/D = 0.5, f_n is 3/2 and the prediction is the same as for the hemispherical nose, when the contribution of the added-mass term containing B_1 is negligible.

For other fully embedded convex axisymmetrical nose shapes, Bernard and Hanagud (Reference 6) gave a method for estimating V_n and V_t at any position on the nose by considering the circumscribed cone tangent to the nose at the point. The base of the cone was in the same plane as the actual nose base, but the tip was forward of the actual tip. The components V_n and V_t at the point of tangency were assumed to be equal to the values of V_n and V_t that would be assumed on the circumscribed cone at the point of tangency if it were an actual conical nose, calculated by the procedure described above for conical noses. This gave a continuous variation of V_t over the nose, dropping to zero at the base of the nose. Explicit formulas for V_p and p_I as a function of position on the nose were given for ogives (Reference 6). For the special case where the ogive is a hemisphere, the distribution of p_I over the nose as calculated by this procedure differs slightly from that given by the previous procedure assuming p_s to vary as the cosine of the polar angle. But the resultant axial force is the same when the added-mass term containing B_1 is negligible.

Because of the formation of a false nose of target material, it does not seem reasonable to apply these assumptions to actual flat-nose projectiles. Neither the X-ray pictures nor post-test examination had shown the actual shape of the false noses formed in the Eglin penetration experiments. In the following analysis of Shots 20 and 21 of the Eglin experiments two kinds of assumptions were made for the shape of the false nose. The first assumption was a hemispherical nose, leading to Equation (21) for the equation of motion. The second kind of assumption was a conical nose, leading to Equation (24). The second assumption was applied for L/D values of 0.5, 0.4, 0.2, and 0.

The material properties for the dry sand target were determined as follows. The shear or deviatoric properties were based on a triaxial test performed in the Civil Engineering Laboratories at the University. Figure 55 shows a plot of $\sigma_1 - \sigma_3$ versus ε_1, where σ_1 and ε_1 are axial compressive stress and strain and σ_3 is the constant lateral confining pressure of

0.589 MPa. The dots denote the experimental curve while the two straight lines are the bilinear fit to it. From the bilinear fit the values of

$$E = 54\ \text{MPa}, \qquad E_t = 1.39\ \text{MPa}, \qquad Y = 1.4\ \text{MPa} \tag{26}$$

were determined for the elastic modulus E, tangent modulus E_t in the plastic regime, and yield stress Y (at the intersection of the two straight lines). The bilinear approximation, required for the simple cavity expansion theory, seems to be quite a reasonable one for the triaxial test curve.

The required approximation to the compressibility properties, determined from a uniaxial strain test as shown in Figure 56 is more extreme and more arbitrary. It is necessary to approximate the curve by two vertical (incompressible) lines joined by a horizontal jump representing the change in density from the locked elastic density at uniaxial strain ε_1, to the locked plastic density at uniaxial strain ε_p upon the passage of the plastic shock wave. The approximations assumed correspond to uniaxial strain values of

$$\text{Elastic } \varepsilon_1 = 0.03 \qquad \text{Plastic } \varepsilon_p = 0.094 \tag{27}$$

The initial density was $\rho_o = 1540\ \text{kg/m}^3$. Then

$$\rho_p = 1700\ \text{kg/m}^3 \quad \text{and} \quad \rho_o/\rho_p = 0.906 \tag{28}$$

leading to the following numerical values for constants in the theory

$$\beta = \frac{Y}{2E} - \frac{1}{3}\varepsilon_1 = 0.00296 \qquad \alpha_p = 1 - (\rho_o/\rho_p) = 0.094$$

$$\delta = 1 - (\rho_o/\rho_p)e^{-3\beta} = 0.1020 \quad B_1 = 1 - \delta^{1/3} = 0.533$$

$$B_2 = 1.5 + (1+\alpha_p)\delta^{1/3} + 0.5\delta^{4/3} = 1.013$$

$$p_s = \frac{4}{9}E(1-e^{-3\beta}) - \frac{2}{3}Y \ln \delta + \frac{2}{27}\pi^2 E_t - \frac{4}{9}E_t\{\sum_{n=1}^{\infty}(\delta^n/n^2)\} = 3.396\ \text{MPa} \tag{29}$$

The formulas for β, α_p, B_1, B_2, and p_s are as given in Hanagud and Ross (Reference 3), and differ slightly from the versions in Bernard and Hanagud (Reference 6). The differences have to do with inclusion of various terms that contribute little to the actual numerical values obtained. With this value of B_1, the added-mass term containing B_1 in Equations (21)or (24) is 0.00285 kg, which is negligible in comparison to the projectile mass m (0.5451 kg in Shot 20 and 0.5443 kg in Shot 25). The equation then takes the form

$$\frac{dV}{dt} = -(A + BV^2) \tag{30}$$

as in the Poncelet force law. Equation (30) is integrated to give

$$x = x_o + \frac{1}{B}\ln\{\cos(\sqrt{AB}\ (t-t_o)) + \sqrt{B/A}\ V_o \sin(\sqrt{AB}\ (t-t_o))\} \tag{31}$$

and

$$V = \{(\frac{A}{B} + V_o^2)e^{-2B(x-x_o)} - \frac{A}{B}\}^{1/2} \tag{32}$$

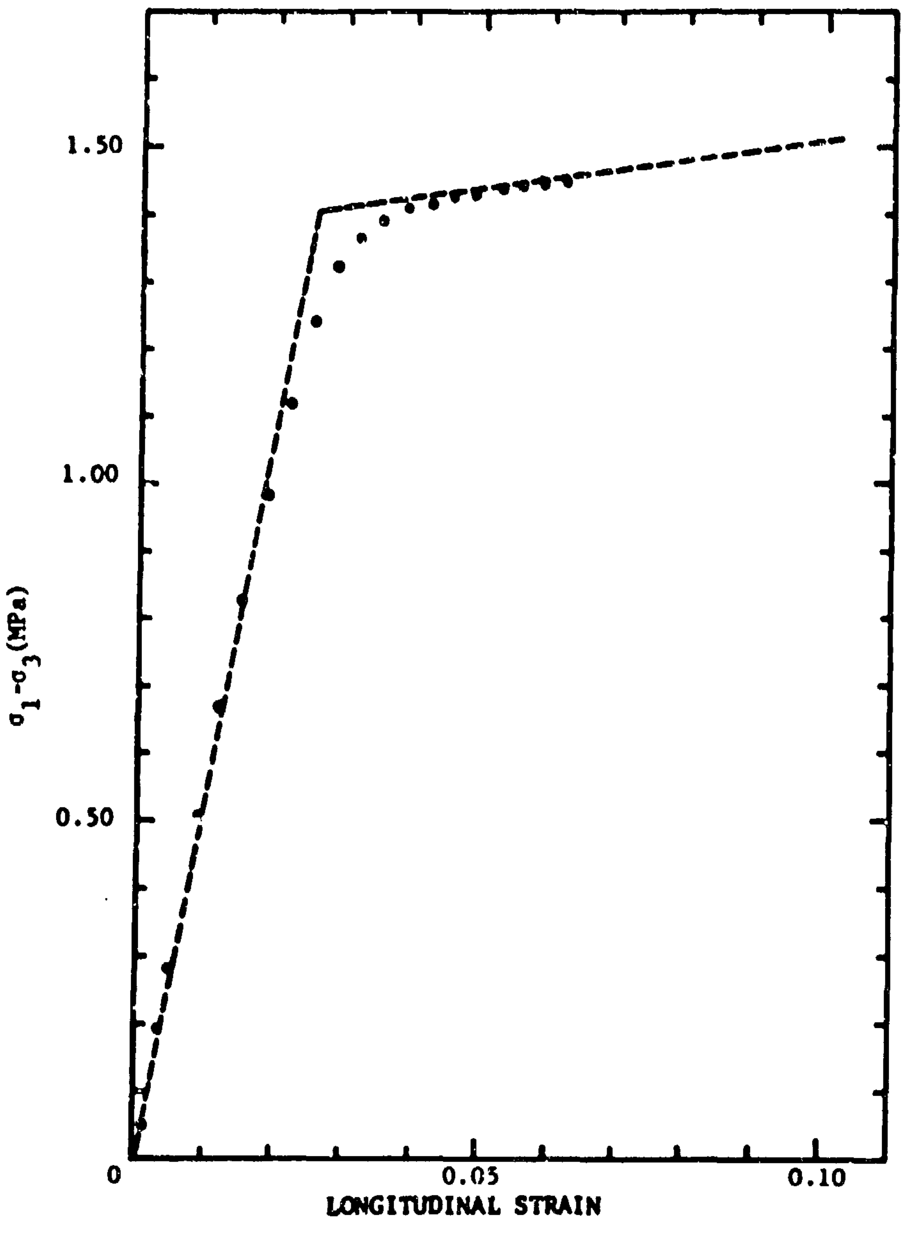

Figure 55. Bilinear Approximation to Triaxial Test Curve for Loose Eglin Sand (ρ_o = 1540 kg/m^3) with σ_3 = 0.589 MPa

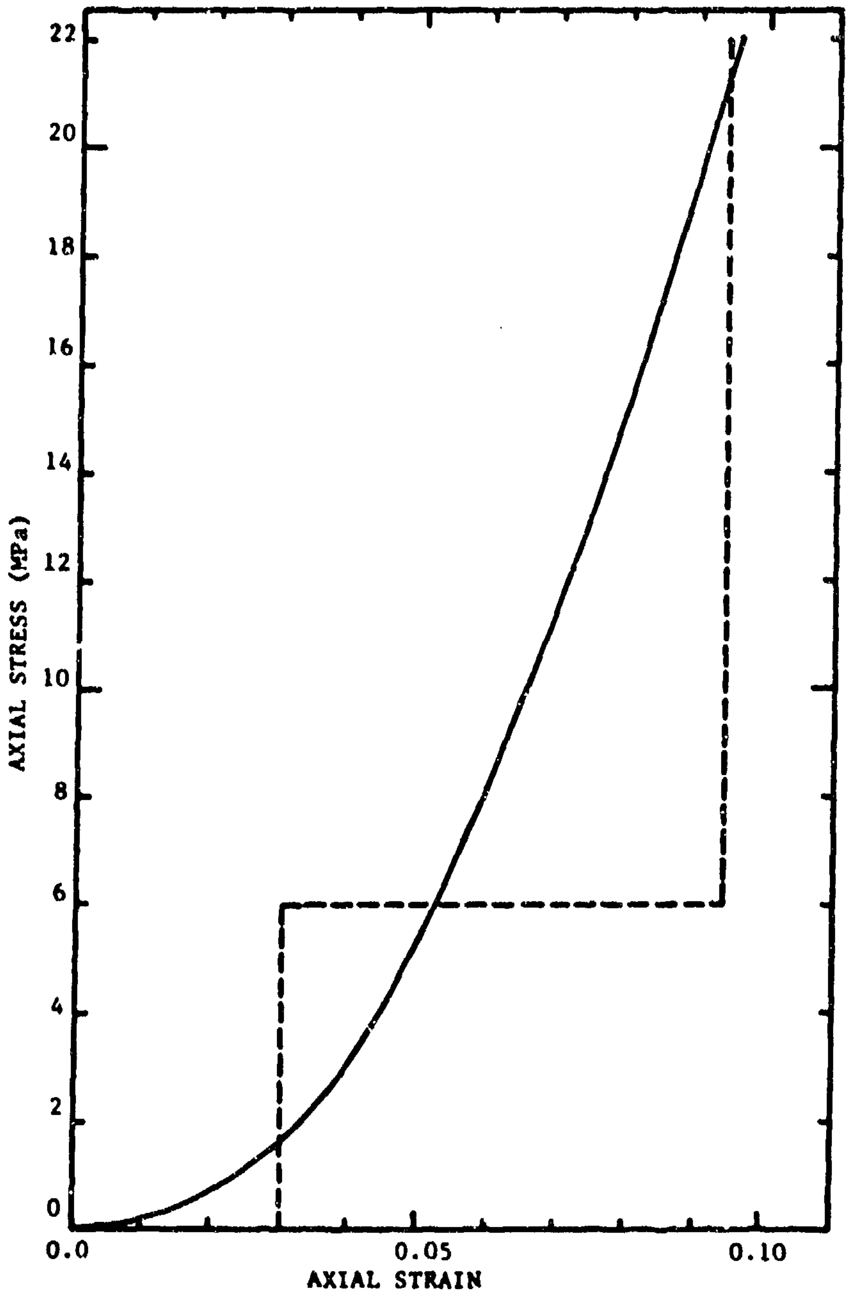

Figure 56. Ideal Locking Approximation to Uniaxial Strain Curve for Loose Eglin Sand (Initial Density 1540 kg/m^3)

These results are plotted in Figure 57 for Shot 20 and Figure 58 for Shot 25. The coefficients A and B for the two shots have the values shown in Table 10.

TABLE 10. COEFFICIENTS FOR CAVITY EXPANSION THEORY PENETRATION CALCULATIONS

Shot 20				Shot 25			
Curve	L/D	$A(m/s^2)$	$B(m^{-1})$	Curve	L/D	$A(m/s^2)$	$B(m^{-1})$
1	0.5	1900	0.6614	1	0.5	1903	0.6624
2	0.4	1900	0.7340	2	0.4	1903	0.7351
3	0.2	1900	0.9009	3	0.2	1903	0.9023
4	0	1900	0.9922	4	0	1903	0.9936

Also plotted in each figure is the fitted Poncelet curve through the experimental points. The agreement is fairly good for the hemispherical nose (Curves 1, L/D = 0.5), overestimating the penetration by 3 to 5 percent and the final velocity by about 11 percent in Shot 20. The xt-curve for L/D = 0.4 (Curve 2) is essentially coincident with the experimental curve in each case. The Vx-curve is also coincident with the experimental curve in Shot 25 and overestimates the final velocity by only 3 percent for Shot 20. It is emphasized that the parameter values used for the prediction were determined from the two static curves as shown in Figures 55 and 56. These parameters were determined before calculation of Figures 57 and 58. No adjustments were made to the parameter values to get a better agreement with the experimental results.

Thus, with an assumed false conical nose with L/D = 0.4 the details of the deceleration history are remarkably well predicted for Shots 20 and 25 in the region of observation. The prediction with an assumed spherical nose (or a cone with L/D = 0.5) is also not bad. The solid Reynolds number for these two shots is R_s = 127 for Shot 20 and R_s = 181 for Shot 25, both above the range of R_s in which the cavity expansion theory was known to give good results. (See the discussion following Equation (19).)

Any attempt to apply the theory directly to the flat-nosed projectiles by using the limiting case of L/D = 0 as in the Curves No. 4 in Figures 57 and 58 would greatly overpredict the drag and underpredict the penetration for Shots 20 and 25.

It is concluded that the cavity expansion theory method has considerable merit despite the strong assumptions involved in its application to penetration theory. For projectiles with actual conical or ogival noses or other nonflat axisymmetric shapes it should prove profitable to consider oblique impacts and attempt to modify the theory to apply locally to a surface area element somewhat in the manner of the assumed differential area force laws to be discussed in Section VI. This has not been done yet for a

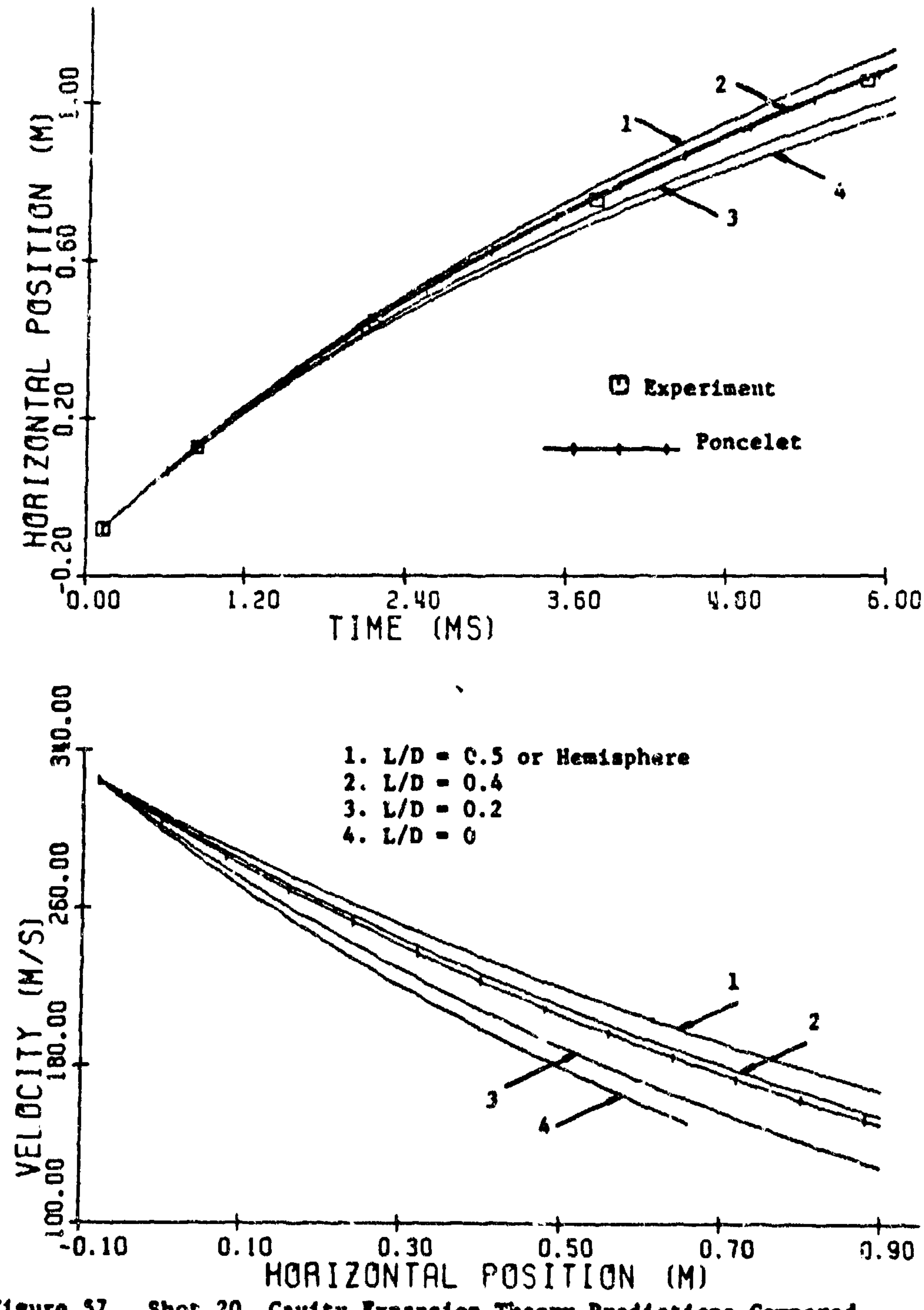

Figure 57. Shot 20, Cavity Expansion Theory Predictions Compared to Experimental Data

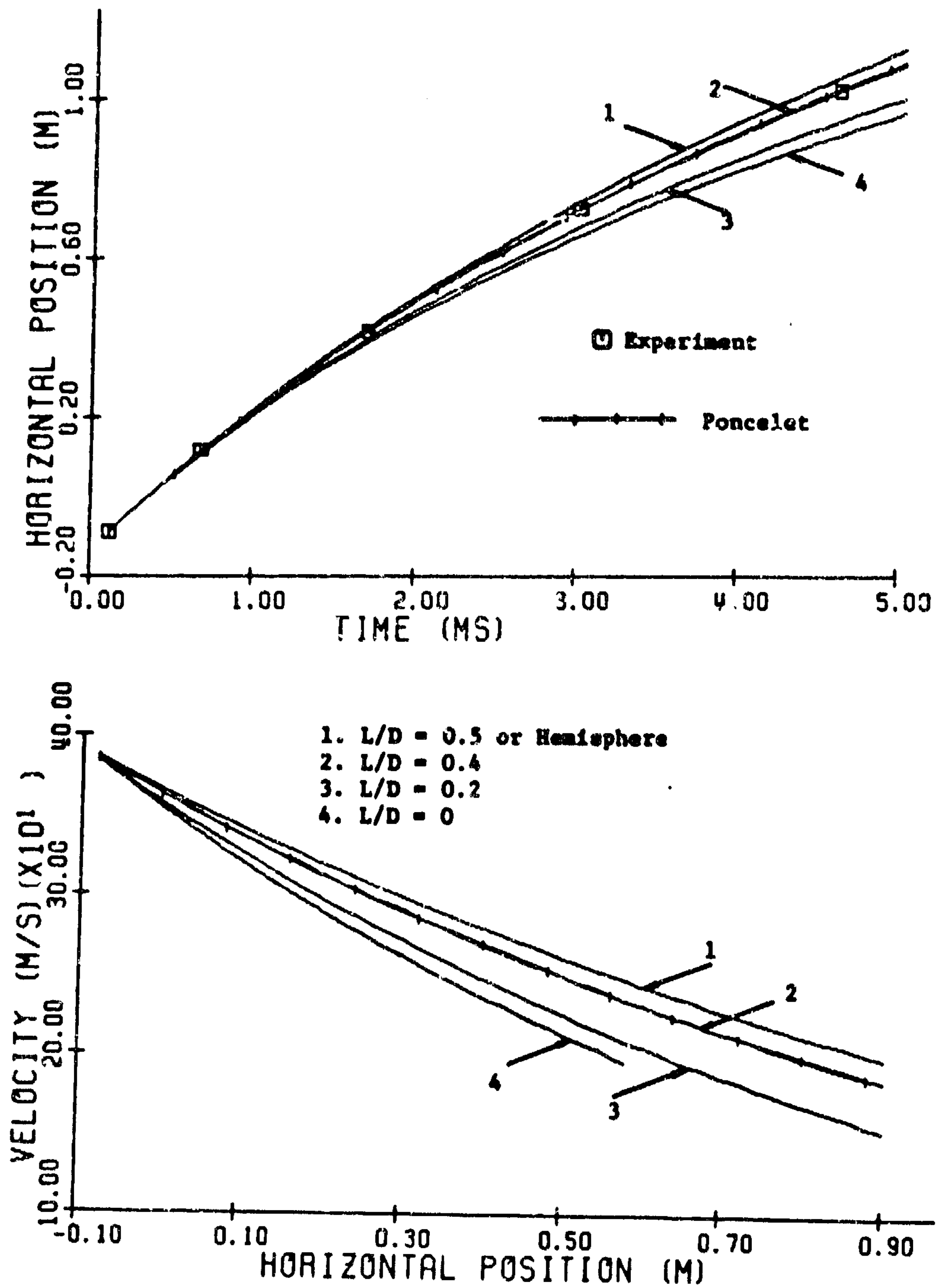

Figure 58. Shot 25, Cavity Expansion Theory Predictions Compared to Experimental Data

complete trajectory, although Bernard and Hanagud (Reference 6) discussed the embedment process at the beginning of an oblique impact for a projectile with a conical nose.

It might also be possible to make similar calculations for the flat-nosed projectile, but this would severely test any assumed false nose shape. It may be possible to obtain some hints about the false nose shape from a study of the separation angles as shown in the X-rays.

SECTION VI

RIGID BODY MOTION IN A SOIL MEDIUM

6.1 EQUATIONS OF MOTION

Soil penetration prediction techniques as classified by Triandafilidis (Reference 1) are considered to fall into two broad categories i.e., mathematical and experimental. Under the broad heading of mathematical further suggested subdivisions are semi-analytical, analytical and theoretical. The semi-analytical techniques listed in Reference 1 were all restricted to completely normal penetration. Even the cavity expansion models, classified as analytical, are also restricted to normal impact. Oblique impact may be analyzed using an analytical Differential Area Force Law (Reference 8). However, a computer program based on this type of analysis has limited access because of proprietary restrictions, as well as being expensive to operate. In light of the above, a study was initiated to develop a simple multidegree-of-freedom set of equations of motion for bodies of revolution in a soil medium. The ground rules for this development are as follows:

1. The projectile was to be a body of revolution with zero rotation rate about the longitudinal axis.
2. Classical six-degree-of-freedom equations of motion would be used with force and moment terms from assumed or empirical force expressions.
3. Force expressions would be selected by joint agreement between the contractor and the project engineer.
4. Results were to be projectile position-time tabulation using Cartesian coordinates for center of mass position and Euler angles for body rotations.

For the derivation a set of body fixed axes x, y, z with unit vectors $\hat{i}$, $\hat{j}$, $\hat{k}$ and an inertial frame x', y', z', with unit vectors $\hat{i}'$, $\hat{j}'$, $\hat{k}'$ fixed in the soil, were selected and are shown schematically in Figure 59.

The generalized six-degree-of-freedom equations of motion for a rigid nonsymmetrical body written relative to the body axes are given as (Reference 27):

$$F_x = m(\dot{U}+QW-RV) \qquad (33)$$

$$F_y = m(\dot{V}+RU-PW) \qquad (34)$$

$$F_z = m(\dot{W}+PV-QU) \qquad (35)$$

$$L = I_{xx}\dot{P}+I_{xy}(PR-\dot{Q})-I_{xz}(\dot{R}+PQ)+RQ(I_{zz}-I_{yy})+I_{yz}(R^2-Q^2) \qquad (36)$$

$$M = -I_{xy}(\dot{P}+RQ)+I_{yy}\dot{Q}+I_{yz}(PQ-\dot{R})+RP(I_{xx}-I_{zz})+I_{xz}(P^2-R^2) \qquad (37)$$

$$N = I_{xz}(QR-\dot{P})-I_{yz}(\dot{Q}+PR)+I_{zz}\dot{R}+I_{xy}(Q^2-P^2)+QP(I_{yy}-I_{xx}) \qquad (38)$$

where:

F_x, F_y, F_z Applied forces in x, y, z directions respectively.

L,M,N — Applied torques or moments about x,y,z axes respectively.

U,V,W — Projectile or body translational velocities relative to x, y, z axes respectively.

P,Q,R — Projectile or body rotational velocities about x, y, z axes respectively.

m — Projectile mass.

I_{xx}, I_{yy}, I_{zz}, I_{xy}, I_{xz}, I_{yz} — Conventional moments of inertia and products of inertia for body axes x, y, z

The dot above any term represents the time derivative or time rate of change of that term.

For a symmetrical body the products of inertia are zero and $I_{yy} = I_{zz}$, and Equations (33) through (38) reduce to

$$F_x = m(\dot{U} + QW - RV) \tag{39}$$

$$F_y = m(\dot{V} + RU - PW) \tag{40}$$

$$F_z = m(\dot{W} + PV - QU) \tag{41}$$

$$L = I_{xx} \dot{P} \tag{42}$$

$$M = I_{yy}\dot{Q} + RP(I_{xx} - I_{yy}) \tag{43}$$

$$N = I_{zz}\dot{R} - QP(I_{xx} - I_{yy}) \tag{44}$$

6.2 FORCE EXPRESSIONS

The force exerted on the projectile by the soil was assumed to be of the form

$$\begin{aligned} \frac{d\bar{F}}{dA} &= n_x(A_x + B_x|U| + C_xU^2)\hat{i} \\ &+ n_y(A_y + B_y|V| + C_yV^2)\hat{j} \\ &+ n_z(A_z + B_z|W| + C_zW^2)\hat{k} \end{aligned} \tag{45}$$

where:

A_x, B_x, C_x, A_y, B_y, C_y, A_z, B_z, C_z — are the force coefficients to be determined from tests performed for a certain projectile shape and a given soil.

n_x, n_y, n_z — are components of outward unit vector normal to surface of projectile.

The forces F_x, F_y, and F_z may then be determined by the projected wetted areas normal to the velocities U, V, W respectively. A force is assured to exist only when the wetted surface has an outward velocity component normal to the projected area. This type of force distribution applicable only to axisymmetric bodies, assumes a uniformly distributed pressure over the projected wetted area, giving rise to a resultant force passing through the geometric center of the projected wetted area. When the geometric center of the projected wetted area coincides with the center of the mass of the projectile then no applied moment L, M, N, exists on the projectile. If the projectile is hollow or if the geometric center of the projected area and the center of mass do not coincide then an applied moment exists and is equal to the applied force times the distance between the geometric center of the projected wetted area and the center of mass. For a body of revolution completely submerged in the medium the force distribution due to a lateral translational velocity V is shown in Figure 60 for the case of zero moment. In a case where the geometric center of the area and the center of mass do not coincide the force distribution is shown in Figure 61. The projected area used to determine the force F_y for a completely submerged axisymmetric projectile is the same as for F_z. The projected area for F_x for the completely submerged projectile is simply the cross section of the projectile normal to the x axis.

If the projectile is only partially submerged then only a portion of the total projected area is in contact with the soil medium and a resultant force and moment will exist as shown in Figure 62. These moments and forces are changing with depth of penetration and become functions of depth. For this case the forces and moments are not simple expressions due to the complicated expressions required to calculate the areas. The derivation of the forces and moments required for partial penetration of a conical nose are given in Appendix B. These equations are not included in the main body of the report as time did not permit complete computer modeling of these equations and therefore are simply included as information.

6.3 COORDINATE TRANSFORMATIONS

Translational and angular positions relative to an inertial frame fixed in the soil may be expressed in terms of angular and translational velocities of the body fixed axes by use of coordinate transformations relating the two systems. The coordinate rotations required for these transformations are given in Reference 28 as:

1. Start with body axis x, aligned with inertial axis x' and rotate about body axis z, through an azimuthal angle Ψ. This produces a new set of body axes X_2, Y_2, Z_2.

2. Rotate about Y_2 through a pitch angle Θ. This produces a new set of body axes X_3, Y_3, Z_3.

3. Finally, rotate about X_3 through a roll angle ϕ, which brings the body into its final body axis system X, Y, Z. (This rotation is not important for a body possessing complete symmetry about the X axis.

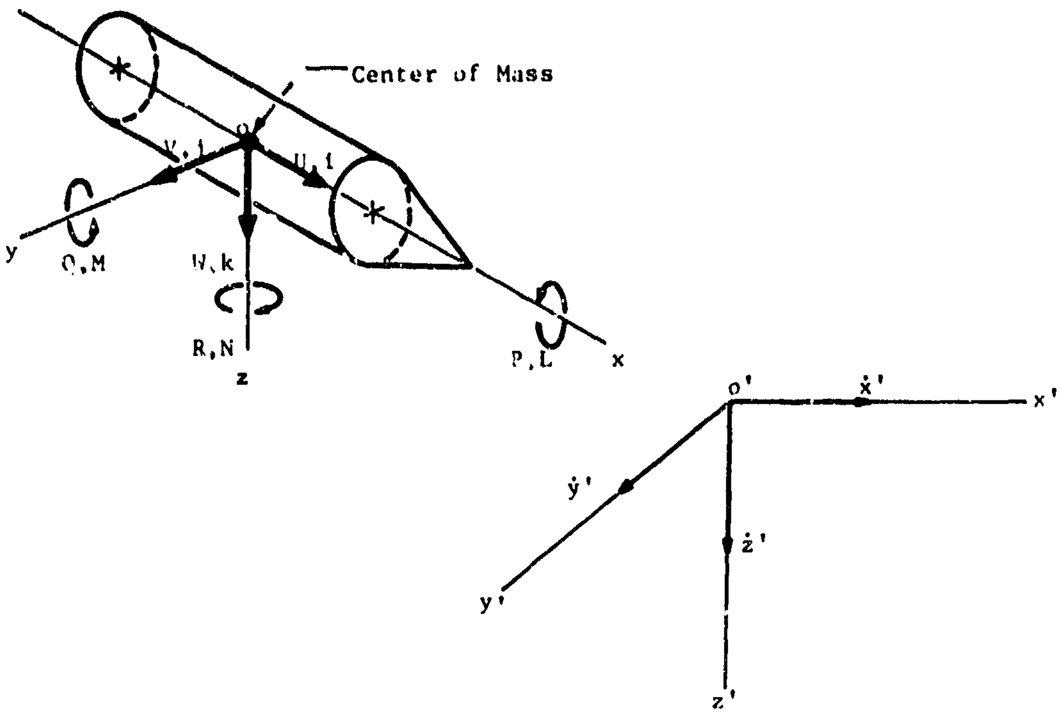

Figure 59. Schematic of Body and Inertial Axes. x' Positive Downward in Soil

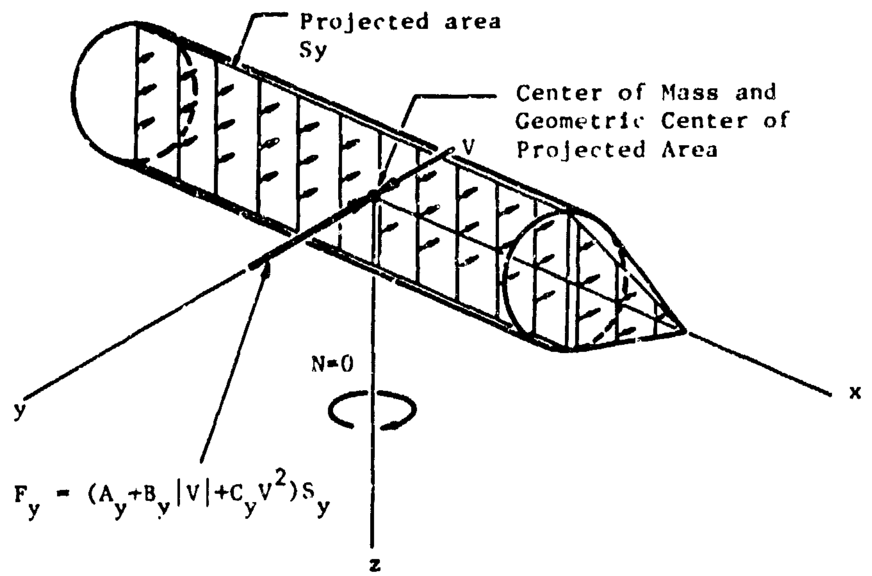

Figure 60. Center of Mass and Geometric Center of Projected Area Coincident

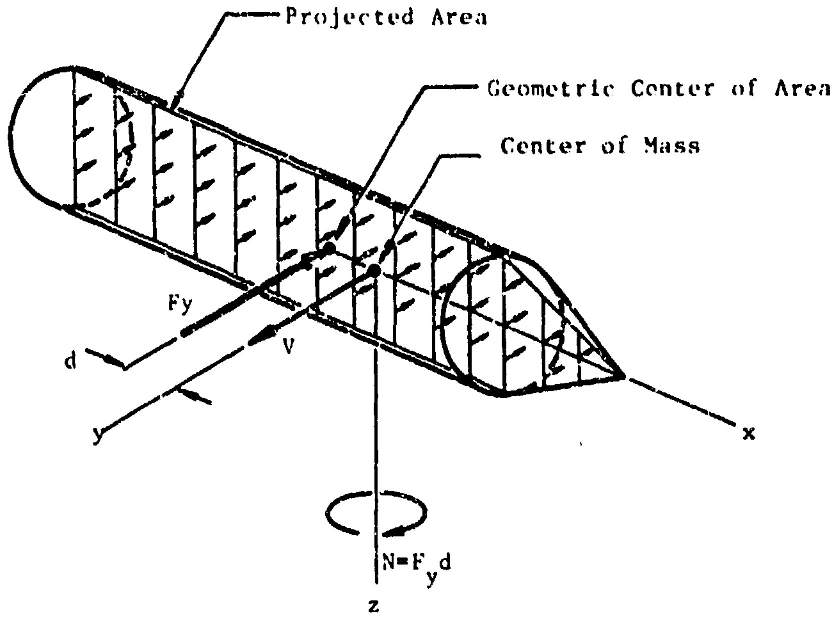

Figure 61. Center of Mass and Geometric Center of Projected Area Not Coincident

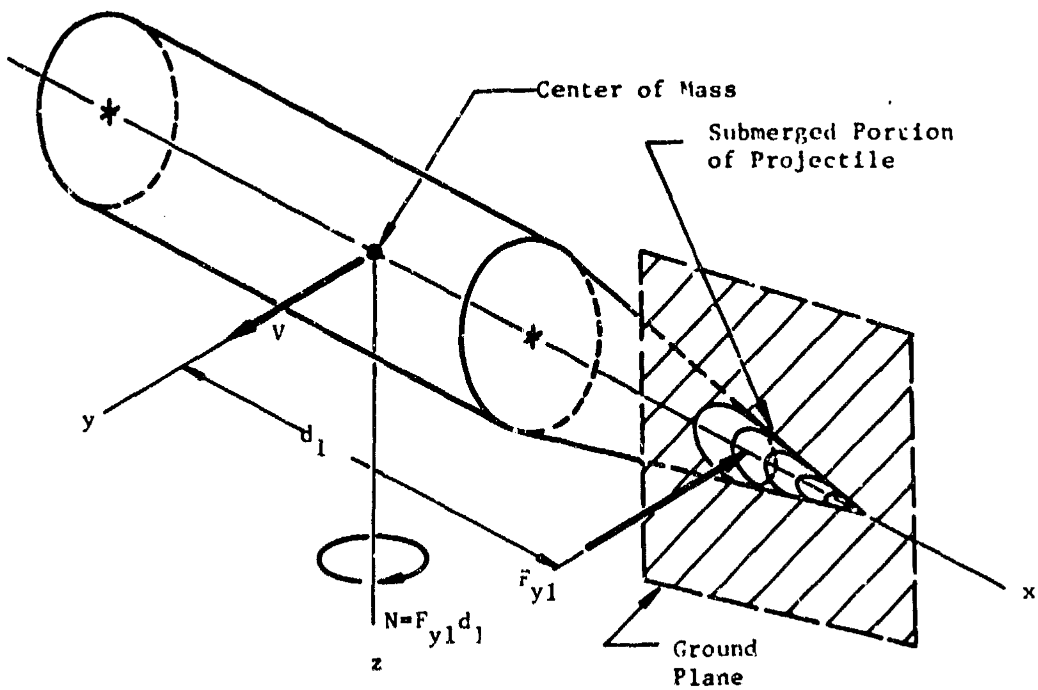

Figure 62. Partially Submerged Projectile

The transformation equation based on these angles is given as

$$\bar{A}_I = T_{BI} \bar{A}_B, \tag{46}$$

which transforms an arbitrary vector $\bar{A}_B$ given in the body system to a vector $\bar{A}_I$ in the inertial system. The transformation matrix T_{BI} is given as

$$T_{BI} = \begin{bmatrix} c\Psi c\Theta & (c\Psi s\Theta s\phi - s\Psi c\phi) & (c\Psi s\Theta c\phi + s\Psi s\phi) \\ s\Psi c\Theta & (s\Psi s\Theta s\phi + c\Psi c\phi) & (s\Psi s\Theta c\phi - c\Psi s\phi) \\ -s\Theta & c\Theta s\phi & c\Theta c\phi \end{bmatrix} \tag{47}$$

where: $c\Theta = \cos\Theta, s\Theta = \sin\Theta$, etc.
For orthogonal transformation such as this the inverse of T_{BI} is equal to the transpose of T_{BI}; therefore the inverse relation of Equation (46) is simply

$$\bar{A}_B = [T_{BI}]^T \bar{A}_I . \tag{48}$$

By using Equation (46) the velocity vectors U, V, W may be transformed to give the velocities $\dot{x}'$, $\dot{y}'$, $\dot{z}'$, in the inertial system. These velocities,

$$\begin{Bmatrix} \dot{x}' \\ \dot{y}' \\ \dot{z}' \end{Bmatrix} = [T_{BI}] \begin{Bmatrix} U \\ V \\ W \end{Bmatrix} \tag{49}$$

may be integrated to determine the position x', y', z' of the center of mass in the inertial frame.

The angular velocities $\dot{\Psi}, \dot{\Theta}, \dot{\phi}$ are related to the angular velocities P, Q, R through a transformation matrix ROT defined by

$$\begin{Bmatrix} P \\ Q \\ R \end{Bmatrix} = [ROT] \begin{Bmatrix} \dot{\phi} \\ \dot{\Theta} \\ \dot{\Psi} \end{Bmatrix} \tag{50}$$

where:

$$[ROT] = \begin{bmatrix} 1 & 0 & -\sin\Theta \\ 0 & \cos\phi & \sin\phi\cos\Theta \\ 0 & -\sin\phi & \cos\phi\cos\Theta \end{bmatrix} \tag{51}$$

Due to the non-orthogonality of [ROT] the inverse of the [ROT] transformation is not $[ROT]^T$. It is given by

$$[ROT]^{-1} = \begin{bmatrix} 1 & \sin\phi\tan\Theta & \cos\phi\tan\Theta \\ 0 & \cos\phi & -\sin\phi \\ 0 & \sin\phi\sec\Theta & \cos\phi\sec\Theta \end{bmatrix} \quad (52)$$

and

$$\begin{Bmatrix} \dot{\phi} \\ \dot{\theta} \\ \dot{\psi} \end{Bmatrix} = [ROT]^{-1} \begin{Bmatrix} P \\ Q \\ R \end{Bmatrix} . \quad (53)$$

Equations (33) through (38), (49) and (53) represent the necessary equations. When solved simultaneously with the proper initial conditions they will yield the position and orientation of the body as functions of time in the inertial frame.

6.4 CALCULATIONS

The solution of Equations (33) through (38), (49) and (53) may be obtained numerically provided expressions for the forces and moments are available. In the general case where impact is not normal the expressions are rather complicated and require considerable computer technique and programming ability. However, a completely submerged projectile could be handled very easily for the force distribution as given by Equation (45). Also if the assumption is made that only the nose of the projectile is in contact with the soil and submersion of the nose is instantaneous, a normal impact can be handled very easily.

The case of complete submersion was programmed using a MIMIC source language program. This program, available on the CDC 6600 in the Mathematical Laboratory at Eglin AFB, is essentially a fourth order Runge-Kutta numerical method for solving simultaneous differential equations. A program shown as Computer Program I of Appendix C was developed for solution of Equations (33) through (38), (49) and (53), for a blunt nosed cylinder, a conical nosed cylinder and a hemispherical nosed cylinder. For this case the force coefficients A_x through C_z are assumed to be constants.

The MIMIC program allows for naming constants or variable parameters and for Program I, Appendix C, all the initial conditions, soil force coefficients, and geometric properties were given a parameter status. Only integration time and print frequency were named constants. A check on this program was accomplished using the data for the blunt nosed cylinder listed in Figure 63. The assumption in this case is that, for normal penetration, nose submersion is instantaneous and only the nose is in contact with the soil.

For this case only the forces parallel to the x axis of the projectile are operative; therefore all other coefficients are set to zero. It is important to note here that the coefficients used for this case were obtained from test data of Reference 14. The results of this case are shown in Figures 64 and 65. Both plots show very

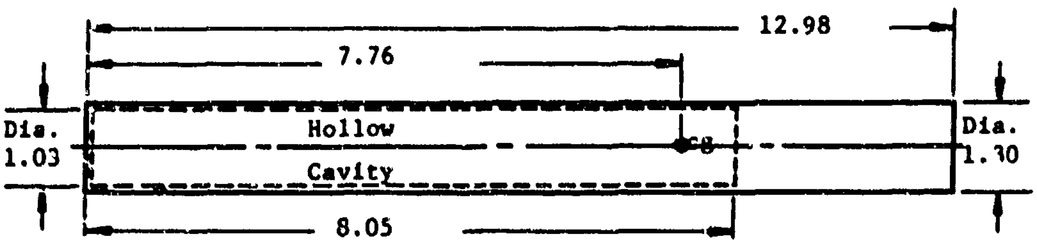

GEOMETRIC VALUES AND INITIAL CONDITIONS

mass = 80 gm

I_{xx} = 20.42 gm-cm^2

I_{yy} = 1000 gm-cm^2

U_o = 6.74 x 10^4cm/sec

$\psi_o = \phi_o = \theta_o = 0$

$I_{yy} = I_{zz}$

$I_{xy} = I_{xz} = I_{yz} = 0$

$V_o = W_o = P_o = Q_o = R_o = 0$

$\dot{Y}'_o = \dot{Z}'_o = 0$

$X'_o = Y'_o = Z'_o = 0$

FORCE COEFFICIENTS

Velocity Range $6.74 \times 10^4 \leq U \leq 1. \times 10^4$ cm/sec

$A_x = B_x = 0 \quad C_x = 1.51$

$A_y = B_y = C_y = A_z = B_z = C_z = 0$

Velocity Range $1. \times 10^4 < U < 0$ cm/sec

$A_x = 2.95 \times 10^6 \quad B_x = 0 \quad C_x = 2.12$

$A_y = B_y = C_y = A_z = B_z = C_z = 0$

Data taken from Reference 14 and all dimensions in cgs units.

Figure 63. Data for Normal Penetration of Blunt Nosed Cylinder

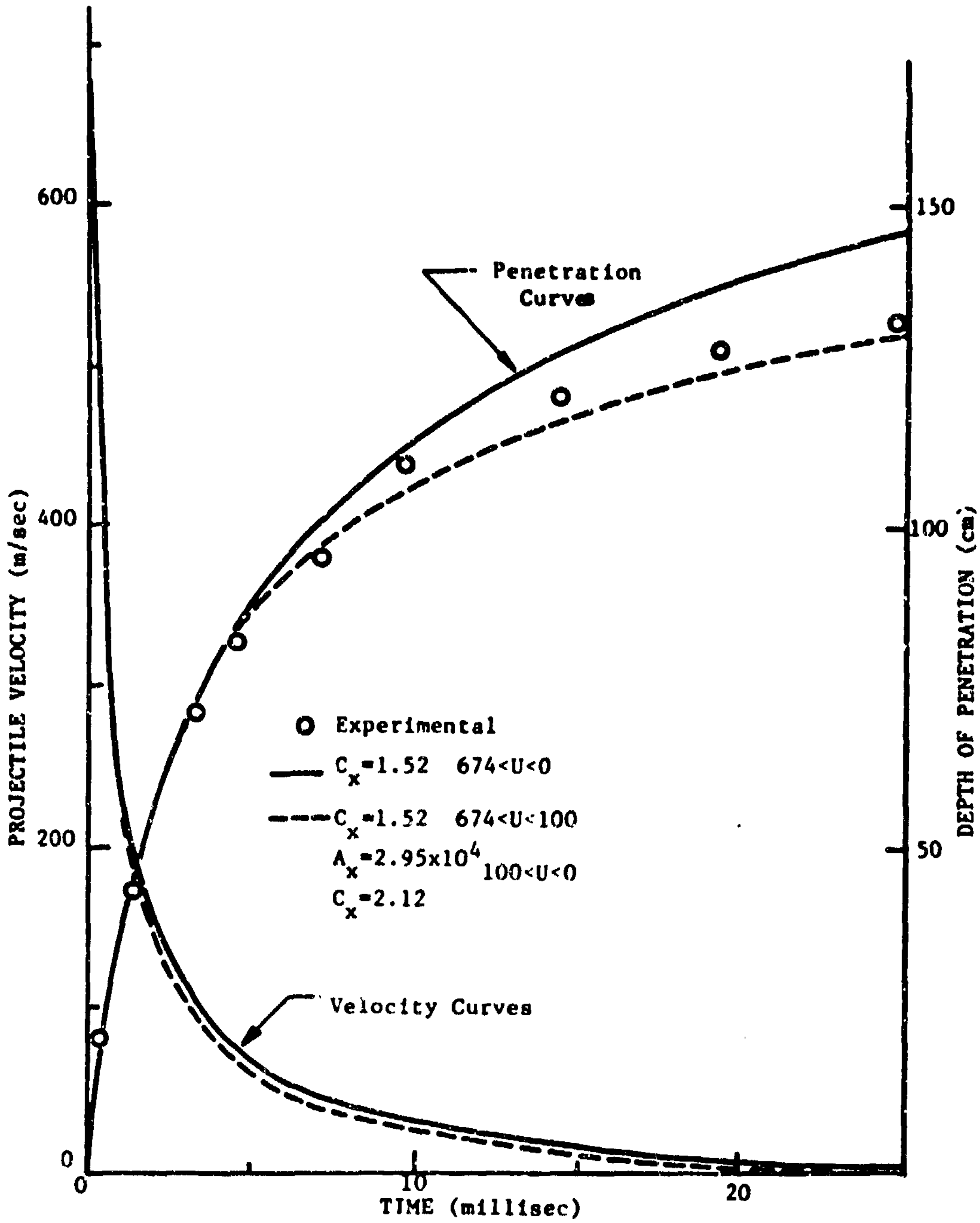

Figure 64. Model Verification Using Data of Reference 14. Projectile Velocity and Depth of Penetration versus Time

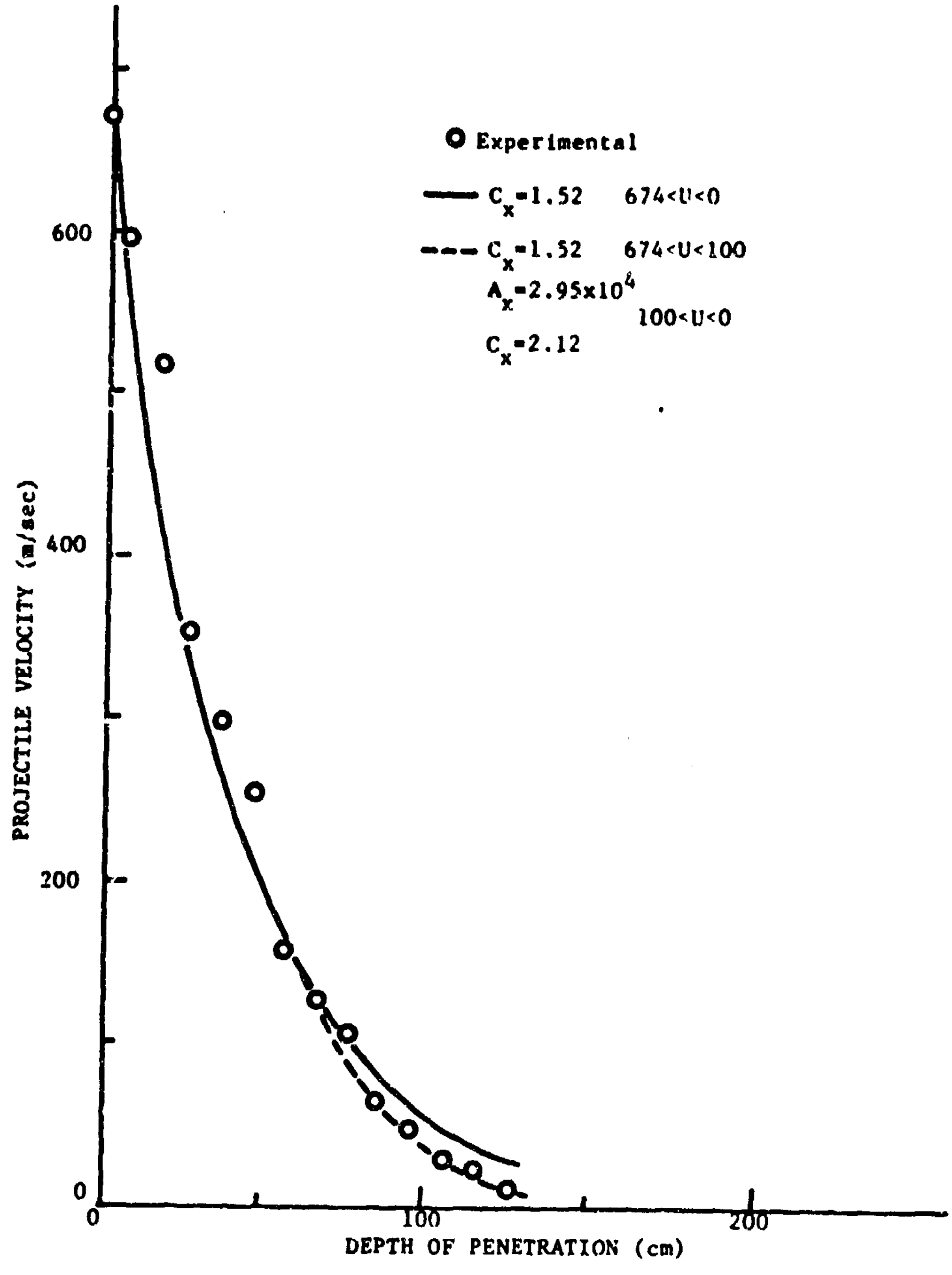

Figure 65. Model Verification Using Data of Reference 14. Projectile Velocity versus Depth of Penetration

good agreement between model and experimental values. Both figures show a comparison between using a constant value of C_x for the whole velocity range and using values for A_x and C_x for velocities below the critical velocity of 100 m/sec. The overall effect of using a value for A_x is to reduce the depth of penetration at the lower velocities and bring the projectile to rest at some finite time. The significant difference of the two cases is shown in the reduction of depth of penetration of Figure 64.

Further verification of the analytical model was obtained by use of experimental data of the Eglin experiments. As discussed in Section II velocity measurements of solid blunt nosed cylinders were made using an X-ray technique. The reduction in velocity during the trajectory was assumed to be attributed to a drag term based on the expression

$$F_x = \frac{1}{2} C_D \rho_s A(\dot{x}')^2 \qquad (54)$$

where C_D is defined as the drag coefficient in the x' direction, ρ_s is the undisturbed soil density and A is the cross sectional area of the projectile. By using this assumption and analyzing the data as in paragraph 4.6, it was found that C_D had a variation with velocity as given in Table 11. Also, if x' and x are assumed to be collinear, then $\dot{x}'$ and U are equal.

TABLE 11. VARIATION OF C_D WITH VELOCITY $\dot{x}'$.

DRY SAND	
$\dot{x}'$ m/sec	C_D
0	4.0
12.7	3.0
25.4	2.2
76.2	2.0
152.4	1.9
228.6	1.25
304.8	1.25
2540.0	1.7

The data of Table 11 fit a power law of the form

$$C_D = aU^b \qquad (55)$$

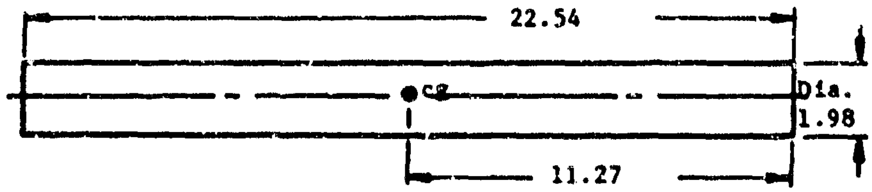

Geometric Values and Initial Conditions

mass = 544 gm

I_{xx} = 268 gm-cm^2

I_{yy} = 23170 gm-cm^2

$I_{yy} = I_{zz}$

$I_{xy} = I_{xz} = I_{yz} = 0$

$U_o = 4.06 \times 10^4$ cm/sec
$= 3.28 \times 10^4$
$= 2.12 \times 10^4$

Three different runs with all other input remaining constant.

$V_o = W_o = P_o = Q_o = R_o = \Psi_o = \phi_o = \theta_o = 0$

$\dot{Y}'_o = \dot{Z}'_o = X'_o = Y'_o = Z'_o = 0$

FORCE COEFFICIENTS

$A_x = B_x = A_y = B_y = C_y = A_z = B_z = C_z = 0$

$C_x = 4.1(U_{crit})^{-0.1}$ for all values above U_{crit}
U_{crit} undetermined but approximately 10^4 cm/sec

Figure 66. Data for Sample Run of Computer Program II

where a = 3.12 and b = -0.1 when U is expressed in cm/sec. If equation (54) is compared to Equation (45) then the relation between C_x and C_D is given as

$$C_x = \frac{1}{2} \rho_s C_D. \tag{56}$$

The density of the soil ρ_s used in the experiment was 1.6 gm/cm^3; therefore $C_X = 0.8C_D$.

Modifying the Computer Program I to include Equations (54) to (56) results in the Computer Program II given in Appendix C. The data used as input for this case are given in Figure 66.

The results of these runs are given in the graphs of Figures 67 and 68. Figure 67 shows the variation of depth of penetration with variations in impact or initial velocity. Figure 68 shows correlation of model prediction with experimentally determined data.

6.5 CONCLUSIONS

The results of the preceding paragraph show that a simple basic terradynamic approach using experimentally determined force coefficients will yield reasonable results. However, it must be emphasized that this method is highly dependent on good data obtained by experiment. The lack of force coefficients for angle of attack and other than normal impact prevents model verification for a general case.

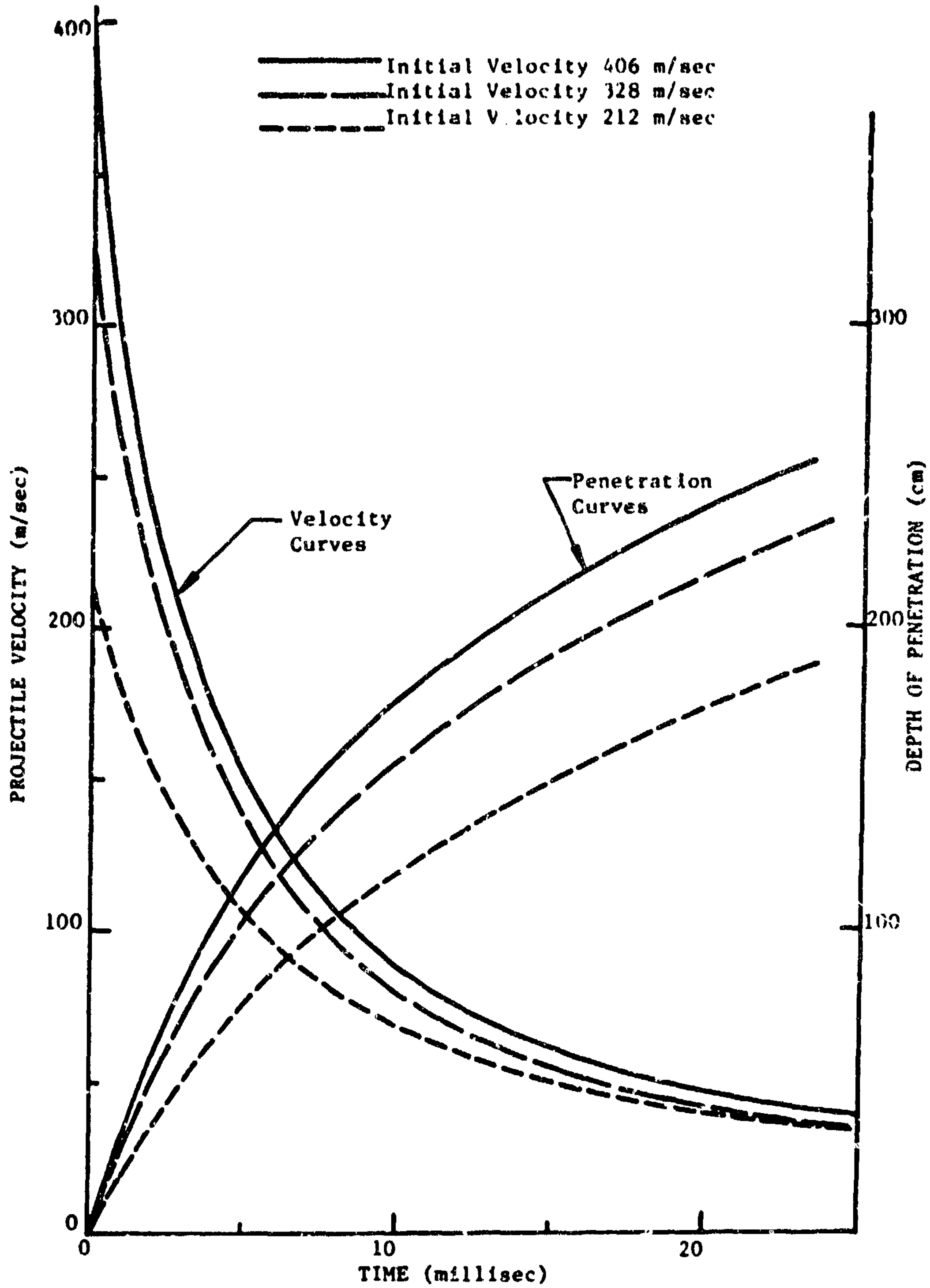

Figure 67. Model Verification Using C_D Data of Table 11

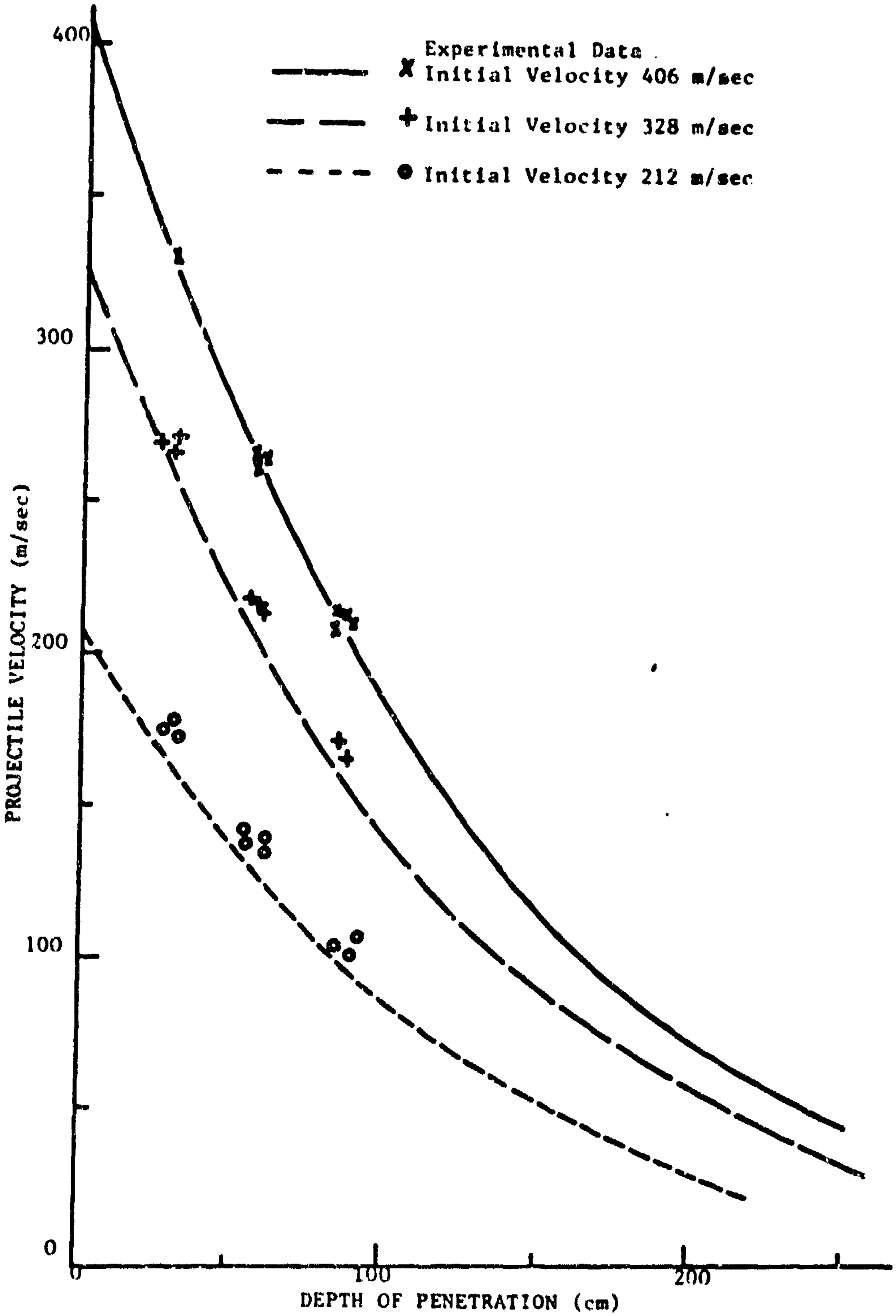

Figure 68. Model Verification Using C_D Data of Figure 66

SECTION VII

SONIC AND ULTRASONIC WAVE SPEED MEASUREMENTS

7.1 INTRODUCTORY REMARKS

The preceding sections have dealt with the testing and performance characteristics of terradynamic vehicles, including trajectory, cavity shape, separation, reattachment and stability. Predictive techniques which allow for a quantitative assessment of earth penetrating vehicle performance require information on certain parameters. Important among these parameters as inputs into terradynamic models are the density and the acoustic impedance of the target medium (Reference 29). The acoustic impedance, which is related to the wave velocity in the material, has particular importance in delineating regimes of application of penetration equations as well as in perhaps predicting bow wave speeds observed in the X-ray studies.

One technique which has been explored in the current test program for obtaining information on the above parameters is ultrasonic wave speed measurement. The use of ultrasound as a diagnostic and measurement tool is well documented. Pohlman (Reference 30), for example, has catalogued ultrasonic research topics in a series of volumes with frequent updating of the literature. Specific descriptions of ultrasonics in diagnostic applications have also been discussed in such references as (References 31,32), while techniques for measurement of mechanical parameters are contained in References 33 through 35. Many mechanical properties measurements by ultrasound have been directed toward obtaining information on the elastic properties of either solid, liquid, or gaseous media using the pulse-echo or through-transmission techniques, as described for example by McSkimin (Reference 36), Papadakis (Reference 37) and others (References 33 through 35). Some recent properties measurements on solid heterogeneous media such as fibrous composite materials and rock media have been reported on in References 40 through 42. These media, while dispersive in nature, remain amenable to conventional ultrasonic testing procedures because of the retention of specimen shape during machining. For granular or solid media, in which three distinct phases are present (solid, liquid and gas), and for which confined samples are not readily produced, measurement of mechanical properties becomes more involved. Some data collection related to soil media has been reported in References 43 through 46. Because of the phase inhomogeneity, properties measurements for soil types such as dry or saturated sands are difficult tasks. For example, dilatational wave speeds through dry sands by sonic radiation provide reasonable properties data, while similar measurements through saturated sand have proved unsatisfactory (Reference 43).

The filled pores allow rapid propagation of dilatational waves, so that measurements of the waves transmitted by the skeletal phase generally require the measurement of shear waves instead. These waves appear to reflect a better standard measurement of the skeletal stiffness and are frequently used in testing soils properties at ultrasonic frequencies. For this reason many of the tests reported in the literature report data on the propagation of shear waves (Reference 44).

In obtaining such data it is important to note that considerable disparity in the reported magnitude of acoustic waves in soils appears in the literature. This discrepancy is partially due to the measuring technique used, type of pulse disturbance used for generating the transmitted signal, and amplitude of resulting disturbances. In any event it is important to note that current analytical models appear inadequate to predict wave velocities and it is necessary to obtain quantitative measures of the wave velocities in real soils by experimental procedures (Reference 44).

In the studies reported in this section, wave speeds in dry or moist Eglin sand (5 to 15 percent moisture by weight) have been investigated with three purposes in mind: (1) to obtain input for existing penetration codes requiring this information or for delineating bounds on the usefulness of terradynamic equations (Reference 29), (2) for potential relationship to observed bow shock wave speeds (Reference 21), and (3) for possible use as a tool for establishing the compaction state of sand.

The major part of the investigation has been concerned with ultrasonic wave speed measurements as a function of compaction and testing pressure. Several difficulties were encountered with the testing program, and it still has had only limited success. The difficulties were associated with the dispersive nature of the sand medium, especially at high frequencies and low testing pressures. The ultrasonic wave speed measurement techniques and results will be described in paragraph 7.2.

A brief discussion will be given in paragraph 7.3 of some low frequency field measurements of sound wave speeds.

7.2 EXPERIMENTAL PROCEDURES AND RESULTS FOR ULTRASONIC WAVE SPEEDS

A Panametrics Ultrasonic Intervalometer system was available at the University that could be used either in a pulse-echo-overlap method with the same transducer used both for sending and for receiving the reflected signal or in a through-transmission method with separate sending and receiving transducers. Because of the dispersive nature of the medium, effort was concentrated on the through-transmission method. The Panameterics system can be used alone with broad band single pulses, or in conjunction with a pulsed radio-frequency (RF) oscillator it can be used with a burst of RF oscillations.

The first testing of sand samples used the single broad band pulse from the Ultrasonic Pulsing Module of Panametrics system as input signal to a Panametrics Type V201 5 MHz longitudinal transducer. The sand was first compacted under conditions of uniaxial strain in a steel cylinder 0.05 meter in diameter under axial pressure of 4.4 to 22 MPa. After unloading, end plates each containing one of the transducers were mounted on the cylinder and the broad band pulse applied to one end. The broad band pulse contains all frequency components, but the received signal resembled a distorted sine wave with the first few oscillations at a frequency 0.02 times the 5 MHz transducer resonant frequency. An example is shown in Figure 69.

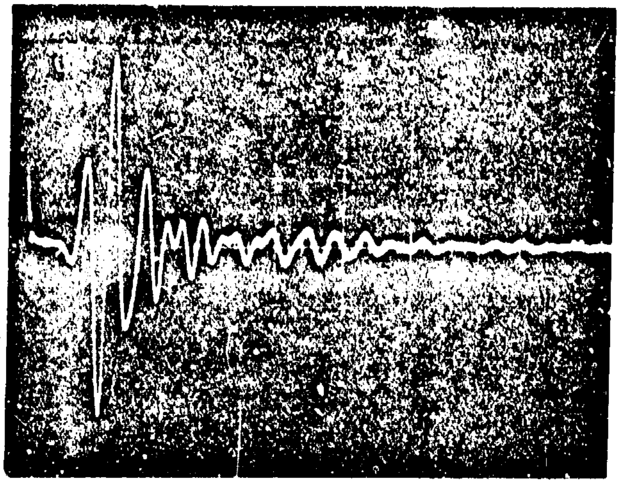

(Sweep Speed 20 μs/cm, vertical 50 mv/cm)

Figure 69. Received Pulse from Broadband Input Pulse

A portion of the input broadband pulse is seen at the beginning of the oscilloscope trace, driving the signal off screen. The received pulse is amplified and mixed with the broadband pulse internally in the Panametrics unit and then displayed on an oscilloscope. Precise timing can be accomplished in a manner similar to that for the RF bursts as will be described later in this section. More details on the operation of the Panametrics system are given in Reference 45.

The pulse displayed in Figure 69 was transmitted through a sand sample 0.0094 meter thick while under an axial pressure of about 0.2 MPa after compaction by an axial pressure of 4.4 MPa in the steel cylinder. The attenuation of the pulse by the sand was so great that this equipment and procedure could not be used with samples much thicker than 0.05 meter. Also the signal became erratic when the applied axial pressure during the wave speed measurement was about 0.1 MPa(approximately 15 psi) and disappeared altogether at some lower pressure. But the most disappointing feature of the results was that the measured wave speed appeared to depend on the thickness of the sample. This is a result of the change in shape of the pulse as it propagates through the dispersive medium. What was measured in these tests was the speed of propagation of the leading edge of the received pulse, which would be the group velocity of the transmitted wave packet of oscillations if the transmitted packet did not change its shape so much.

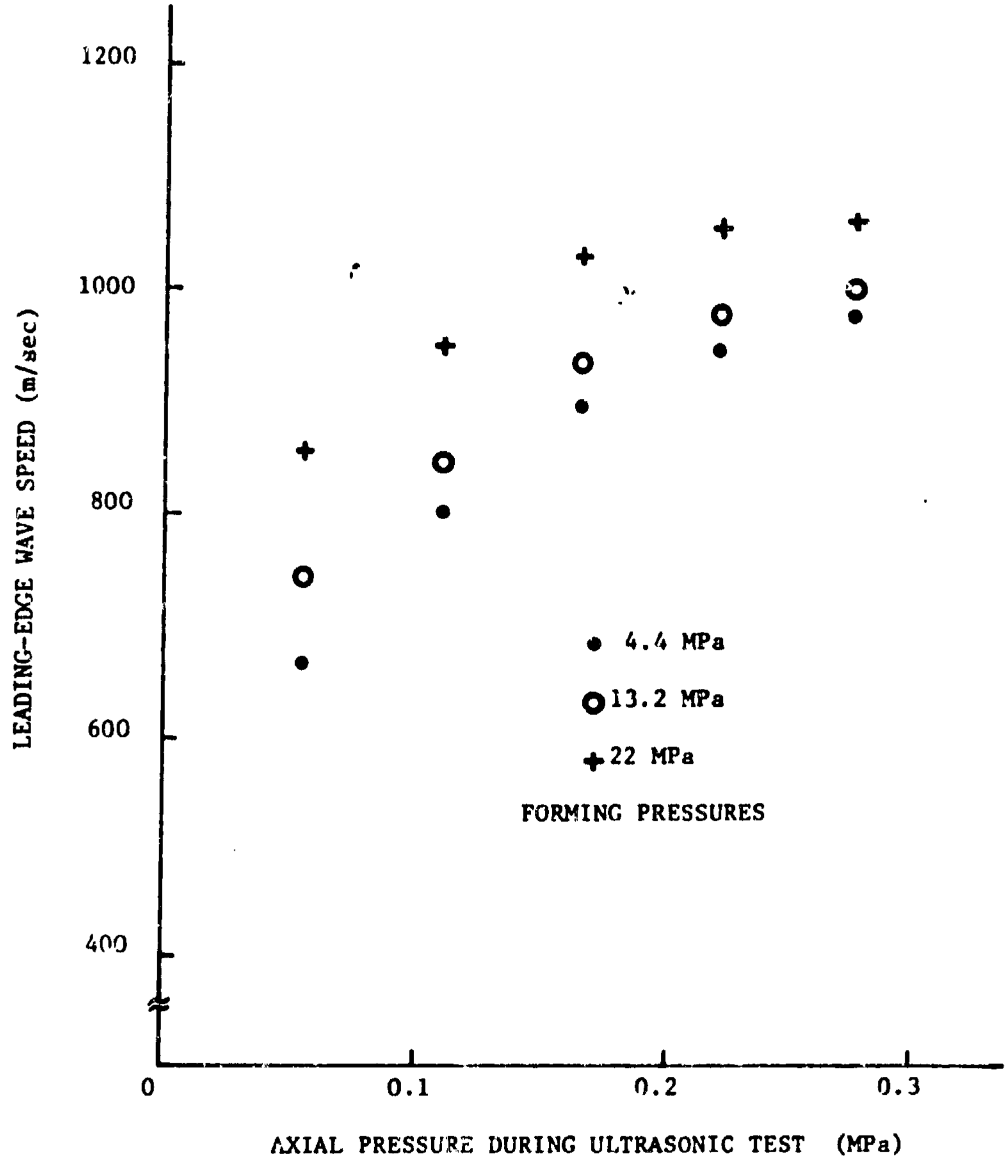

Figure 70. Leading-Edge Wave Speeds for a 0.01-meter-thick Dry Sand Sample

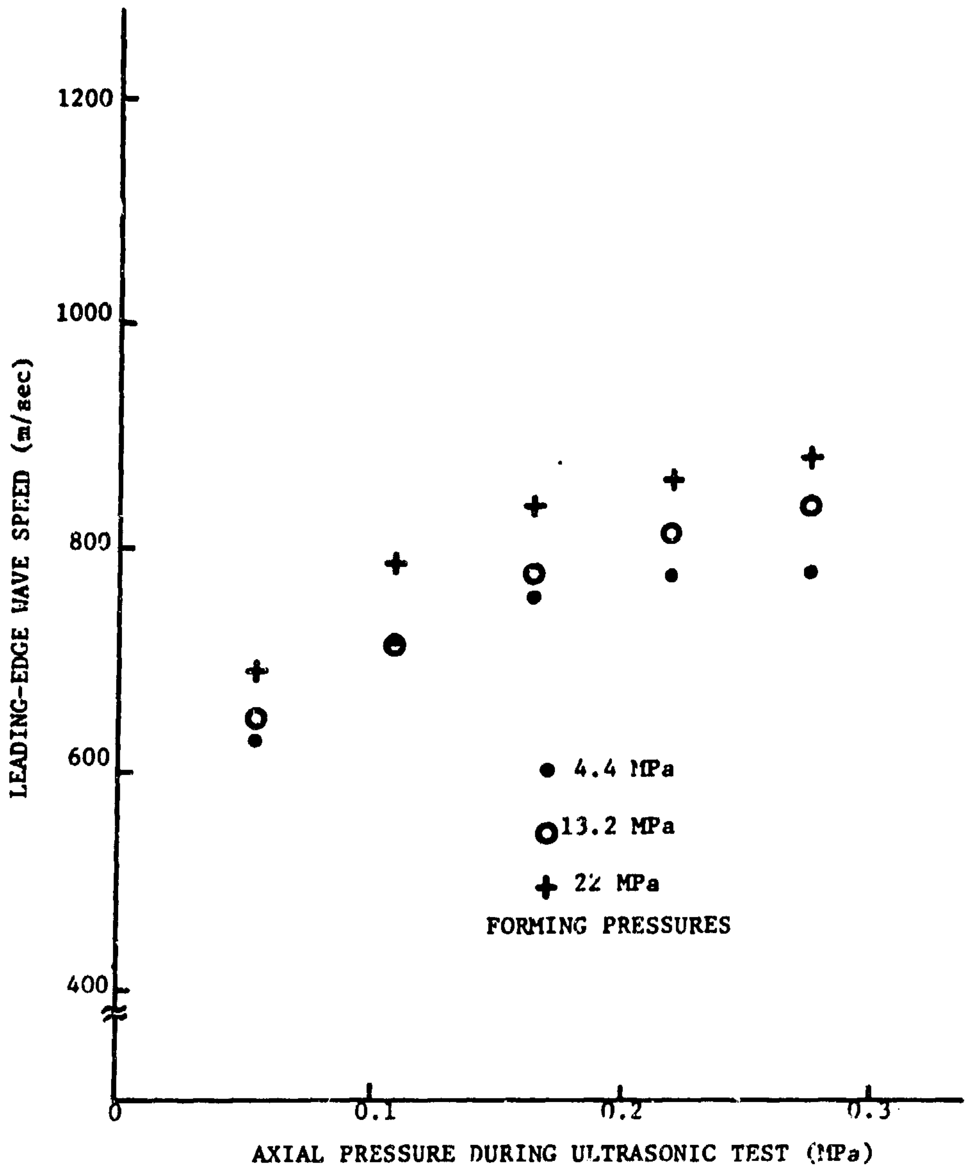

Figure 71. Leading-Edge Wave Speeds for a 0.023-meter-thick Dry Sand Sample

Figure 70 shows the leading-edge wave speed for a 0.01-meter-thick dry sand sample versus axial testing pressure varying from about 0.05 MPa to about 0.30 MPa for specimens previously compacted at three different axial pressures. Figure 71 shows the same kind of plot for a 0.023-meter-thick dry sand sample. Figure 72 is a photograph of the steel cylinder in place in a fixture mounted in a Tinius Olsen universal testing machine to provide the axial force during testing. The two transducer leads can be seen coming out of the fixutre. In this setup the transducers (not visible) are inside the end plates in direct contact with the sand.

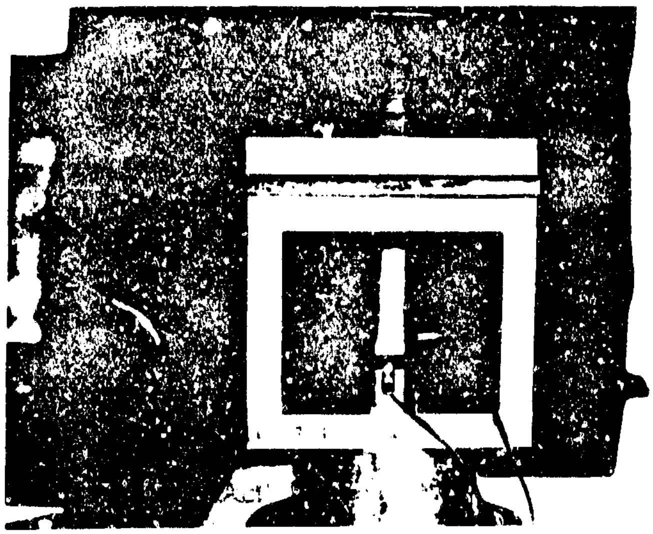

Figure 72. Fixture for Ultrasonic Wave Speed Measurements in Sand Contained in Cylinder Under Axial Load

Some additional tests of this type were performed on samples with moisture contents of 5, 10, and 15 percent by weight. At the highest forming pressure the 15 percent sample was saturated. The other samples were not saturated. The results indicated that increasing the moisture content increases the attenuation and decreases the wave speed, but the leading-edge speed results were again imprecise because of the changing shape of the transmitted pulse.

It was proposed then to obtain an RF pulser, since it was believed that the RF bursts, containing a single dominant RF frequency could be used to measure group velocity of the RF burst in a manner that would not appear to depend upon specimen thickness. It was also proposed to use the new equipment to study the effect of various amounts of air and water in the three-phase sand medium. In particular it was proposed to compare results with the predictions of an equation derived by Liahov (Reference 46) and discussed by Cristescu (Reference 47).

An Arenberg Ultrasonic Laboratory oscillator, Model II (PG-65-2-C) with 400 watts peak power was obtained. It was furnished with three coils for the RF frequency ranges of 4.3 to 7.5 MHz, 0.81 to 1.1 MHz, and 0.45 to 0.62 MHz. Additional coils can extend the range to operate anywhere in the 0.13 to 190 MHz frequency range with some loss of power at the lower frequencies.

Figure 73 shows a block diagram of the Arenberg oscillator (RF pulser) connections with the Panametrics unit. The single pulse from the Pulsing Module of the Panametrics unit triggers the Arenberg RF Pulser which then emits an RF frequency burst of variable length (e.g. 5 to 20 cycles at 0.5 MHz). This input pulse travels to the sending transducer which sends a mechanical stress wave burst through the sample to the receiver and preamplifier and then to the oscilloscope (CRO). The input pulse is also attenuated and fed directly to the CRO y-input terminal for comparison with the received signal.

If the transmitted signal has the same wave form as the input signal, very precise timing can be obtained as follows. After the attenuated input signal and amplified output signal have been displayed on the oscilloscope (CRO) using the internal sweep of the CRO, the final precise measurement is made by switching to a sweep provided by the variable-frequency CW oscillator of the Panametrics system. The sweep frequency is adjusted so that the transmitted and received signals are made to overlap. The time interval between the two signals is then measured by the frequency counter of the Panametrics system.

In actuality the transmitted wave pulse is modulated by the transducers and the transmission through the sand, so that the output resembles the received signal from the broadband input (see Figure 69) more than it resembles the input RF signal, which has an essentially square envelope. But the oscillations within the pulse are at the frequency of the RF, and the overlapping technique can still be applied, except at low testing pressures where there is excessive distortion. For best results the RF burst should contain at least 20 cycles and the overlapping should be made to coincide at the middle of the burst, since there is some distortion at the beginning and at the end of the burst. Because the great attenuation made it necessary to use a very short specimen path, it was not possible to use such a long pulse, and usually the overlapping was performed on the second or third peak in the burst. This use of the RF technique did succeed in removing the apparent dependence of the measured wave speed on the thickness of the sample when the test was performed at axial pressures above about 0.5 MPa. Differences in wave speed between the different specimens was within 3 percent which is considered very close agreement for different sand samples. The sand specimen holder was redesigned so that the transducers were not in direct contact with the sand but transmitted the signal through the steel end plates without themselves being subjected to the static axial loads. They could thus be left in place during the axial loading to compact the sand and could measure wave speed at various times during the loading and unloading.

Figure 74 shows a stress-strain curve for a uniaxial strain test carried out in the steel cylinder. At the points marked on the curve, wave speed measurements were performed, with the results shown in Table 12.

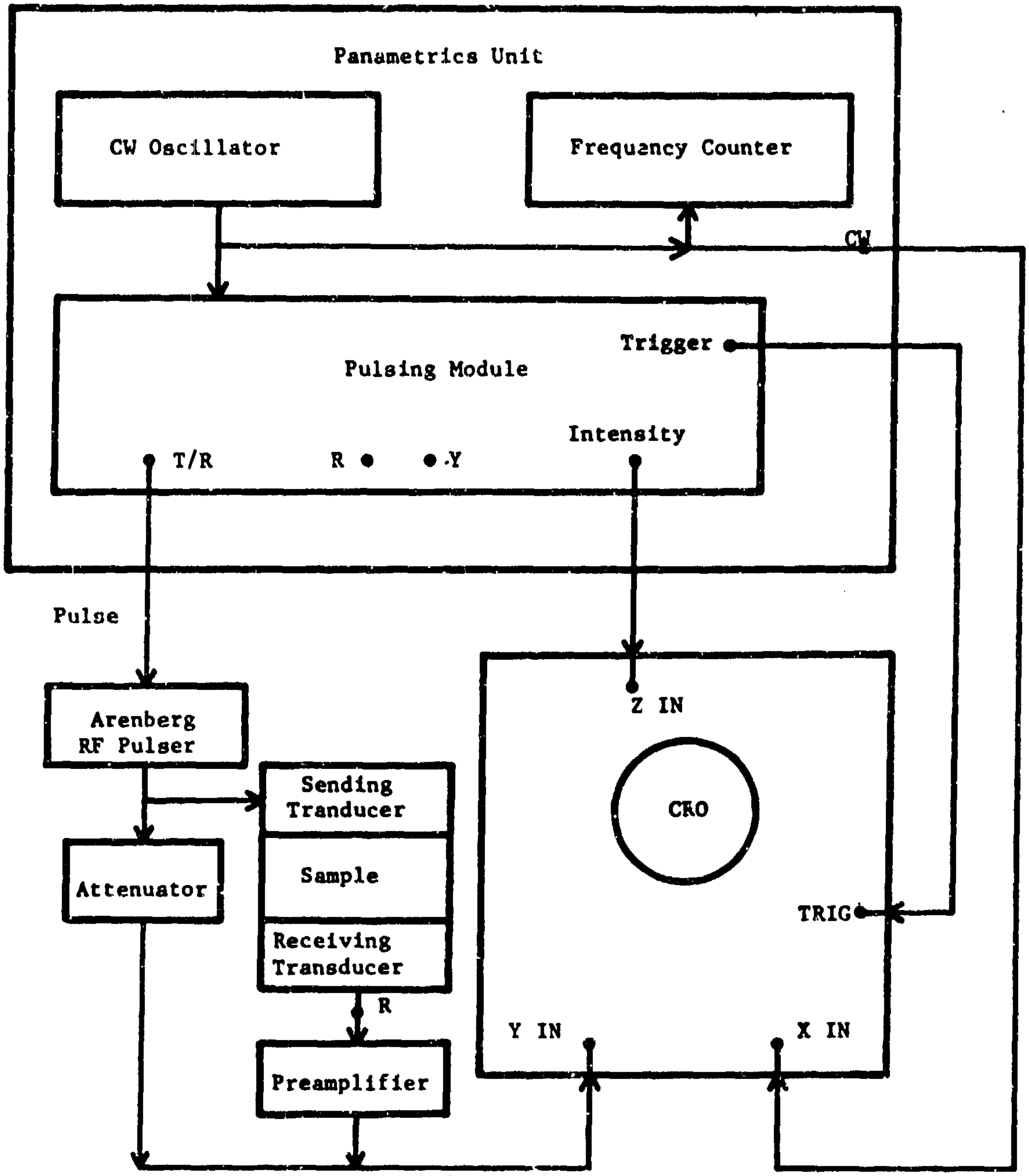

For use with broad band pulse, the T/R terminal is connected directly to the sending transducer, and the receiving transducer is connected to the R terminal on the Panametrics unit for internal amplification and mixing with the input pulse.

Figure 73. Block Diagram of Interconnections Between Arenberg Oscillator (RF Pulser) and Panametrics Unit

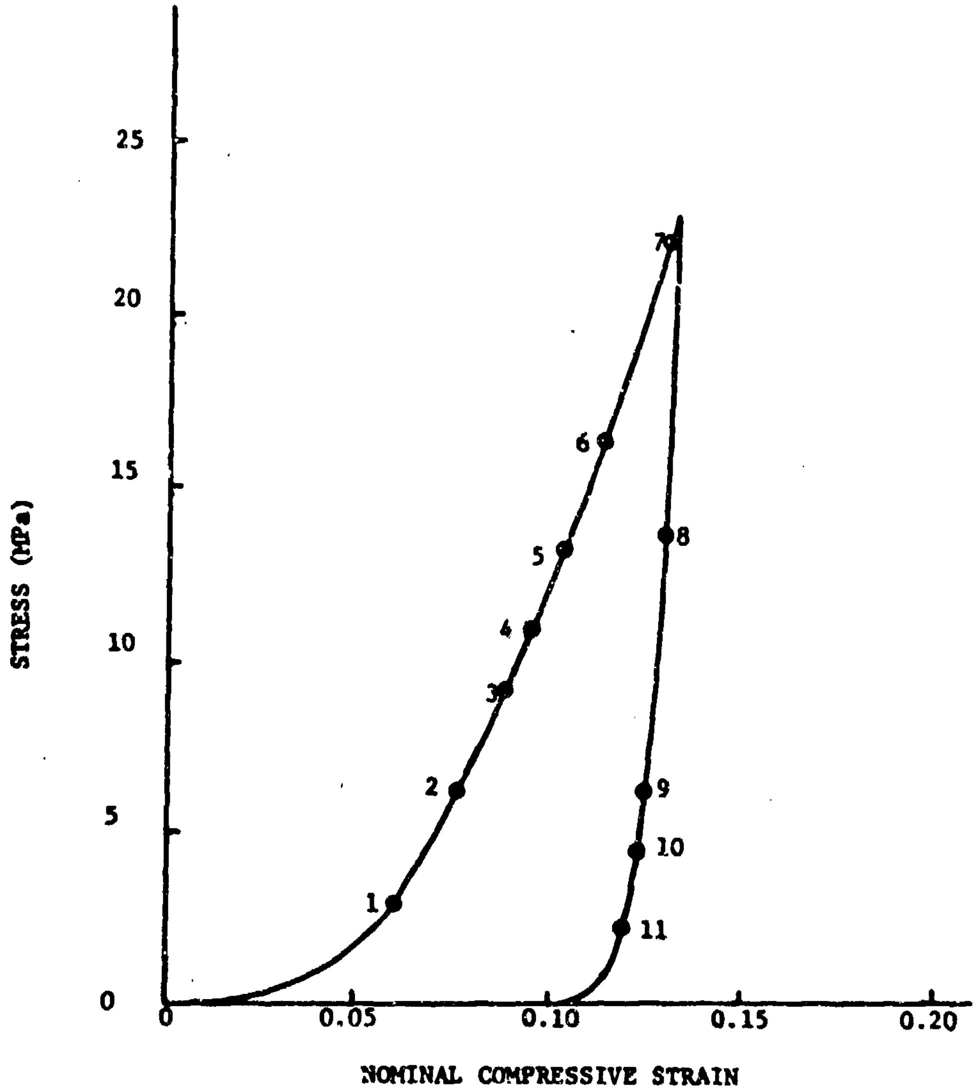

Figure 74. Stress-Strain Curve of Dry Eglin Sand in Uniaxial Strain (Numbers mark points where wave speeds were measured)

TABLE 12. WAVE SPEEDS DURING UNIAXIAL STRAIN TEST

Point	Stress (MPa)	Density Ratio ρ/ρ_o	Wave Speed (m/sec)
Loading			
1	3.08	1.065	910
2	6.14	1.081	1195
3	9.22	1.097	1280
4	10.98	1.106	1340
5	13.17	1.114	1390
6	16.48	1.128	1470
7	22.17	1.152	1600
Unloading			
8	13.61	1.150	1420
9	8.78	1.145	1280
10	6.14	1.142	1165
11	4.39	1.140	1070
12	2.19	1.136	960

These wave speeds are group velocities of the RF bursts. They show a very strong dependence on the testing pressure. It is remarkable how little difference was measured between the velocities during unloading and those during loading, despite the different compaction states and the different slopes of the loading and unloading curves. It seems clear that ultrasonic wave speed measurement will not be a good tool for determining the compaction condition.

For the last series of tests the 5 MHz transducer was replaced by a 1 MHz Panametrics Type V103 transducer, and testing was again performed with bursts of 0.5 MHz. By operating nearer the transducer resonance and by using the larger 1 MHz transducers with 4 times as much frontal area a greater power could be transmitted. It was hoped that this would permit testing at much lower axial pressures more like the ambient pressures in the penetration experiments. A signal was in fact received at pressures well below the previous minimum testing pressure of 0.5 MPa, but the transmitted signals were so badly distorted that the pulse overlap technique could not be used. The oscillations in the transmitted pulse appeared to be at a frequency about 20 percent below the RF frequency of the input signal. The reason for this is not clear, but it is believed to be related to the fact that at these low pressures the phase velocity is so low that the wave length approaches the order of magnitude of the sand particle size. Thus the medium no longer responds as a continuum. Because of the distortion, only leading-edge wave speeds could be measured at the low pressures and these with the same kind of errors and apparent dependence of the wave speed on specimen thickness as were previously observed with the broadband pulses at all testing pressures.

At higher testing pressures, however, good clean RF bursts were transmitted by the 1 MHz transducers operating at 0.5 MHz, and the group velocities could be measured quite accurately by the overlap technique.

The last series of tests examined the variation of the group velocity with testing pressure for pairs of dry sand specimens all of about 0.025 meter thickness with different initial densities. The two different initial compaction states at the same pressure were achieved by shaking one of the two specimens (by tapping the side of the steel container with a hammer) to compact the sand instead of by initially compressing it under axial load. Results for three such pairs of specimens, tested by loading to three different maximum values of axial pressure are shown in Figures 75 to 77. Each figure thus gives one curve for an initially loose sand (solid curve) and one for an initially dense sand tested over the same range of pressures. The so-called dense sand had an initial density 4 to 7 percent greater than that for the initially loose sand. The additional density increase during the test varied from about 1 percent for the dense sand in Figure 75 to about 5 percent for the loose sand tested to a higher pressure in Figure 77. The arrows on each curve indicate the direction of loading or unloading. Although the loading and unloading curves are not identical, the wave speeds at any testing pressure do not vary a great deal from the loading curve to the unloading curve. The extreme values from the three curves are listed in Table 13. The last-point densities upon unloading were not recorded, but they are approximately equal to the maximum densities.

Evidently the wave speeds are much more dependent on testing pressure than on the compaction state, so that wave speed measurements are not a good measure of compaction state.

Because of the difficulties encountered in the program, time did not permit further testing of wave speeds and attenuation as a function of moisture content. The Liahov equation (References 46,47) predicts significant differences in sound wave speeds in almost saturated sands for very small changes in the air content. Variations in the air volume fraction from 0.005 to 0.04 would change the wave speed by a factor of a third. It was not possible to attempt any verification of this theoretical prediction in the present program because of the difficulty in controlling the air content as well as the difficulty in measuring ultrasonic velocities at low pressures in sand.

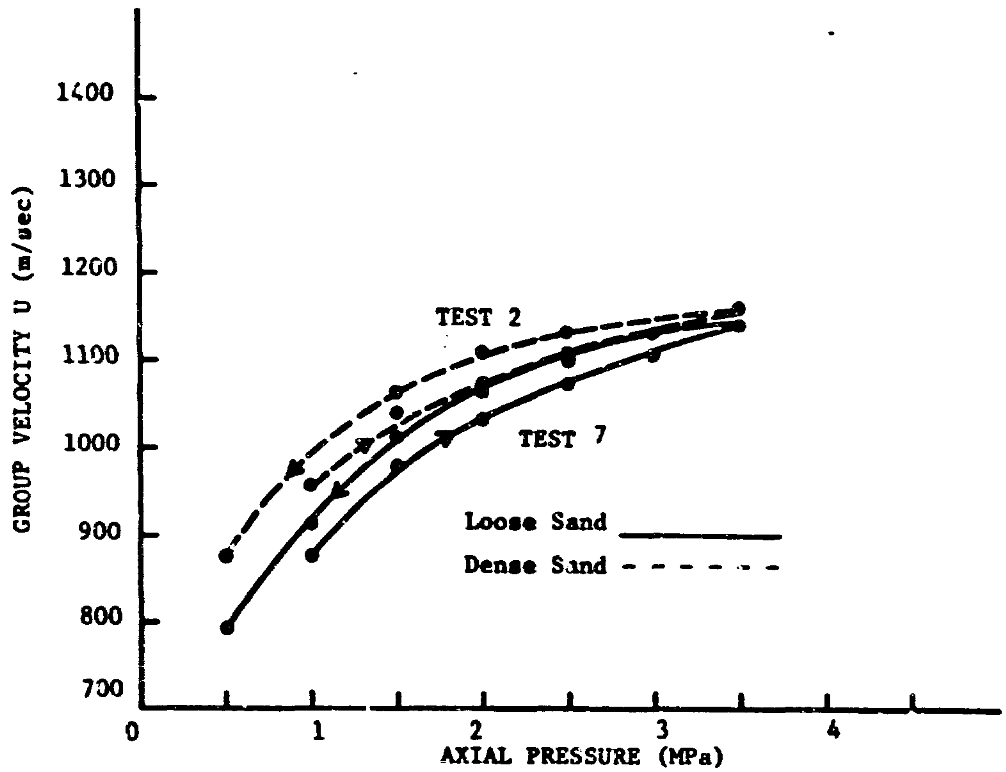

Figure 75. RF Wave Burst Wave Speed versus Axial Pressure in Uniaxial Strain Test to 3.5 MPa

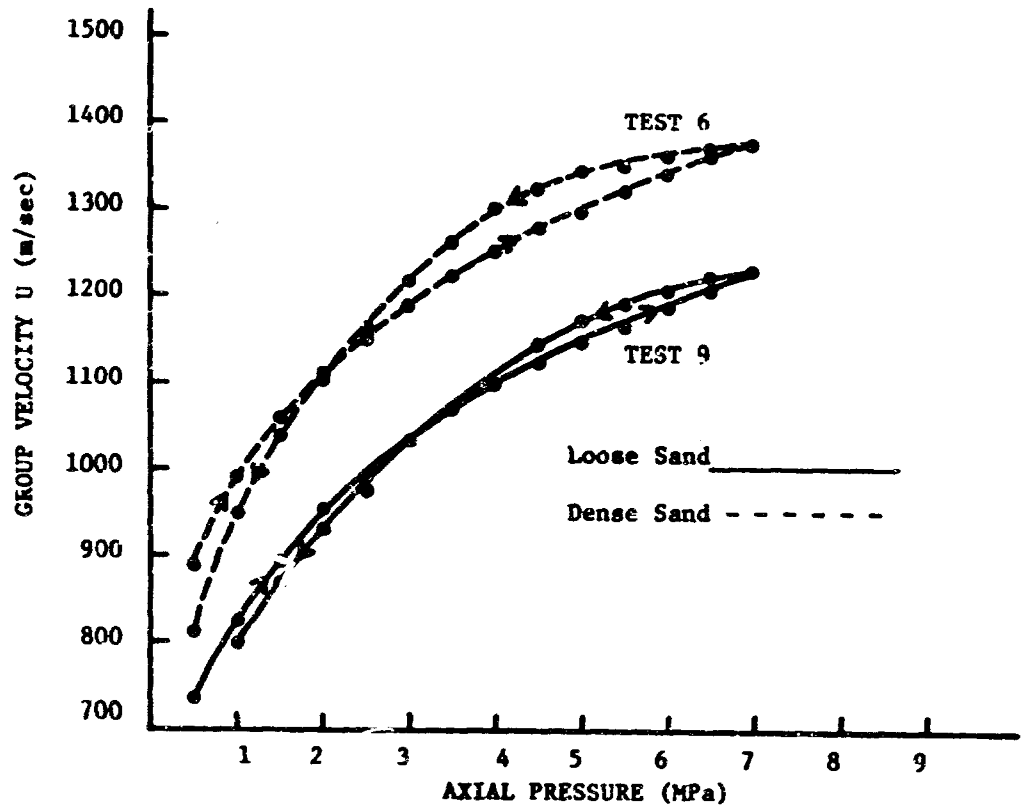

Figure 76. RF Wave Burst Wave Speed versus Axial Pressure in Uniaxial Strain Test to 7.0 MPa

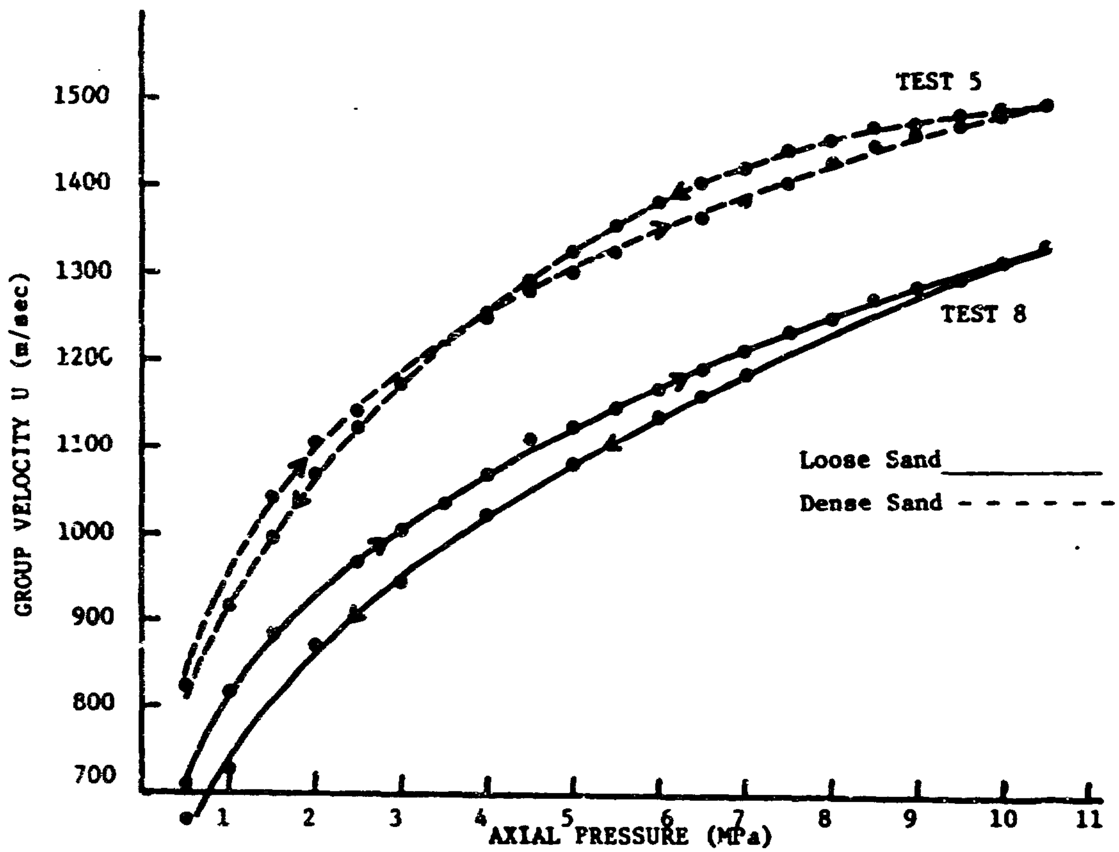

Figure 77. RF Wave Burst Wave Speed versus Axial Pressure in Uniaxial Strain Test to 10.5 MPa

TABLE 13. EXTREME VALUES OF PRESSURE AND WAVE SPEED IN FIGURES 75 to 77

		Density (kg/m^3)	Pressure (MPa)	Wave Speed (m/sec)
Figure 75				
Loose Sand	First Point	1638	1.0	875
Test 7	Maximum	1666	3.5	1140
	Last Point		0.5	790
Dense Sand	First Point	1726	1.0	960
Test 2	Maximum	1742	3.5	1170
	Last Point		0.5	875
Figure 76				
Loose Sand	First Point	1573	1.0	735
Test 9	Maximum	1636	7.0	1230
	Last Point		0.5	810
Dense Sand	First Point	1677	1.0	890
Test 6	Maximum	1723	7.0	1370
	Last Point		0.5	810
Figure 77				
Loose Sand	First Point	1585	0.5	710
Test 8	Maximum	1653	10.5	1335
	Last Point		0.5	670
Dense Sand	First Point	1644	0.5	835
Test 5	Maximum	1723	10.5	1500
	Last Point		0.5	810

The difficulty at the lower pressures is now believed to be caused by the fact that the lower wave speeds at the lower confining pressures lead to wave lengths of the order of magnitude of particle size. At low pressures, wave speeds of the order of 250 m/sec have been reported (Reference 14) although not at ultrasonic frequencies. The relationship between phase velocity c, frequency f, and wave length λ is (Reference 48)

$$c = f\lambda \tag{57}$$

At f = 1 MHz, and c = 1000 m/sec (the order of magnitude of the group velocities observed in the present program under high pressures) the wave length is 10^{-3} meters while the sand grain size is of the order of 10^{-4} to 2×10^{-4} meters. If at low pressures a speed of c = 250 m/sec could be expected, this would give a wave length at 1 MHz of 2.5×10^{-4} meters, about the same as the grain size. If the same speed 250 m/sec prevailed at lower frequencies, it would give $\lambda = 5 \times 10^{-4}$ meters at 0.5 MHz and $\lambda = 10^{-3}$ meters at 0.25 MHz.

This suggests that the high frequencies are not suitable for use in the sand. A brief discussion of some lower frequency testing is given in paragraph 7.3. The discussion of Equation (57) applies to phase velocities, while the measurements reported in this section have all been group velocities. In a dispersive medium, the phase velocity of a dilatational plane wave is a function of wave length, say $c = c(\lambda)$. A wave packet, such as the RF bursts of the experiments described, contains a spectrum of phase velocities with a dominant mean phase velocity, say c_o at wave length λ_o. The packet containing wave lengths predominantly near λ_o travels at a group velocity U, which is related to c_o by the following equation (Reference 48)

$$U = c_o - \lambda_o \left(\frac{dc}{d\lambda}\right)_o \tag{58}$$

If the medium is nondispersive $dc/d\lambda = 0$. Then $U = c_o$ and U is independent of wave length and frequency. But if the medium is dispersive, $dc/d\lambda \neq 0$, and the group velocity may differ markedly from the phase velocity. The phase velocities for the sand are not known at these frequencies, so an evaluation of U by Equation (58) is not feasible. It was observed in some preliminary tests that the group velocity of the RF was somewhat frequency dependent, but time and available equipment did not permit a determination of the frequency dependence over a wide frequency range.

The pulsed RF measurements can be used to determine phase velocity by using a specimen of thickness equal to one wave length (Reference 39), but this is not easy to do with the short wave lengths of the ultrasound. The technique is similar to that used with continuous waves. Some preliminary tests with continuous waves at lower frequencies are described in paragraph 7.3.

7.3 SOUND WAVE PHASE VELOCITIES

In July 1976 some preliminary field tests of low-frequency sonic phase velocities were performed at Eglin. The source for the sound waves was a 50-pound dynamic force MB vibration-testing shaker and power amplifier belonging to the University. A 0.1-meter-diameter aluminum plate was fabricated at the University and mounted on a shaft attached to the shaker armature and extending 0.15 meter outside a wooden box containing the shaker. The box was partly buried in the ground.

The tryout of the equipment was conducted jointly with the Mines Branch AFATL/DLJM, which provided geophones, recording equipment, and spectrum analysis. The setup worked well. A good strong continuous wave signal was obtained at a distance of 3.7 meters from the shaker, even when the power amplifier driving the shaker was operating at very low power. Higher power sometimes led to distortion of the sine-wave signal. The technique involved recording the signal at two stations. Frequency was increased slowly until the two signals were in phase, indicating that the two stations were one wave length λ apart. The dilatational phase velocity c is then given by $c = f\lambda$.

The preliminary tests indicate some dependence of wave speed on frequency, varying from about 108 m/sec at 59 Hz to 170 to 180 m/sec at around 100 Hz for two receiving stations 1.85 meters apart. The phase velocity at 100 Hz was comparable to the speed of 168 m/sec determined from the leading edge wave speeds of pulses produced by hammer blows. Higher frequency tests (up to about 19,000 Hz) were also recorded on magnetic tape for later analysis by methods not requiring the two signals to be in phase. Further tests of this type should be performed. It seems to be a good method for low-frequency sound-wave speed measurements, although care must be exercised in interpreting the results, which may be affected by reflections from the free surface and/or from internal boundaries in stratified media, especially when the two geophones are more than one wave length apart.

SECTION VIII

SUMMARY AND CONCLUSIONS

The results and conclusions of each phase of the investigation have been reported in previous sections. This final section summarizes them and indicates where more detail about them may be found. Section II described the Eglin experimental program and the various types of sensors used in it or evaluated for possible use. The sequential flash X-ray technique was judged to be the most successful method investigated, since it not only gave more complete and precise information about the trajectory and the projectile's position and attitude at various times than did any other method but also gave information on cavity formation and separation points and, in some cases, showed a shock wave ahead of the projectile. This investigation is believed to be the most extensive use ever made of flash radiography in terradynamic research. The magnetic sensors also provided good information about horizontal velocity.

The results of the experiments were described in Section III and interpreted in Section IV. The trajectory plots of paragraph 4.2 for the primary test program showed that the flat-nosed and step-tier projectiles had followed remarkably straight and stable horizontal paths through the 1.2-meters-long test chamber, although most of them exhibited a slight rise. Because the paths were so nearly straight, analysis by one-dimensional terradynamic models was feasible. A cubic interpolation formula gave a very accurate representation of the horizontal position-time data, and of the velocity near the middle of the interval. A classical Poncelet force-law penetration model, discussed in paragraph 4.3.2, gave an excellent account of the observed parts of the trajectories in dry sand, with a drag coefficient essentially independent of the striking velocity in the range of velocities observed. In saturated sand, each shot could be fitted by the Poncelet model, but the drag coefficient appeared to depend on the striking velocity, which showed that the Poncelet model does not really apply.

Drag coefficient variation along the trajectory was exhibited in paragraph 4.6. Although the velocity calculations of that section, each based on average velocity between only two stations, tend to magnify an error at one of the stations, they do show a trend of variation along the path, more pronounced in the wet sand cases than in the dry. The classical Poncelet force law gave more consistent results than a modification of the Sandia empirical method. In all of the analyses of Section IV, force law coefficients were determined to fit observed penetration data, and the success of a model was judged on the basis of agreement between the coefficient values fitted to the different shots.

The cavity-expansion penetration model of Section V, on the other hand, attempts to predict the penetration behavior from statically measured soil properties. Despite the rather strong assumptions involved in this simple analytical model, it gave very good results in predicting the behavior for two flat-nosed projectiles in dry sand. It was necessary to assume a shape for the false nose of sand carried along by the flat-nosed projectile.

An assumed hemispherical nose or a conical nose with length-to-diameter ratio of 0.4 to 0.5 led to very close agreement between the predicted and observed position-time and velocity-position curves, even for shots in a velocity range higher than the range for which previous investigations had validated the method. The success of this model suggests that it should be considered further, possibly for oblique impacts.

A three-dimensional trajectory analysis based on an assumed three-dimensional differential force law was presented in Section VI. The procedure was carried through for a case of a straight trajectory with a drag coefficient varying with velocity according to a power law, with reasonable results. It could be applied to a trajectory with an angle of attack or an oblique impact if suitable force coefficients could be determined or estimated.

Section VII reported on an independent investigation of ultrasonic wave speeds as a function of sand compaction and testing pressure. Several difficulties were encountered in the investigation. Pulse shape changes made it impossible to establish single broadband pulse propagation speeds that were independent of path length. This difficulty was overcome by using RF bursts instead of single pulses. Group velocities measured for these bursts gave (with an RF frequency of 0.5 MHz) consistent results for ambient testing pressures greater than about 0.5 MPa, but at lower pressures the signals were too badly distorted to give consistent results. This is believed to be a result of the fact that the lower pressures lead to lower wave speeds and a wave length of the order of sand grain dimensions. It is recommended that in further studies of sound wave speeds in sand attention be concentrated on lower frequencies. The group velocities showed a greater dependence on the testing pressure than on the compaction state.

REFERENCES

1. Triandafilidis, G.E., State of the Art of Earth Penetration Technology, TR CE-42(76)DNA-297, May 1976.

2. Poncelet, J.V., Cours de Mécanique Industrielle, First Edition, Paris, 1829.

3. Hanagud, S. and Ross, B., "Large Deformation, Deep Penetration Theory for a Compressible Strain Hardening Target Material", AIAA Journal, Vol. 9, No. 5, pp. 905-911, May 1971.

4. Rohani, B., "High Velocity Fragment Penetration of Soil Targets", Proc., Conference on Rapid Penetration of Terrestrial Materials, Texas A & M University, College Station, Texas, 1972.

5. Norwood, F.R., Cylindrical Cavity Expansion in a Locking Soil, Sandia Laboratories, SLA-74-0201, Albuquerque, New Mexico, July 1974.

6. Bernard, R.S. and Hanagud, S.V., Development of a Projectile Penetration Theory, Report I, Penetration Theory for Shallow to Moderate Depths, U.S. Army Engineers Waterways Experiment Station, Technical Report S-75-9, Vicksburg, Mississippi, June 1975.

7. Bernard, R., Development of a Projectile Penetration Theory, Report 2, Deep Penetration Theory for Homogeneous and Layered Targets, U.S. Army Engineers Waterways Experiment Station, Technical Report S-75-9, Vicksburg, Mississippi, February 1976.

8. Henderson, D. and Stephens, R.L. "Impact and Penetration Technology" paper presented at the Fuze-Munitions Environment Characterization Symposium at Picatinny Arsenal, New Jersey, by AVCO Corp., November 1972.

9. Hermann, W. A Lagrangian Finite Difference Method for Two-Dimensional Motion Including Material Strength, AFWL, Technical Report WL-TR-64-107, November 1967.

10. Hageman, L.J. and Walsh, J.M. HELP--A Multi-Material Eulerian Program for Compressible Fluid and Elastic-Plastic Flows in Two Space Dimensions and Time, Systems, Science and Software, 3SIR-350, Vol.I, La Jolla, California, 1970.

11. Sedgwick, R.T. Theoretical Terminal Ballistic Investigation and Studies of Impact at Low and Very High Velocities, General Electric Co., Space Sciences Laboratory, Technical Report AFATL-TR-68-61, King of Prussia, Pennsylvania, 1968.

12. Young, C.W. The Development of Empirical Equations for Predicting Depth of an Earth-Penetrating Projectile, Sandia Laboratories, SC-DR-67-60, May 1967.

13. Young, C.W. Empirical Equations for Predicting Penetration Performance in Layered Earth Materials for Complex Penetrator Configurations, Sandia Laboratories, SC-DR-72-0523, December 1972.

14. Allen, W.A., Mayfield, E.B. and Morrison, H. L. "Dynamics of a Projectile Penetrating Sand," Journal of Applied Physics, Vol. 28, pp 370-376 and 1331-1335, 1957.

15. Hakala, W.W. "Resistance of a Granular Medium to Normal Impact of a Rigid Projectile", Ph.D. Dissertation, Virginia Polytechnic Institute, Blacksburg, Virginia, June 1965.

16. Robertson, H.P., Terminal Ballistics, National Research Council, Washington, D.C., 1941.

17. McNeill, R.L., "Rapid Penetration of Terrestrial Materials - The State of the Art", Proc., Conference on Rapid Penetration of Terrestrial Materials, Texas A & M University, College Station, Texas, 1972.

18. Colp, J.L., Caudle, W.N., and Romine, K.L., An Annotated Bibliography of Sandia Laboratories Publications Related to Terradynamics, Sandia Laboratories, SLA-73-0345, March 1974.

19. Wood, W.R., "Instrumentation of Penetration Projectiles Using Hard Wire & RF Data Transmission", Proc., Conference on Rapid Penetration of Terrestrial Materials, Texas A. & M University, College Station, Texas, 1972.

20. Murff, J.D. and Coyle, H.M., "A Laboratory Investigation of Low-Speed Penetration," Proc., Conference on Rapid Penetration of Terrestrial Materials, Texas A & M University, College Station, Texas, 1972.

21. Culp, M.F., Submunition Penetration into Tactical Targets, Lockheed Missiles and Space Co.,D434546, December 1975.

22. Culp, M.F., "Flash X-Ray Investigation of Penetrator Terradynamics," paper presented at 2'nd International Symposium on Ballistics, sponsored by American Defense Preparedness Association, Daytona Beach, Florida, March 1976.

23. Hoffman, P.R., McMath, R.R., and Migotsky, E., Projectile Penetration Studies, AFWL-TR-64-102, December 1964. (RTD-WL-TR-64-102)

24. Biele, A., An Investigation of the Terradynamic Stability of a Scaled Model Projectile, Masters Thesis, Mississippi State University, August 1973.

25. Lambe, T.W. Soil Testing for Engineers, John Wiley & Sons, New York, 1951.

26. Goodier, J.N. "On the Mechanics of Indentation and Cratering in Solid Targets of Strain Hardening Metal by Impact of Hard and Soft Spheres", Proc., 7th Symposium on Hypervelocity Impact, Vol. III, AIAA, New York, 1965, pp. 215-259.

27. Etkin, B., Dynamics of Flight, John Wiley and Sons, N.Y., N.Y., 1959.

28. Etkin, B., Dynamics of Atmospheric Flight, John Wiley and Sons, N.Y., N.Y., 1972.

29. Hadala, P.F. Evaluation of Empirical and Analytical Procedures used for Predicting the Rigid Body Motion of an Earth Penetrator, WES Report No. S-75-15, June, 1975.

30. Pohlman, R. Documentation in Ultrasonics (a citation series), Published by Laboratory for Ultrasonics, Aachen, Germany, 1970-1976.

31. Sharpe, R.S. Research Techniques in Nondestructive Testing, Academic Press, 1970.

32. Nondestructive Testing, NASA SP-5113, 1973.

33. KrautKramer J. and KrautKramer, H. Ultrasonic Testing of Materials, Springer-Verlag, N.Y. Inc., 1969.

34. Green, R.E., Jr., "Ultrasonic Investigations of Mechanical Properties" in Treatise on Materials Science and Technology, Vol. 3, Academic Press, 1973.

35. Schreiber, E., Anderson, O.L., Soga, N. Elastic Constants and Their Measurements, McGraw-Hill Book Co., 1973.

36. McSkimin, H.J. "Pulse Superposition Method for Measuring Ultrasonic Wave Velocities in Solids", J.Acoustical Society of America, Vo. 33, pp. 12-16 1961.

37. Papadakis, E.P. "Absolute Accuracy of the Pulse-Echo Overlap Method and the Pulse-Superposition Method for Ultrasonic Velocity", J.Acoustical Society of America, Vol. 52, pp. 843-949, 1972.

38. Ross, C.A. and Sierakowski, R.L. "Elastic Waves in Fiber-Reinforced Composites", Shock and Vibration Digest, Vol. 7, pp. 1-12, 1975.

39. Martin, A.G. "Ultrasonic Phase Velocity Measurement by Phase Comparison of Continuous or Pulsed Waves", Private Communication, 1976.

40. Friedman, M. and Bur, T.R. "Investigations of the Relations among Residual Strain, Fabric, Fracture and Ultrasonic Attenuation and Velocity in Rocks", Int.J.Rock Mech. Min. Sci. and Geomech. Abstra. Vol. 11, pp. 221-234, 1974.

41. Johnson, J.N., Lingle, R., Swolfs, H.S. The Determination of In Situ Anisotropic Elastic Moduli from Laboratory Ultrasonic and Field Seismic Measurements, Terra Tek TR 75-28, June, 1975.

42. Barker, L.M., Lingle, R., Hendrickson, R.R., Johnson, J.N. Measurement of Low-Pressure Static Elastic Moduli of Rock and Comparison with Ultrasonic Data, Terra Tek, TR 75-30, October, 1975.

43. Lawrence, F.V., Jr. The Response of Soils to Dynamic Loadings; Ultrasonic Shear Wave Velocities in Sand and Clay, WES Research Report R 65-05, January, 1965.

44. Richart, I.E., Jr., Hall, J.R., Jr., and Woods, R.D. Vibrations of Soils and Foundations, Prentice-Hall Co. 1970.

45. Operations Manual for Ultrasonic Time Intervalometer Pulsing Module 5053, Panametrics, Walthem, Mass., 1975.

46. Liahov, G.M., The Fundamentals of the Dynamics of Explosions in Soils and in Liquid Media [in Russian], Moscow, 1964.

47. Cristescu, N. Dynamic Plasticity, North-Holland Publ. Co., 1967.

48. Lindsay, R.B., Mechanical Radiation, McGraw-Hill Book Co.,1960.

APPENDIX A

DATA FROM EGLIN PENETRATION EXPERIMENTS

This appendix tabulates data from 74 shots of the Eglin experimental program, using one page for each shot, and listed in order by Shot Numbers. Descriptions of the various kinds of entries in the tables, both of experimentally measured data and of several kinds of information calculated in the data analysis, are given in paragraph 3. Further explanations of some of the calculated data groups may be found in paragraphs 3.3 and 4.4.

SHOT 14 (10 MARCH 1976, NO. 3)

SAND: DRY, DENSITY:1538. KG/M**3; APPROACHING VELOCITY: 420. M/S
PROJECTILE: SOLID FLAT NOSE MASS:0.5451 KG, D=0.02 M, L=0.225 M

X-RAY STATION	NO.1	NO.2	NO.3	NO.4	NO.5
TIME (SECOND)	.000224	.001304	.003401	.005621	.009161
CENTER OF GRAVITY POSITION (M)					
HORIZONTAL	-0.081	0.109	18.515	18.820	0.900
VERTICAL	0.127	0.132	18.232	18.232	0.167
INCLINATION ANGLE(DEG).	0.0	1.0	*****	*****	-6.5
SEPARATION ANGLE(DEGREE)					
ABOVE	****	****	****	****	****
BELOW	****	****	****	****	****
NOSE WIDTH (M ON FILM).	0.0250	0.0230	******	******	0.0230
NOSE POSITION (M)					
HORIZONTAL	0.032	0.222	18.535	18.839	1.013
VERTICAL	0.127	0.134	18.121	18.121	0.154
INPUT NOSE POSITION (M)					
HORIZONTAL	0.030	0.221	******	******	0.993
VERTICAL	-0.090	-0.083	******	******	-0.060

SHOT 15 (16 MARCH, 1976, NO. 4)

SAND: DRY, DENSITY:1538. KG/M**3; APPROACHING VELOCITY: 209. M/S
PROJECTILE: SOLID FLAT NOSE MASS:0.5452 KG, D=0.02 M, L=0.225 M

X-RAY STATION	NO.1	NO.2	NO.3	NO.4	NO.5
TIME (SECOND)	.000202	.001273	.003323	.005932	.009099
CENTER OF GRAVITY POSITION (M)					
HORIZONTAL	-0.084	0.058	0.361	18.820	19.125
VERTICAL	0.119	0.124	0.130	18.232	18.232
INCLINATION ANGLE(DEG).	0.5	0.5	0.0	*****	*****
SEPARATION ANGLE(DEGREE)					
ABOVE	****	****	****	****	****
BELOW	****	****	****	****	****
NOSE WIDTH (M ON FILM).	0.0245	0.0225	0.0225	******	******.
NOSE POSITION (M)					
HORIZONTAL	0.029	0.171	0.474	18.839	19.144
VERTICAL	0.120	0.125	0.130	18.121	18.121
INPUT NOSE POSITION (M)					
HORIZONTAL	0.027	0.164	0.467	******	******
VERTICAL	-0.095	-0.093	-0.088	******	******

SHOT 16 (11 MARCH, 1976, NO. 1)

SAND: DRY, DENSITY:1538. KG/M**3; APPROACHING VELOCITY: 212. M/S
PROJECTILE: SOLID FLAT NOSE MASS:0.5451 KG, D=0.02 M, L=0.225 M

X-RAY STATION	NO.1	NO.2	NO.3	NO.4	NO.5
TIME (SECOND)	.000170	.000898	.003034	.005808	*******
CENTER OF GRAVITY POSITION (M)					
HORIZONTAL	-0.085	0.057	0.403	0.748	19.125
VERTICAL	0.120	0.128	0.132	0.153	18.232
INCLINATION ANGLE(DEG).	2.0	1.0	5.0	7.0	*****
SEPARATION ANGLE(DEGREE)					
ABOVE	****	****	7.0	****	****
BELOW	****	****	2.0	****	****
NOSE WIDTH (M ON FILM).	0.0250	0.0230	0.0240	0.0250	******
NOSE POSITION (M)					
HORIZONTAL	0.028	0.170	0.515	0.860	19.144
VERTICAL	0.124	0.130	0.142	0.167	18.121
INPUT NOSE POSITION (M)					
HORIZONTAL	0.028	0.161	0.512	0.866	******
VERTICAL	-0.094	-0.087	-0.072	-0.040	******

SHOT 17 (11 MARCH, 1976, NO. 2)

SAND: DRY, DENSITY:1538. KG/M**3; APPROACHING VELOCITY: 212. M/S
PROJECTILE: SOLID FLAT NOSE MASS:0.5461 KG, D=0.02 M, L=0.225 M

X-RAY STATION	NO.1	NO.2	NO.3	NO.4	NO.5
TIME (SECOND)	.000217	.001307	.003540	.006220	.009140
CENTER OF GRAVITY POSITION (M)					
HORIZONTAL	-0.071	0.140	0.486	0.816	1.092
VERTICAL	0.120	0.128	0.135	0.143	0.162
INCLINATION ANGLE(DEG).	1.5	2.3	4.0	9.0	12.5
SEPARATION ANGLE(DEGREE)					
ABOVE	****	4.0	5.0	9.0	9.5
BELOW	****	2.5	1.8	1.0	1.[illegible]
NOSE WIDTH (M ON FILM).	0.0240	0.0230	0.0230	0.0230	0.02[illegible]
NOSE POSITION (M)					
HORIZONTAL	0.042	0.252	0.599	0.928	1.202
VERTICAL	0.123	0.132	0.143	0.161	0.187
INPUT NOSE POSITION (M)					
HORIZONTAL	0.043	0.256	0.609	0.941	1.211
VERTICAL	-0.095	-0.085	-0.072	-0.052	-0.022

NOSE VEL. Y-COMP. (M/S): 7. 6. 6. 7. 12.
COEFFICIENTS OF CUBIC POLYNOMIAL/STANDARD DEVIATION
0.1220E 00 0.7758E 01 -0.6430E 03 0.6267E 05 / 0.0013 (M)

NOSE VEL. X-COMP. (M/S): 201. 178. 139. 106. 86.
COEFFICIENTS OF CUBIC POLYNOMIAL/STANDARD DEVIATION
-0.4578E-03 0.2054E 03 -0.1116E 05 0.3377E 06 / 0.0043 (M)

NOSE VEL. DIRECTION(DEG)	2.1	2.1	2.3	3.8	7.8
SEPARATION ANGLE(DEGREE), RELATIVE TO NOSE VELOCITY					
ABOVE	****	3.8	3.3	3.8	4.8
BELOW	****	2.7	3.5	6.2	5.7

C.G. VEL. Y-COMP. (M/S): 8. 5. 3. 4. 10.
COEFFICIENTS OF CUBIC POLYNOMIAL/STANDARD DEVIATION
0.1185E 00 0.8457E 01 -0.1420E 04 0.1117E 06 / 0.0002 (M)

C.G. VEL. X-COMP. (M/S): 200. 178. 139. 106. 86.
COEFFICIENTS OF CUBIC POLYNOMIAL/STANDARD DEVIATION
-0.1133E 00 0.2051E 03 -0.1108E 05 0.3338E 06 / 0.0045 (M)

PONCELET DRAG COEFF. = 1.644
VO = 139. STAND. DEVIA. = 0.0087 (M)
C.G. VEL. X-COMP. (M/S): 210. 180. 139. 109. 89.

SHOT 18 (11 MARCH. 1976. NO. 3)

SAND: DRY. DENSITY:1538. KG/M**3; APPROACHING VELOCITY: 213. M/S
PROJECTILE: SOLID FLAT NOSE MASS:0.5451 KG. D=0.02 M. L=0.225 M

X-RAY STATION	NO.1	NO.2	NO.3	NO.4	NO.5
TIME (SECOND)	.000224	.001304	.003401	.005970	.009161
CENTER OF GRAVITY POSITION (M)					
HORIZONTAL	-0.073	0.136	0.462	0.778	1.065
VERTICAL	0.120	0.128	0.133	0.143	0.159
INCLINATION ANGLE(DEG).	1.6	2.0	4.6	7.4	8.5
SEPARATION ANGLE(DEGREE)					
ABOVE	****	5.5	5.0	6.5	9.5
BELOW	9.9	4.0	1.4	1.0	1.0
NOSE WIDTH (M ON FILM).	0.0255	0.0235	0.0230	0.0240	0.0255
NOSE POSITION (M)					
HORIZONTAL	0.040	0.249	0.575	0.890	1.177
VERTICAL	0.123	0.132	0.142	0.157	0.175
INPUT NOSE POSITION (M)					
HORIZONTAL	0.041	0.252	0.581	0.901	1.186
VERTICAL	-0.095	-0.085	-0.073	-0.054	-0.028

NOSE VEL. Y-COMP. (M/S): 7. 7. 6. 5. 7.
COEFFICIENTS OF CUBIC POLYNOMIAL/STANDARD DEVIATION
0.1217E 00 0.7488E 01 -0.4320E 03 0.2787E 05 / 0.0014 (M)

NOSE VEL. X-COMP. (M/S): 200. 178. 140. 105. 78.
COEFFICIENTS OF CUBIC POLYNOMIAL/STANDARD DEVIATION
-0.3601E-02 0.2051E 03 -0.1114E 05 0.3059E 06 / 0.0044 (M)

NOSE VEL. DIRECTION(DEG)	2.1	2.1	2.3	2.9	4.8
SEPARATION ANGLE(DEGREE), RELATIVE TO NOSE VELOCITY					
ABOVE	****	5.6	2.7	2.0	5.8
BELOW	9.4	3.9	3.7	5.5	4.7

C.G. VEL. Y-COMP. (M/S): 7. 5. 3. 3. 8.
COEFFICIENTS OF CUBIC POLYNOMIAL/STANDARD DEVIATION
0.1189E 00 0.6934E 01 -0.9250E 03 0.7026E 05 / 0.0019 (M)

C.G. VEL. X-COMP. (M/S): 200. 178. 140. 105. 78.
COEFFICIENTS OF CUBIC POLYNOMIAL/STANDARD DEVIATION
-0.1165E 00 0.2050E 03 -0.1107E 05 0.3011E 06 / 0.0045 (M)

PONCELET DRAG COEFF. = 1.624
VO = 200. STAND. DEVIA. = 0.0129 (M)
C.G. VEL. X-COMP. (M/S): 200. 173. 137. 109. 87.

```
SHOT 19   ( 11 MARCH. 1976. NO. 4 )

SAND: DRY. DENSITY:1538. KG/M**3: APPROACHING VELOCITY: 211. M/S
PROJECTILE: SOLID FLAT NOSE MASS:0.5459 KG. D=0.02 M. L=0.225 M

X-RAY STATION .........    NO.1      NO.2      NO.3      NO.4      NO.5

TIME (SECOND) ......... .000202  .001273  .003323  .005932  .009099
CENTER OF GRAVITY POSITION (M)
  HORIZONTAL .......... -0.068    0.141    0.464    0.783    1.072
  VERTICAL ............  0.121    0.126    0.136    0.151    0.183

INCLINATION ANGLE(DEG).   2.0      3.3      7.0     12.0     16.5
SEPARATION ANGLE(DEGREE)
  ABOVE ...............   4.0      5.0      6.5     11.0     11.0
  BELOW ...............   4.0      2.5      1.0      0.5      0.5
NOSE WIDTH (M ON FILM).  0.0243   0.0225   0.0225   0.0220   0.0225
NOSE POSITION (M)
  HORIZONTAL ..........  0.045    0.254    0.577    0.893    1.180
  VERTICAL ............  0.125    0.134    0.150    0.174    0.215
INPUT NOSE POSITION (M)
  HORIZONTAL ..........  0.047    0.257    0.582    0.899    1.185
  VERTICAL ............ -0.093   -0.083   -0.065   -0.039    0.008


NOSE VEL. Y-COMP. (M/S):    9.       8.       8.      10.      16.
COEFFICIENTS OF CUBIC POLYNOMIAL/STANDARD DEVIATION
  0.1232E 00  0.8648E 01 -0.3090E 03  0.6144E 05 / 0.0005 (M)

NOSE VEL. X-COMP. (M/S): 205.     180.     140.     104.      82.
COEFFICIENTS OF CUBIC POLYNOMIAL/STANDARD DEVIATION
  0.4456E-02  0.2097E 03 -0.1249E 05  0.3988E 06 / 0.0030 (M)


NOSE VEL. DIRECTION(DEG)  2.4      2.6      3.4      5.7     11.0
SEPARATION ANGLE(DEGREE). RELATIVE TO NOSE VELOCITY
  ABOVE ...............   4.4      4.3      2.9      4.7      5.5
  BELOW ...............   3.6      3.2      4.6      6.8      6.0


C.G. VEL. Y-COMP. (M/S):    6.       5.       5.       7.      14.
COEFFICIENTS OF CUBIC POLYNOMIAL/STANDARD DEVIATION
  0.1197E 00  0.6648E 01 -0.7450E 03  0.8547E 05 / 0.0007 (M)

C.G. VEL. X-COMP. (M/S): 205.     180.     140.     104.      82.
COEFFICIENTS OF CUBIC POLYNOMIAL/STANDARD DEVIATION
 -0.1084E 00  0.2096E 03 -0.1236E 05  0.3930E 06 / 0.0029 (M)

PONCELET DRAG COEFF. = 1.694
 VO = 205. STAND. DEVIA. = 0.0098 (M)
C.G. VEL. X-COMP. (M/S): 205.     176.     138.     109.      87.
```

```
                    SHOT 20    ( 11 MARCH, 1976, NO. 5 )

SAND: DRY, DENSITY:1338. KG/M**3; APPROACHING VELOCITY: 340. M/S
PROJECTILE: SOLID FLAT NOSE MASS:0.5481 KG, D=0.02 M, L=0.225 M

X-RAY STATION ..........   NO.1     NO.2     NO.3     NO.4     NO.5

TIME (SECOND) .........  .000130  .004832  .002143  .003795  .005807
CENTER OF GRAVITY POSITION (M)
  HORIZONTAL .......... -0.080    0.120    0.444    0.753    1.054
  VERTICAL ............  0.125    0.131    0.138    0.144    0.144

INCLINATION ANGLE(DEG).  0.0      0.8      0.0     -1.7     -2.3
SEPARATION ANGLE(DEGREE)
  ABOVE ...............  ****     6.0      4.6      2.5      2.5
  BELOW ...............  ****     7.4      5.7      7.0      6.8
NOSE WIDTH (M ON FILM). 0.0240   0.0225   0.0225   0.0225   0.0220
NOSE POSITION (M)
  HORIZONTAL ..........  0.033    0.239    0.557    0.866    1.167
  VERTICAL ............  0.125    0.132    0.138    0.140    0.140
INPUT NOSE POSITION (M)
  HORIZONTAL ..........  0.032    0.240    0.560    0.870    1.169
  VERTICAL ............ -0.093   -0.085   -0.079   -0.076   -0.077


NOSE VEL. Y-COMP. (M/S):  11.       8.       3.      -0.       1.
COEFFICIENTS OF CUBIC POLYNOMIAL/STANDARD DEVIATION
  0.1237E 00   0.1166E 02 -0.2712E 04  0.2035E 06 / 0.0010 (M)

NOSE VEL. X-COMP. (M/S): 313.     274.     215.     165.     141.
COEFFICIENTS OF CUBIC POLYNOMIAL/STANDARD DEVIATION
 -0.6087E-02  0.3206E 03 -0.3011E 05  0.1678E 07 / 0.0003 (M)


NOSE VEL. DIRECTION(DEG)  2.0     1.6      0.8     -0.0      0.3
SEPARATION ANGLE(DEGREE), RELATIVE TO NOSE VELOCITY
  ABOVE ...............  ****     6.8      5.4      4.2      5.1
  BELOW ...............  ****     6.6      4.9      5.3      4.2


C.G. VEL. Y-COMP. (M/S):   8.       7.       5.       2.      -1.
COEFFICIENTS OF CUBIC POLYNOMIAL/STANDARD DEVIATION
  0.1239E 00   0.8469E 01 -0.9080E 03  0.9984E 04 / 0.0006 (M)

C.G. VEL. X-COMP. (M/S): 313.     274.     215.     165.     141.
COEFFICIENTS OF CUBIC POLYNOMIAL/STANDARD DEVIATION
 -0.1211E 00   0.3206E 03 -0.3010E 05  0.1680E 07 / 0.0012 (M)

PONCELET DRAG COEFF. = 1.769
 VO = 215. STAND. DEVIA. = 0.0036 (M)
C.G. VEL. X-COMP. (M/S): 325.     276.     215.     168.     133.
```

SHOT 22 (11 MARCH, 1976, NO. 7)

SAND: DRY, DENSITY:1538. KG/M**3; APPROACHING VELOCITY: 328. M/S
PROJECTILE: SOLID FLAT NOSE MASS:0.5451 KG, D=0.02 M, L=0.225 M

X-RAY STATION	NO.1	NO.2	NO.3	NO.4	NO.5
TIME (SECOND)	.000165	.000697	.002198	.003855	.005820
CENTER OF GRAVITY POSITION (M)					
HORIZONTAL	-0.075	0.129	0.442	0.693	1.049
VERTICAL	0.123	0.130	0.135	0.139	0.152
INCLINATION ANGLE(DEG).	1.5	2.5	4.0	7.0	9.0
SEPARATION ANGLE(DEGREE)					
ABOVE	****	6.0	7.0	10.0	11.0
BELOW	****	3.0	3.0	2.0	1.5
NOSE WIDTH (M ON FILM).	0.0260	0.0230	0.0235	0.0240	0.0230
NOSE POSITION (M)					
HORIZONTAL	0.038	0.242	0.555	0.805	1.160
VERTICAL	0.126	0.135	0.143	0.152	0.169
INPUT NOSE POSITION (M)					
HORIZONTAL	0.038	0.244	0.559	0.799	1.163
VERTICAL	-0.091	-0.082	-0.072	-0.060	-0.042

NOSE VEL. Y-COMP. (M/S): 13. 10. 5. 5. 14.
COEFFICIENTS OF CUBIC POLYNOMIAL/STANDARD DEVIATION
0.1247E 00 0.1428E 02 -0.3347E 04 0.3809E 06 / 0.0021 (M)

NOSE VEL. X-COMP. (M/S): 372. 300. 167. 137. 259.
COEFFICIENTS OF CUBIC POLYNOMIAL/STANDARD DEVIATION
-0.1326E-01 0.3953E 03 -0.7622E 05 0.7393E 07 / 0.0202 (M)

NOSE VEL. DIRECTION(DEG)	2.0	1.9	1.7	2.3	3.1
SEPARATION ANGLE(DEGREE), RELATIVE TO NOSE VELOCITY					
ABOVE	****	5.4	4.7	5.3	5.1
BELOW	****	3.6	5.3	6.7	7.4

C.G. VEL. Y-COMP. (M/S): 12. 8. 2. 3. 13.
COEFFICIENTS OF CUBIC POLYNOMIAL/STANDARD DEVIATION
0.1215E 00 0.1304E 02 -0.4045E 04 0.4636E 06 / 0.0013 (M)

C.G. VEL. X-COMP. (M/S): 372. 300. 167. 137. 259.
COEFFICIENTS OF CUBIC POLYNOMIAL/STANDARD DEVIATION
-0.1262E 00 0.3951E 03 -0.7611E 05 0.7381E 07 / 0.0202 (M)

PONCELET DRAG COEFF. = 2.498
VO = 372. STAND. DEVIA. = 0.0503 (M)
C.G. VEL. X-COMP. (M/S): 372. 304. 202. 147. 112.

SHOT 23 (11 MARCH, 1976, NO. 8)

SAND: DRY, DENSITY:1538. KG/M**3; APPROACHING VELOCITY: 328. M/S
PROJECTILE: SOLID FLAT NOSE MASS:0.5451 KG, D=0.02 M, L=0.225 M

X-RAY STATION	NO.1	NO.2	NO.3	NO.4	NO.5
TIME (SECOND)	.000124	.000805	.002105	.003777	.005789
CENTER OF GRAVITY POSITION (M)					
HORIZONTAL	-0.071	0.133	0.444	0.766	1.057
VERTICAL	0.121	0.130	0.136	0.143	0.148
INCLINATION ANGLE(DEG).	2.0	1.5	2.2	3.7	6.5
SEPARATION ANGLE(DEGREE)					
ABOVE	****	6.0	4.5	5.5	9.0
BELOW	****	5.0	2.5	2.0	1.5
NOSE WIDTH (M ON FILM).	0.0250	0.0230	0.0230	0.0235	0.0240
NOSE POSITION (M)					
HORIZONTAL	0.042	0.246	0.557	0.879	1.170
VERTICAL	0.125	0.133	0.141	0.150	0.157
INPUT NOSE POSITION (M)					
HORIZONTAL	0.043	0.248	0.561	0.886	1.175
VERTICAL	-0.092	-0.084	-0.075	-0.063	-0.054

NOSE VEL. Y-COMP. (M/S): 10. 8. 6. 4. 3.
COEFFICIENTS OF CUBIC POLYNOMIAL/STANDARD DEVIATION
0.1246E 00 0.1003E 02 -0.1069E 04 0.5402E 05 / 0.0013 (M)

NOSE VEL. X-COMP. (M/S): 309. 274. 218. 165. 131.
COEFFICIENTS OF CUBIC POLYNOMIAL/STANDARD DEVIATION
0.4990E-02 0.3155E 03 -0.2726E 05 0.1305E 07 / 0.0053 (M)

NOSE VEL. DIRECTION (DEG)	1.8	1.8	1.6	1.5	1.3
SEPARATION ANGLE(DEGREE), RELATIVE TO NOSE VELOCITY					
ABOVE	****	6.3	3.9	3.3	3.0
BELOW	****	4.7	3.1	4.2	6.7

C.G. VEL. Y-COMP. (M/S): 11. 9. 5. 2. 0.
COEFFICIENTS OF CUBIC POLYNOMIAL/STANDARD DEVIATION
0.1206E 00 0.1153E 02 -0.1924E 04 0.1119E 06 / 0.0018 (M)

C.G. VEL. X-COMP. (M/S): 309. 274. 218. 166. 132.
COEFFICIENTS OF CUBIC POLYNOMIAL/STANDARD DEVIATION
-0.1079E 00 0.3154E 03 -0.2723E 05 0.1309E 07 / 0.0055 (M)

PONCELET DRAG COEFF. = 1.723
VO = 218. STAND. DEVIA. = 0.0106 (M)
C.G. VEL. X-COMP. (M/S): 326. 279. 218. 171. 135.

SHOT 24 (12 MARCH, 1976, NO. 1)

SAND: DRY, DENSITY:1638. KG/M**3; APPROACHING VELOCITY: 327. M/S
PROJECTILE: SOLID FLAT NOSE MASS:0.6443 KG, D=0.02 M, L=0.225 M

X-RAY STATION	NO.1	NO.2	NO.3	NO.4	NO.5
TIME (SECOND)	.000130	.000836	.002019	.003616	.005696
CENTER OF GRAVITY POSITION (M)					
HORIZONTAL	-0.089	0.115	0.402	0.710	1.024
VERTICAL	0.126	0.130	0.135	0.139	0.145
INCLINATION ANGLE(DEG).	0.0	2.0	2.5	4.0	5.0
SEPARATION ANGLE(DEGREE)					
ABOVE	****	5.0	5.0	5.0	5.0
BELOW	****	4.0	3.0	2.5	1.[illegible]
NOSE WIDTH (M ON FILM).	0.0240	0.0223	0.0223	0.0220	0.0220
NOSE POSITION (M)					
HORIZONTAL	0.024	0.228	0.515	0.823	1.137
VERTICAL	0.126	0.134	0.140	0.147	0.154
INPUT NOSE POSITION (M)					
HORIZONTAL	0.021	0.228	0.513	0.821	1.136
VERTICAL	-0.091	-0.083	-0.077	-0.069	-0.061

NOSE VEL. Y-COMP. (M/S):	10.	8.	5.	3.	5.

COEFFICIENTS OF CUBIC POLYNOMIAL/STANDARD DEVIATION
0.1256E 00 0.1046E 02 -0.1841E 04 0.1567E 06 / 0.0015 (M)

NOSE VEL. X-COMP. (M/S):	307.	270.	219.	170.	140.

COEFFICIENTS OF CUBIC POLYNOMIAL/STANDARD DEVIATION
-0.1628E-01 0.3142E 03 -0.2816E 05 0.1505E 07 / 0.0016 (M)

NOSE VEL. DIRECTION(DEG)	1.9	1.6	1.3	1.1	1.9
SEPARATION ANGLE(DEGREE), RELATIVE TO NOSE VELOCITY					
ABOVE	****	4.6	3.8	2.1	1.9
BELOW	****	4.4	4.2	5.4	4.6

C.G. VEL. Y-COMP. (M/S):	6.	5.	3.	2.	3.

COEFFICIENTS OF CUBIC POLYNOMIAL/STANDARD DEVIATION
0.1258E 00 0.5902E 01 -0.8590E 03 0.7040E 05 / 0.0002 (M)

C.G. VEL. X-COMP. (M/S):	307.	270.	219.	170.	140.

COEFFICIENTS OF CUBIC POLYNOMIAL/STANDARD DEVIATION
-0.1293E 00 0.3142E 03 -0.2814E 05 0.1500E 07 / 0.0010 (M)

PONCELET DRAG COEFF. = 1.724
VO = 219. STAND. DEVIA. = 0.0048 (M)

C.G. VEL. X-COMP. (M/S):	320.	273.	219.	173.	135.

RECORDED TIME OF MAXIMUM/MINIMUM COIL VOLTAGE (S)				
MAX	.000126	.001926	.003529	.005418
MIN	.000712	.002771	.004675	.006904
COMPUTED NOSE POSITION AT MAX/MIN COIL VOLTAGE (M)				
AT MAX	0.022	0.494	0.808	1.099
AT MIN	0.194	0.670	0.931	1.306
RECORDED COIL POSITION (M)				
	0.0	0.486	0.778	1.076
DIFFERENCE BETWEEN COIL AND NOSE AT MAX/MIN VOLTAGE (M)				
AT MAX	0.022	0.008	0.030	0.023
AT MIN	0.194	0.184	0.213	0.230

SHOT 25 (12 MARCH, 1976, NO. 2)

SAND: DRY, DENSITY:1538. KG/M**3; APPROACHING VELOCITY: 408. M/S
PROJECTILE, SOLID FLAT NOSE MASS:0.6443 KG, D=0.02 M, L=0.225 M

X-RAY STATION	NO.1	NO.2	NO.3	NO.4	NO.5
TIME (SECOND)	.000121	.000681	.001703	.003009	.004613
CENTER OF GRAVITY POSITION (M)					
HORIZONTAL	-0.087	0.118	0.417	0.726	1.024
VERTICAL	0.132	0.137	0.143	0.145	0.154
INCLINATION ANGLE(DEG).	0.0	2.0	3.5	7.0	9.0
SEPARATION ANGLE(DEGREE)					
ABOVE	****	6.0	6.5	7.0	10.0
BELOW	****	4.5	3.0	1.5	0.0
NOSE WIDTH (M ON FILM).	0.0240	0.0230	0.0225	0.0225	0.0225
NOSE POSITION (M)					
HORIZONTAL	0.026	0.231	0.529	0.838	1.136
VERTICAL	0.132	0.141	0.150	0.159	0.171
INPUT NOSE POSITION (M)					
HORIZONTAL	0.023	0.231	0.529	0.838	1.135
VERTICAL	-0.084	-0.075	-0.035	-0.055	-0.041

NOSE VEL. Y-COMP. (M/S): 16. 12. 8. 6. 11.
COEFFICIENTS OF CUBIC POLYNOMIAL/STANDARD DEVIATION
0.1305E 00 0.1706E 02 -0.3958E 04 0.4746E 06 / 0.0005 (M)

NOSE VEL. X-COMP. (M/S): 381. 335. 266. 206. 176.
COEFFICIENTS OF CUBIC POLYNOMIAL/STANDARD DEVIATION
-0.1964E-01 0.3917E 03 -0.4494E 05 0.3121E 07 / 0.0052 (M)

NOSE VEL. DIRECTION(DEG)	2.4	2.1	1.7	1.7	3.5
SEPARATION ANGLE(DEGREE), RELATIVE TO NOSE VELOCITY					
ABOVE	****	6.1	4.7	1.7	4.5
BELOW	****	4.4	4.8	6.8	5.5

C.G. VEL. Y-COMP. (M/S): 12. 8. 3. 2. 9.
COEFFICIENTS OF CUBIC POLYNOMIAL/STANDARD DEVIATION
0.1305E 00 0.1266E 02 -0.4363E 04 0.5778E 06 / 0.0010 (M)

C.G. VEL. X-COMP. (M/S): 381. 335. 266. 207. 177.
COEFFICIENTS OF CUBIC POLYNOMIAL/STANDARD DEVIATION
-0.1326E 00 0.3918E 03 -0.4469E 05 0.3092E 07 / 0.0054 (M)

PONCELET DRAG COEFF. = 1.684
VO = 266. STAND. DEVIA. = 0.0039 (M)
C.G. VEL. X-COMP. (M/S): 389. 334. 266. 211. 169.

```
                    SHOT 26    ( 18 MARCH, 1976, NO. 3 )

SAND: DRY, DENSITY:1538. KG/M**3; APPROACHING VELOCITY: 406. M/S
PROJECTILE: SOLID FLAT NOSE MASS:0.5443 KG. D=0.02 M. L=0.225 M

X-RAY STATION .........   NO.1     NO.2     NO.3     NO.4     NO.5

TIME (SECOND) ......... .000108  .000675  .001687  .003003  .004582
CENTER OF GRAVITY POSITION (M)
  HORIZONTAL .......... -0.086    0.119    0.420    0.730    1.035
  VERTICAL ............  0.134    0.140    0.146    0.153    0.160

INCLINATION ANGLE(DEG).  0.0      1.0      0.5     -1.5     -6.0
SEPARATION ANGLE(DEGREE)
  ABOVE ...............  ****     5.0      3.5      2.5      0.5
  BELOW ...............  ****     4.5      4.5      5.5      8.
NOSE WIDTH (M ON FILM). 0.0250   0.0228   0.0230   0.0230   0.0225
NOSE POSITION (M)
  HORIZONTAL ..........  0.027    0.232    0.533    0.843    1.147
  VERTICAL ............  0.134    0.142    0.147    0.150    0.148
INPUT NOSE POSITION (M)
  HORIZONTAL ..........  0.024    0.232    0.533    0.844    1.148
  VERTICAL ............ -0.081   -0.074   -0.068   -0.064   -0.067


NOSE VEL. Y-COMP. (M/S):  13.       9.       4.      -0.      -1.
COEFFICIENTS OF CUBIC POLYNOMIAL/STANDARD DEVIATION
  0.1332E 00  0.1376E 02 -0.3564E 04  0.2793E 06 / 0.0013 (M)

NOSE VEL. X-COMP. (M/S): 383.     336.     267.     209.     185.
COEFFICIENTS OF CUBIC POLYNOMIAL/STANDARD DEVIATION
 -0.1469E-01  0.3931E 03 -0.4603E 05  0.3396E 07 / 0.0015 (M)


NOSE VEL. DIRECTION(DEG)  1.9      1.6      0.9     -0.0     -0.4
SEPARATION ANGLE(DEGREE), RELATIVE TO NOSE VELOCITY
  ABOVE ...............  ****     5.6      3.9      4.0      6.1
  BELOW ...............  ****     3.9      4.1      4.0      2.9


C.G. VEL. Y-COMP. (M/S):   9.       8.       6.       5.       5.
COEFFICIENTS OF CUBIC POLYNOMIAL/STANDARD DEVIATION
  0.1334E 00  0.9680E 01 -0.1439E 04  0.1306E 06 / 0.0007 (M)

C.G. VEL. X-COMP. (M/S): 383.     336.     267.     209.     187.
COEFFICIENTS OF CUBIC POLYNOMIAL/STANDARD DEVIATION
 -0.1277E 00  0.3932E 03 -0.4614E 05  0.3432E 07 / 0.0014 (M)

PONCELET DRAG COEFF. = 1.649
 VO = 267. STAND. DEVIA. = 0.0025 (M)
C.G. VEL. X-COMP. (M/S): 386.     333.     267.     212.     170.


RECORDED TIME OF MAXIMUM/MINIMUM COIL VOLTAGE (S)
  MAX         .000099     .001594     .002864     .004427
  MIN         .000625     .002307     .003947     .005650
COMPUTED NOSE POSITION AT MAX/MIN COIL VOLTAGE (M)
  AT MAX      0.024       0.509       0.813       1.118
  AT MIN      0.214       0.689       1.029       1.349
RECORDED COIL POSITION (M)
              0.0         0.486       0.778       1.076
DIFFERENCE BETWEEN COIL AND NOSE AT MAX/MIN VOLTAGE (M)
  AT MAX      0.024       0.023       0.035       0.042
  AT MIN      0.214       0.203       0.251       0.273
```

SHOT 27 (12 MARCH, 1976, NO. 4)

SAND: DRY, DENSITY:1538. KG/M**3; APPROACHING VELOCITY: 409. M/S
PROJECTILE: SOLID FLAT NOSE MASS:0.5443 KG, D=0.02 M, L=0.225 M

X-RAY STATION	NO.1	NO.2	NO.3	NO.4	NO.5
TIME (SECOND)	.000118	.000681	.001703	.003018	.004628
CENTER OF GRAVITY POSITION (M)					
HORIZONTAL	-0.087	0.119	0.422	0.732	0.950
VERTICAL	0.143	0.152	0.161	0.169	0.176
INCLINATION ANGLE(DEG).	0.0	0.0	-0.5	-2.5	-2.5
SEPARATION ANGLE(DEGREE)					
ABOVE	****	4.5	2.5	1.0	2.5
BELOW	****	6.0	7.0	7.0	7.0
NOSE WIDTH (M ON FILM).	0.0250	0.0230	0.0230	0.0230	0.0230
NOSE POSITION (M)					
HORIZONTAL	0.026	0.232	0.535	0.845	1.063
VERTICAL	0.143	0.152	0.160	0.164	0.171
INPUT NOSE POSITION (M)					
HORIZONTAL	0.023	0.233	0.535	0.846	1.051
VERTICAL	-0.070	-0.062	-0.053	-0.048	-0.040

NOSE VEL. Y-COMP. (M/S): 18. 12. 5. 2. 8.
COEFFICIENTS OF CUBIC POLYNOMIAL/STANDARD DEVIATION
0.1409E 00 0.1959E 02 -0.6071E 04 0.7017E 06 / 0.0005 (M)

NOSE VEL. X-COMP. (M/S): 371. 336. 273. 189. 84.
COEFFICIENTS OF CUBIC POLYNOMIAL/STANDARD DEVIATION
-0.1585E-01 0.3779E 03 -0.3029E 05 -0.2130E 06 / 0.0072 (M)

NOSE VEL. DIRECTION(DEG) 2.8 2.1 1.1 0.6 5.8
SEPARATION ANGLE(DEGREE), RELATIVE TO NOSE VELOCITY
ABOVE .... **** 6.6 4.1 4.1 10.8
BELOW .... **** 3.9 5.4 3.9 -1.3

C.G. VEL. Y-COMP. (M/S): 16. 13. 8. 4. 6.
COEFFICIENTS OF CUBIC POLYNOMIAL/STANDARD DEVIATION
0.1413E 00 0.1705E 02 -0.3688E 04 0.3517E 06 / 0.0010 (M)

C.G. VEL. X-COMP. (M/S): 371. 337. 273. 189. 84.
COEFFICIENTS OF CUBIC POLYNOMIAL/STANDARD DEVIATION
-0.1269E 00 0.3781E 03 -0.3029E 05 -0.2130E 06 / 0.0073 (M)

PONCELET DRAG COEFF. = 1.764
VO = 273. STAND. DEVIA. = 0.0550 (M)
C.G. VEL. X-COMP. (M/S): 413. 349. 273. 213. 168.

SHOT 29 (12 MARCH, 1976, NO. 6)

```
SAND: DRY, DENSITY:1538. KG/M**3; APPROACHING VELOCITY: 405. M/S
PROJECTILE: SOLID FLAT NOSE MASS:0.5447 KG, D=0.02 M, L=0.225 M

X-RAY STATION .........   NO.1     NO.2     NO.3     NO.4     NO.5

TIME (SECOND) ......... .000077  .000635  .001656  .002834  .004567
CENTER OF GRAVITY POSITION (M)
  HORIZONTAL .......... -0.088    0.120    0.421    0.701    1.031
  VERTICAL ............  0.115    0.122    0.130    0.132    0.126

INCLINATION ANGLE(DEG).  -1.0    -1.5     -4.0     -6.5     -6.0
SEPARATION ANGLE(DEGREE)
  ABOVE ...............  ****     4.0      3.0      1.5      1.0
  BELOW ...............  ****     9.0     10.5     11.0     10.0
NOSE WIDTH (M ON FILM). 0.0250   0.0230   0.0230   0.0230   0.0230
NOSE POSITION (M)
  HORIZONTAL ..........  0.028    0.232    0.534    0.813    1.144
  VERTICAL ............  0.113    0.119    0.122    0.119    0.115
INPUT NOSE POSITION (M)
  HORIZONTAL ..........  0.025    0.233    0.534    0.809    1.144
  VERTICAL ............ -0.108   -0.100   -0.096   -0.100   -0.105


NOSE VEL. Y-COMP. (M/S):  15.      8.      -0.      -4.       2.
COEFFICIENTS OF CUBIC POLYNOMIAL/STANDARD DEVIATION
  0.1114E 00  0.1598E 02 -0.6907E 04  0.7803E 06 / 0.0000 (M)

NOSE VEL. X-COMP. (M/S): 387.     337.     265.     210.     185.
COEFFICIENTS OF CUBIC POLYNOMIAL/STANDARD DEVIATION
 -0.1460E-02  0.3943E 03 -0.4837E 05  0.3711E 07 / 0.0031 (M)


NOSE VEL. DIRECTION(DEG)  2.2     1.4     -0.1     -1.2      0.5
SEPARATION ANGLE(DEGREE), RELATIVE TO NOSE VELOCITY
  ABOVE ...............  ****     6.9      6.9      6.8      7.5
  BELOW ...............  ****     6.1      6.6      5.7      3.5


C.G. VEL. Y-COMP. (M/S):  16.     11.      4.      -1.      -4.
COEFFICIENTS OF CUBIC POLYNOMIAL/STANDARD DEVIATION
  0.1132E 00  0.1693E 02 -0.4593E 04  0.3328E 06 / 0.0003 (M)

C.G. VEL. X-COMP. (M/S): 387.     338.     265.     210.     185.
COEFFICIENTS OF CUBIC POLYNOMIAL/STANDARD DEVIATION
 -0.1145E 00  0.3941E 03 -0.4806E 05  0.3670E 07 / 0.0033 (M)

PONCELET DRAG COEFF. = 1.706
 V0 = 265. STAND. DEVIA. = 0.0025 (M)
C.G. VEL. X-COMP. (M/S): 388.     333.     265.     214.     167.


RECORDED TIME OF MAXIMUM/MINIMUM COIL VOLTAGE (S)
  MAX         .000062     .001564     .002664     .004474
  MIN         .000557     .002276     .003762     .005542
COMPUTED NOSE POSITION AT MAX/MIN COIL VOLTAGE (M)
  AT MAX      0.023       0.511       0.818       1.127
  AT MIN      0.204       0.689       0.995       1.330
RECORDED COIL POSITION (M)
              0.0         0.486       0.778       1.076
DIFFERENCE BETWEEN COIL AND NOSE AT MAX/MIN VOLTAGE (M)
  AT MAX      0.023       0.025       0.040       0.051
  AT MIN      0.204       0.203       0.217       0.254
```

```
                     SHOT 30    ( 12 MARCH, 1976, NO. 7 )

SAND: DRY, DENSITY:1638. KG/M**3; APPROACHING VELOCITY: 352. M/S
PROJECTILE: SOLID BICONIC    MASS:0.4964 KG, D=0.02 M, L=0.226 M

X-RAY STATION ..........  NO.1      NO.2      NO.3      NO.4      NO.5

TIME (SECOND) .......... .000115  .000681  .001703  .002879  .004613
CENTER OF GRAVITY POSITION (M)
  HORIZONTAL ........... -0.092    0.100    0.408    0.718    1.094
  VERTICAL ............. 0.114     0.119    0.124    0.130    0.162

INCLINATION ANGLE(DEG).   0.0      1.0      2.5      6.0      11.0
SEPARATION ANGLE(DEGREE)
  ABOVE ...............   ****     ****     4.5      5.0      6.5
  BELOW ...............   ****     ****     2.0      1.0      1.5
NOSE WIDTH (M ON FILM). 0.0250   0.0230   0.0225   0.0220   0.0203
NOSE POSITION (M)
  HORIZONTAL ..........   0.030    0.222    0.529    0.839    1.214
  VERTICAL ............   0.114    0.122    0.130    0.143    0.185
INPUT NOSE POSITION (M)
  HORIZONTAL ..........   0.028    0.221    0.529    0.839    1.215
  VERTICAL ............  -0.106   -0.097   -0.088   -0.074   -0.033


NOSE VEL. Y-COMP. (M/S):  14.      10.       8.       14.       38.
COEFFICIENTS OF CUBIC POLYNOMIAL/STANDARD DEVIATION
  0.1127E 00  0.1497E 02 -0.4550E 04  0.1019E 07 / 0.0007 (M)

NOSE VEL. X-COMP. (M/S): 349.     324.     283.     242.      193.
COEFFICIENTS OF CUBIC POLYNOMIAL/STANDARD DEVIATION
 -0.9872E-02  0.3539E 03 -0.2290E 05  0.7905E 06 / 0.0019 (M)


NOSE VEL. DIRECTION(DEG)  2.3      1.8      1.7      3.3      11.1
SEPARATION ANGLE(DEGREE), RELATIVE TO NOSE VELOCITY
  ABOVE ...............   ****     ****     3.7      2.3       6.6
  BELOW ...............   ****     ****     2.8      3.7       1.4


C.G. VEL. Y-COMP. (M/S):  12.      7.       3.       8.        32.
COEFFICIENTS OF CUBIC POLYNOMIAL/STANDARD DEVIATION
  0.1127E 00  0.1368E 02 -0.6010E 04  0.1159E 07 / 0.0001 (M)

C.G. VEL. X-COMP. (M/S): 349.     324.     283.     243.      195.
COEFFICIENTS OF CUBIC POLYNOMIAL/STANDARD DEVIATION
 -0.1318E 00  0.3538E 03 -0.2275E 05  0.8028E 06 / 0.0019 (M)

PONCELET DRAG COEFF. = 0.910
 V0 = 349. STAND. DEVIA. = 0.0058 (M)
C.G. VEL. X-COMP. (M/S): 349.     321.     286.     244.      206.
```

SHOT 31 (12 MARCH, 1976, NO. 8)

```
SAND: DRY, DENSITY:1538. KG/M**3; APPROACHING VELOCITY: 352. M/S
PROJECTILE: SOLID BICONIC    MASS:0.4964 KG, D=0.02 M, L=0.226 M

X-RAY STATION ..........   NO.1     NO.2     NO.3     NO.4     NO.5

TIME (SECOND) .......... .000139  .000672  .001694  .002796  .004303
CENTER OF GRAVITY POSITION (M)
  HORIZONTAL .......... -0.081    0.100    0.406    0.697    1.019
  VERTICAL ............  0.110    0.114    0.123    0.136    0.190

INCLINATION ANGLE(DEG).   1.5      3.0      5.5     12.0     19.0
SEPARATION ANGLE(DEGREE)
  ABOVE ...............   ****     ****     6.0      8.0     10.0
  BELOW ...............   ****     ****     1.0      1.0     ****
NOSE WIDTH (M ON FILM).  0.0245   0.0235   0.0225   0.0220   0.0210
NOSE POSITION (M)
  HORIZONTAL ..........  0.041    0.222    0.528    0.816    1.134
  VERTICAL ............  0.113    0.121    0.135    0.162    0.229
INPUT NOSE POSITION (M)
  HORIZONTAL ..........  0.042    0.221    0.527    0.814    1.134
  VERTICAL ............ -0.107   -0.098   -0.082   -0.053    0.016

NOSE VEL. Y-COMP. (M/S):  13.      13.      18.      31.      62.
COEFFICIENTS OF CUBIC POLYNOMIAL/STANDARD DEVIATION
  0.1117E 00  0.1331E 02 -0.1442E 04  0.1094E 07 / 0.0007 (M)

NOSE VEL. X-COMP. (M/S): 346.     323.     201.     239.     185.
COEFFICIENTS OF CUBIC POLYNOMIAL/STANDARD DEVIATION
 -0.6516E-02  0.3524E 03 -0.2206E 05  0.4055E 06 / 0.0026 (M)

NOSE VEL. DIRECTION(DEG)  2.1      2.3      3.6      7.4     18.4
SEPARATION ANGLE(DEGREE), RELATIVE TO NOSE VELOCITY
  ABOVE ...............   ****     ****     4.1      3.4      9.4
  BELOW ...............   ****     ****     2.9      5.6     ****

C.G. VEL. Y-COMP. (M/S):  12.       8.       8.      20.      54.
COEFFICIENTS OF CUBIC POLYNOMIAL/STANDARD DEVIATION
  0.1079E 00  0.1393E 02 -0.5891E 04  0.1642E 07 / 0.0012 (M)

C.G. VEL. X-COMP. (M/S): 346.     323.     282.     241.     189.
COEFFICIENTS OF CUBIC POLYNOMIAL/STANDARD DEVIATION
 -0.1283E 00  0.3518E 03 -0.2146E 05  0.3850E 06 / 0.0028 (M)

PONCELET DRAG COEFF. = 0.937
 VO = 346. STAND. DEVIA. = 0.0083 (M)
C.G. VEL. X-COMP. (M/S): 346.     319.     278.     244.     209.
```

```
                    SHOT 32    ( 1" MARCH, 1976, NO. 1 )

SAND: DRY, DENSITY:1538. KG/M**3; APPROACHING VELOCITY: 334. M/S
PROJECTILE: SOLID B'CONIC    MASS:0.4965 KG, D=0.02 M, L=0.226 M

X-RAY STATION ..........  NO.1     NO.2     NO.3     NO.4     NO.5

TIME (SECOND) .......... .000124  .000672  .001694  .002981  .004288
CENTER OF  RAVITY POSITION (M)
  HORIZONTAL ........... -0.074    0.105    0.407    0.739    1.007
  VERTICAL ............   0.103    0.109    0.116    0.140    0.183

INCLINATION ANGLE(DEG).   2.0      2.5      6.8      15.0     29.0
SEPARATION ANGLE(DEGREE)
  ABOVE ...............   ****     ****     ****     ****     ****
  BELOW ...............   ****     ****     ****     ****     ****
NOSE WIDTH (M ON FILM).   0.0250   0.0230   0.0230   0.0240   0.0265
NOSE POSITION (M)
  HORIZONTAL ..........   0.048    0.227    0.529    0.857    1.114
  VERTICAL ............   0.107    0.115    0.130    0.171    0.242
INPUT NOSE POSITION (M)
  HORIZONTAL ..........   0.050    0.227    0.528    0.861    1.104
  VERTICAL ............  -0.115   -0.105   -0.087   -0.037    0.063


NOSE VEL. Y-COMP. (M/S):  10.      13.      22.      41.      69.
COEFFICIENTS OF CUBIC POLYNOMIAL/STANDARD DEVIATION
  0.1062E 00  0.9629E 01  0.1641E 04  0.8218E 06 / 0.0015 (M)

NOSE VEL. X-COMP. (M/S): 332.     315.     280.     228.     166.
COEFFICIENTS OF CUBIC POLYNOMIAL/STANDARD DEVIATION
  0.6912E-02  0.3361E 03 -0.1451E 05 -0.8233E 06 / 0.0037 (M)


NOSE VEL. DIRECTION(DEG)  1.7      2.4      4.5      10.3     22.6
SEPARATION ANGLE(DEGREE), RELATIVE TO NOSE VELOCITY
  ABOVE ...............   ****     ****     ****     ****     ****
  BELOW ...............   ****     ****     ****     ****     ****


C.G. VEL. Y-COMP. (M/S):   9.       8.      12.      24.      45.
COEFFICIENTS OF CUBIC POLYNOMIAL/STANDARD DEVIATION
  0.1022E 00  0.9176E 01 -0.1509E 04  0.8817E 06 / 0.0020 (M)

C.G. VEL. X-COMP. (M/S): 333.     316.     281.     232.     178.
COEFFICIENTS OF CUBIC POLYNOMIAL/STANDARD DEVIATION
 -0.1151E 00  0.3369E 03 -0.1531E 05 -0.4915E 06 / 0.0032 (M)

PONCELET DRAG COEFF. = 0.865
 V0 = 333. STAND. DEVIA. = 0.0116 (M)
C.G. VEL. X-COMP. (M/S): 333.     309.     273.     238.     210.
```

SHOT 33 (13 MARCH, 1976, NO. 2)

SAND: DRY, DENSITY:1538. KG/M**3; APPROACHING VELOCITY: 400. M/S
PROJECTILE: HOLLOW BICONIC MASS:0.3439 KG, D=0.02 M, L=0.226 M

X-RAY STATION	NO.1	NO.2	NO.3	NO.4	NO.5
TIME (SECOND)	.000155	.000780	.001703	.002817	.004303
CENTER OF GRAVITY POSITION (M)					
HORIZONTAL	-0.051	0.190	0.458	18.737	19.042
VERTICAL	0.102	0.104	0.060	18.121	18.121
INCLINATION ANGLE(DEG).	-4.0	-11.0	-16.0	0.0	0.0
SEPARATION ANGLE(DEGREE)					
ABOVE	****	1.0	****	****	****
BELOW	****	9.0	****	****	****
NOSE WIDTH (M ON FILM).	0.0250	0.0230	0.0230	******	******
NOSE POSITION (M)					
HORIZONTAL	0.051	0.290	0.556	18.839	19.144
VERTICAL	0.095	0.084	0.032	18.121	18.121
INPUT NOSE POSITION (M)					
HORIZONTAL	0.054	0.299	0.560	******	******
VERTICAL	-0.130	-0.140	-0.200	******	******

SHOT 34 (13 MARCH, 1976, NO. 3)

SAND: DRY, DENSITY:1538. KG/M**3; APPROACHING VELOCITY: 413. M/S
PROJECTILE: HOLLOW BICONIC MASS:0.3436 KG, D=0.02 M, L=0.226 M

X-RAY STATION	NO.1	NO.2	NO.3	NO.4	NO.5
TIME (SECOND)	.000139	.000774	.001703	.002811	.004319
CENTER OF GRAVITY POSITION (M)					
HORIZONTAL	-0.053	0.190	0.475	18.737	19.042
VERTICAL	0.102	0.107	0.092	18.121	18.121
INCLINATION ANGLE(DEG).	-1.7	-5.0	-8.5	0.0	0.0
SEPARATION ANGLE(DEGREE)					
ABOVE	****	1.0	1.0	****	****
BELOW	****	6.5	6.0	****	****
NOSE WIDTH (M ON FILM).	0.02[illegible]0	0.0235	0.0250	******	******
NOSE POSITION (M)					
HORIZONTAL	0.049	0.291	0.576	18.839	19.144
VERTICAL	0.099	0.098	0.077	18.121	18.121
INPUT NOSE POSITION (M)					
HORIZONTAL	0.052	0.302	0.587	******	******
VERTICAL	-0.125	-0.125	-0.153	******	******

SHOT 35 (13 MARCH, 1976, NO. 4)

SAND: DRY, DENSITY:1536. KG/M**3; APPROACHING VELOCITY: 362. M/S
PROJECTILE: HOLLOW BICONIC MASS:0.3435 KG, D=0.02 M, L=0.226 M

X-RAY STATION	NO.1	NO.2	NO.3	NO.4	NO.5
TIME (SECOND)	.000139	.000790	.001919	.003514	.005418
CENTER OF GRAVITY POSITION (M)					
HORIZONTAL	-0.063	0.146	0.440	0.774	1.092
VERTICAL	0.096	0.102	0.115	0.143	0.190
INCLINATION ANGLE(DEG).	1.5	4.0	6.0	7.5	14.0
SEPARATION ANGLE(DEGREE)					
ABOVE	****	****	5.0	7.0	****
BELOW	****	****	1.0	4.0	****
NOSE WIDTH (M ON FILM).	0.0245	0.0230	0.0240	0.0250	0.0310
NOSE POSITION (M)					
HORIZONTAL	0.039	0.247	0.541	0.876	1.191
VERTICAL	0.099	0.109	0.126	0.157	0.215
INPUT NOSE POSITION (M)					
HORIZONTAL	0.039	0.250	0.543	0.885	1.218
VERTICAL	-0.125	-0.111	-0.092	-0.053	0.049

NOSE VEL. Y-COMP. (M/S): 16. 15. 16. 23. 40.
COEFFICIENTS OF CUBIC POLYNOMIAL/STANDARD DEVIATION
0.9659E-01 0.1635E 02 -0.1343E 04 0.4349E 06 / 0.0008 (M)

NOSE VEL. X-COMP. (M/S): 335. 295. 238. 183. 157.
COEFFICIENTS OF CUBIC POLYNOMIAL/STANDARD DEVIATION
-0.7080E-02 0.3437E 03 -0.3338E 05 0.1991E 07 / 0.0038 (M)

NOSE VEL. DIRECTION(DEG)	2.7	2.9	3.9	7.2	14.3
SEPARATION ANGLE(DEGREE), RELATIVE TO NOSE VELOCITY					
ABOVE	****	****	2.9	6.7	****
BELOW	****	****	3.1	4.3	****

C.G. VEL. Y-COMP. (M/S): 8. 10. 14. 21. 29.
COEFFICIENTS OF CUBIC POLYNOMIAL/STANDARD DEVIATION
0.9512E-01 0.7102E 01 0.1731E 04 0.3738E 05 / 0.0007 (M)

C.G. VEL. X-COMP. (M/S): 335. 295. 238. 183. 159.
COEFFICIENTS OF CUBIC POLYNOMIAL/STANDARD DEVIATION
-0.1092E 00 0.3444E 03 -0.3368E 05 0.2042E 07 / 0.0038 (M)

PONCELET DRAG COEFF. = 1.011
VO = 238. STAND. DEVIA. = 0.0021 (M)
C.G. VEL. X-COMP. (M/S): 349. 294. 238. 187. 149.

SHOT 36 (13 MARCH, 1976, NO. 5)

SAND: WET, DENSITY:2050. KG/M**3; APPROACHING VELOCITY: 336. M/S
PROJECTILE: SOLID FLAT NOSE MASS:0.5450 KG, D=0.02 M, L=0.225 M

X-RAY STATION	NO.1	NO.2	NO.3	NO.4	NO.5
TIME (SECOND)	.000130	.000836	.002217	.003901	.006094
CENTER OF GRAVITY POSITION (M)					
HORIZONTAL	-0.074	0.142	0.490	0.844	19.031
VERTICAL	0.098	0.095	0.106	0.108	18.121
INCLINATION ANGLE(DEG).	0.0	0.0	0.5	0.5	0.0
SEPARATION ANGLE(DEGREE)					
ABOVE	****	17.0	7.5	5.0	****
BELOW	****	17.0	8.5	8.0	****
NOSE WIDTH (M ON FILM).	0.0250	0.0230	0.0230	0.0230	******
NOSE POSITION (M)					
HORIZONTAL	0.039	0.255	0.693	0.957	19.144
VERTICAL	0.098	0.095	0.107	0.109	18.121
INPUT NOSE POSITION (M)					
HORIZONTAL	0.039	0.259	0.613	0.975	******
VERTICAL	-0.126	-0.126	-0.114	-0.111	******

SHOT 37 (24 MARCH, 1976, NO. 1)

SAND: WET, DENSITY:2050. KG/M**3; APPROACHING VELOCITY: 336. M/S
PROJECTILE: SOLID FLAT NOSE MASS:0.5449 KG, D=0.02 M, L=0.225 M

X-RAY STATION	NO.1	NO.2	NO.3	NO.4	NO.5
TIME (SECOND)	.000130	.000805	.002074	.003560	.005365
CENTER OF GRAVITY POSITION (M)					
HORIZONTAL	-0.079	0.126	0.451	0.776	1.090
VERTICAL	0.095	0.100	0.102	0.103	0.105
INCLINATION ANGLE(DEG).	1.0	1.0	2.0	2.5	4.0
SEPARATION ANGLE(DEGREE)					
ABOVE	20.0	****	11.0	8.0	9.5
BELOW	20.0	****	9.0	6.5	4.0
NOSE WIDTH (M ON FILM).	0.0250	0.0225	0.0230	0.0230	0.0230
NOSE POSITION (M)					
HORIZONTAL	0.034	0.239	0.563	0.888	1.203
VERTICAL	0.097	0.102	0.106	0.108	0.113
INPUT NOSE POSITION (M)					
HORIZONTAL	0.033	0.240	0.568	0.896	1.212
VERTICAL	-0.127	-0.119	-0.115	-0.113	-0.107

NOSE VEL. Y-COMP. (M/S): 8. 5. 2. 1. 5.
COEFFICIENTS OF CUBIC POLYNOMIAL/STANDARD DEVIATION
0.9633E-01 0.8092E 01 -0.2690E 04 0.2954E 06 / 0.0002 (M)

NOSE VEL. X-COMP. (M/S): 311. 283. 238. 195. 157.
COEFFICIENTS OF CUBIC POLYNOMIAL/STANDARD DEVIATION
-0.5356E-02 0.3161E 03 -0.2123E 05 0.7992E 06 / 0.0045 (M)

NOSE VEL. DIRECTION(DEG)	1.5	1.1	0.4	0.3	2.1
SEPARATION ANGLE(DEGREE), RELATIVE TO NOSE VELOCITY					
ABOVE	20.5	****	9.4	5.8	7.6
BELOW	19.5	****	10.6	8.7	5.9

C.G. VEL. Y-COMP. (M/S): 7. 4. 1. -0. 4.
COEFFICIENTS OF CUBIC POLYNOMIAL/STANDARD DEVIATION
0.9469E-01 0.7996E 01 -0.2613E 04 0.2755E 06 / 0.0009 (M)

C.G. VEL. X-COMP. (M/S): 311. 284. 238. 195. 157.
COEFFICIENTS OF CUBIC POLYNOMIAL/STANDARD DEVIATION
-0.1183E 00 0.3161E 03 -0.2123E 05 0.8008E 06 / 0.0044 (M)

PONCELET DRAG COEFF. = 0.948
VO = 238. STAND. DEVIA. = 0.0084 (M)
C.G. VEL. X-COMP. (M/S): 322. 287. 238. 199. 166.

RECORDED TIME OF MAXIMUM/MINIMUM COIL VOLTAGE (S)				
MAX	.000133	.001811	.003229	.004892
MIN	.000697	.002666	.004235	.006068
COMPUTED NOSE POSITION AT MAX/MIN COIL VOLTAGE (M)				
AT MAX	0.036	0.502	0.821	1.127
AT MIN	0.205	0.702	1.013	1.310
RECORDED COIL POSITION (M)				
	0.0	0.486	0.794	1.092
DIFFERENCE BETWEEN COIL AND NOSE AT MAX/MIN VOLTAGE (M)				
AT MAX	0.035	0.016	0.027	0.035
AT MIN	0.205	0.216	0.219	0.218

```
SHOT 38   ( 24 MARCH, 1976, NO. 2 )

SAND: WET, DENSITY:2050. KG/M**3; APPROACHING VELOCITY: 333. M/S
PROJECTILE: SOLID FLAT NOSE MASS:0.5446 KG, D=0.02 M, L=0.225 M

X-RAY STATION ..........   NO.1      NO.2      NO.3      NO.4      NO.5

TIME (SECOND) .......... .000130  .000805  .002068  .003560  .005418
CENTER OF GRAVITY POSITION (M)
  HORIZONTAL ........... -0.076    0.131    0.461    0.788    1.124
  VERTICAL .............  0.069    0.097    0.100    0.100    0.110

INCLINATION ANGLE(DEG).   2.5      1.0      1.5      2.0      3.5
SEPARATION ANGLE(DEGREE)
  ABOVE ................  ****     16.0     8.5      8.5      10.0
  BELOW ................  ****     12.0     6.5      0.0      5.0
NOSE WIDTH (M ON FILM). 0.0250   0.0230   0.0230   0.0230   0.0230
NOSE POSITION (M)
  HORIZONTAL ...........  0.037    0.244    0.574    0.901    1.237
  VERTICAL .............  0.094    0.099    0.103    0.104    0.117
INPUT NOSE POSITION (M)
  HORIZONTAL ...........  0.037    0.246    0.580    0.910    1.251
  VERTICAL ............. -0.131   -0.123   -0.118   -0.117   -0.102


NOSE VEL. Y-COMP. (M/S):  10.      6.       1.       2.       14.
COEFFICIENTS OF CUBIC POLYNOMIAL/STANDARD DEVIATION
  0.9262E-01  0.1144E 02 -0.4229E 04  0.5450E 06 / 0.0006 (M)

NOSE VEL. X-COMP. (M/S): 319.     288.     240.     198.     168.
COEFFICIENTS OF CUBIC POLYNOMIAL/STANDARD DEVIATION
 -0.4028E-02  0.3250E 03 -0.2426E 05  0.1207E 07 / 0.0019 (M)


NOSE VEL. DIRECTION(DEG)  1.9      1.1      0.2      0.6      4.6
SEPARATION ANGLE(DEGREE). RELATIVE TO NOSE VELOCITY
  ABOVE ...............   ****     16.1     7.2      7.1      11.1
  BELOW ...............   ****     11.9     7.8      9.4      3.9


C.G. VEL. Y-COMP. (M/S):  14.      7.       6.       0.       13.
COEFFICIENTS OF CUBIC POLYNOMIAL/STANDARD DEVIATION
  0.8757E-01  0.1541E 02 -0.5785E 04  0.6853E 06 / 0.0007 (M)

C.G. VEL. X-COMP. (M/S): 319.     288.     240.     198.     169.
COEFFICIENTS OF CUBIC POLYNOMIAL/STANDARD DEVIATION
 -0.1169E 00  0.3249E 03 -0.2421E 05  0.1207E 07 / 0.0019 (M)

PONCELET DRAG COEFF. = 0.937
 VO = 240. STAND. DEVIA. = 0.0021 (M)
C.G. VEL. X-COMP. (M/S): 324.     289.     240.     200.     166.
```

```
SHOT 39   ( 24 MARCH, 1976, NO. 3 )

SAND: WET, DENSITY:2050. KG/M**3; APPROACHING VELOCITY: 330. M/S
PROJECTILE: SOLID STEP-TIER MASS:0.5646 KG, D=0.02 M, L=0.238 M

X-RAY STATION ..........   NO.1      NO.2      NO.3      NO.4      NO.5

TIME (SECOND) .......... .000130  .001799  .001904     3**    .005108
CENTER OF GRAVITY POSITION (M)
  HORIZONTAL ........... -0.096    0.218     0.425     0.774     1.121
  VERTICAL .............  0.104    0.111     0.116     0.123     0.152

INCLINATION ANGLE(DEG).   3.0      3.0       5.5       9.5      10.0
SEPARATION ANGLE(DEGREE)
  ABOVE ................  ****     14.0      11.5      13.0      ****
  BELOW ................  ****      9.5       6.0       1.5      ****
NOSE WIDTH (M ON FILM). 0.0250   0.0230    0.0225    0.0220    0.0220
NOSE POSITION (M)
  HORIZONTAL ...........  0.032    0.238     0.546     0.894     1.241
  VERTICAL .............  0.110    0.117     0.128     0.144     0.174
INPUT NOSE POSITION (M)
  HORIZONTAL ...........  0.036    0.239     0.548     0.900     1.251
  VERTICAL ............. -0.111   -0.102    -0.090    -0.073    -0.040

NOSE VEL. Y-COMP. (M/S):  11.      10.       10.       13.       22.
COEFFICIENTS OF CUBIC POLYNOMIAL/STANDARD DEVIATION
  0.1087E 00  0.1166E 02 -0.1478E 04  0.3259E 06 / 0.0003 (M)

NOSE VEL. X-COMP. (M/S): 318.     297.      253.      221.      173.
COEFFICIENTS OF CUBIC POLYNOMIAL/STANDARD DEVIATION
 -0.9964E-02  0.3227E 03 -0.1643E 05  0.2335E 06 / 0.0006 (M)

NOSE VEL. DIRECTION(DEG)  2.0      1.9       2.1       3.3       7.3
SEPARATION ANGLE(DEGREE), RELATIVE TO NOSE VELOCITY
  ABOVE ...............   ****     12.9       8.1       6.5      ****
  BELOW ...............   ****     10.6       9.4       7.7      ****

C.G. VEL. Y-COMP. (M/S):  13.       9.        4.        8.       28.
COEFFICIENTS OF CUBIC POLYNOMIAL/STANDARD DEVIATION
  0.1021E 00  0.1446E 02 -0.5314E 04  0.8614E 06 / 0.0004 (M)

C.G. VEL. X-COMP. (M/S): 318.     297.      263.      221.      173.
COEFFICIENTS OF CUBIC POLYNOMIAL/STANDARD DEVIATION
 -0.1317E 00  0.3221E 03 -0.1590E 05  0.1651E 06 / 0.0006 (M)

PONCELET DRAG COEFF. = 0.720
 VO = 318. STAND. DEVIA. = 0.0092 (M)
C.G. VEL. X-COMP. (M/S): 318.     292.      258.      224.      193.
```

SHOT 49 (25 MARCH, 1976, NO. 2)

SANDS WET, DENSITY:2050. KG/M**3; APPROACHING VELOCITY: 326. M/S
PROJECTILE: SOLID STEP-TIER MASS:0.5638 KG, D=0.02 M, L=0.238 M

X-RAY STATION	NO.1	NO.2	NO.3	NO.4	NO.5
TIME (SECOND)	.000124	*******	.001920	.003251	.004836
CENTER OF GRAVITY POSITION (M)					
HORIZONTAL	-0.092	18.210	0.418	0.735	1.041
VERTICAL	0.068	18.241	0.102	0.105	0.122
INCLINATION ANGLE(DEG).	3.0	*****	4.0	8.5	9.5
SEPARATION ANGLE(DEGREE)					
ABOVE	****	****	9.0	16.0	12.0
BELOW	****	****	4.5	5.0	1.5
NOSE WIDTH (M ON FILM).	0.0260	******	0.0230	0.0230	0.0230
NOSE POSITION (M)					
HORIZONTAL	0.030	18.231	0.540	0.855	1.161
VERTICAL	0.094	18.121	0.110	0.123	0.142
INPUT NOSE POSITION (M)					
HORIZONTAL	0.027	******	0.541	0.858	1.164
VERTICAL	-0.132	******	-0.110	-0.095	-0.073

SHOT 41 (25 MARCH, 1976, NO. 3)

SAND: WET. DENSITY:2050. KG/M**3; APPROACHING VELOCITY: 320. M/S
PROJECTILE: SOLID STEP-TIER MASS:0.5645 KG. D=0.02 M. L=0.238 M

X-RAY STATION	NO.1	NO.2	NO.3	NO.4	NO.5
TIME (SECOND)	.000093	*******	.001858	.003220	.004830
CENTER OF GRAVITY POSITION (M)					
HORIZONTAL	-0.091	18.210	0.428	0.767	1.106
VERTICAL	0.088	18.241	0.099	0.105	0.112
INCLINATION ANGLE(DEG).	1.0	*****	1.0	1.0	2.0
SEPARATION ANGLE(DEGREE)					
ABOVE	****	****	5.0	11.0	13.0
BELOW	****	****	4.0	10.0	13.
NOSE WIDTH (M ON FILM).	0.0270	******	0.0235	0.0230	0.0230
NOSE POSITION (M)					
HORIZONTAL	0.031	18.231	0.550	0.889	1.228
VERTICAL	0.090	18.121	0.102	0.107	0.116
INPUT NOSE POSITION (M)					
HORIZONTAL	0.029	******	0.553	0.897	1.241
VERTICAL	-0.139	******	-0.120	-0.114	-0.103

SHOT 42 (25 MARCH, 1976, NO. 6)

SAND: WET, DENSITY:2080. KG/M**3; APPROACHING VELOCITY: 217. M/S
PROJECTILE: SOLID STEP-TIER MASS:0.5649 KG, D=0.02 M, L=0.238 M

X-RAY STATION	NO.1	NO.2	NO.3	NO.4	NO.5
TIME (SECOND)	.000170	*******	.004536	.008263	.007740
CENTER OF GRAVITY POSITION (M)					
HORIZONTAL	-0.091	18.210	18.[illegible]	0.709	0.968
VERTICAL	0.092	18.241	18.241	0.096	0.107
INCLINATION ANGLE(DEG).	0.0	*****	*****	-4.5	-8.0
SEPARATION ANGLE(DEGREE)					
ABOVE	****	****	****	****	****
BELOW	****	****	****	****	****
NOSE WIDTH (M ON FILM).	0.0260	******	******	0.0230	0.0230
NOSE POSITION (M)					
HORIZONTAL	0.031	18.231	18.535	0.831	1.089
VERTICAL	0.092	18.121	18.121	0.085	0.090
INPUT NOSE POSITION (M)					
HORIZONTAL	0.029	******	******	0.830	1.081
VERTICAL	-0.135	******	******	-0.138	-0.133

SHOT 43 (25 MARCH, 1976, NO. 5)

SAND: WET, DENSITY:2050. KG/M**3; APPROACHING VELOCITY: 210. M/S
PROJECTILE: SOLID STEP-TIER MASS=0.5648 KG, D=0.02 M, L=0.238 M

X-RAY STATION	NO.1	NO.2	NO.3	NO.4	NO.5
TIME (SECOND)	.000149	*******	.003198	.005461	.008142
CENTER OF GRAVITY POSITION (M)					
HORIZONTAL	18.019	18.210	0.437	0.725	0.997
VERTICAL	18.241	18.241	0.098	0.101	0.104
INCLINATION ANGLE(DEG).	*****	*****	-1.0	-5.0	-7.5
SEPARATION ANGLE(DEGREE)					
ABOVE	****	****	3.5	****	****
BELOW	****	****	5.0	****	***
NOSE WIDTH (M ON FILM).	******	******	0.0230	0.0230	0.0230
NOSE POSITION (M)					
HORIZONTAL	18.040	18.231	0.559	0.847	1.118
VERTICAL	18.121	18.121	0.096	0.090	0.089
INPUT NOSE POSITION (M)					
HORIZONTAL	******	******	0.563	0.848	1.114
VERTICAL	******	******	-0.127	-0.133	-0.135

SHOT 44 (25 MARCH, 1976, NO. 6)

SAND: WET, DENSITY:2050. KG/M**3; APPROACHING VELOCITY: 213. M/S
PROJECTILE: SOLID STEP-TIER MASS:0.0659 KG, D=0.02 M, L=0.238 M

X-RAY STATION	NO.1	NO.2	NO.3	NO.4	NO.5
TIME (SECOND)	.000173	*******	.003297	.005650	.008421
CENTER OF GRAVITY POSITION (M)					
HORIZONTAL	17.916	18.210	0.438	0.732	1.004
VERTICAL	18.121	18.241	0.093	0.098	0.104
INCLINATION ANGLE(DEG).	0.0	*****	1.0	-2.5	-4.5
SEPARATION ANGLE(DEGREE)					
ABOVE	****	****	4.0	0.0	3.0
BELOW	****	****	4.0	5.0	6.0
NOSE WIDTH (M ON FILM).	******	******	0.0230	0.0230	0.0230
NOSE POSITION (M)					
HORIZONTAL	18.040	18.231	0.560	0.854	1.126
VERTICAL	18.121	18.121	0.096	0.093	0.095
INPUT NOSE POSITION (M)					
HORIZONTAL	******	******	0.564	0.856	1.123
VERTICAL	******	******	-0.127	-0.130	-0.128

```
SHOT 45   ( 08 APRIL. 1976. NO. 1 )

SAND: WET. DENSITY:2050. KG/M**3; APPROACHING VELOCITY: 210. M/S
PROJECTILE: SOLID STEP-TIER MASS:0.5662 KG. D=0.02 M. L=0.238 M

X-RAY STATION ..........   NO.1     NO.2     NO.3     NO.4     NO.5

TIME (SECOND) ..........  .000192  .001238  .003300  .005628  .008365
CENTER OF GRAVITY POSITION (M)
  HORIZONTAL ........... -0.087    0.110    0.442    0.742    1.013
  VERTICAL .............  0.104    0.110    0.115    0.118    0.122

INCLINATION ANGLE(DEG).   1.6      1.0      2.5      5.0      6.0
SEPARATION ANGLE(DEGREE)
  ABOVE ...............   ****     7.0      4.5      8.5     10.0
  BELOW ...............   ****     5.5      3.5      5.0      1.0
NOSE WIDTH (M ON FILM). 0.0250   0.0230   0.0230   0.0230   0.0230
NOSE POSITION (M)
  HORIZONTAL ..........   0.035    0.232    0.563    0.863    1.134
  VERTICAL ............   0.106    0.112    0.121    0.129    0.135
INPUT NOSE POSITION (M)
  HORIZONTAL ..........   0.034    0.233    0.568    0.867    1.133
  VERTICAL ............  -0.116   -0.108   -0.098   -0.089   -0.082


NOSE VEL. Y-COMP. (M/S):    6.       5.       4.       3.       2.
COEFFICIENTS OF CUBIC POLYNOMIAL/STANDARD DEVIATION
  0.1052E 00  0.5801E 01 -0.3430E 03  0.8368E 04 / 0.0003 (M)

NOSE VEL. X-COMP. (M/S): 198.     179.     145.     113.      86.
COEFFICIENTS OF CUBIC POLYNOMIAL/STANDARD DEVIATION
 -0.3281E-02  0.2018E 03 -0.9825E 04  0.2332E 06 / 0.0011 (M)


NOSE VEL. DIRECTION(DEG)  1.6      1.6      1.5      1.4      1.2
SEPARATION ANGLE(DEGREE). RELATIVE TO NOSE VELOCITY
  ABOVE ...............   ****     7.6      3.5      4.9      5.2
  BELOW ...............   ****     4.9      4.5      8.6      5.8


C.G. VEL. Y-COMP. (M/S):    6.       4.       2.       1.       3.
COEFFICIENTS OF CUBIC POLYNOMIAL/STANDARD DEVIATION
  0.1029E 00  0.6875E 01 -0.1156E 04  0.7251E 05 / 0.0003 (M)

C.G. VEL. X-COMP. (M/S): 198.     179.     145.     113.      86.
COEFFICIENTS OF CUBIC POLYNOMIAL/STANDARD DEVIATION
 -0.1252E 00  0.2017E 03 -0.9772E 04  0.2296E 06 / 0.0012 (M)

PONCELET DRAG COEFF. = 1.241
 V0 = 145. STAND. DEVIA. = 0.0134 (M)
C.G. VEL. X-COMP. (M/S): 212.     183.     145.     117.      95.
```

SHOT 46 (08 APRIL, 1976, NO. 2)

SAND: WET, DENSITY:2060. KG/M**3; APPROACHING VELOCITY: 251. M/S
PROJECTILE: A.M.M. MASS:0.0811 KG, D=0.02 M, L=0.070 M

X-RAY STATION	NO.1	NO.2	NO.3	NO.4	NO.5
TIME (SECOND)	.000099	.000901	.005000	.019317	.063951
CENTER OF GRAVITY POSITION (M)					
HORIZONTAL	0.024	0.152	18.535	18.839	19.144
VERTICAL	0.111	0.118	18.121	18.121	18.121
INCLINATION ANGLE(DEG).	3.5	13.0	*****	*****	*****
SEPARATION ANGLE(DEGREE)					
ABOVE	****	20.0	****	****	****
BELOW	****	1.0	****	****	****
NOSE WIDTH (M ON FILM).	0.0250	0.0230	******	******	******
NOSE POSITION (M)					
HORIZONTAL	0.024	0.152	18.535	18.839	19.144
VERTICAL	0.111	0.118	18.121	18.121	18.121
INPUT NOSE POSITION (M)					
HORIZONTAL	0.021	0.141	******	******	******
VERTICAL	-0.110	-0.101	******	******	******

SHOT 47 (06 APRIL, 1970, NO. 3)

SAND: WET, DENSITY:2050. KG/M**3: APPROACHING VELOCITY: 552. M/S
PROJECTILE: A.M.H. MASS:0.0812 KG. D=0.02 M. L=0.070 M

X-RAY STATION	NO.1	NO.2	NO.3	NO.4	NO.5
TIME (SECOND)	.000093	.000970	.005000	.019192	.063951
CENTER OF GRAVITY POSITION (M)					
HORIZONTAL	0.037	0.264	0.398	18.839	19.144
VERTICAL	0.111	0.121	0.164	18.121	18.121
INCLINATION ANGLE(DEG).	8.0	20.0	152.0	*****	*****
SEPARATION ANGLE(DEGREE)					
ABOVE	****	24.0	****	****	****
BELOW	****	****	****	****	****
NOSE WIDTH (M ON FILM).	0.0250	0.0235	0.0220	******	******
NOSE POSITION (M)					
HORIZONTAL	0.037	0.264	0.398	18.839	19.144
VERTICAL	0.111	0.121	0.164	18.121	18.121
INPUT NOSE POSITION (M)					
HORIZONTAL	0.037	0.270	0.385	******	******
VERTICAL	-0.110	-0.098	-0.051	******	******

SHOT 48 (08 APRIL, 1976, NO. 4)

SAND: WET. DENSITY:2050. KG/M**3; APPROACHING VELOCITY: 538. M/S
PROJECTILE: A.M.M. MASS:0.0811 KG. D=0.02 M. L=0.070 M

X-RAY STATION	NO.1	NO.2	NO.3	NO.4	NO.5
TIME (SECOND)	.000155	.001200	.008044	.019969	.100000
CENTER OF GRAVITY POSITION (M)					
HORIZONTAL	0.063	18.231	0.423	18.839	19.144
VERTICAL	0.101	18.121	0.076	18.121	18.121
INCLINATION ANGLE(DEG).	-1.0	*****	*****	*****	*****
SEPARATION ANGLE(DEGREE)					
ABOVE	****	****	****	****	****
BELOW	****	****	****	****	****
NOSE WIDTH (M ON FILM).	0.0260	******	0.0230	******	******
NOSE POSITION (M)					
HORIZONTAL	0.063	18.231	0.423	18.839	19.144
VERTICAL	0.101	18.121	0.076	18.121	18.121
INPUT NOSE POSITION (M)					
HORIZONTAL	0.071	******	0.406	******	******
VERTICAL	-0.123	******	-0.150	******	******

SHOT 49 (09 APRIL, 1976, NO. 1)

SAND: WET, DENSITY:2050. KG/M**3; APPROACHING VELOCITY: 327. M/S
PROJECTILE: SOLID STEP-TIER MASS:0.5660 KG, D=0.02 M, L=0.238 M

X-RAY STATION	NO.1	NO.2	NO.3	NO.4	NO.5
TIME (SECOND)	.000127	.000780	.001876	.003220	.004768
CENTER OF GRAVITY POSITION (M)					
HORIZONTAL	-0.093	0.117	0.426	0.753	1.071
VERTICAL	0.093	0.098	0.105	0.110	0.116
INCLINATION ANGLE(DEG).	0.5	0.5	0.5	0.5	-0.5
SEPARATION ANGLE(DEGREE)					
ABOVE	****	11.0	10.5	9.0	8.0
BELOW	****	11.0	7.5	7.0	10.0
NOSE WIDTH (M ON FILM).	0.0250	0.0230	0.0230	0.0230	0.0230
NOSE POSITION (M)					
HORIZONTAL	0.029	0.239	0.548	0.875	1.193
VERTICAL	0.094	0.099	0.106	0.111	0.115
INPUT NOSE POSITION (M)					
HORIZONTAL	0.027	0.241	0.550	0.880	1.201
VERTICAL	-0.131	-0.123	-0.115	-0.109	-0.105

NOSE VEL. Y-COMP. (M/S): 8. 7. 5. 3. 1.
COEFFICIENTS OF CUBIC POLYNOMIAL/STANDARD DEVIATION
0.9305E-01 0.8645E 01 -0.1072E 04 0.4224E 05 / 0.0003 (M)

NOSE VEL. X-COMP. (M/S): 334. 305. 263. 223. 192.
COEFFICIENTS OF CUBIC POLYNOMIAL/STANDARD DEVIATION
-0.1309E-01 0.3401E 03 -0.2382E 05 0.1163E 07 / 0.0018 (M)

NOSE VEL. DIRECTION(DEG)	1.4	1.3	1.1	0.8	0.4
SEPARATION ANGLE(DEGREE), RELATIVE TO NOSE VELOCITY					
ABOVE	****	11.8	11.1	9.3	8.9
BELOW	****	10.2	6.9	6.7	9.1

C.G. VEL. Y-COMP. (M/S): 9. 7. 5. 4. 4.
COEFFICIENTS OF CUBIC POLYNOMIAL/STANDARD DEVIATION
0.9190E-01 0.9129E 01 -0.1491E 04 0.1293E 06 / 0.0004 (M)

C.G. VEL. X-COMP. (M/S): 334. 305. 263. 223. 193.
COEFFICIENTS OF CUBIC POLYNOMIAL/STANDARD DEVIATION
-0.1351E 00 0.3401E 03 -0.2384E 05 0.1171E 07 / 0.0017 (M)

PONCELET DRAG COEFF. = 0.822
VO = 334. STAND. DEVIA. = 0.0025 (M)
C.G. VEL. X-COMP. (M/S): 334. 303. 262. 225. 194.

RECORDED TIME OF MAXIMUM/MINIMUM COIL VOLTAGE (S)				
MAX	.000155	.001894	.003137	.004658
MIN	.000705	.002773	*******	.005621
COMPUTED NOSE POSITION AT MAX/MIN COIL VOLTAGE (M)				
AT MAX	0.039	0.554	0.855	1.172
AT MIN	0.215	0.772	********	1.353
RECORDED COIL POSITION (M)				
	0.0	0.487	0.792	1.085
DIFFERENCE BETWEEN COIL AND NOSE AT MAX/MIN VOLTAGE (M)				
AT MAX	0.039	0.067	0.063	0.086
AT MIN	0.215	0.265	********	0.267

```
                    SHOT 50     ( 09 APRIL, 1976, NO. 2 )

SAND: WET, DENSITY:2050. KG/M**3; APPROACHING VELOCITY: 395. M/S
PROJECTILE: SOLID STEP-TIER MASS:0.5560 KG, D=0.02 M, L=0.230 M

X-RAY STATION ..........    NO.1     NO.2     NO.3     NO.4     NO.5

TIME (SECOND) .......... .000108  .000635  .001579  .002771  .004288
CENTER OF GRAVITY POSITION (M)
  HORIZONTAL ........... -0.095    0.107    0.430    0.781    1.119
  VERTICAL .............  0.094    0.099    0.107    0.112    0.112

INCLINATION ANGLE(DEG).    1.5      1.5      2.0      3.5      7.5
SEPARATION ANGLE(DEGREE)
  ABOVE ................   ****     10.0     9.0      15.0     ****
  BELOW ................   ****     11.0     8.0      9.0      ****
NOSE WIDTH (M ON FILM).  0.0255   0.0230   0.0230   0.0230   0.0230
NOSE POSITION (M)
  HORIZONTAL ...........   0.027    0.229    0.552    0.902    1.240
  VERTICAL .............   0.097    0.102    0.111    0.119    0.128
INPUT NOSE POSITION (M)
  HORIZONTAL ...........   0.024    0.229    0.555    0.912    1.255
  VERTICAL ............. -0.128   -0.119   -0.109   -0.100   -0.090


NOSE VEL. Y-COMP. (M/S):   12.      10.      8.       6.       6.
COEFFICIENTS OF CUBIC POLYNOMIAL/STANDARD DEVIATION
  0.9567E-01  0.1207E 02 -0.1727E 04  0.1531E 06 / 0.0003 (M)

NOSE VEL. X-COMP. (M/S): 392.     368.     322.     263.     183.
COEFFICIENTS OF CUBIC POLYNOMIAL/STANDARD DEVIATION
 -0.1501E-01  0.3971E 03 -0.2302E 05 -0.2949E 06 / 0.0021 (M)


NOSE VEL. DIRECTION(DEG)  1.7      1.6      1.4      1.3      1.8
SEPARATION ANGLE(DEGREE), RELATIVE TO NOSE VELOCITY
  ABOVE ...............    ****     10.1     8.4      12.8     ****
  BELOW ...............    ****     10.9     6.6      11.2     ****


C.G. VEL. Y-COMP. (M/S):   12.      10.      6.       2.      -2.
COEFFICIENTS OF CUBIC POLYNOMIAL/STANDARD DEVIATION
  0.9248E-01  0.1230E 02 -0.2173E 04  0.8346E 05 / 0.0002 (M)

C.G. VEL. X-COMP. (M/S): 392.     368.     322.     263.     184.
COEFFICIENTS OF CUBIC POLYNOMIAL/STANDARD DEVIATION
 -0.1370E 00  0.3972E 03 -0.2304E 05 -0.2785E 06 / 0.0023 (M)

PONCELET DRAG COEFF. = 0.788
 VO = 392. STAND. DEVIA. = 0.0156 (M)
C.G. VEL. X-COMP. (M/S): 392.     359.     312.     267.     226.


RECORDED TIME OF MAXIMUM/MINIMUM COIL VOLTAGE (S)
  MAX          .000124      .001566      .002485      .003804
  MIN          .000606      .002236      .003137      .004665
COMPUTED NOSE POSITION AT MAX/MIN COIL VOLTAGE (M)
  AT MAX        0.034        0.550        0.825        1.146
  AT MIN        0.217        0.755        0.995        1.307
RECORDED COIL POSITION (M)
                0.0          0.487        0.792        1.086
DIFFERENCE BETWEEN COIL AND NOSE AT MAX/MIN VOLTAGE (M)
  AT MAX        0.034        0.063        0.033        0.060
  AT MIN        0.217        0.268        0.203        0.221
```

SHOT 51 (09 APRIL, 1976, NO. 3)

SAND: WET, DENSITY:2050. KG/M**3; APPROACHING VELOCITY: 402. M/S
PROJECTILE: SOLID STEP-TIER MASS:0.5657 KG. D=0.02 M, L=0.238 M

X-RAY STATION	NO.1	NO.2	NO.3	NO.4	NO.5
TIME (SECOND)	.000118	.000644	.001691	.002495	.003848
CENTER OF GRAVITY POSITION (M)					
HORIZONTAL	18.019	0.111	18.514	0.667	19.124
VERTICAL	18.241	0.102	18.241	0.111	18.241
INCLINATION ANGLE(DEG).	*****	1.5	*****	6.0	*****
SEPARATION ANGLE(DEGREE)					
ABOVE	****	14.0	****	14.0	****
BELOW	****	11.0	****	6.5	****
NOSE WIDTH (M ON FILM).	******	0.0230	******	0.0230	******
NOSE POSITION (M)					
HORIZONTAL	18.040	0.233	18.535	0.788	19.144
VERTICAL	18.121	0.105	18.121	0.124	18.121
INPUT NOSE POSITION (M)					
HORIZONTAL	******	0.234	******	0.781	******
VERTICAL	******	-0.116	******	-0.094	******

SHOT 52 (10 APRIL, 1976, NO. 1)

SAND: DRY, DENSITY:1538. KG/M**3; APPROACHING VELOCITY: 210. M/S
PROJECTILE: SOLID STEP-TIER MASS:0.5662 KG, D=0.02 M, L=0.238 M

X-RAY STATION	NO.1	NO.2	NO.3	NO.4	NO.5
TIME (SECOND)	.000166	.001217	.003251	.005471	.008136
CENTER OF GRAVITY POSITION (M)					
HORIZONTAL	-0.094	0.109	0.428	0.708	0.975
VERTICAL	0.106	0.115	0.120	0.128	0.129
INCLINATION ANGLE(DEG).	0.0	0.0	-1.0	-3.5	-5.5
SEPARATION ANGLE(DEGREE)					
ABOVE	****	5.5	4.0	3.0	0.0
BELOW	****	5.5	6.0	5.0	3.0
NOSE WIDTH (M ON FILM).	0.0250	0.0230	0.0230	0.0230	0.0230
NOSE POSITION (M)					
HORIZONTAL	0.028	0.231	0.550	0.829	1.096
VERTICAL	0.106	0.115	0.118	0.121	0.117
INPUT NOSE POSITION (M)					
HORIZONTAL	0.025	0.231	0.552	0.828	1.089
VERTICAL	-0.116	-0.105	-0.101	-0.098	-0.102

NOSE VEL. Y-COMP. (M/S):	7.	5.	1.	-1.	-1.

COEFFICIENTS OF CUBIC POLYNOMIAL/STANDARD DEVIATION
0.1055E 00 0.7758E 01 -0.1255E 04 0.5922E 05 / 0.0022 (M)

NOSE VEL. X-COMP. (M/S):	206.	181.	140.	110.	94.

COEFFICIENTS OF CUBIC POLYNOMIAL/STANDARD DEVIATION
-0.9796E-02 0.2107E 03 -0.1327E 05 0.5007E 06 / 0.0044 (M)

NOSE VEL. DIRECTION(DEG)	2.0	1.6	0.6	-0.3	-0.5
SEPARATION ANGLE(DEGREE), RELATIVE TO NOSE VELOCITY					
ABOVE	****	7.1	5.6	6.2	5.0
BELOW	****	3.9	4.4	1.8	-2.0

C.G. VEL. Y-COMP. (M/S):	6.	5.	3.	2.	-0.

COEFFICIENTS OF CUBIC POLYNOMIAL/STANDARD DEVIATION
0.1058E 00 0.6473E 01 -0.4980E 03 0.6752E 04 / 0.0026 (M)

C.G. VEL. X-COMP. (M/S):	206.	181.	140.	111.	94.

COEFFICIENTS OF CUBIC POLYNOMIAL/STANDARD DEVIATION
-0.1318E 00 0.2106E 03 -0.1326E 05 0.5005E 06 / 0.0045 (M)

PONCELET DRAG COEFF. = 1.811
VO = 140. STAND. DEVIA. = 0.0028 (M)

C.G. VEL. X-COMP. (M/S):	210.	180.	140.	113.	92.

SHOT 5J (10 APRIL, 1976, NO. 2)

SAND: DRY, DENSITY:1538. KG/M**3; APPROACHING VELOCITY: 212. M/S
PROJECTILE: SOLID STEP-TIER MASS:0.5652 KG, D=0.02 M, L=0.238 M

X-RAY STATION	NO.1	NO.2	NO.3	NO.4	NO.5
TIME (SECOND)	.000186	.001227	.003233	.005575	.008168
CENTER OF GRAVITY POSITION (M)					
HORIZONTAL	-0.095	0.108	0.429	18.819	0.963
VERTICAL	0.106	0.114	0.116	18.241	0.091
INCLINATION ANGLE(DEG).	1.0	0.5	-5.0	*****	-14.5
SEPARATION ANGLE(DEGREE)					
ABOVE	****	3.0	2.0	****	****
BELOW	****	3.0	7.0	****	****
NOSE WIDTH (M ON FILM).	0.0240	0.0235	0.0235	******	0.0250
NOSE POSITION (M)					
HORIZONTAL	0.027	0.230	0.551	18.839	1.078
VERTICAL	0.108	0.115	0.105	18.121	0.061
INPUT NOSE POSITION (M)					
HORIZONTAL	0.025	0.230	0.554	******	1.062
VERTICAL	-0.113	-0.105	-0.116	******	-0.173

SHOT 54 (10 APRIL, 1976, NO. 3)

SAND: DRY, DENSITY:1636. KG/M**3; APPROACHING VELOCITY: 208. M/S
PROJECTILE: SOLID STEP-TIER MASS:0.5662 KG. D=0.02 M. L=0.238 M

X-RAY STATION	NO.1	NO.2	NO.3	NO.4	NO.5
TIME (SECOND)	.000155	.001196	.003199	.005730	.008556
CENTER OF GRAVITY POSITION (M)					
HORIZONTAL	-0.099	0.100	0.415	0.722	0.990
VERTICAL	0.102	0.110	0.114	0.117	0.121
INCLINATION ANGLE(DEG).	2.0	2.0	2.0	2.5	2.5
SEPARATION ANGLE(DEGREE)					
ABOVE	****	6.0	5.0	6.0	5.0
BELOW	****	6.0	4.0	3.0	3.0
NOSE WIDTH (M ON FILM).	0.0260	0.0240	0.0230	0.0235	0.0240
NOSE POSITION (M)					
HORIZONTAL	0.023	0.221	0.536	0.844	1.112
VERTICAL	0.106	0.114	0.118	0.122	0.126
INPUT NOSE POSITION (M)					
HORIZONTAL	0.019	0.220	0.537	0.845	1.106
VERTICAL	-0.117	-0.106	-0.101	-0.096	-0.091

NOSE VEL. Y-COMP. (M/S):	7.	5.	2.	1.	3.

COEFFICIENTS OF CUBIC POLYNOMIAL/STANDARD DEVIATION
0.1654E 00 0.7578E 01 -0.1208E 04 0.7875E 05 / 0.0018 (M)

NOSE VEL. X-COMP. (M/S):	202.	178.	139.	106.	88.

COEFFICIENTS OF CUBIC POLYNOMIAL/STANDARD DEVIATION
-0.7965E-02 0.2058E 03 -0.1243E 05 0.4311E 06 / 0.0008 (M)

NOSE VEL. DIRECTION(DEG)	2.0	1.6	0.8	0.4	2.1
SEPARATION ANGLE(DEGREE), RELATIVE TO NOSE VELOCITY					
ABOVE	****	5.6	3.8	3.9	4.6
BELOW	****	6.4	5.2	5.1	3.4

C.G. VEL. Y-COMP. (M/S):	8.	5.	2.	1.	4.

COEFFICIENTS OF CUBIC POLYNOMIAL/STANDARD DEVIATION
0.1010E 00 0.8031E 01 -0.1454E 04 0.9274E 05 / 0.0016 (M)

C.G. VEL. X-COMP. (M/S):	202.	178.	139.	106.	87.

COEFFICIENTS OF CUBIC POLYNOMIAL/STANDARD DEVIATION
-0.1299E 00 0.2057E 03 -0.1243E 05 0.4303E 06 / 0.0012 (M)

PONCELET DRAG COEFF. = 1.900
VO = 139. STAND. DEVIA. = 0.0063 (M)

C.G. VEL. X-COMP. (M/S):	212.	180.	139.	108.	87.

RECORDED TIME OF MAXIMUM/MINIMUM COIL VOLTAGE (S)

MAX	.000124	.003044	.005621	.008789
MIN	.001180	.004658	.007516	.011056
COMPUTED NOSE POSITION AT MAX/MIN COIL VOLTAGE (M)				
AT MAX	0.017	0.515	0.832	1.133
AT MIN	0.216	0.724	1.019	1.330
RECORDED COIL POSITION (M)				
	0.0	0.486	0.791	1.086
DIFFERENCE BETWEEN COIL AND NOSE AT MAX/MIN VOLTAGE (M)				
AT MAX	0.017	0.029	0.041	0.047
AT MIN	0.216	0.238	0.228	0.244

SHOT 58 (10 APRIL, 1976, NO. 4)

SAND: DRY, DENSITY:1538. KG/M**3; APPROACHING VELOCITY: 206. M/S
PROJECTILE: SOLID STEP-TIER MASS:0.5653 KG, D=0.02 M, L=0.238 M

X-RAY STATION	NO.1	NO.2	NO.3	NO.4	NO.5
TIME (SECOND)	.000202	.001242	.003283	.005814	.008618
CENTER OF GRAVITY POSITION (M)					
HORIZONTAL	-0.095	0.100	0.411	0.713	0.975
VERTICAL	0.106	0.112	0.118	0.122	0.115
INCLINATION ANGLE(DEG).	0.0	0.0	-2.0	-5.0	-5.5
SEPARATION ANGLE(DEGREE)					
ABOVE	****	4.5	6.5	****	1.0
BELOW	****	5.0	2.5	****	7.0
NOSE WIDTH (M ON FILM).	0.0250	0.0230	0.0230	0.0220	0.0220
NOSE POSITION (M)					
HORIZONTAL	0.027	0.222	0.533	0.834	1.097
VERTICAL	0.105	0.112	0.114	0.112	0.104
INPUT NOSE POSITION (M)					
HORIZONTAL	0.024	0.221	0.533	0.834	1.092
VERTICAL	-0.117	-0.109	-0.106	-0.108	-0.117

NOSE VEL. Y-COMP. (M/S): 6. 4. 0. -2. -3.
COEFFICIENTS OF CUBIC POLYNOMIAL/STANDARD DEVIATION
0.1046E 00 0.6631E 01 -0.1271E 04 0.5683E 05 / 0.0015 (M)

NOSE VEL. X-COMP. (M/S): 197. 174. 136. 103. 87.
COEFFICIENTS OF CUBIC POLYNOMIAL/STANDARD DEVIATION
-0.1282E-01 0.2024E 03 -0.1232E 05 0.4362E 06 / 0.0025 (M)

NOSE VEL. DIRECTION(DEG)	1.8	1.2	0.1	-1.3	-1.7
SEPARATION ANGLE(DEGREE), RELATIVE TO NOSE VELOCITY					
ABOVE	****	5.7	8.6	****	4.8
BELOW	****	3.8	0.4	****	3.2

C.G. VEL. Y-COMP. (M/S): 5. 5. 3. -0. -5.
COEFFICIENTS OF CUBIC POLYNOMIAL/STANDARD DEVIATION
0.1047E 00 0.5641E 01 -0.3470E 03 -0.1907E 05 / 0.0013 (M)

C.G. VEL. X-COMP. (M/S): 197. 174. 136. 104. 87.
COEFFICIENTS OF CUBIC POLYNOMIAL/STANDARD DEVIATION
-0.1348E 00 0.2023E 03 -0.1223E 05 0.4319E 06 / 0.0026 (M)

PONCELET DRAG COEFF. = 1.894
VO = 136. STAND. DEVIA. = 0.0046 (M)
C.G. VEL. X-COMP. (M/S): 205. 175. 136. 106. 86.

RECORDED TIME OF MAXIMUM/MINIMUM COIL VOLTAGE (S)				
MAX	.000140	.003137	.005730	.008882
MIN	.001242	.004845	.007686	.011211
COMPUTED NOSE POSITION AT MAX/MIN COIL VOLTAGE (M)				
AT MAX	0.015	0.514	0.825	1.119
AT MIN	0.220	0.728	1.013	1.323
RECORDED COIL POSITION (M)				
	0.0	0.486	0.791	1.086
DIFFERENCE BETWEEN COIL AND NOSE AT MAX/MIN VOLTAGE (M)				
AT MAX	0.015	0.028	0.034	0.033
AT MIN	0.220	0.242	0.222	0.237

SHOT 56 (10 APRIL, 1976, NO. 5)

```
SAND: DRY, DENSITY:1538. KG/M**3; APPROACHING VELOCITY: 324. M/S
PROJECTILE: SOLID STEP-TIER MASS:0.5653 KG, D=0.02 M, L=0.238 M

X-RAY STATION ..........  NO.1      NO.2      NO.3      NO.4      NO.5

TIME (SECOND) .......... .000166  .000820  .001919  .003263  .004808
CENTER OF GRAVITY POSITION (M)
  HORIZONTAL .......... -0.089    0.106     0.376     0.652     0.880
  VERTICAL ............  0.106    0.112     0.117     0.120     0.119

INCLINATION ANGLE(DEG).   0.0      0.5      -1.0      -2.5      -5.0
SEPARATION ANGLE(DEGREE)
  ABOVE ...............   ****     7.0       5.0      ****       2.0
  BELOW ...............   ****     5.5       5.0      ****       4.0
NOSE WIDTH (M ON FILM).  0.0250   0.0230    0.0230    0.0230    0.0220
NOSE POSITION (M)
  HORIZONTAL ..........  0.033    0.228     0.498     0.774     1.001
  VERTICAL ............  0.106    0.113     0.115     0.115     0.108
INPUT NOSE POSITION (M)
  HORIZONTAL ..........  0.032    0.228     0.493     0.764     0.987
  VERTICAL ............ -0.116   -0.107    -0.105    -0.105    -0.112


NOSE VEL. Y-COMP. (M/S):  10.       6.        1.       -3.       -4.
COEFFICIENTS OF CUBIC POLYNOMIAL/STANDARD DEVIATION
  0.1047E 00  0.1120E 02 -0.3321E 04  0.2360E 06 / 0.0017 (M)

NOSE VEL. X-COMP. (M/S): 314.     281.      228.      174.      126.
COEFFICIENTS OF CUBIC POLYNOMIAL/STANDARD DEVIATION
 -0.2419E-01  0.3243E 03 -0.2794E 05  0.1012E 07 / 0.0069 (M)


NOSE VEL. DIRECTION(DEG)  1.8      1.3       0.3      -1.0      -2.0
SEPARATION ANGLE(DEGREE), RELATIVE TO NOSE VELOCITY
  ABOVE ...............   ****     7.8       6.3      ****       5.0
  BELOW ...............   ****     4.7       3.7      ****       1.0


C.G. VEL. Y-COMP. (M/S):   9.       7.        4.        0.       -2.
COEFFICIENTS OF CUBIC POLYNOMIAL/STANDARD DEVIATION
  0.1046E 00  0.9832E 01 -0.1919E 04  0.9958E 05 / 0.0006 (M)

C.G. VEL. X-COMP. (M/S): 314.     280.      228.      174.      126.
COEFFICIENTS OF CUBIC POLYNOMIAL/STANDARD DEVIATION
 -0.1462E 00  0.3243E 03 -0.2800E 05  0.1020E 07 / 0.0069 (M)

PONCELET DRAG COEFF. = 1.760
 VO = 314. STAND. DEVIA. = 0.0133 (M)
C.G. VEL. X-COMP. (M/S): 314.     273.      223.      182.      150.


RECORDED TIME OF MAXIMUM/MINIMUM COIL VOLTAGE (S)
  MAX          .000124     .001957     .003571     .005839
  MIN          .000714     .002950     .004752     .007298
COMPUTED NOSE POSITION AT MAX/MIN COIL VOLTAGE (M)
  AT MAX       0.016       0.511       0.824       1.118
  AT MIN       0.194       0.715       0.995       1.248
RECORDED COIL POSITION (M)
               0.0         0.486       0.791       1.086
DIFFERENCE BETWEEN COIL AND NOSE AT MAX/MIN VOLTACE (M)
  AT MAX       0.016       0.025       0.033       0.032
  AT MIN       0.194       0.229       0.204       0.162
```

SHOT 57 (10 APRIL, 1976, NO. 6)

SAND: DRY, DENSITY:1538. KG/M**3; APPROACHING VELOCITY: 198. M/S
PROJECTILE: SOLID STEP-TIER MASS:0.565. KG, D=0.02 M, L=0.238 M

X-RAY STATION	NO.1	NO.2	NO.3	NO.4	NO.5
TIME (SECOND)	.000279	.001422	.003090	.005512	.0084[illegible]9
CENTER OF GRAVITY POSITION (M)					
HORIZONTAL	-0.087	0.117	0.356	0.664	0.934
VERTICAL	0.100	0.108	0.113	0.119	0.142
INCLINATION ANGLE(DEG).	1.0	1.0	3.0	8.0	10.5
SEPARATION ANGLE(DEGREE)					
ABOVE	****	3.5	2.5	****	1.5
BELOW	****	4.5	5.0	****	1.5
NOSE WIDTH (M ON FILM).	0.0250	0.0230	0.0230	0.0240	0.0250
NOSE POSITION (M)					
HORIZONTAL	0.035	0.239	0.477	0.785	1.054
VERTICAL	0.102	0.110	0.119	0.136	0.164
INPUT NOSE POSITION (M)					
HORIZONTAL	0.034	0.241	0.469	0.774	1.032
VERTICAL	-0.121	-0.110	-0.100	-0.080	-0.044

NOSE VEL. Y-COMP. (M/S): 7. 6. 6. 8. 12.
COEFFICIENTS OF CUBIC POLYNOMIAL/STANDARD DEVIATION
0.1005E 00 0.6977E 01 -0.4550E 03 0.6165E 05 / 0.0009 (M)

NOSE VEL. X-COMP. (M/S): 180. 162. 139. 109. 79.
COEFFICIENTS OF CUBIC POLYNOMIAL/STANDARD DEVIATION
-0.1329E-01 0.1842E 03 -0.7988E 04 0.1388E 06 / 0.0098 (M)

NOSE VEL. DIRECTION(DEG)	2.1	2.1	2.4	4.0	8.9
SEPARATION ANGLE(DEGREE), RELATIVE TO NOSE VELOCITY					
ABOVE	****	4.0	1.9	****	-0.1
BELOW	****	3.4	5.6	****	3.1

C.G. VEL. Y-COMP. (M/S): 8. 5. 2. 4. 14.
COEFFICIENTS OF CUBIC POLYNOMIAL/STANDARD DEVIATION
0.9773E-01 0.9586E 01 -0.2064E 04 0.1834E 06 / 0.0007 (M)

C.G. VEL. X-COMP. (M/S): 179. 162. 139. 109. 79.
COEFFICIENTS OF CUBIC POLYNOMIAL/STANDARD DEVIATION
-0.1351E 00 0.1838E 03 -0.7651E 04 0.1298E 06 / 0.0099 (M)

PONCELET DRAG COEFF. = 1.604
VO = 139. STAND. DEVIA. = 0.0167 (M)
C.G. VEL. X-COMP. (M/S): 190. 165. 139. 113. 92.

```
SHOT 58   ( 22 APRIL, 1976, NO. 1 )

SAND: DRY, DENSITY:1536. KG/M**3; APPROACHING VELOCITY: 334. M/S
PROJECTILE: SOLID STEP-TIER MASS:0.5647 KG, D=0.02 M, L=0.238 M

X-RAY STATION ..........  NO.1     NO.2     NO.3     NO.4     NO.5

TIME (SECOND) .......... .000127  .000780  .001975  .003404  .005100
CENTER OF GRAVITY POSITION (M)
  HORIZONTAL ........... -0.091    0.066    0.381    0.643    0.914
  VERTICAL .............  0.095    0.098    0.102    0.104    0.108

INCLINATION ANGLE(DEG).   0.0      0.0      0.0     -1.0     -2.5
SEPARATION ANGLE(DEGREE)
  ABOVE ................  ****     3.0      2.8      ****     2.5
  BELOW ................  ****     6.5      4.0      ****     5.0
NOSE WIDTH (M ON FILM).  0.0260   0.0230   0.0240   0.0240   0.0240
NOSE POSITION (M)
  HORIZONTAL ...........  0.031    0.208    0.503    0.765    1.036
  VERTICAL .............  0.095    0.098    0.102    0.102    0.102
INPUT NOSE POSITION (M)
  HORIZONTAL ...........  0.029    0.205    0.497    0.750    1.015
  VERTICAL ............. -0.131   -0.124   -0.120   -0.120   -0.120


NOSE VEL. Y-COMP. (M/S):    7.      4.      1.     -0.       0.
COEFFICIENTS OF CUBIC POLYNOMIAL/STANDARD DEVIATION
  0.9407E-01  0.7207E 01 -0.1977E 04  0.1715E 06 / 0.0007 (M)

NOSE VEL. X-COMP. (M/S): 303.     266.     212.     170.     153.
COEFFICIENTS OF CUBIC POLYNOMIAL/STANDARD DEVIATION
 -0.1060E-01  0.3113E 03 -0.3136E 05  0.2070E 07 / 0.0088 (M)


NOSE VEL. DIRECTION(DEG)  1.3     1.0      0.4     -0.1       0.2
SEPARATION ANGLE(DEGREE), RELATIVE TO NOSE VELOCITY
  ABOVE ...............  ****     4.0      2.9     ****       5.2
  BELOW ...............  ****     5.5      3.6     ****       2.3


C.G. VEL. Y-COMP. (M/S):    6.      4.      2.      1.       3.
COEFFICIENTS OF CUBIC POLYNOMIAL/STANDARD DEVIATION
  0.9429E-01  0.6230E 01 -0.1423E 04  0.1385E 06 / 0.0004 (M)

C.G. VEL. X-COMP. (M/S): 303.     266.     212.     170.     153.
COEFFICIENTS OF CUBIC POLYNOMIAL/STANDARD DEVIATION
 -0.1326E 00  0.3112E 03 -0.3138E 05  0.2074E 07 / 0.0088 (M)

PONCELET DRAG COEFF. = 1.913
 VO = 212. STAND. DEVIA. = 0.0088 (M)
C.G. VEL. X-COMP. (M/S): 311.     267.     212.     170.     137.


RECORDED TIME OF MAXIMUM/MININUM COIL VOLTAGE (S)
  MAX        .000155     .001916     .003494     .005516
  MIN        .000745     .002929     .004801     .007075
COMPUTED NOSE POSITION AT MAX/MIN COIL VOLTAGE (M)
  AT MAX      0.037       0.465       0.782       1.100
  AT MIN      0.205       0.684       0.990       1.355
RECORDED COIL POSITION (M)
              0.0         0.486       0.810       1.086
DIFFERENCE BETWEEN COIL AND NOSE AT MAX/MIN VOLTAGE (M)
  AT MAX      0.037      -0.001      -0.028       0.014
  AT MIN      0.205       0.198       0.180       0.269
```

SHOT 59 (22 APRIL, 1976, NO. 2)

```
SAND: DRY, DENSITY:1538. KG/M**3; APPROACHING VELOCITY: 335. M/S
PROJECTILE: SOLID STEP-TIER MASS:0.5649 KG, D=0.02 M, L=0.238 M

X-RAY STATION .........     NO.1     NO.2     NO.3     NO.4     NO.5

TIME (SECOND) .........  .000127  .000795  .002050  .003491  .005696
CENTER OF GRAVITY POSITION (M)
  HORIZONTAL ..........   -0.081    0.097    0.396    0.680    0.989
  VERTICAL ............    0.106    0.108    0.109    0.115    0.108

INCLINATION ANGLE(DEG).      0.0      0.5     -1.0     -3.5     -4.5
SEPARATION ANGLE(DEGREE)
  ABOVE ...............     ****      6.5      3.5      2.5      2.0
  BELOW ...............     ****      6.5      5.0      6.0      7.
NOSE WIDTH (M ON FILM).   0.0240   0.0230   0.0220   0.0220   0.0210
NOSE POSITION (M)
  HORIZONTAL ..........    0.041    0.219    0.518    0.802    1.111
  VERTICAL ............    0.106    0.109    0.107    0.107    0.098
INPUT NOSE POSITION (M)
  HORIZONTAL ..........    0.042    0.217    0.517    0.798    1.109
  VERTICAL ............   -0.116   -0.112   -0.113   -0.113   -0.122


NOSE VEL. Y-COMP. (M/S):      2.       1.      -0.      -2.      -6.
COEFFICIENTS OF CUBIC POLYNOMIAL/STANDARD DEVIATION
  0.1059E 00  0.2160E 01 -0.4530E 03 -0.2998E 05 / 0.0017 (M)

NOSE VEL. X-COMP. (M/S): 277.     257.     219.     175.     105.
COEFFICIENTS OF CUBIC POLYNOMIAL/STANDARD DEVIATION
  0.5737E-02  0.2802E 03 -0.1459E 05 -0.9062E 05 / 0.0016 (M)


NOSE VEL. DIRECTION(DEG)     0.4      0.3     -0.0     -0.7     -3.2
SEPARATION ANGLE(DEGREE), RELATIVE TO NOSE VELOCITY
  ABOVE ...............     ****      6.3      4.5      5.3      3.3
  BELOW ...............     ****      6.7      4.0      3.2      5.7


C.G. VEL. Y-COMP. (M/S):    -0.       2.       3.       2.      -9.
COEFFICIENTS OF CUBIC POLYNOMIAL/STANDARD DEVIATION
  0.1062E 00 -0.1004E 01  0.2105E 04 -0.3305E 06 / 0.0014 (M)

C.G. VEL. X-COMP. (M/S): 276.     257.     219.     175.     105.
COEFFICIENTS OF CUBIC POLYNOMIAL/STANDARD DEVIATION
 -0.1163E 00  0.2801E 03 -0.1451E 05 -0.9933E 05 / 0.0016 (M)

PONCELET DRAG COEFF. = 1.667
 V0 = 219. STAND. DEVIA. = 0.0276 (M)
C.G. VEL. X-COMP. (M/S): 314.     273.     219.     179.     140.


RECORDED TIME OF MAXIMUM/MINIMUM COIL VOLTAGE (S)
  MAX          .006062     .001916     .003500     .005466
  MIN          .000739     .003000     .004839     .007205
COMPUTED NOSE POSITION AT MAX/MIN COIL VOLTAGE (M)
  AT MAX       0.023       0.468       0.804       1.087
  AT MIN       0.205       0.713       1.010       1.233
RECORDED COIL POSITION (M)
               0.0         0.486       0.810       1.086
DIFFERENCE BETWEEN COIL AND NOSE AT MAX/MIN VOLTAGE (M)
  AT MAX       0.023       0.002      -0.006       0.001
  AT MIN       0.205       0.227       0.200       0.147
```

SHOT 61 (22 APRIL, 1976, NO. 4)

SAND: DRY, DENSITY:1538. KG/M**3; APPROACHING VELOCITY: 336. M/S
PROJECTILE: SOLID STEP-TIER MASS:0.5636 KG, D=0.02 M, L=0.238 M

X-RAY STATION	NO.1	NO.2	NO.3	NO.4	NO.5
TIME (SECOND)	.000140	.000783	.002056	.003509	.005714
CENTER OF GRAVITY POSITION (M)					
HORIZONTAL	-0.087	0.088	0.388	0.669	0.973
VERTICAL	0.107	0.103	0.105	0.111	0.108
INCLINATION ANGLE(DEG).	0.0	-0.5	-1.5	-4.5	-4.5
SEPARATION ANGLE(DEGREE)					
ABOVE	****	8.0	6.0	4.0	2.0
BELOW	****	8.0	7.0	8.0	8.0
NOSE WIDTH (M ON FILM).	0.0250	0.0230	0.0230	0.0230	0.0235
NOSE POSITION (M)					
HORIZONTAL	0.035	0.210	0.510	0.790	1.094
VERTICAL	0.107	0.102	0.102	0.102	0.099
INPUT NOSE POSITION (M)					
HORIZONTAL	0.034	0.207	0.507	0.783	1.086
VERTICAL	-0.115	-0.120	-0.120	-0.120	-0.124

NOSE VEL. Y-COMP. (M/S): -8. -4. 0. 1. -6.
COEFFICIENTS OF CUBIC POLYNOMIAL/STANDARD DEVIATION
0.1075E 00 -0.8371E 01 0.3126E 04 -0.3400E 06 / 0.0017 (M)

NOSE VEL. X-COMP. (M/S): 284. 260. 215. 169. 109.
COEFFICIENTS OF CUBIC POLYNOMIAL/STANDARD DEVIATION
-0.5295E-02 0.2896E 03 -0.1939E 05 0.4221E 06 / 0.0010 (M)

NOSE VEL. DIRECTION(DEG)	-1.5	-0.9	0.0	0.3	-3.1
SEPARATION ANGLE(DEGREE), RELATIVE TO NOSE VELOCITY					
ABOVE	****	7.6	7.5	8.8	3.4
BELOW	****	8.4	5.5	3.2	6.6

C.G. VEL. Y-COMP. (M/S): -9. -3. 4. 4. -10.
COEFFICIENTS OF CUBIC POLYNOMIAL/STANDARD DEVIATION
0.1081E 00 -0.1013E 02 0.5343E 04 -0.6252E 06 / 0.0007 (M)

C.G. VEL. X-COMP. (M/S): 284. 260. 216. 169. 109.
COEFFICIENTS OF CUBIC POLYNOMIAL/STANDARD DEVIATION
-0.1272E 00 0.2895E 03 -0.1926E 05 0.4076E 06 / 0.0011 (M)

PONCELET DRAG COEFF. = 1.815
VO = 216. STAND. DEVIA. = 0.0221 (M)
C.G. VEL. X-COMP. (M/S): 317. 274. 216. 173. 134.

RECORDED TIME OF MAXIMUM/MINIMUM COIL VOLTAGE (S)				
MAX	.000109	.001929	.003603	.005767
MIN	.000699	.002957	.004944	.007491
COMPUTED NOSE POSITION AT MAX/MIN COIL VOLTAGE (M)				
AT MAX	0.026	0.484	0.806	1.101
AT MIN	0.188	0.693	1.004	1.254
RECORDED COIL POSITION (M)				
	0.0	0.486	0.810	1.086
DIFFERENCE BETWEEN COIL AND NOSE AT MAX/MIN VOLTAGE (M)				
AT MAX	0.026	-0.002	-0.004	0.015
AT MIN	0.188	0.207	0.194	0.168

```
                    SHOT 62   ( 22 APRIL, 1976, NO. 5 )

SAND: DRY, DENSITY:1538. KG/M**3; APPROACHING VELOCITY: [illegible] M/S
PROJECTILE: SOLID STEP-TIER MASS:0.5633 KG, D=0.02 M, L=0.238 M

X-RAY STATION .........  NO.1      NO.2      NO.3      NO.4      NO.5

TIME (SECOND) .........  .000127   .000683   .001646   .002702   .004006
CENTER OF GRAVITY POSITION (M)
  HORIZONTAL .......... -0.077     0.107     0.379     0.624     0.847
  VERTICAL ............  0.103     0.106     0.106     0.103     0.116

INCLINATION ANGLE(DEG).  1.5       1.5       3.5       5.5       8.0
SEPARATION ANGLE(DEGREE)
  ABOVE ...............  ****      9.5       9.5       9.0       ****
  BELOW ...............  ****      5.5       3.0       1.5       ****
NOSE WIDTH (M ON FILM).  0.0250    0.0230    0.0230    0.0230    0.0220
NOSE POSITION (M)
  HORIZONTAL ..........  0.045     0.229     0.501     0.746     0.968
  VERTICAL ............  0.106     0.109     0.114     0.115     0.133
INPUT NOSE POSITION (M)
  HORIZONTAL ..........  0.047     0.229     0.496     0.732     0.950
  VERTICAL ............ -0.116    -0.111    -0.106    -0.105    -0.085

NOSE VEL. Y-COMP. (M/S):  12.       5.        1.        5.        24.
COEFFICIENTS OF CUBIC POLYNOMIAL/STANDARD DEVIATION
  0.1042E 00  0.1356E 02 -0.7442E 04  0.1455E 07 / 0.0015 (M)

NOSE VEL. X-COMP. (M/S): 344.      312.      258.      203.      139.
COEFFICIENTS OF CUBIC POLYNOMIAL/STANDARD DEVIATION
  0.1633E-02  0.3510E 03 -0.2930E 05  0.4710E 06 / 0.0019 (M)

NOSE VEL. DIRECTION(DEG)  2.0       1.0       0.2       1.5       9.8
SEPARATION ANGLE(DEGREE), RELATIVE TO NOSE VELOCITY
  ABOVE ...............  ****      9.0       6.2       5.0       ****
  BELOW ...............  ****      6.0       6.3       5.5       ****

C.G. VEL. Y-COMP. (M/S):  12.       3.       -3.        0.        22.
COEFFICIENTS OF CUBIC POLYNOMIAL/STANDARD DEVIATION
  0.1012E 00  0.1389E 02 -0.9613E 04  0.1759E 07 / 0.0008 (M)

C.G. VEL. X-COMP. (M/S): 344.      312.      259.      204.      140.
COEFFICIENTS OF CUBIC POLYNOMIAL/STANDARD DEVIATION
 -0.1203E 00  0.3510E 03 -0.2918E 05  0.4669E 06 / 0.0020 (M)

PONCELET DRAG COEFF. = 1.827
 VO = 259. STAND. DEVIA. = 0.0200 (M)
C.G. VEL. X-COMP. (M/S): 374.      321.      259.      213.      175.
```

SHOT 63 (22 APRIL, 1976, NO. 6)

SAND: DRY, DENSITY:1538. KG/M**3; APPROACHING VELOCITY: 415. M/S
PROJECTILE: SOLID STEP-TIER MASS:0.5633 KG, D=0.02 M, L=0.238 M

X-RAY STATION	NO.1	NO.2	NO.3	NO.4	NO.5
TIME (SECOND)	.000146	.000683	.001708	.003084	.004798
CENTER OF GRAVITY POSITION (M)					
HORIZONTAL	-0.071	0.109	0.396	0.711	0.989
VERTICAL	0.102	0.104	0.104	0.114	0.136
INCLINATION ANGLE(DEG).	2.5	3.5	8.0	11.5	11.5
SEPARATION ANGLE(DEGREE)					
ABOVE	****	10.0	12.0	12.0	11.0
BELOW	****	4.0	1.5	[illegible]	1.0
NOSE WIDTH (M ON FILM).	0.0250	0.0230	0.0230	0.0230	0.0230
NOSE POSITION (M)					
HORIZONTAL	0.051	0.231	0.516	0.831	1.108
VERTICAL	0.107	0.111	0.121	0.138	0.161
INPUT NOSE POSITION (M)					
HORIZONTAL	0.054	0.231	0.514	0.830	1.103
VERTICAL	-0.115	-0.109	-0.098	-0.078	-0.052

NOSE VEL. Y-COMP. (M/S): 6. 8. 11. 13. 13.
COEFFICIENTS OF CUBIC POLYNOMIAL/STANDARD DEVIATION
0.1063E 00 0.5346E 01 0.2234E 04 -0.2063E 06 / 0.0004 (M)

NOSE VEL. X-COMP. (M/S): 341. 311. 258. 195. 131.
COEFFICIENTS OF CUBIC POLYNOMIAL/STANDARD DEVIATION
0.1801E-02 0.3499E 03 -0.2920E 05 0.8929E 06 / 0.0046 (M)

NOSE VEL. DIRECTION(DEG)	1.0	1.5	2.5	3.9	5.4
SEPARATION ANGLE(DEGREE), RELATIVE TO NOSE VELOCITY					
ABOVE	****	6.0	5.5	4.4	4.9
BELOW	****	6.0	7.0	8.6	7.1

C.G. VEL. Y-COMP. (M/S): -0. 1. 4. 9. 18.
COEFFICIENTS OF CUBIC POLYNOMIAL/STANDARD DEVIATION
0.1023E 00 -0.4180E 00 0.6070E 03 0.1577E 06 / 0.0018 (M)

C.G. VEL. X-COMP. (M/S): 342. 312. 259. 196. 131.
COEFFICIENTS OF CUBIC POLYNOMIAL/STANDARD DEVIATION
-0.1201E 00 0.3499E 03 -0.2662E 05 0.8028E 06 / 0.0044 (M)

PONCELET DRAG COEFF. = 1.811
VO = 259. STAND. DEVIA. = 0.0214 (M)
C.G. VEL. X-COMP. (M/S): 378. 327. 259. 203. 160.

SHOT 64 (22 APRIL, 1976, NO. 7)

SAND: DRY, DENSITY:1536. KG/M**3; APPROACHING VELOCITY: 409. M/S
PROJECTILE: SOLID STEP-TIER MASS:0.5633 KG, D=0.02 M, L=0.238 M

X-RAY STATION	NO.1	NO.2	NO.3	NO.4	NO.5
TIME (SECOND)	.000146	.000674	.001693	.003100	.004801
CENTER OF GRAVITY POSITION (M)					
HORIZONTAL	-0.060	0.099	0.386	0.704	0.978
VERTICAL	0.094	0.098	0.099	0.102	0.122
INCLINATION ANGLE(DEG).	1.0	1.5	5.0	10.0	9.5
SEPARATION ANGLE(DEGREE)					
ABOVE	****	8.5	7.0	13.0	11.0
BELOW	****	6.5	4.5	2.0	1.5
NOSE WIDTH (M ON FILM).	0.0250	0.0230	0.0230	0.0225	0.0220
NOSE POSITION (M)					
HORIZONTAL	0.042	0.221	0.508	0.824	1.098
VERTICAL	0.097	0.101	0.109	0.123	0.142
INPUT NOSE POSITION (M)					
HORIZONTAL	0.043	0.220	0.504	0.822	1.094
VERTICAL	-0.128	-0.121	-0.111	-0.095	-0.075

NOSE VEL. Y-COMP. (M/S):	7.	8.	9.	10.	11.

COEFFICIENTS OF CUBIC POLYNUMIAL/STANDARD DEVIATION
0.9560E-01 0.6984E 01 0.8090E 03 -0.5632E 05 / 0.0002 (M)

NOSE VEL. X-COMP. (M/S):	350.	316.	257.	191.	137.

COEFFICIENTS OF CUBIC POLYNUMIAL/STANDARD DEVIATION
-0.8636E-02 0.3598E 03 -0.3429E 05 0.1536E 07 / 0.0034 (M)

NOSE VEL. DIRECTION(DEG)	1.2	1.5	2.1	3.1	4.5
SEPARATION ANGLE(DEGREE). RELATIVE TO NOSE VELOCITY					
ABOVE	****	8.5	4.1	6.1	6.0
BELOW	****	6.5	7.4	8.9	6.5

C.G. VEL. Y-COMP. (M/S):	6.	3.	1.	5.	20.

COEFFICIENTS OF CUBIC POLYNUMIAL/STANDARD DEVIATION
0.9364E-01 0.7402E 01 -0.3646E 04 0.6899E 06 / 0.0005 (M)

C.G. VEL. X-COMP. (M/S):	349.	316.	258.	192.	135.

COEFFICIENTS OF CUBIC POLYNUMIAL/STANDARD DEVIATION
-0.1305E 00 0.3590E 03 -0.3350E 05 0.1417E 07 / 0.0036 (M)

PONCELET DRAG COEFF. = 1.917
VO = 258. STAND. DEVIA. = 0.0174 (M)

C.C. VEL. X-COMP. (M/S):	383.	329.	258.	199.	155.

RECORDED TIME OF MAXIMUM/MINIMUM COIL VOLTAGE (S)				
MAX	.000124	.001646	.002972	.004770
MIN	.000668	.002547	.004146	.006124
COMPUTED NOSE POSITION AT MAX/MIN COIL VOLTAGE (M)				
AT MAX	0.035	0.497	0.798	1.094
AT MIN	0.217	0.711	1.003	1.261
RECORDED COIL POSITION (M)				
	0.0	0.486	0.810	1.086
DIFFERENCE BETWEEN COIL AND NOSE AT MAX/MIN VOLTAGE (M)				
AT MAX	0.035	0.011	-0.012	0.008
AT MIN	0.217	0.225	0.193	0.175

SHOT 65 (22 APRIL, 1976, NO. 8) 1

SAND: DRY, DENSITY:5380. KG/M**3; APPROACHING VELOCITY: 407. M/S
PROJECTILE: SOLID STEP-TIER MASS:0.5631 KG, D=0.02 M, L=0.230 M

X-RAY STATION	NO.1	NO.2	NO.3	NO.4	NO.5
TIME (SECOND)	.000155	.000693	.001708	.003121	.004804
CENTER OF GRAVITY POSITION (M)					
HORIZONTAL	-0.070	0.110	0.396	0.713	0.993
VERTICAL	0.100	0.104	0.103	0.108	0.111
INCLINATION ANGLE(DEG).	0.0	0.0	0.5	-1.0	-3.5
SEPARATION ANGLE(DEGREE)					
ABOVE	****	7.0	6.5	5.5	2.0
BELOW	****	6.5	4.5	4.5	6.0
NOSE WIDTH (M ON FILM),	0.0250	0.0235	0.0240	0.0230	0.0230
NOSE POSITION (M)					
HORIZONTAL	0.052	0.232	0.518	0.835	1.115
VERTICAL	0.100	0.104	0.104	0.106	0.103
INPUT NOSE POSITION (M)					
HORIZONTAL	0.055	0.232	0.515	0.835	1.111
VERTICAL	-0.124	-0.116	-0.118	-0.115	-0.118

NOSE VEL. Y-COMP. (M/S): 5. 3. 1. -1. -2.
COEFFICIENTS OF CUBIC POLYNOMIAL/STANDARD DEVIATION
0.5963E-01 0.4867E 01 -0.1143E 04 0.5990E 05 / 0.0017 (M)

NOSE VEL. X-COMP. (M/S): 348. 314. 257. 193. 144.
COEFFICIENTS OF CUBIC POLYNOMIAL/STANDARD DEVIATION
-0.2609E-02 0.3588E 03 -0.3408E 05 0.1622E 07 / 0.0022 (M)

NOSE VEL. DIRECTION(DEG) 0.7 0.6 0.3 -0.2 -0.8
SEPARATION ANGLE(DEGREE), RELATIVE TO NOSE VELOCITY
ABOVE .... **** 7.6 6.3 6.3 4.7
BELOW .... **** 5.9 4.7 3.7 3.3

C.G. VEL. Y-COMP. (M/S): 2. 2. 2. 2. 2.
COEFFICIENTS OF CUBIC POLYNOMIAL/STANDARD DEVIATION
0.1003E 00 0.2379E 01 0.1000E 02 -0.1075E 05 / 0.0025 (M)

C.G. VEL. X-COMP. (M/S): 348. 314. 257. 194. 144.
COEFFICIENTS OF CUBIC POLYNOMIAL/STANDARD DEVIATION
-0.1246E 00 0.3569E 03 -0.3408E 05 0.1626E 07 / 0.0018 (M)

PONCELET DRAG COEFF. = 0.536
VO = 257. STAND. DEVIA. = 0.0133 (M)
C.G. VEL. X-COMP. (M/S): 378. 325. 257. 199. 157.

SHOT 66 (24 APRIL, 1976, NO. 9)

SAND: DRY, DENSITY:1538. KG/M**3; APPROACHING VELOCITY: 588. M/S
PROJECTILE: A.M.H. MASS:0.0824 KG, D=0.02 M, L=0.076 M

X-RAY STATION	NO.1	NO.2	NO.3	NO.4	NO.5
TIME (SECOND)	.000124	.001158	.007981	.020000	.100000
CENTER OF GRAVITY POSITION (M)					
HORIZONTAL	0.062	0.267	0.395	18.839	19.144
VERTICAL	0.088	0.071	0.055	18.121	18.121
INCLINATION ANGLE(DEG).	-6.0	-49.0	*****	*****	*****
SEPARATION ANGLE(DEGREE)					
ABOVE	****	****	****	****	****
BELOW	****	****	****	****	***
NOSE WIDTH (M ON FILM).	0.0260	0.0235	0.0240	******	******
NOSE POSITION (M)					
HORIZONTAL	0.062	0.267	0.395	18.839	19.144
VERTICAL	0.088	0.071	0.055	18.121	18.121
INPUT NOSE POSITION (M)					
HORIZONTAL	0.069	0.274	0.367	******	******
VERTICAL	-0.140	-0.156	-0.177	******	******

SHOT 67 (22 APRIL, 1976, NO.10)

SAND: DRY, DENSITY:1538. KG/M**3; APPROACHING VELOCITY: 575. M/S
PROJECTILE: A.M.M. MASS:0.0812 KG, D=0.02 M, L=0.070 M

X-RAY STATION	NO.1	NO.2	NO.3	NO.4	NO.5
TIME (SECOND)	.000146	.001186	.007981	.020000	.100000
CENTER OF GRAVITY POSITION (M)					
HORIZONTAL	0.066	0.248	0.364	18.839	19.144
VERTICAL	0.086	0.069	0.062	18.121	18.121
INCLINATION ANGLE(DEG),	-7.5	-58.5	*****	*****	*****
SEPARATION ANGLE(DEGREE)					
ABOVE	4.0	****	****	****	****
BELOW	14.0	****	****	****	****
NOSE WIDTH (M ON FILM).	0.0266	0.0240	0.0240	******	******
NOSE POSITION (M)					
HORIZONTAL	0.066	0.248	0.364	18.839	19.144
VERTICAL	0.086	0.069	0.062	18.121	18.121
INPUT NOSE POSITION (M)					
HORIZONTAL	0.075	0.252	0.330	******	******
VERTICAL	-0.143	-0.160	-0.168	******	******

```
SHOT 68    ( 23 APRIL, 1976, NO. 1 )

SAND: WET, DENSITY:2050. KG/M**3; APPROACHING VELOCITY: 397. M/S
PROJECTILE: SOLID STEP-TIER MASS:0.5664 KG, D=0.02 M, L=0.238 M

X-RAY STATION .........   NO.1     NO.2     NO.3     NO.4     NO.5

TIME (SECOND) .........  .000118  .000637  .001593  .002491  .003845
CENTER OF GRAVITY POSITION (M)
  HORIZONTAL .........  -0.082    0.099    0.421    0.693    1.039
  VERTICAL ...........   0.099    0.103    0.105    0.109    0.113

INCLINATION ANGLE(DEG).  0.0      0.0      0.0     -1.0     -3.0
SEPARATION ANGLE(DEGREE)
  ABOVE ..............   ****     13.0     14.0     12.0     7.0
  BELOW ..............   ****     11.0     14.0     12.0     12.
NOSE WIDTH (M ON FILM).  0.0250   0.0230   0.0230   0.0230   0.0230
NOSE POSITION (M)
  HORIZONTAL .........   0.040    0.221    0.543    0.815    1.161
  VERTICAL ...........   0.099    0.103    0.105    0.107    0.107
INPUT NOSE POSITION (M)
  HORIZONTAL .........   0.041    0.220    0.544    0.812    1.164
  VERTICAL ...........  -0.125   -0.118   -0.116   -0.114   -0.114


NOSE VEL. Y-COMP. (M/S):    8.       5.       2.       0.       1.
COEFFICIENTS OF CUBIC POLYNOMIAL/STANDARD DEVIATION
  0.9832E-01  0.8637E 01 -0.3050E 04  0.3592E 06 / 0.0011 (M)

NOSE VEL. X-COMP. (M/S): 355.     346.     321.     288.     218.
COEFFICIENTS OF CUBIC POLYNOMIAL/STANDARD DEVIATION
 -0.1862E-02  0.3561E 03 -0.6032E 04 -0.2060E 07 / 0.0013 (M)


NOSE VEL. DIRECTION(DEG)  1.3      0.9      0.3      0.0      0.3
SEPARATION ANGLE(DEGREE), RELATIVE TO NOSE VELOCITY
  ABOVE ..............   ****     13.9     14.3     13.0     10.3
  BELOW ..............   ****     10.1     13.7     11.0      8.7


C.G. VEL. Y-COMP. (M/S):    7.       5.       3.       3.       5.
COEFFICIENTS OF CUBIC POLYNOMIAL/STANDARD DEVIATION
  0.9858E-01  0.7234E 01 -0.2100E 04  0.3144E 06 / 0.0015 (M)

C.G. VEL. X-COMP. (M/S): 354.     346.     321.     288.     218.
COEFFICIENTS OF CUBIC POLYNOMIAL/STANDARD DEVIATION
 -0.1239E 00  0.3560E 03 -0.6000E 04 -0.2064E 07 / 0.0014 (M)

PONCELET DRAG COEFF. = 0.614
 VO = 321. STAND. DEVIA. = 0.0177 (M)
C.G. VEL. X-COMP. (M/S): 385.     360.     321.     292.     256.


RECORDED TIME OF MAXIMUM/MINIMUM COIL VOLTAGE (S)
  MAX        .000084     .001494     .002457     .003615
  MIN        .000565     .002149     *******     .004394
COMPUTED NOSE POSITION AT MAX/MIN COIL VOLTAGE (M)
  AT MAX     0.028       0.510       0.806       1.109
  AT MIN     0.197       0.715      ********     1.271
RECORDED COIL POSITION (M)
             0.0         0.486       0.810       1.086
DIFFERENCE BETWEEN COIL AND NOSE AT MAX/MIN VOLTAGE (M)
  AT MAX     0.028       0.024      -0.004       0.023
  AT MIN     0.197       0.229      ********     0.185
```

```
SHOT 69    ( 23 APRIL, 1976, NO. 2 )

SAND: WET, DENSITY:2050. KG/M**3; APPROACHING VELOCITY: 395. M/S
PROJECTILE: SOLID STEP-TIER MASS:0.5643 KG, D=0.02 M, L=0.238 M

X-RAY STATION .........   NO.1     NO.2     NO.3     NO.4     NO.5

TIME (SECOND) ......... .000103  .000618  .001596  .002472  .003845
CENTER OF GRAVITY POSITION (M)
  HORIZONTAL .......... -0.092    0.111    0.448    0.719    1.075
  VERTICAL ............  0.120    0.128    0.132    0.136    0.138

INCLINATION ANGLE(DEG).   0.5      0.0      0.0      0.0     -3.0
SEPARATION ANGLE(DEGREE)
  ABOVE ...............   ****     7.0      9.0      ****     6.0
  BELOW ...............   ****     7.0     12.0      ****    11.0
NOSE WIDTH (M ON FILM).  0.0200   0.0230   0.0240   0.0230   0.0240
NOSE POSITION (M)
  HORIZONTAL ..........   0.030    0.233    0.570    0.841    1.197
  VERTICAL ............   0.121    0.126    0.132    0.136    0.131
INPUT NOSE POSITION (M)
  HORIZONTAL ..........   0.028    0.234    0.577    0.842    1.208
  VERTICAL ............  -0.097   -0.090   -0.084   -0.080   -0.085


NOSE VEL. Y-COMP. (M/S):  10.       9.       5.       1.      -7.
COEFFICIENTS OF CUBIC POLYNOMIAL/STANDARD DEVIATION
  0.1206E 00  0.1079E 02 -0.1553E 04 -0.1359E 06 / 0.0016 (M)

NOSE VEL. X-COMP. (M/S): 401.     374.     325.     287.     235.
COEFFICIENTS OF CUBIC POLYNOMIAL/STANDARD DEVIATION
 -0.1024E-01  0.4069E 03 -0.2784E 05  0.9462E 06 / 0.0041 (M)


NOSE VEL. DIRECTION(DEG)  1.5      1.3      0.8      0.1     -1.8
SEPARATION ANGLE(DEGREE), RELATIVE TO NOSE VELOCITY
  ABOVE ...............   ****     8.3      9.8      ****     7.2
  BELOW ...............   ****     5.7     11.2      ****     9.8


C.G. VEL. Y-COMP. (M/S):  14.      10.       4.       2.       2.
COEFFICIENTS OF CUBIC POLYNOMIAL/STANDARD DEVIATION
  0.1192E 00  0.1470E 02 -0.4452E 04  0.4882E 06 / 0.0016 (M)

C.G. VEL. X-COMP. (M/S): 401.     374.     325.     287.     235.
COEFFICIENTS OF CUBIC POLYNOMIAL/STANDARD DEVIATION
 -0.1322E 00  0.4066E 03 -0.2782E 05  0.9462E 06 / 0.0042 (M)

PONCELET DRAG COEFF. = 0.711
 VO = 401. STAND. DEVIA. = 0.0062 (M)
C.G. VEL. X-COMP. (M/S): 401.     370.     323.     289.     249.


RECORDED TIME OF MAXIMUM/MINIMUM COIL VOLTAGE (S)
  MAX         .000112     .001407     .002416     .003562
  MIN         .000559     .002028     .003158     .004404
COMPUTED NOSE POSITION AT MAX/MIN COIL VOLTAGE (M)
  AT MAX      0.035       0.510       0.824       1.129
  AT MIN      0.209       0.708       1.027       1.322
RECORDED COIL POSITION (M)
              0.0         0.486       0.810       1.086
DIFFERENCE BETWEEN COIL AND NOSE AT MAX/MIN VOLTAGE (M)
  AT MAX      0.035       0.024       0.014       0.043
  AT MIN      0.209       0.222       0.217       0.236
```

```
                SHOT 70    ( 23 APRIL, 1976, NO. 3 )

SAND: WET, DENSITY:2050. KG/M**3; APPROACHING VELOCITY: 209. M/S
PROJECTILE: SOLID FLAT NOSE MASS:0.5451 KG, D=0.02 M, L=0.225 M

X-RAY STATION .........   NO.1     NO.2     NO.3     NO.4     NO.5

TIME (SECOND) ......... .000202  .001130  .003220  .005503  .008428
CENTER OF GRAVITY POSITION (M)
  HORIZONTAL .......... -0.085    0.094    0.408    0.667    0.885
  VERTICAL ............  0.115    0.125    0.133    0.138    0.131

INCLINATION ANGLE(DEG).  0.0      0.0     -1.5     -4.0     -5.0
SEPARATION ANGLE(DEGREE)
  ABOVE ...............  ****     ****     3.0      ****     ****
  BELOW ...............  ****     ****     7.5      ****     ****
NOSE WIDTH (M ON FILM). 0.0260   0.0240   0.0240   0.0235   0.0240
NOSE POSITION (M)
  HORIZONTAL ..........  0.028    0.207    0.520    0.780    0.998
  VERTICAL ............  0.115    0.125    0.130    0.130    0.121
INPUT NOSE POSITION (M)
  HORIZONTAL ..........  0.025    0.203    0.518    0.770    0.969
  VERTICAL ............ -0.105   -0.093   -0.087   -0.087   -0.098


NOSE VEL. Y-COMP. (M/S):  10.       7.       1.      -2.      -3.
COEFFICIENTS OF CUBIC POLYNOMIAL/STANDARD DEVIATION
  0.1139E 00  0.1025E 02 -0.1781E 04  0.7843E 05 / 0.0022 (M)

NOSE VEL. X-COMP. (M/S): 199.     176.     132.      93.      59.
COEFFICIENTS OF CUBIC POLYNOMIAL/STANDARD DEVIATION
 -0.1074E-01  0.2038E 03 -0.1283E 05  0.3377E 06 / 0.0055 (M)


NOSE VEL. DIRECTION(DEG)  2.8      2.1      0.5     -1.4     -2.9
SEPARATION ANGLE(DEGREE), RELATIVE TO NOSE VELOCITY
  ABOVE ...............  ****     ****     5.0      ****     ****
  BELOW ...............  ****     ****     5.5      ****     ****


C.G. VEL. Y-COMP. (M/S):   9.       7.       3.      -0.      -4.
COEFFICIENTS OF CUBIC POLYNOMIAL/STANDARD DEVIATION
  0.1141E 00  0.9265E 01 -0.1015E 04  0.1742E 05 / 0.0022 (M)

C.G. VEL. X-COMP. (M/S): 199.     176.     132.      93.      60.
COEFFICIENTS OF CUBIC POLYNOMIAL/STANDARD DEVIATION
 -0.1237E 00  0.2036E 03 -0.1279E 05  0.3351E 06 / 0.0055 (M)

PONCELET DRAG COEFF. = 1.587
 V0 = 199. STAND. DEVIA. = 0.0199 (M)
C.G. VEL. X-COMP. (M/S): 199.     169.     127.     100.      78.


RECORDED TIME OF MAXIMUM/MINIMUM COIL VOLTAGE (S)
  MAX        .000233    .003276    .006006    .010435
  MIN        .001168    .004733    .008376    .014876
COMPUTED NOSE POSITION AT MAX/MIN COIL VOLTAGE (M)
  AT MAX     0.036      0.531      0.823      1.102
  AT MIN     0.210      0.702      0.994      1.293
RECORDED COIL POSITION (M)
             0.0        0.486      0.810      1.086
DIFFERENCE BETWEEN COIL AND NOSE AT MAX/MIN VOLTAGE (M)
  AT MAX     0.036      0.045      0.013      0.016
  AT MIN     0.210      0.216      0.184      0.207
```

SHOT 71 (23 APRIL, 1976, NO. 4)

SAND: WET, DENSITY:2050. KG/M**3; APPROACHING VELOCITY: 208. M/S
PROJECTILE: SOLID FLAT NOSE MASS:0.5450 KG, D=0.02 M, L=0.225 M

X-RAY STATION	NO.1	NO.2	NO.3	NO.4	NO.5
TIME (SECOND)	.000211	.001124	.003227	.005910	.009438
CENTER OF GRAVITY POSITION (M)					
HORIZONTAL	-0.102	0.091	0.413	0.722	1.013
VERTICAL	0.111	0.1[illegible]7	0.124	0.122	0.128
INCLINATION ANGLE(DEG).	2.5	3.5	3.0	5.0	0.5
SEPARATION ANGLE(DEGREE)					
ABOVE	****	****	6.5	****	****
BELOW	****	****	3.3	****	****
NOSE WIDTH (M ON FILM).	0.0270	0.0230	0.0240	0.0240	0.0240
NOSE POSITION (M)					
HORIZONTAL	0.011	0.204	0.525	0.835	1.125
VERTICAL	0.116	0.124	0.130	0.132	0.129
INPUT NOSE POSITION (M)					
HORIZONTAL	0.002	0.200	0.524	0.834	1.122
VERTICAL	-0.104	-0.094	-0.087	-0.084	-0.088

NOSE VEL. Y-COMP. (M/S):	8.	6.	2.	-1.	-0.

COEFFICIENTS OF CUBIC POLYNOMIAL/STANDARD DEVIATION
0.1150E 00 0.8418E 01 -0.1285E 04 0.5813E 05 / 0.0018 (M)

NOSE VEL. X-COMP. (M/S):	212.	185.	135.	94.	79.

COEFFICIENTS OF CUBIC POLYNOMIAL/STANDARD DEVIATION
-0.3027E-01 0.2188E 03 -0.1589E 05 0.5996E 06 / 0.0102 (M)

NOSE VEL. DIRECTION(DEG)	2.1	1.8	0.8	-0.4	-0.2
SEPARATION ANGLE(DEGREE), RELATIVE TO NOSE VELOCITY					
ABOVE	****	****	4.3	****	****
BELOW	****	****	5.7	****	****

C.G. VEL. Y-COMP. (M/S):	9.	6.	1.	-1.	5.

COEFFICIENTS OF CUBIC POLYNOMIAL/STANDARD DEVIATION
0.1090E 00 0.9646E 01 -0.1978E 04 0.1236E 06 / 0.0004 (M)

C.G. VEL. X-COMP. (M/S):	212.	185.	135.	94.	79.

COEFFICIENTS OF CUBIC POLYNOMIAL/STANDARD DEVIATION
-0.1431E 00 0.2187E 03 -0.1583E 05 0.5955E 06 / 0.0102 (M)

PONCELET DRAG COEFF. = 1.543
VO = 212. STAND. DEVIA. = 0.0125 (M)

C.G. VEL. X-COMP. (M/S):	212.	180.	134.	101.	76.

RECORDED TIME OF MAXIMUM/MINIMUM COIL VOLTAGE (S)				
MAX	.000208	.003112	.005699	.009317
MIN	.001155	.004621	.007736	.012270
COMPUTED NOSE POSITION AT MAX/MIN COIL VOLTAGE (M)				
AT MAX	0.015	0.515	0.812	1.115
AT MIN	0.202	0.701	0.990	1.371
RECORDED COIL POSITION (M)				
	0.0	0.486	0.810	1.086
DIFFERENCE BETWEEN COIL AND NOSE AT MAX/MIN VOLTAGE (M)				
AT MAX	0.015	0.029	0.002	0.029
AT MIN	0.202	0.215	0.180	0.285

SHOT 72 (23 APRIL, 1976, NO. 5)

SAND: WET, DENSITY:2050. KG/M**3; APPROACHING VELOCITY: 214. M/S
PROJECTILE: SOLID FLAT NOSE MASS:0.5448 KG, D=0.02 M, L=0.225 M

X-RAY STATION	NO.1	NO.2	NO.3	NO.4	NO.5
TIME (SECOND)	.000166	.001103	.003146	.005870	.009410
CENTER OF GRAVITY POSITION (M)					
HORIZONTAL	-0.086	0.096	0.430	0.760	1.075
VERTICAL	0.114	0.122	0.129	0.132	0.139
INCLINATION ANGLE(DEG).	0.0	0.0	0.5	-1.5	-5.0
SEPARATION ANGLE(DEGREE)					
ABOVE	****	****	6.0	3.0	4.0
BELOW	****	****	5.5	8.0	8.0
NOSE WIDTH (M ON FILM).	0.0260	0.0230	0.0230	0.0240	0.0240
NOSE POSITION (M)					
HORIZONTAL	0.027	0.209	0.543	0.873	1.187
VERTICAL	0.114	0.122	0.130	0.129	0.129
INPUT NOSE POSITION (M)					
HORIZONTAL	0.024	0.206	0.545	0.880	1.196
VERTICAL	-0.107	-0.097	-0.087	-0.088	-0.088

NOSE VEL. Y-COMP. (M/S): 11. 7. 2. -1. 3.
COEFFICIENTS OF CUBIC POLYNOMIAL/STANDARD DEVIATION
0.1114E 00 0.1165E 02 -0.2190E 04 0.1224E 06 / 0.0003 (M)

NOSE VEL. X-COMP. (M/S): 210. 187. 143. 102. 81.
COEFFICIENTS OF CUBIC POLYNOMIAL/STANDARD DEVIATION
-0.1222E-01 0.2151E 03 -0.1365E 05 0.4608E 06 / 0.0004 (M)

NOSE VEL. DIRECTION(DEG)	3.0	2.2	0.6	-0.8	2.1
SEPARATION ANGLE(DEGREE), RELATIVE TO NOSE VELOCITY					
ABOVE	****	****	6.1	3.7	11.1
BELOW	****	****	5.4	7.3	0.9

C.G. VEL. Y-COMP. (M/S): 10. 7. 2. 0. 5.
COEFFICIENTS OF CUBIC POLYNOMIAL/STANDARD DEVIATION
0.1120E 00 0.1015E 02 -0.1779E 04 0.1068E 06 / 0.0006 (M)

C.G. VEL. X-COMP. (M/S): 210. 187. 143. 102. 81.
COEFFICIENTS OF CUBIC POLYNOMIAL/STANDARD DEVIATION
-0.1252E 00 0.2151E 03 -0.1367E 05 0.4623E 06 / 0.0011 (M)

PONCELET DRAG COEFF. = 1.359
V0 = 210. STAND. DEVIA. = 0.0098 (M)
C.G. VEL. X-COMP. (M/S): 210. 182. 140. 107. 82.

RECORDED TIME OF MAXIMUM/MINIMUM COIL VOLTAGE (S)				
MAX	.000155	.003031	.005326	.008634
MIN	.001099	.004379	.007174	.011031
COMPUTED NOSE POSITION AT MAX/MIN COIL VOLTAGE (M)				
AT MAX	0.021	0.527	0.816	1.124
AT MIN	0.208	0.707	0.998	1.318
RECORDED COIL POSITION (M)				
	0.0	0.486	0.810	1.086
DIFFERENCE BETWEEN COIL AND NOSE AT MAX/MIN VOLTAGE (M)				
AT MAX	0.021	0.041	0.006	0.038
AT MIN	0.206	0.221	0.188	0.232

```
                    SHOT 73    ( 23 APRIL, 1976, NO. 6 )

SAND: WET, DENSITY:2050. KG/M**3; APPROACHING VELOCITY: 213. M/S
PROJECTILE: SOLID FLAT NOSE MASS:0.5446 KG. D=0.02 M. L=0.225 M

X-RAY STATION .........   NO.1      NO.2      NO.3      NO.4      NO.5

TIME (SECOND) .........  .000180   .001121   .003220   .005904   .009410
CENTER OF GRAVITY POSITION (M)
  HORIZONTAL .......... -0.089     0.098     0.437     0.774     1.093
  VERTICAL ............  0.115     0.125     0.134     0.139     0.144

INCLINATION ANGLE(DEG).  0.0       0.0       0.0      -2.0      -5.0
SEPARATION ANGLE(DEGREE)
  ABOVE ...............  ****      ****      5.5       2.5       ****
  BELOW ...............  ****      ****      7.0       8.0       ****
NOSE WIDTH (M ON FILM).  0.0260    0.0230    0.0230    0.0230    0.0230
NOSE POSITION (M)
  HORIZONTAL ..........  0.024     0.211     0.550     0.887     1.206
  VERTICAL ............  0.115     0.125     0.134     0.136     0.134
INPUT NOSE POSITION (M)
  HORIZONTAL ..........  0.020     0.208     0.553     0.894     1.215
  VERTICAL ............ -0.105    -0.093    -0.083    -0.081    -0.083


NOSE VEL. Y-COMP. (M/S):  11.       8.        2.       -1.        1.
COEFFICIENTS OF CUBIC POLYNOMIAL/STANDARD DEVIATION
  0.1135E 00  0.1171E 02 -0.1934E 04  0.9779E 05 / 0.0011 (M)

NOSE VEL. X-COMP. (M/S): 206.     185.      145.      107.       80.
COEFFICIENTS OF CUBIC POLYNOMIAL/STANDARD DEVIATION
 -0.1317E-01  0.2164E 03 -0.1193E 05  0.3543E 06 / 0.0036 (M)


NOSE VEL. DIRECTION(DEG)  3.1      2.4       0.9      -0.5       0.9
SEPARATION ANGLE(DEGREE), RELATIVE TO NOSE VELOCITY
  ABOVE ...............  ****      ****      6.4       4.0       ****
  BELOW ...............  ****      ****      6.1       6.5       ****


C.G. VEL. Y-COMP. (M/S):  10.       7.        3.        1.        3.
COEFFICIENTS OF CUBIC POLYNOMIAL/STANDARD DEVIATION
  0.1138E 00  0.1061E 02 -0.1546E 04  0.8040E 05 / 0.0016 (M)

C.G. VEL. X-COMP. (M/S): 206.     185.      148.      107.       80.
COEFFICIENTS OF CUBIC POLYNOMIAL/STANDARD DEVIATION
 -0.1262E 00  0.2104E 03 -0.1193E 05  0.3553E 06 / 0.0036 (M)

PONCELET DRAG COEFF. = 1.233
 VO = 205. STAND. DEVIA. = 0.0120 (M)
C.G. VEL. X-COMP. (M/S): 206.     181.      142.      111.       86.


RECORDED TIME OF MAXIMUM/MINIMUM COIL VOLTAGE (S)
  MAX          .000134     .002957     .005248     .008400
  MIN          .001134     .004354     .007106     .010776
COMPUTED NOSE POSITION AT MAX/MIN COIL VOLTAGE (M)
  AT MAX       0.015       0.514       0.814       1.122
  AT MIN       0.211       0.706       1.007       1.312
RECORDED COIL POSITION (M)
               0.0         0.486       0.810       1.086
DIFFERENCE BETWEEN COIL AND NOSE AT MAX/MIN VOLTAGE (M)
  AT MAX       0.015       0.028       0.004       0.036
  AT MIN       0.211       0.220       0.197       0.226
```

SHOT 74   (23 APRIL, 1976, NO. 7)

```
SAND: WET, DENSITY:2050. KG/M**3; APPROACHING VELOCITY: 334. M/S
PROJECTILE: SOLID FLAT NOSE MASS:0.5450 KG. D=0.02 M. L=0.225 M

X-RAY STATION ..........   NO.1      NO.2      NO.3      NO.4      NO.5

TIME (SECOND) ..........  .000155   .000835   .002174   .003831   .005714
CENTER OF GRAVITY POSITION (M)
   HORIZONTAL ........... -0.080     0.131     0.472     0.817     1.137
   VERTICAL .............  0.116     0.128     0.137     0.138     0.144

INCLINATION ANGLE(DEG).    1.0       0.5       0.0       0.5       1.5
SEPARATION ANGLE(DEGREE)
   ABOVE ................  ****      9.0       7.0       8.0       ****
   BELOW ................  ****      9.0       7.0       7.0       ***
NOSE WIDTH (M ON FILM).   0.0260    0.0230    0.0230    0.0230    0.0230
NOSE POSITION (M)
   HORIZONTAL ...........  0.033     0.244     0.585     0.930     1.250
   VERTICAL .............  0.120     0.129     0.137     0.139     0.147
INPUT NOSE POSITION (M)
   HORIZONTAL ...........  0.032     0.246     0.593     0.944     1.266
   VERTICAL ............. -0.099    -0.088    -0.079    -0.077    -0.068


NOSE VEL. Y-COMP. (M/S):  17.       11.       3.        1.        10.
COEFFICIENTS OF CUBIC POLYNOMIAL/STANDARD DEVIATION
   0.1171E 00  0.1872E 02 -0.5503E 04  0.5489E 06 / 0.0003 (M)

NOSE VEL. X-COMP. (M/S): 318.       287.      235.      187.      153.
COEFFICIENTS OF CUBIC POLYNOMIAL/STANDARD DEVIATION
  -0.1479E-01  0.3251E 03 -0.2430E 05  0.1082E 07 / 0.0051 (M)


NOSE VEL. DIRECTION(DEG)  3.1       2.1       0.6       0.2       3.6
SEPARATION ANGLE(DEGREE), RELATIVE TO NOSE VELOCITY
   ABOVE ................  ****      10.6      7.6       7.7       ****
   BELOW ................  ****      7.4       6.4       7.3       ****


C.G. VEL. Y-COMP. (M/S):  19.       12.       3.       -0.        9.
COEFFICIENTS OF CUBIC POLYNOMIAL/STANDARD DEVIATION
   0.1147E 00  0.2105E 02 -0.6193E 04  0.5949E 06 / 0.0002 (M)

C.G. VEL. X-COMP. (M/S): 318.       287.      235.      187.      153.
COEFFICIENTS OF CUBIC POLYNOMIAL/STANDARD DEVIATION
  -0.1278E 00  0.3251E 03 -0.2432E 05  0.1080E 07 / 0.0050 (M)

PONCELET DRAG COEFF. = 1.017
 VO = 235. STAND. DEVIA. = 0.0075 (M)
C.G. VEL. X-COMP. (M/S): 328.       289.      235.      191.      157.
```

SHOT 76 (24 APRIL, 1976, NO. 2)

```
SAND: WET, DENSITY:2050. KG/M**3; APPROACHING VELOCITY: 406. M/S
PROJECTILE: SOLID FLAT NOSE MASS:0.5448 KG, D=0.02 M, L=0.225 M

X-RAY STATION ..........  NO.1     NO.2     NO.3     NO.4     NO.5

TIME (SECOND) .......... .000124  .000655  .001714  .002991  .004826
CENTER OF GRAVITY POSITION (M)
  HORIZONTAL .......... -0.070    0.135    0.463    0.811    1.177
  VERTICAL ............  0.120    0.130    0.137    0.138    ******

INCLINATION ANGLE(DEG).  0.0      0.0      0.0      0.0      0.0
SEPARATION ANGLE(DEGREE)
  ABOVE ...............  20.0     13.0     9.0      9.0      ****
  BELOW ...............  20.0     14.0     9.0      8.0      ****
NOSE WIDTH (M ON FILM).  0.0260   0.0240   0.0230   0.0240   0.0240
NOSE POSITION (M)
  HORIZONTAL ..........  0.043    0.248    0.576    0.924    1.290
  VERTICAL ............  0.120    0.130    0.137    0.138    ******
INPUT NOSE POSITION (M)
  HORIZONTAL ..........  0.045    0.252    0.582    0.941    1.320
  VERTICAL ............ -0.099   -0.087   -0.079   -0.077    ******


NOSE VEL. Y-COMP. (M/S):*****   *****    *****    *****    *****
COEFFICIENTS OF CUBIC POLYNOMIAL/STANDARD DEVIATION
 -0.2520E 04  0.1401E 08 -0.1264E 11  0.2781E 13 / ****** (M)

NOSE VEL. X-COMP. (M/S): 379.   350.     295.     237.     168.
COEFFICIENTS OF CUBIC POLYNOMIAL/STANDARD DEVIATION
 -0.4425E-03  0.3863E 03 -0.2869E 05  0.8356E 06 / 0.0109 (M)


NOSE VEL. DIRECTION(DEG) 90.0   90.0    -90.0     90.0     90.0
SEPARATION ANGLE(DEGREE), RELATIVE TO NOSE VELOCITY
  ABOVE ...............  ****     ****     ****     99.0     ****
  BELOW ...............  ****     ****     99.0     ****     ****


C.G. VEL. Y-COMP. (M/S):*****   *****    *****    *****    *****
COEFFICIENTS OF CUBIC POLYNOMIAL/STANDARD DEVIATION
 -0.2520E 04  0.1401E 08 -0.1264E 11  0.2781E 13 / ****** (M)

C.G. VEL. X-COMP. (M/S): 379.   350.     295.     237.     168.
COEFFICIENTS OF CUBIC POLYNOMIAL/STANDARD DEVIATION
 -0.1134E 00  0.3864E 03 -0.2874E 05  0.8438E 06 / 0.0108 (M)

PONCELET DRAG COEFF. = 0.964
 V0 = 295. STAND. DEVIA. = 0.0194 (M)
C.G. VEL. X-COMP. (M/S): 403.   359.     298.     243.     194.


RECORDED TIME OF MAXIMUM/MINIMUM COIL VOLTAGE (S)
  MAX        .000093     *******     .002655     .003711
  MIN        .000590     *******     .003385     .004643
COMPUTED NOSE POSITION AT MAX/MIN COIL VOLTAGE (M)
  AT MAX     0.035       ********    0.839       1.081
  AT MIN     0.218       ********    1.011       1.258
RECORDED COIL POSITION (M)
             0.0         0.486       0.810       1.086
DIFFERENCE BETWEEN COIL AND NOSE AT MAX/MIN VOLTAGE (M)
  AT MAX     0.035       ********    0.029      -0.005
  AT MIN     0.218       ********    0.201       0.172
```

SHOT 77 (24 APRIL, 1976, NO. 3)

SAND: DRY, DENSITY:1536. KG/M**3; APPROACHING VELOCITY: 242. M/S
PROJECTILE: FLAT 6-INCH CYL.MASS:0.3687 KG, D=0.02 M, L=0.152 M

X-RAY STATION	NO.1	NO.2	NO.3	NO.4	NO.5
TIME (SECOND)	.000118	.000786	.002323	.004522	.008432
CENTER OF GRAVITY POSITION (M)					
HORIZONTAL	-0.012	0.081	0.341	0.882	19.132
VERTICAL	0.120	0.126	0.129	0.098	18.196
INCLINATION ANGLE(DEG).	-1.0	0.0	-4.0	-8.0	*****
SEPARATION ANGLE(DEGREE)					
ABOVE	****	****	****	****	****
BELOW	****	****	****	****	***
NOSE WIDTH (M ON FILM).	0.0260	0.0240	0.0235	0.0250	****.*
NOSE POSITION (M)					
HORIZONTAL	0.064	0.157	0.417	0.957	19.144
VERTICAL	0.119	0.126	0.123	0.087	18.121
INPUT NOSE POSITION (M)					
HORIZONTAL	0.072	0.143	0.397	0.987	******
VERTICAL	-0.100	-0.092	-0.095	-0.140	******

SHOT 76 (24 APRIL, 1970, NO. 4)

SAND: DRY, DENSITY:1538. KG/M**3; APPROACHING VELOCITY: 242. M/S
PROJECTILE: FLAT 6-INCH CYL.MASS:0.3687 KG, D=0.02 M, L=0.152 M

X-RAY STATION	NO.1	NO.2	NO.3	NO.4	NO.5
TIME (SECOND)	.000137	.000904	.002950	.005832	.010000
CENTER OF GRAVITY POSITION (M)					
HORIZONTAL	-0.059	0.151	0.404	0.748	1.096
VERTICAL	0.122	0.130	0.129	0.144	0.176
INCLINATION ANGLE(DEG).	[illegible]	2.5	6.0	11.0	16.5
SEPARATION ANGLE(DEGREE)					
ABOVE	****	****	10.0	****	11.0
BELOW	****	****	2.0	****	3.0
NOSE WIDTH (M ON FILM).	0.0260	0.0230	0.0230	0.0230	0.0215
NOSE POSITION (M)					
HORIZONTAL	0.017	0.177	0.480	0.822	1.169
VERTICAL	0.126	0.134	0.137	0.158	0.198
INPUT NOSE POSITION (M)					
HORIZONTAL	0.011	0.169	0.472	0.820	1.171
VERTICAL	-0.091	-0.083	-0.079	-0.055	-0.015

NOSE VEL. Y-COMP. (M/S): 3. 0. 5. 6. 12.
COEFFICIENTS OF CUBIC POLYNOMIAL/STANDARD DEVIATION
0.1274E 00 0.3027E 01 0.3050E 03 0.1003E 05 / 0.0044 (M)

NOSE VEL. X-COMP. (M/S): 195. 177. 137. 98. 76.
COEFFICIENTS OF CUBIC POLYNOMIAL/STANDARD DEVIATION
-0.3510E-02 0.1904E 03 -0.1237E 05 0.4047E 06 / 0.0140 (M)

NOSE VEL. DIRECTION(DEG) 0.9 1.2 2.1 4.4 9.0
SEPARATION ANGLE(DEGREE), RELATIVE TO NOSE VELOCITY

	NO.1	NO.2	NO.3	NO.4	NO.5
ABOVE	****	****	6.1	****	3.5
BELOW	****	****	5.9	****	10.5

C.G. VEL. Y-COMP. (M/S): 3. [illegible] 3. 5. 12.
COEFFICIENTS OF CUBIC POLYNOMIAL/STANDARD DEVIATION
0.1239E 00 0.2789E 01 -0.1650E 03 0.4141E 05 / 0.0054 (M)

C.G. VEL. X-COMP. (M/S): 195. 177. 137. 98. 77.
COEFFICIENTS OF CUBIC POLYNOMIAL/STANDARD DEVIATION
-0.7941E-01 0.1983E 03 -0.1209E 05 0.4017E 06 / 0.0140 (M)

PONCELET DRAG COEFF. = 1.311
V0 = 137. STAND. DEVIA. = 0.0139 (M)
C.G. VEL. X-COMP. (M/S): 206. 181. 137. 103. 75.

SHOT 79 (24 APRIL, 1976, NO. 5)

SANDI DRY, DENSITY:1538. KG/M**3; APPROACHING VELOCITY: 234. M/S
PROJECTILE: HOLLOW STEP-TIEMMASS:0.4218 KG. D=0.02 M. L=0.238 M

X-RAY STATION	NO.1	NO.2	NO.3	NO.4	NO.5
TIME (SECOND)	.000124	.000876	.002882	.005807	.010025
CENTER OF GRAVITY POSITION (M)					
HORIZONTAL	-0.089	0.073	0.390	0.736	1.078
VERTICAL	0.120	0.126	0.129	0.136	0.132
INCLINATION ANGLE(DEG).	-0.5	0.0	-1.5	-5.0	-5.5
SEPARATION ANGLE(DEGREE)					
ABOVE	****	8.5	2.0	****	1.5
BELOW	****	8.0	6.5	****	10.5
NOSE WIDTH (M ON FILM).	0.0200	0.0240	0.0230	0.0235	0.0240
NOSE POSITION (M)					
HORIZONTAL	0.016	0.178	0.503	0.841	1.183
VERTICAL	0.119	0.126	0.126	0.127	0.121
INPUT NOSE POSITION (M)					
HORIZONTAL	0.010	0.168	0.498	0.841	1.191
VERTICAL	-0.100	-0.092	-0.092	-0.091	-0.097

NOSE VEL. Y-COMP. (M/S): 5. 3. 1. -1. -0.
COEFFICIENTS OF CUBIC POLYNOMIAL/STANDARD DEVIATION
0.1198E 00 0.4815E 01 -0.6610E 03 0.4165E 05 / 0.0031 (M)

NOSE VEL. X-COMP. (M/S): 216. 193. 141. 93. 81.
COEFFICIENTS OF CUBIC POLYNOMIAL/STANDARD DEVIATION
-0.7645E-02 0.2204E 03 -0.1654E 05 0.6369E 06 / 0.0069 (M)

NOSE VEL. DIRECTION(DEG) 1.2 1.0 0.3 -0.7 -0.2
SEPARATION ANGLE(DEGREE), RELATIVE TO NOSE VELOCITY

ABOVE	****	9.5	3.8	****	6.8
BELOW	****	7.0	4.7	****	5.2

C.G. VEL. Y-COMP. (M/S): 4. 3. 3. 1. -3.
COEFFICIENTS OF CUBIC POLYNOMIAL/STANDARD DEVIATION
0.1206E 00 0.3590E 01 -0.8300E 02 -0.1658E 05 / 0.0026 (M)

C.G. VEL. X-COMP. (M/S): 216. 193. 141. 93. 81.
COEFFICIENTS OF CUBIC POLYNOMIAL/STANDARD DEVIATION
-0.1126E 00 0.2203E 03 -0.1648E 05 0.6333E 06 / 0.0067 (M)

PONCELET DRAG COEFF. = 1.789
VO = 141. STAND. DEVIA. = 0.0110 (M)
C.G. VEL. X-COMP. (M/S): 235. 199. 141. 99. 69.

RECORDED TIME OF MAXIMUM/MINIMUM COIL VOLTAGE (S)

MAX	.000127	.003009	.005559	.009217
MIN	.001047	.004637	.007624	.012025

COMPUTED NOSE POSITION AT MAX/MIN COIL VOLTAGE (M)

AT MAX	0.020	0.523	0.816	1.117
AT MIN	0.206	0.722	0.993	1.358

RECORDED COIL POSITION (M)

0.0	0.486	0.810	1.086

DIFFERENCE BETWEEN COIL AND NOSE AT MAX/MIN VOLTAGE (M)

AT MAX	0.020	0.037	0.006	0.031
AT MIN	0.206	0.236	0.183	0.272

SHOT 66 (24 APRIL, 1976, NO. 6)

SAND: DRY, DENSITY:1538. KG/M**3; APPROACHING VELOCITY: 234. M/S
PROJECTILE: HOLLOW STEP-TIERMASS:0.4218 KG, D=0.02 M, L=0.238 M

X-RAY STATION	NO.1	NO.2	NO.3	NO.4	NO.5
TIME (SECOND)	.000140	.000907	.002926	.005845	.010062
CENTER OF GRAVITY POSITION (M)					
HORIZONTAL	-0.091	0.073	0.403	0.730	1.048
VERTICAL	0.124	0.129	0.128	0.118	0.094
INCLINATION ANGLE(DEG).	0.0	0.0	-6.5	-10.0	-10.5
SEPARATION ANGLE(DEGREE)					
ABOVE	****	6.0	1.5	1.0	****
BELOW	****	5.0	9.0	11.0	****
NOSE WIDTH (M ON FILM).	0.0260	0.0235	0.0230	0.0240	0.0250
NOSE POSITION (M)					
HORIZONTAL	0.014	0.178	0.507	0.833	1.151
VERTICAL	0.124	0.129	0.116	0.100	0.075
INPUT NOSE POSITION (M)					
HORIZONTAL	0.007	0.169	0.503	0.832	1.153
VERTICAL	-0.094	-0.088	-0.103	-0.123	-0.155

NOSE VEL. Y-COMP. (M/S): 1. -1. -5. -7. -3.
COEFFICIENTS OF CUBIC POLYNOMIAL/STANDARD DEVIATION
0.1256E 00 0.1230E 01 -0.1491E 04 0.8648E 05 / 0.0048 (M)

NOSE VEL. X-COMP. (M/S): 220. 194. 139. 88. 75.
COEFFICIENTS OF CUBIC POLYNOMIAL/STANDARD DEVIATION
-0.1503E-01 0.2246E 03 -0.1751E 05 0.6666E 06 / 0.0042 (M)

NOSE VEL. DIRECTION(DEG)	0.2	-0.4	-2.2	-4.8	-1.9
SEPARATION ANGLE(DEGREE), RELATIVE TO NOSE VELOCITY					
ABOVE	****	5.6	5.8	6.2	****
BELOW	****	5.4	4.7	5.8	****

C.G. VEL. Y-COMP. (M/S): 6. 3. -2. -5. -4.
COEFFICIENTS OF CUBIC POLYNOMIAL/STANDARD DEVIATION
0.1230E 00 0.6038E 01 -0.1636E 04 0.7408E 05 / 0.0019 (M)

C.G. VEL. X-COMP. (M/S): 220. 195. 140. 89. 74.
COEFFICIENTS OF CUBIC POLYNOMIAL/STANDARD DEVIATION
-0.1201E 00 0.2246E 03 -0.1743E 05 0.6602E 06 / 0.0042 (M)

PONCELET DRAG COEFF. = 1.772
VO = 220. STAND. DEVIA. = 0.0145 (M)
C.G. VEL. X-COMP. (M/S): 220. 188. 136. 97. 68.

```
SHOT 81    ( 24 APRIL, 1976, NO. 7 )

SAND: WET, DENSITY:2050. KG/M**3: APPROACHING VELOCITY: 334. M/S
PROJECTILE: SOLID FLAT NOSE MASS:0.5448 KG, D=0.02 M, L=0.225 M

X-RAY STATION .........  NO.1     NO.2     NO.3     NO.4     NO.5

TIME (SECOND) ......... .000155  .000839  .002174  .003634  .005450
CENTER OF GRAVITY POSITION (M)
  HORIZONTAL ..........  -0.078   0.128    0.470    0.786    1.097
  VERTICAL ............   0.128   0.135    0.134    0.133    0.136

INCLINATION ANGLE(DEG).   1.5      1.0      2.0      5.0      8.0
SEPARATION ANGLE(DEGREE)
  ABOVE ...............   ****     10.0     9.0      9.0      10.0
  BELOW ...............   ****     8.0      6.0      3.5      1.5
NOSE WIDTH (M ON FILM). 0.0260   0.0240   0.0240   0.0230   0.0235
NOSE POSITION (M)
  HORIZONTAL ..........   0.035    0.241    0.583    0.899    1.209
  VERTICAL ............   0.131    0.136    0.138    0.142    0.151
INPUT NOSE POSITION (M)
  HORIZONTAL ..........   0.034    0.243    0.593    0.908    1.221
  VERTICAL ............  -0.085   -0.079   -0.077   -0.073   -0.062


NOSE VEL. Y-COMP. (M/S):   8.       5.       2.       2.       9.
COEFFICIENTS OF CUBIC POLYNOMIAL/STANDARD DEVIATION
  0.1299E 00   0.8052E 01 -0.2554E 04   0.3187E 06 / 0.0019 (M)

NOSE VEL. X-COMP. (M/S): 310.     283.     236.     193.     151.
COEFFICIENTS OF CUBIC POLYNOMIAL/STANDARD DEVIATION
 -0.1259E-01   0.3161E 03 -0.2042E 05   0.6477E 06 / 0.0033 (M)


NOSE VEL. DIRECTION(DEG)  1.4      1.0      0.4      0.7      3.4
SEPARATION ANGLE(DEGREE), RELATIVE TO NOSE VELOCITY
  ABOVE ...............   ****     10.0     7.4      4.7      5.4
  BELOW ...............   ****     8.0      7.6      7.8      6.1


C.G. VEL. Y-COMP. (M/S):   11.      5.      -1.      -2.       7.
COEFFICIENTS OF CUBIC POLYNOMIAL/STANDARD DEVIATION
  0.1263E 00   0.1214E 02 -0.4691E 04   0.5450E 06 / 0.0017 (M)

C.G. VEL. X-COMP. (M/S): 310.     283.     237.     194.     152.
COEFFICIENTS OF CUBIC POLYNOMIAL/STANDARD DEVIATION
 -0.1255E 00   0.3159E 03 -0.2034E 05   0.6446E 06 / 0.0033 (M)

PONCELET DRAG COEFF. = 0.964
 V0 = 237. STAND. DEVIA. = 0.0107 (M)
C.G. VEL. X-COMP. (M/S): 325.     289.     237.     198.     164.

RECORDED TIME OF MAXIMUM/MINIMUM COIL VOLTAGE (S)
  MAX        .000137     .001863     .003199     .004900
  MIN        .000708     .002671     .004193     .006103
COMPUTED NOSE POSITION AT MAX/MIN COIL VOLTAGE (M)
  AT MAX      0.030       0.510       0.811       1.122
  AT MIN      0.201       0.696       1.001       1.303
RECORDED COIL POSITION (M)
              0.0         0.486       0.810       1.086
DIFFERENCE BETWEEN COIL AND NOSE AT MAX/MIN VOLTAGE (M)
  AT MAX      0.030       0.024       0.001       0.036
  AT MIN      0.201       0.212       0.191       0.217
```

SHOT 62 (24 APRIL, 1976, NO. 8)

SAND: WET, DENSITY:2050. KG/M**3; APPROACHING VELOCITY: 405. M/S
PROJECTILE: SOLID FLAT NOSE MASS:0.5447 KG, D=0.02 M, L=0.225 M

X-RAY STATION	NO.1	NO.2	NO.3	NO.4	NO.5
TIME (SECOND)	.000130	.000680	.001724	.002811	.004068
CENTER OF GRAVITY POSITION (M)					
HORIZONTAL	-0.072	0.131	0.462	0.768	1.091
VERTICAL	0.124	0.131	0.132	0.134	0.138
INCLINATION ANGLE(DEG).	1.0	1.0	1.0	1.0	1.0
SEPARATION ANGLE(DEGREE)					
ABOVE	****	15.0	15.0	15.0	15.0
BELOW	****	14.0	11.5	10.0	9.0
NOSE WIDTH (M ON FILM).	0.0260	0.0240	0.0230	0.0230	0.0230
NOSE POSITION (M)					
HORIZONTAL	0.041	0.244	0.575	0.881	1.204
VERTICAL	0.126	0.133	0.134	0.136	0.140
INPUT NOSE POSITION (M)					
HORIZONTAL	0.042	0.247	0.581	0.886	1.213
VERTICAL	-0.091	-0.083	-0.083	-0.080	-0.076

NOSE VEL. Y-COMP. (M/S): 12. 7. 1. 1. 8.
COEFFICIENTS OF CUBIC POLYNOMIAL/STANDARD DEVIATION
0.1249E 00 0.1345E 02 -0.5757E 04 0.8271E 06 / 0.0023 (M)

NOSE VEL. X-COMP. (M/S): 381. 347. 297. 265. 254.
COEFFICIENTS OF CUBIC POLYNOMIAL/STANDARD DEVIATION
-0.8148E-02 0.3901E 03 -0.3459E 05 0.2916E 07 / 0.0031 (M)

NOSE VEL. DIRECTION(DEG)	1.8	1.1	0.2	0.1	1.7
SEPARATION ANGLE(DEGREE), RELATIVE TO NOSE VELOCITY					
ABOVE	****	15.1	14.2	14.1	15.7
BELOW	****	13.9	12.3	10.9	8.3

C.G. VEL. Y-COMP. (M/S): 12. 7. 1. 1. 8.
COEFFICIENTS OF CUBIC POLYNOMIAL/STANDARD DEVIATION
0.1230E 00 0.1345E 02 -0.5752E 04 0.8264E 06 / 0.0023 (M)

C.G. VEL. X-COMP. (M/S): 381. 347. 297. 265. 254.
COEFFICIENTS OF CUBIC POLYNOMIAL/STANDARD DEVIATION
-0.1212E 00 0.3902E 03 -0.3454E 05 0.2925E 07 / 0.0031 (M)

PONCELET DRAG COEFF. = 0.729
VO = 381. STAND. DEVIA. = 0.0061 (M)
C.G. VEL. X-COMP. (M/S): 381. 350. 302. 265. 232.

SHOT 83 (25 APRIL, 1976, NO. 1)

SAND: WET, DENSITY:2050. KG/M**3; APPROACHING VELOCITY: 419. M/S
PROJECTILE: SOLID FLAT NOSE MASS:0.5450 KG, D=0.02 M, L=0.225 M

X-RAY STATION	NO.1	NO.2	NO.3	NO.4	NO.5
TIME (SECOND)	.000109	.000652	.001693	.002655	.003882
CENTER OF GRAVITY POSITION (M)					
HORIZONTAL	-0.072	0.134	0.461	0.733	1.021
VERTICAL	0.113	0.125	0.130	0.133	0.131
INCLINATION ANGLE(DEG).	2.0	1.0	1.5	1.5	0.5
SEPARATION ANGLE(DEGREE)					
ABOVE	****	****	12.0	12.0	12.
BELOW	****	****	10.0	10.0	10.
NOSE WIDTH (M ON FILM).	0.0260	0.0240	0.0230	0.0240	0.0232
NOSE POSITION (M)					
HORIZONTAL	0.041	0.246	0.574	0.845	1.134
VERTICAL	0.117	0.126	0.133	0.136	0.132
INPUT NOSE POSITION (M)					
HORIZONTAL	0.042	0.250	0.580	0.847	1.132
VERTICAL	-0.103	-0.091	-0.084	-0.080	-0.085

NOSE VEL. Y-COMP. (M/S): 19. 13. 4. -1. -3.
COEFFICIENTS OF CUBIC POLYNOMIAL/STANDARD DEVIATION
0.1150E 00 0.1987E 02 -0.6034E 04 0.5268E 06 / 0.0016 (M)

NOSE VEL. X-COMP. (M/S): 385. 351. 296. 256. 221.
COEFFICIENTS OF CUBIC POLYNOMIAL/STANDARD DEVIATION
0.5493E-03 0.3917E 03 -0.3306E 05 0.1892E 07 / 0.0067 (M)

NOSE VEL. DIRECTION(DEG)	2.8	2.1	0.8	-0.2	-0.8
SEPARATION ANGLE(DEGREE), RELATIVE TO NOSE VELOCITY					
ABOVE	****	****	11.3	10.3	10.7
BELOW	****	****	10.7	11.7	11.3

C.G. VEL. Y-COMP. (M/S): 22. 14. 3. -1. 1.
COEFFICIENTS OF CUBIC POLYNOMIAL/STANDARD DEVIATION
0.1108E 00 0.2417E 02 -0.8803E 04 0.1010E 07 / 0.0023 (M)

C.G. VEL. X-COMP. (M/S): 384. 351. 296. 256. 220.
COEFFICIENTS OF CUBIC POLYNOMIAL/STANDARD DEVIATION
-0.1124E 00 0.3915E 03 -0.3299E 05 0.1880E 07 / 0.0067 (M)

PONCELET DRAG COEFF. = 0.820
VO = 296. STAND. DEVIA. = 0.0051 (M)
C.G. VEL. X-COMP. (M/S): 383. 348. 296. 260. 225.

RECORDED TIME OF MAXIMUM/MINIMUM COIL VOLTAGE (S)				
MAX	.000078	.001413	.002509	.003758
MIN	.000544	.002034	.003230	.004627
COMPUTED NOSE POSITION AT MAX/MIN COIL VOLTAGE (M)				
AT MAX	0.031	0.493	0.805	1.106
AT MIN	0.204	0.676	0.985	1.293
RECORDED COIL POSITION (M)				
	0.0	0.486	0.810	1.086
DIFFERENCE BETWEEN COIL AND NOSE AT MAX/MIN VOLTAGE (M)				
AT MAX	0.031	0.007	-0.005	0.020
AT MIN	0.204	0.190	0.175	0.207

SHOT 84 (25 APRIL, 1976, NO. 2)

SAND: WET, DENSITY:2050. KG/M**3; APPROACHING VELOCITY: 406. M/S
PROJECTILE: SOLID FLAT NOSE MASS:0.5450 KG, D=0.02 M, L=0.225 M

X-RAY STATION	NO.1	NO.2	NO.3	NO.4	NO.5
TIME (SECOND)	.000137	.000699	.001739	.002702	.003929
CENTER OF GRAVITY POSITION (M)					
HORIZONTAL	-0.065	0.137	0.457	0.726	1.004
VERTICAL	0.115	0.122	0.127	0.129	0.125
INCLINATION ANGLE(DEG).	2.5	2.5	2.0	2.5	3.8
SEPARATION ANGLE(DEGREE)					
ABOVE	****	14.0	17.0	15.0	12.0
BELOW	****	13.0	9.0	9.0	4.0
NOSE WIDTH (M ON FILM).	0.0255	0.0235	0.0230	0.0230	0.0230
NOSE POSITION (M)					
HORIZONTAL	0.048	0.249	0.570	0.839	1.117
VERTICAL	0.120	0.127	0.131	0.134	0.132
INPUT NOSE POSITION (M)					
HORIZONTAL	0.051	0.253	0.576	0.839	1.113
VERTICAL	-0.099	-0.091	-0.086	-0.083	-0.085

NOSE VEL. Y-COMP. (M/S):	12.	9.	3.	-0.	-2.

COEFFICIENTS OF CUBIC POLYNOMIAL/STANDARD DEVIATION
0.1183E 00 0.1337E 02 -0.3727E 04 0.3087E 06 / 0.0012 (M)

NOSE VEL. X-COMP. (M/S):	362.	337.	293.	253.	204.

COEFFICIENTS OF CUBIC POLYNOMIAL/STANDARD DEVIATION
-0.4120E-03 0.3682E 03 -0.2218E 05 0.2130E 06 / 0.0054 (M)

NOSE VEL. DIRECTION(DEG)	2.0	1.5	0.6	-0.0	-0.5
SEPARATION ANGLE(DEGREE), RELATIVE TO NOSE VELOCITY					
ABOVE	****	13.0	15.6	12.5	7.7
BELOW	****	14.0	10.4	11.5	8.3

C.G. VEL. Y-COMP. (M/S):	13.	9.	3.	-1.	-5.

COEFFICIENTS OF CUBIC POLYNOMIAL/STANDARD DEVIATION
0.1132E 00 0.1409E 02 -0.3662E 04 0.2068E 06 / 0.0007 (M)

C.G. VEL. X-COMP. (M/S):	362.	337.	293.	253.	204.

COEFFICIENTS OF CUBIC POLYNOMIAL/STANDARD DEVIATION
-0.1133E 00 0.3682E 03 -0.2219E 05 0.2212E 06 / 0.0054 (M)

PONCELET DRAG COEFF. = 0.777
V0 = 293. STAND. DEVIA. = 0.0108 (M)

C.G. VEL. X-COMP. (M/S):	374.	341.	293.	259.	226.

RECORDED TIME OF MAXIMUM/MINIMUM COIL VOLTAGE (S)

MAX	.000062	.001522	.002562	.003842
MIN	.000509	*******	.003317	.004752
COMPUTED NOSE POSITION AT MAX/MIN COIL VOLTAGE (M)				
AT MAX	0.022	0.509	0.801	1.099
AT MIN	0.181	********	0.985	1.271
RECORDED COIL POSITION (M)				
	0.0	0.486	0.810	1.086
DIFFERENCE BETWEEN COIL AND NOSE AT MAX/MIN VOLTAGE (M)				
AT MAX	0.022	0.023	-0.009	0.013
AT MIN	0.181	********	0.175	0.185

SHOT 85 (25 APRIL, 1976, NO. 3)

SAND:H-OH, DENSITY:1000. KG/M**3; APPROACHING VELOCITY: 237. M/S
PROJECTILE: HOLLOW STEP-TIERMASS:0.4230 KG. D=0.02 M. L=0.238 M

X RAY STATION	NO.1	NO.2	NO.3	NO.4	NO.5
TIME (SECOND)	.000155	.000865	.002298	.004596	.008612
CENTER OF GRAVITY POSITION (M)					
HORIZONTAL	-0.061	0.090	0.393	0.862	19.127
VERTICAL	0.105	0.113	0.116	0.121	18.224
INCLINATION ANGLE(DEG).	1.0	0.0	0.0	1.0	*****
SEPARATION ANGLE(DEGREE)					
ABOVE	****	****	****	****	****
BELOW	****	****	****	****	***
NOSE WIDTH (M ON FILM).	0.0262	0.0230	0.0231	0.0230	******
NOSE POSITION (M)					
HORIZONTAL	0.024	0.195	0.498	0.967	19.144
VERTICAL	0.107	0.113	0.116	0.122	18.121
INPUT NOSE POSITION (M)					
HORIZONTAL	0.020	0.190	0.493	0.986	******
VERTICAL	-0.116	-0.107	-0.104	-0.096	******

SHOT 66 (25 APRIL, 1976, NO. 4)

SAND:H-OH, DENSITY:1000. KG/M**3; APPROACHING VELOCITY: 237. M/S
PROJECTILE: HOLLOW STEP-TIE MASS:0.4230 KG, D=0.02 M, L=0.238 M

X-RAY STATION	NO.1	NO.2	NO.3	NO.4	NO.5
TIME (SECOND)	.000171	.000978	.002339	.004379	.006444
CENTER OF GRAVITY POSITION (M)					
HORIZONTAL	-0.080	0.106	0.398	0.764	1.099
VERTICAL	0.104	0.111	0.114	0.119	0.129
INCLINATION ANGLE(DEG).	1.0	0.5	0.5	-3.0	-8.0
SEPARATION ANGLE(DEGREE)					
ABOVE	****	****	****	****	****
BELOW	****	****	****	****	****
NOSE WIDTH (M ON FILM).	0.0260	0.0240	0.0240	0.0240	0.0240
NOSE POSITION (M)					
HORIZONTAL	0.025	0.211	0.503	0.869	1.203
VERTICAL	0.106	0.112	0.115	0.113	0.115
INPUT NOSE POSITION (M)					
HORIZONTAL	0.021	0.207	0.497	0.875	1.215
VERTICAL	-0.117	-0.108	-0.105	-0.107	-0.105

NOSE VEL. Y-COMP. (M/S): 9. 5. 0. -1. 4.
COEFFICIENTS OF CUBIC POLYNOMIAL/STANDARD DEVIATION
0.1044E 00 0.1046E 02 -0.3145E 04 0.2753E 06 / 0.0006 (M)

NOSE VEL. X-COMP. (M/S): 246. 226. 197. 168. 157.
COEFFICIENTS OF CUBIC POLYNOMIAL/STANDARD DEVIATION
-0.1897E-01 0.2511E 03 -0.1402E 05 0.6966E 06 / 0.0045 (M)

NOSE VEL. DIRECTION(DEG) 2.2 1.3 0.1 -0.4 1.5
SEPARATION ANGLE(DEGREE), RELATIVE TO NOSE VELOCITY

ABOVE	****	****	****	****	****
BELOW	****	****	****	****	****

C.G. VEL. Y-COMP. (M/S): 9. 5. 2. 2. 10.
COEFFICIENTS OF CUBIC POLYNOMIAL/STANDARD DEVIATION
0.1030E 00 0.9602E 01 -0.2561E 04 0.2650E 06 / 0.0017 (M)

C.G. VEL. X-COMP. (M/S): 246. 226. 197. 168. 158.
COEFFICIENTS OF CUBIC POLYNOMIAL/STANDARD DEVIATION
-0.1239E 00 0.2511E 03 -0.1408E 05 0.7058E 06 / 0.0045 (M)

PONCELET DRAG COEFF. = 1.131
VO = 197. STAND. DEVIA. = 0.0078 (M)
C.G. VEL. X-COMP. (M/S): 240. 222. 197. 168. 147.

RECORDED TIME OF MAXIMUM/MINIMUM COIL VOLTAGE (S)

MAX	.000155	.002391	.003960	.005528
MIN	.001009	.003354	.004985	.006584
COMPUTED NOSE POSITION AT MAX/MIN COIL VOLTAGE (M)				
AT MAX	0.020	0.511	0.799	1.058
AT MIN	0.221	0.692	0.971	1.225
RECORDED COIL POSITION (M)				
	0.0	0.486	0.810	1.086
DIFFERENCE BETWEEN COIL AND NOSE AT MAX/MIN VOLTAGE (M)				
AT MAX	0.020	0.025	-0.011	-0.028
AT MIN	0.221	0.206	0.161	0.139

SHOT 87   (25 APRIL. 1976. NO. 5)

```
SAND:H-OH. DENSITY:1000. KG/M**3; APPROACHING VELOCITY: 241. M/S
PROJECTILE: HOLLOW STEP-TIERMASS:0.4227 KG. D=0.02 M. L=0.238 M

X-RAY STATION .........   NO.1      NO.2      NO.3      NO.4      NO.5

TIME (SECOND) .........  .000174   .000994   .002391   .004193   .006081
CENTER OF GRAVITY POSITION (M)
  HORIZONTAL ..........  -0.076     0.112     0.406     0.775     1.122
  VERTICAL ............   0.105     0.111     0.114     0.120     0.123

INCLINATION ANGLE(DEG).  -1.5      -1.0      -0.8      -1.7      -2.0
SEPARATION ANGLE(DEGREE)
  ABOVE ...............   ****      ****      ****      17.0      15.0
  BELOW ...............   ****      ****      ****      20.0      20.0
NOSE WIDTH (M ON FILM).  0.0260    0.0235    0.0240    0.0245    0.0245
NOSE POSITION (M)
  HORIZONTAL ..........   0.029     0.217     0.511     0.880     1.227
  VERTICAL ............   0.102     0.109     0.112     0.117     0.119
INPUT NOSE POSITION (M)
  HORIZONTAL ..........   0.026     0.215     0.507     0.889     1.246
  VERTICAL ............  -0.122    -0.112    -0.108    -0.103    -0.100


NOSE VEL. Y-COMP. (M/S)     8.        5.        3.        1.        2.
COEFFICIENTS OF CUBIC POLYNOMIAL/STANDARD DEVIATION
  0.1011E 00  0.8328E 01 -0.1679E 04  0.1308E 06 / 0.0014 (M)

NOSE VEL. X-COMP. (M/S : 227.      221.      210.      194.      176.
COEFFICIENTS OF CUBIC POLYNOMIAL/STANDARD DEVIATION
 -0.9338E-02  0.2281E 03 -0.3552E 04 -0.7910E 05 / 0.0052 (M)


NOSE VEL. DIRECTION(DEG)  2.0       1.4       0.7       0.3       0.8
SEPARATION ANGLE(DEGREE). RELATIVE TO NOSE VELOCITY
  ABOVE ...............   ****      ****      ****      19.0      17.8
  BELOW ...............   ****      ****      ****      18.0      17.2


C.G. VEL. Y-COMP. (M/S):    6.        5.        3.        2.        2.
COEFFICIENTS OF CUBIC POLYNOMIAL/STANDARD DEVIATION
  0.1043E 00  0.6035E 01 -0.6080E 03  0.5197E 05 / 0.0016 (M)

C.G. VEL. X-COMP. (M/S): 227.      221.      210.      194.      176.
COEFFICIENTS OF CUBIC POLYNOMIAL/STANDARD DEVIATION
 -0.1143E 00  0.2280E 03 -0.3520E 04 -0.8422E 05 / 0.0051 (M)

PONCELET DRAG COEFF. = 0.506
 VO = 210. STAND. DEVIA. = 0.0064 (M)
C.G. VEL. X-COMP. (M/S): 230.      222.      210.      196.      183.


RECORDED TIME OF MAXIMUM/MINIMUM COIL VOLTAGE (S)
  MAX        .000149     .002376     .003929     .005419
  MIN        .001009     .003332     .004891     .006503
COMPUTED NOSE POSITION AT MAX/MIN COIL VOLTAGE (M)
  AT MAX      0.025       0.511       0.827       1.110
  AT MIN      0.217       0.708       1.012       1.302
RECORDED COIL POSITION (M)
              0.0         0.486       0.810       1.086
DIFFERENCE BETWEEN COIL AND NOSE AT MAX/MIN VOLTAGE (M)
  AT MAX      0.025       0.025       0.017       0.024
  AT MIN      0.217       0.222       0.202       0.216
```

SHOT 86 (24 MAY, 1976, NO. 1)

SAND: DRY, DENSITY:1538. KG/M**3; APPROACHING VELOCITY: 233. M/S
PROJECTILE: HOLLOW STEP-TIERMASS:0.4219 KG, D=0.02 M, L=0.238 M

X-RAY STATION	NO.1	NO.2	NO.3	NO.4	NO.5
TIME (SECOND)	.000134	.000898	.002919	.005792	.010028
CENTER OF GRAVITY POSITION (M)					
HORIZONTAL	18.022	0.080	0.400	0.723	1.051
VERTICAL	18.224	0.117	0.122	0.124	0.108
INCLINATION ANGLE(DEG).	*****	0.0	-2.8	-7.3	-7.5
SEPARATION ANGLE(DEGREE)					
ABOVE	****	****	****	1.0	2.5
BELOW	****	****	****	6.5	9.0
NOSE WIDTH (M ON FILM).	******	0.0230	0.0230	0.0230	0.0230
NOSE POSITION (M)					
HORIZONTAL	18.040	0.185	0.505	0.828	1.155
VERTICAL	18.121	0.117	0.117	0.110	0.095
INPUT NOSE POSITION (M)					
HORIZONTAL	******	0.170	0.501	0.826	1.157
VERTICAL	******	-0.102	-0.102	-0.110	-0.128

SHOT 69 (24 MAY. 1976. NO. 2)

SAND: DRY. DENSITY:1538. KG/M**3; APPROACHING VELOCITY: 227. M/S
PROJECTILE: HOLLOW STEP-TIERMASS:0.4219 KG. D=0.02 M. L=0.238 M

X-RAY STATION	NO.1	NO.2	NO.3	NO.4	NO.5
TIME (SECOND)	.000143	.000901	.002938	.005811	.010047
CENTER OF GRAVITY POSITION (M)					
HORIZONTAL	-0.094	0.068	0.393	0.715	1.043
VERTICAL	0.114	0.119	0.125	0.113	0.084
INCLINATION ANGLE(DEG).	0.0	-0.5	-8.0	-10.0	-11.0
SEPARATION ANGLE(DEGREE)					
ABOVE	****	6.0	****	****	****
BELOW	****	5.0	****	****	****
NOSE WIDTH (M ON FILM).	0.0260	0.0235	0.0230	0.0235	0.0230
NOSE POSITION (M)					
HORIZONTAL	0.011	0.173	0.496	0.818	1.146
VERTICAL	0.114	0.118	0.110	0.095	0.064
INPUT NOSE POSITION (M)					
HORIZONTAL	0.003	0.163	0.491	0.815	1.146
VERTICAL	-0.106	-0.101	-0.110	-0.126	-0.163

NOSE VEL. Y-COMP. (M/S):	2.	-0.	-4.	-7.	-6.

COEFFICIENTS OF CUBIC POLYNOMIAL/STANDARD DEVIATION
0.1153E 00 0.2012E 01 -0.1297E 04 0.5877E 05 / 0.0027 (M)

NOSE VEL. X-COMP. (M/S):	215.	191.	137.	89.	77.

COEFFICIENTS OF CUBIC POLYNOMIAL/STANDARD DEVIATION
-0.1706E-01 0.2199E 03 -0.1693E 05 0.6508E 06 / 0.0071 (M)

NOSE VEL. DIRECTION(DEG)	0.4	-0.1	-1.7	-4.6	-4.7
SEPARATION ANGLE(DEGREE), RELATIVE TO NOSE VELOCITY					
ABOVE	****	6.4	****	****	****
BELOW	****	4.6	****	****	****

C.G. VEL. Y-COMP. (M/S):	9.	6.	-1.	-6.	-6.

COEFFICIENTS OF CUBIC POLYNOMIAL/STANDARD DEVIATION
0.1127E 00 0.9586E 01 -0.2160E 04 0.9181E 05 / 0.0008 (M)

C.G. VEL. X-COMP. (M/S):	215.	191.	138.	89.	77.

COEFFICIENTS OF CUBIC POLYNOMIAL/STANDARD DEVIATION
-0.1222E 00 0.2203E 03 -0.1693E 05 0.6505E 06 / 0.0064 (M)

PONCELET DRAG COEFF. = 1.734
VO = 215. STAND. DEVIA. = 0.0126 (M)

C.G. VEL. X-COMP. (M/S):	215.	185.	135.	97.	69.

SHOT 90 (26 MAY. 1976. NO. 3)

SAND: WET. DENSITY:2050. KG/M**3; APPROACHING VELOCITY: 445. M/S
PROJECTILE: HOLLOW STEP-TIERMASS:0.4220 KG. D=0.032 M. L=0.238 M

X-RAY STATION	NO.1	NO.2	NO.3	NO.4	NO.5
TIME (SECOND)	.000146	.000700	.001708	.002800	.004354
CENTER OF GRAVITY POSITION (M)					
HORIZONTAL	-0.055	18.213	0.577	0.885	1.174
VERTICAL	0.121	18.224	0.136	0.137	0.135
INCLINATION ANGLE(DEG).	0.0	*****	-3.0	-3.0	-2.2
SEPARATION ANGLE(DEGREE)					
ABOVE	****	****	7.0	2.0	****
BELOW	****	****	11.0	7.0	***0
NOSE WIDTH (M ON FILM).	0.0260	******	0.0230	0.0235	0.0220
NOSE POSITION (M)					
HORIZONTAL	0.056	18.231	0.682	0.990	1.279
VERTICAL	0.121	18.121	0.130	0.132	0.131
INPUT NOSE POSITION (M)					
HORIZONTAL	0.054	******	0.704	1.017	1.293
VERTICAL	-0.097	******	-0.087	-0.085	-0.087

SHOT 91 (24 MAY. 1976. NO. 4)

SAND:H-OH. DENSITY:1000. KG/M**3; APPROACHING VELOCITY: 23[illegible] . M/S
PROJECTILE: HOLLOW STEP-TIERMASS:0.0422 KG. D=0.02 M. L=0.238 M

X-RAY STATION	NO.1	NO.2	NO.3	NO.4	NO.5
TIME (SECOND)	.000180	.001000	.002350	.004192	.[illegible]6.55
CENTER OF GRAVITY POSITION (M)					
HORIZONTAL	-0.009	0.115	0.407	0.835	1.129
VERTICAL	0.100	0.106	0.111	0.117	0.119
INCLINATION ANGLE(DEG).	0.0	0.0	-0.5	-3.0	-4.5
SEPARATION ANGLE(DEGREE)					
ABOVE	****	13.0	****	****	9.0
BELOW	****	14.5	****	****	16.5
NOSE WIDTH (M ON FILM).	0.0[illegible]	0.0230	0.0237	0.0230	0.02[illegible]
NOSE POSITION (M)					
HORIZONTAL	0.036	0.220	0.512	0.940	1.233
VERTICAL	0.100	0.106	0.111	0.111	0.111
INPUT NOSE POSITION (M)					
HORIZONTAL	0.036	0.219	0.508	0.955	1.247
VERTICAL	-0.124	-0.115	-0.112	-0.109	-0.109

NOSE VEL. Y-COMP. (M/S): 9. 6. 2. -0. 1.
COEFFICIENTS OF CUBIC POLYNOMIAL/STANDARD DEVIATION
0.9845E-01 0.9017E 01 -0.2315E 04 0.1771E 06 / 0.0001 (M)

NOSE VEL. X-COMP. (M/S): 192. 219. 236. 204. 106.
COEFFICIENTS OF CUBIC POLYNOMIAL/STANDARD DEVIATION
0.6862E-02 0.1045E 03 0.2200E 05 -0.3132E 07 / 0.0150 (M)

NOSE VEL. DIRECTION(DEG)	2.6	1.4	0.4	-0.1	0.6
SEPARATION ANGLE(DEGREE). RELATIVE TO NOSE VELOCITY					
ABOVE	****	14.4	****	****	14.1
BELOW	****	13.1	****	****	11.4

C.G. VEL. Y-COMP. (M/S): 7. 6. 4. 2. 2.
COEFFICIENTS OF CUBIC POLYNOMIAL/STANDARD DEVIATION
0.9688E-01 0.7824E 01 -0.1155E 04 0.7014E 05 / 0.0005 (M)

C.G. VEL. X-COMP. (M/S): 192. 219. 236. 204. 106.
COEFFICIENTS OF CUBIC POLYNOMIAL/STANDARD DEVIATION
-0.9811E-01 0.1044E 03 0.2202E 05 -0.3135E 07 / 0.0150 (M)

PONCELET DRAG COEFF. = -.000
VO = 192. STAND. DEVIA. = 0.0990 (M)
C.G. VEL. X-COMP. (M/S): 192. 192. 192. 192. 192.

APPENDIX B

DERIVATION OF FORCES AND MOMENTS ON A RIGID BODY IN A SOIL MEDIUM

The purpose of this section is to develop the expressions for the forces and moments applied to a projectile in a soil medium. The forces are represented by F_x, F_y and F_z along a body fixed set of axes x,y,z with the origin at the center of mass of the vehicle. The moments are about the x,y and z axes and are denoted L, M and N respectively and the velocity components are designated U, V, W respectively. It is assumed that the force exerted by the soil on a differential surface area of the body is of the form

$$\frac{dF}{dA} \propto (A_x+B_x|U|+C_xU^2)n_x\hat{i} + (A_y+B_y|V|+C_yV^2)n_y\hat{j} + (A_z+B_z|W|+C_zW^2)n_z\hat{k} \quad , \tag{B-1}$$

where n_x,n_y,n_z are components of the outward unit vector $\hat{n}$ normal to the surface of the body. The force is assumed to exist only when the velocity is directed toward the elemental area. The flow is assumed to be separated from the body aft of the nose.

The nose shape that is treated is conical, with nomenclature as shown in Figure B-1. In the cylindrical coordinate system the equation for the surface of the conical nose is given by

$$\rho = \frac{r}{L_N}(\bar{x}-x) \quad . \tag{B-2}$$

The unit vector normal to the surface of the nose is

$$\hat{n} = \text{Sin}\ \gamma\ \hat{i} + \text{Cos}\ \gamma\ \text{Cos}\ \beta\hat{j} + \text{Cos}\ \gamma\ \text{Sin}\ \beta\hat{k} \quad . \tag{B-3}$$

The area of a differential surface element is given by

$$dA = \frac{\rho\ dx\ d\beta}{\text{Cos}\ \gamma} \quad . \tag{B-4}$$

The inertial reference frame x'y'z', a rectangular Cartesian system, is chosen with x' perpendicular to the surface of the target and pointing inward and y' and z' chosen in any convenient direction. In order to write the equation of the target surface prior to impact, in the body fixed axis system, a coordinate system x_1,y_1,z_1 is chosen oriented parallel to the body axis system but whose origin is coincident with that of the inertial axis system. The equation of the target plane in the inertial system is x' = 0. Using the Euler transformation matrix introduced in Section VI the relation between the primed and sub-one system can be written as

$$\begin{Bmatrix} x' \\ y' \\ z' \end{Bmatrix} = T_{BI} \begin{Bmatrix} x_1 \\ y_1 \\ z_1 \end{Bmatrix} . \qquad \text{(B-5)}$$

This yields

$$x' = T_{11}x_1 + T_{12}y_1 + T_{13}Z_1 = 0 , \qquad \text{(B-6)}$$

where

$$T_{11} = \text{Cos } \Psi \text{ Cos } \theta$$

$$T_{12} = \text{Cos } \Psi \text{ Sin } \theta \text{ Sin } \phi - \text{Sin } \Psi \text{ Cos } \phi$$

$$T_{13} = \text{Cos } \Psi \text{ Sin } \theta \text{ Cos } \phi + \text{Sin } \Psi \text{ Sin } \phi .$$

Equation (B-6) can be written in the body axis system by a simple translation

$$\begin{aligned} x &= x_1 + d \\ y &= y_1 \\ z &= z_1 , \end{aligned} \qquad \text{(B-7)}$$

where d is the distance from the body axis origin to the inertial axis origin and is

$$d = \sqrt{(x')^2 + (y')^2 + (z')^2} .$$

Substituting Equation (B-7) into Equation (B-6) results in

$$T_{11}x + T_{12}y + T_{13}z = T_{11}d , \qquad \text{(B-8)}$$

the equation of the target plane in the body axis system. It is convenient to write this equation in a cylindrical body axis system as shown in Figure B-1.

$$T_{11}x + T_{12}\rho \text{Cos}\beta + T_{13}\rho \text{Sin}\beta = T_{11}d. \qquad \text{(B-9)}$$

Consider the case where the nose has impacted the target and is partially immersed in the soil as shown in Figure B-2. The locus of the intersection of the nose and the target plane will be given by the simultaneous solution of Equation (B-9) and Equation (B-2) which yields

$$x = \frac{T_{11}d - (r/L_N)\bar{x}[T_{12}\text{Cos}\beta + T_{13}\text{Sin } \beta]}{T_{11} - (r/L_N)[T_{12}\text{Cos}\beta + T_{13}\text{Sin } \beta]} = f_1(x',y',z',\Psi,\theta,\phi,\beta). \qquad \text{(B-10)}$$

Using Equation (B-1) the differential force in the x direction becomes

$$dF_x = (A_x + B_x|U| + C_xU^2)n_x \, dA$$

and realizing that a positive value of U will produce a negative force on the projectile, this force is rewritten as

$$dF_x = -\frac{U}{|U|}(A_x+B_x|U|+C_xU^2)n_x\ dA\ .$$

By using Equations (B-2), (B-3) and (B-4) and $\frac{r}{L_N} = \tan\gamma$ the above expression may be written as

$$dF_x = -\frac{U}{|U|}(A_x+B_x|U|+C_xU^2)(r/L_N)^2(\bar{x}-x)\ dx\ d\beta\ ,$$

and upon integration, yields

$$F_x = -\frac{U}{|U|}(A_x+B_x|U|+C_xU^2)(r/L_N)^2\iint(\bar{x}-x)\ dx\ d\beta$$

where the limits for the integrals are chosen so that the integration is over the portion of the submerged area having a velocity component toward that surface. The integration with respect to x is performed first. The upper limit for the x integral is simply $\bar{x}$. The lower limit for x is a bit more complicated as shown by Figure B-3 which shows the x-z plane for a case where $\theta = \phi = 0$. As long as the projectile has not penetrated very far the lower limit is simply given by the equation of the intersection of the cone and the target plane, that is f_1 of Equation (B-10). As shown in Figure B-3 when the penetration reaches the base of the nose this limit is no longer correct since integration where $x < L_1$ gives a contribution over the dashed part of the cone that does not exist. For this reason the lower limit becomes f_1, unless $f_1 < L_1$ in which case the lower limit becomes L_1.

The limit on the β integral will depend upon the magnitude of the angle of attack, α given below, as compared with the cone half angle γ. If the angle of attack is less than γ the limit will be from 0 to 2π. This is expressed as

$$\alpha = \cos^{-1}\left[\frac{|U|}{\sqrt{U^2+V^2+W^2}}\right] < \gamma = \tan^{-1}\left[\frac{r}{L_N}\right].$$

To summarize

$$F_x = -\frac{U}{|U|}(A_x+B_x|U|+C_xU^2)\left[\frac{r}{L_N}\right]^2\int_0^{2\pi}\int_{f_1\geq L_1}^{\bar{x}}(\bar{x}-x)\ dx\ d\beta\ , \qquad \text{(B-11)}$$

for $\alpha<\gamma$ and for $\bar{x}\geq f_1\geq L_1$. For the case where $\alpha>\gamma$ one side of the cone will be blanketed and the β integral will be integrated only over 180 degrees. In order to determine the proper range of β consider the y-z coordinates (x into the plane of the paper) as shown in Figure B-4. The V and W components determine the projected or wetted area in contact with the soil. Let $\delta_t = \tan^{-1}\frac{W}{V}$, and limits on β will be $\pm\frac{\pi}{2}$ radians from the angle δ_t or from $-\frac{\pi}{2}+\delta_t$ to $\frac{\pi}{2}+\delta_t$. Collecting this we write

$$F_x = -\frac{U}{|U|}(A_x+B_x|U|+C_xU^2)\left[\frac{r}{L_N}\right]^2\int_{-\frac{\pi}{2}+\delta_t}^{\frac{\pi}{2}+\delta_t}\int_{f_1\geq L_1}^{\bar{x}}(\bar{x}-x)\ dx\ d\beta\ , \qquad \text{(B-12)}$$

for

$\alpha>\gamma$, $\bar{x}\geq f_1\geq L_1$ and $V\geq 0$.

If $V<0$ a different set of limits on β are applicable. In this case

$$F_x = \frac{-U}{|U|}(A_x+B_x|U|+C_xU^2)\left[\frac{r}{L_N}\right]^2 \int_{\frac{\pi}{2}+\delta_t}^{\frac{3\pi}{2}+\delta_t} \int_{f_1\geq L_1}^{\bar{x}} (\bar{x}-x)dx\, d\beta \quad , \qquad \text{(B-13)}$$

for $\alpha>\gamma$, $\bar{x}\geq f_1\geq L_1$ and $V<0$.

Once the nose has penetrated so that it is totally submerged the force becomes

$$F_x = -\frac{U}{|U|}(A_x+B_x|U|+C_xU^2)\frac{\pi r^2}{n} \qquad \text{(B-14)}$$

where $n = 1$ for $\alpha<\gamma$ and $n = 2$ for $\alpha>\gamma$.

In developing expressions for F_y and F_z the velocity components in the y and z directions would be made up of a velocity term due to translation plus a term due to rotation. Specifically, for a point on the axis of symmetry the velocity component in the y direction is $V + Rx$ and the velocity component in the z direction is $W - Qx$. If these velocity terms are used, the angle δ_t becomes a function of x, namely $\delta_t = \tan^{-1}[(V+Rx)/(W-Qx)]$. Since δ_t appears in the limits of integration with respect to β, these limits now become functions of x, and the integration is extremely cumbersome.

One approach to this problem is to treat the two velocity terms separately and add the resulting forces. This neglects the cross product terms $2VRx$ and $-2WQx$ in the velocity squared terms of the differential force in Equation (B-1). Another approach would be to sum the two velocity terms first and replace the longitudinal integration with respect to x by integrations over several strips of finite length Δx. Then sum these segmental integrations to obtain the resultant forces. Only the first method is presented here, and further consideration of this problem is left for later research in which the possiblity of modifying the assumed force law should also be considered.

The expression for F_y is written as the sum of two parts. The first is due to translation, $(F_y)_T$, and is obtained in a manner similar to the detailed procedure outlined above for F_x and the other is a component of force due to a rotation rate R radians per second about the z-axis. This component is denoted $(F_y)_r$. The rotation rate will give the differential surface element a velocity component in the y direction equal to Rx. This component is treated in the same manner as the translational velocity V in order to determine the F_y that it produces. The results are as follows:

$$F_y = (F_y)_T + (F_y)_r \qquad \text{(B-15)}$$

$$(F_y)_T = -\frac{V}{|V|}(A_y+B_y|V|+C_yV^2)\left[\frac{r}{L_N}\right]\int_{-\frac{\pi}{2}+\delta_t}^{\frac{\pi}{2}+\delta_t}\int_{f_1\geq L_1}^{\bar{x}}(\bar{x}-x)dx\,\text{Cos}\beta\,d\beta \qquad \text{(B-16)}$$

for $V\geq 0$ and $\bar{x}\geq f_1\geq L_1$. For the case where $V<0$ the limits on the β integral become $\frac{\pi}{2}+\delta_t$ to $\frac{3\pi}{2}+\delta_t$.

$$(F_y)_r = -\frac{R}{|R|}\left[\frac{r}{L_N}\right]\int_{-\frac{\pi}{2}+\delta_r}^{\frac{\pi}{2}+\delta_r}\int_{f_1\geq L_1}^{\bar{x}}(A_y+B_yx|R|+C_yx^2R^2)\,(\bar{x}-x)\,dx\,\text{Cos}\beta\,d\beta \qquad \text{(B-17)}$$

for $R\geq 0$, $\bar{x}\geq f_1\geq L_1$ and $\delta_r = -\tan^{-1}\frac{Q}{R}$. For $R<0$ the limits on the β integral become $\frac{\pi}{2}+\delta_r$ to $\frac{3\pi}{2}+\delta_r$.

Once the projectile has penetrated so that the nose is totally submerged the lower limit on all of the x integrals becomes L_1.

In a similar manner F_z is composed of $(F_z)_T$ and $(F_z)_r$.

$$F_z = (F_z)_T + (F_z)_r \,. \qquad \text{(B-18)}$$

Where

$$(F_z)_T = -\frac{W}{|W|}\left[\frac{r}{L_N}\right](A_z+B_z|W|+C_zW^2)\int_{-\frac{\pi}{2}+\delta_t}^{\frac{\pi}{2}+\delta_t}\int_{f_1\geq L_1}^{\bar{x}}(\bar{x}-x)\,dx\,\text{Sin}\,\beta\,d\beta \qquad \text{(B-19)}$$

for $V\geq 0$ and $\bar{x}\geq f_1\geq L_1$. For $V<0$ the limits on the β integral become $\frac{\pi}{2}+\delta_t$ to $\frac{3\pi}{2}+\delta_t$.

The component due to rotation is

$$(F_z)_r = \frac{Q}{|Q|}\left[\frac{r}{L_N}\right]\int_{-\frac{\pi}{2}+\delta_r}^{\frac{\pi}{2}+\delta_r}\int_{f_1\geq L_1}^{\bar{x}}(A_z+B_zx|Q|+C_zx^2Q^2)(\bar{x}-x)\,dx\,\text{Sin}\beta\,d\beta \qquad \text{(B-20)}$$

for $R\geq 0$ and $\bar{x}\geq f_1\geq L_1$. For $R<0$ the limits on the β integral become $\frac{\pi}{2}+\delta_r$ to $\frac{3\pi}{2}+\delta_r$.

Once the projectile has penetrated so that the nose is totally submerged in the target the lower limit on the x integrals becomes L_1.

The moments follow from the fact that there is a force on the differential element of area which is located a distance x from the center of mass. See Figure B-6. The force dF_y applied to the area dA will produce a moment about the z-axis, denoted N, whose magnitude will be $x\,dF_y$.

The moment N will be made up of two parts, one due to translation, $(N)_T$ and one due to rotation rate $(N)_r$.

$$N = (N)_T + (N)_r \tag{B-21}$$

The results for $(N)_T$ are as follows:

$$(N)_T = -\frac{V}{|V|}(A_y+B_y|V|+C_yV^2)\left[\frac{r}{L_N}\right]\int_{-\frac{\pi}{2}+\delta_t}^{\frac{\pi}{2}+\delta_t}\int_{f_1\geq L_1}^{\bar{x}} x(\bar{x}-x)\ dx\ \text{Cos}\beta\ d\beta \tag{B-22}$$

for $V\geq 0$ and $\bar{x}\geq f_1\geq L_1$. For $V<0$ the limits on the β integral become

$\frac{\pi}{2}+\delta_r$ to $\frac{3\pi}{2}+\delta_r$.

The values of moment due to rotation rate are

$$(N)_r = -\frac{R}{|R|}\left[\frac{r}{L_N}\right]\int_{-\frac{\pi}{2}+\delta_r}^{\frac{\pi}{2}+\delta_r}\int_{f_1\geq L_1}^{\bar{x}} (A_y+B_yx|R|+C_yx^2R^2)x(\bar{x}-x)\ dx\ \text{Cos}\beta\ d\beta \tag{B-23}$$

for $R\geq 0$ and $\bar{x}\geq f_1\geq L_1$. For $R<0$ the limits on the β integral become

$\frac{\pi}{2}+\delta_r$ to $\frac{3\pi}{2}+\delta_r$.

When the complete nose is submerged in the target the lower limit on the x integrals becomes L_1.

In a similar manner the moment about the y-axis,

$$M = (M)_T+(M)_r. \tag{B-24}$$

$$(M)_T = \frac{W}{|W|}\left[\frac{r}{L_N}\right](A_z+B_z|W|+C_zW^2)\int_{-\frac{\pi}{2}+\delta_t}^{\frac{\pi}{2}+\delta_t}\int_{f_1\geq L_1}^{\bar{x}} x(\bar{x}-x)\ dx\ \text{Sin}\beta\ d\beta \tag{B-25}$$

when $V\geq 0$, $\bar{x}\geq f_1\geq L_1$. For $V<0$ the limits on the β integral become

$\frac{\pi}{2}+\delta_t$ to $\frac{3\pi}{2}+\delta_t$.

$$(M)_r = \frac{Q}{|Q|}\left[\frac{r}{L_N}\right]\int_{-\frac{\pi}{2}+\delta_r}^{\frac{\pi}{2}+\delta_r}\int_{f_1\geq L_1}^{\bar{x}} (A_z+B_zx|Q|+C_zx^2Q^2)x(\bar{x}-x)\ dx\ \text{Sin}\beta\ d\beta \tag{B-26}$$

when $R \geq 0$, $\bar{x} \geq f_1 \geq L_1$. For $R<0$ the limits on the β integral become

$\frac{\pi}{2}+\delta_r$ to $\frac{3\pi}{2}+\delta_r$.

When the nose is completely submerged the lower limit on the x integrals becomes L_1.

Under the assumptions of this force model the moment about the x-axis, L, will be equal to zero for reasonable angles of attack and obliquity.

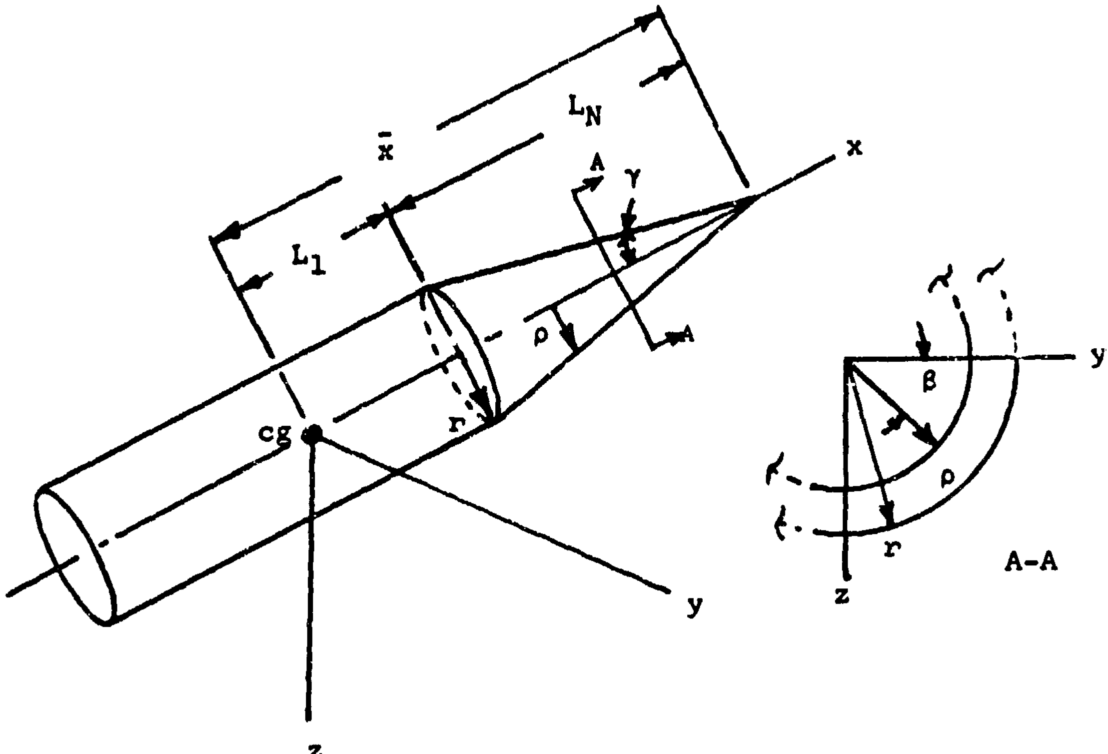

Figure B-1. Nomenclature and Coordinate Systems

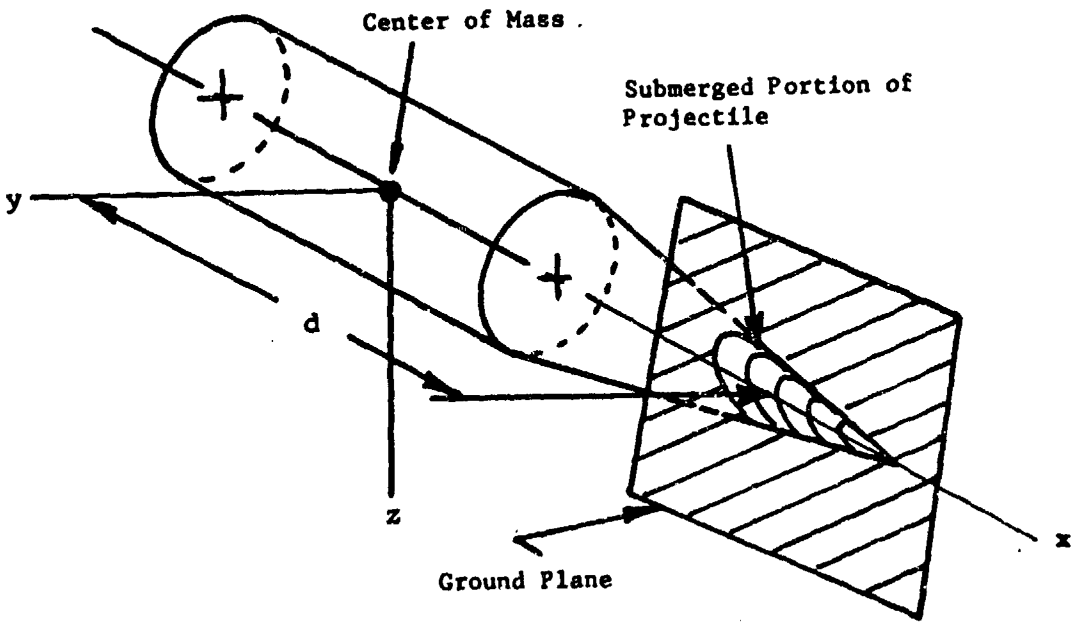

Figure B-2. Partially Submerged Projectile

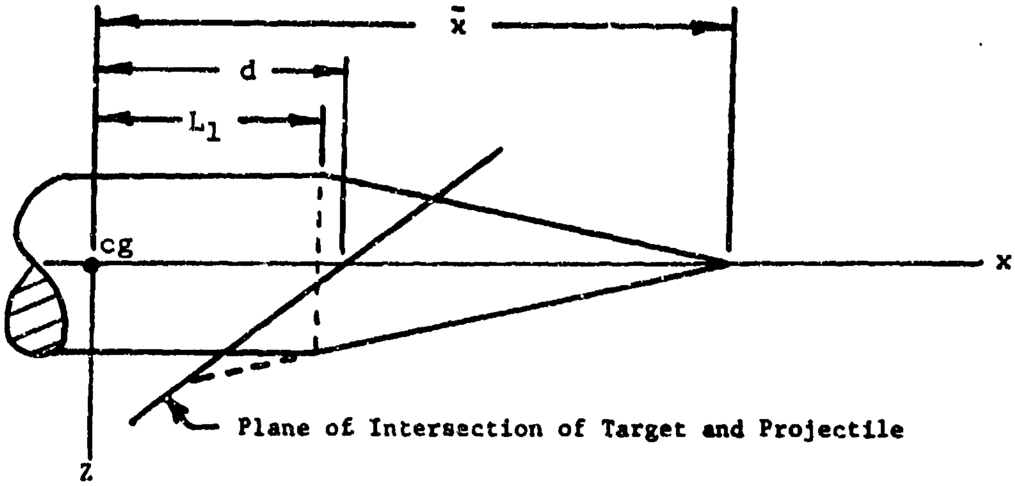

Figure B-3. Schematic Showing Plane of Intersection of Target and Projectile

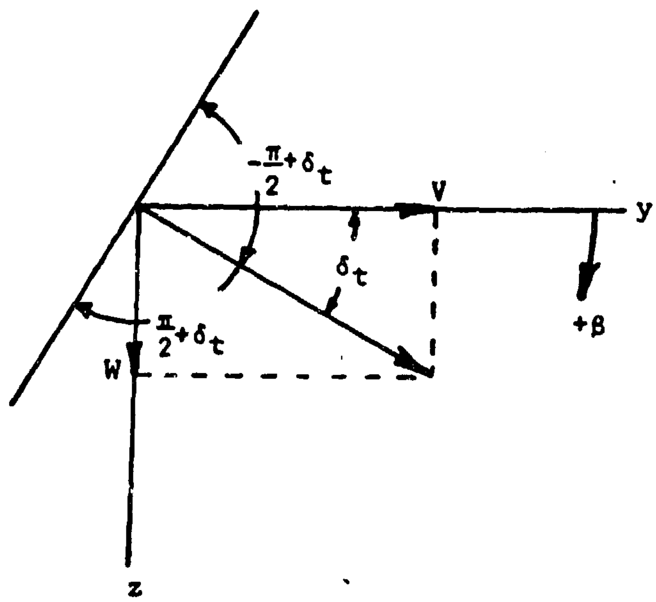

Figure B-4. Range of Angle β Shown in y-z Plane

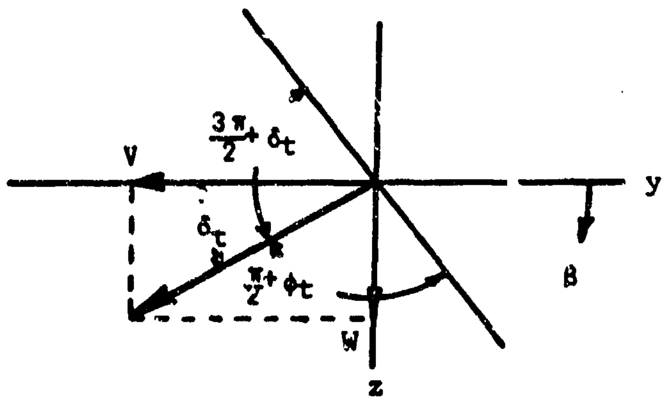

Figure B-5. Range of Angle β Shown in y-z Plane

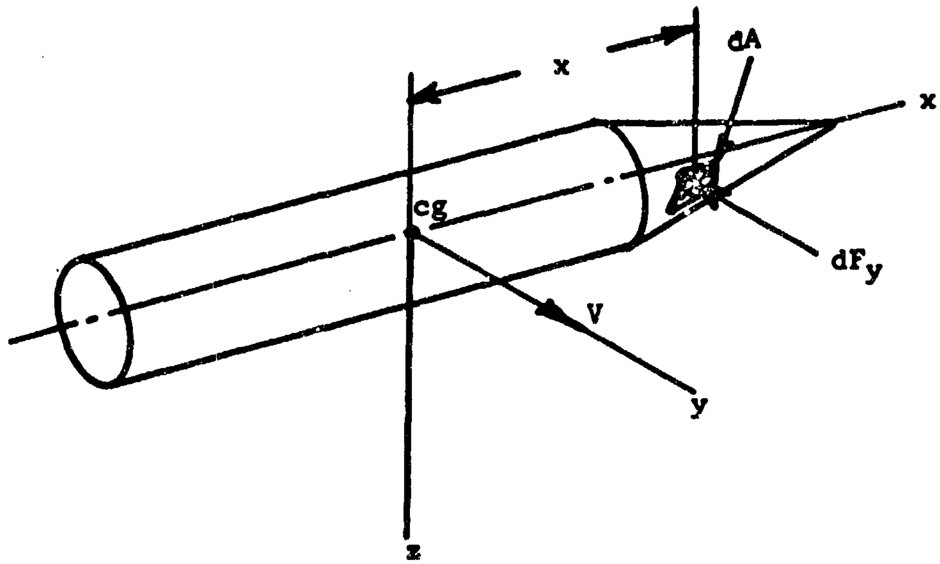

Figure B-6. Schematic Showing Differential Force dF_y

APPENDIX C

1. LIST OF COMPUTER SYMBOLS

AX	Force coefficient, A_x
AY	Force coefficient, A_y
AZ	Force coefficient, A_z
BX	Force coefficient, B_x
BY	Force coefficient, B_y
BZ	Force coefficient, B_z
CD	Drag coefficient, C_D
CMX	x coordinate center of mass
CMY	y coordinate center of mass
CMZ	z coordinate center of mass
CX	Force coefficient, C_x
CY	Force coefficient, C_y
CZ	Force coefficient, C_z
DT	Print time frequency
DTMAX	Maximum integration time
DTMIN	Minimum integration time
FIN	MIMIC finish statements
FX	Total force component x direction, F_x
FY	Total force component y direction, F_y
FYCO	Force component y direction for cone only
FYCY	Force component y direction for cylinder only
FYHE	Force component y direction for hemisphere only
FZ	Total force component z direction, F_z
FZCO	Force component z direction for cone only
FZCY	Force component z direction for cylinder only
FZHE	Force component z direction for hemisphere only
HDR	Output headings
INT	MIMIC integration symbol
IXX	Moment of inertia, I_{xx}
IYY	Moment of inertia, I_{yy}
K1,K2,K3	Constants used to select proper force terms
K4,K5,K6	Constants used to select proper moment terms
L	Total applied moment about x axis

LCO	Applied moment about x axis due to cone only
LCX	Natural logarithm of C_x
LCY	Applied moment about x axis due to cylinder only
LHE	Applied moment about x axis due to hemisphere only
LNCY	Length of cylinder
LNCO	Length of nose cone
M	Total applied moment about y axis
MAS	Mass of projectile
MCO	Applied moment about y axis due to cone only
MCY	Applied moment about y axis due to cylinder only
MHE	Applied moment about y axis due to hemisphere only
N	Total applied moment about z axis
OUT	Output to be listed
NCO	Applied moment about z axis due to cone only
NCY	Applied moment about z axis due to cylinder only
P	Rotation velocity about x axis
PD	Rotation acceleration about x axis, $\dot{P}$
PI	Universal constant π = 3.14159
PHI	Euler angle ϕ
PHID	Euler angular velocity, $\dot{\phi}$
PHIO	Initial Euler angle, ϕ_o
PO	Initail rotational velocity, P_o
PRESU	Pressure exerted by velocity U
PRESV	Pressure exerted by velocity V
PRESW	Pressure exerted by velocity W
PSI	Euler angle, ψ
PSID	Euler angular velocity, $\dot{\psi}$
PSIO	Initial Euler angle, ψ_o
Q	Rotational velocity about y axis
QD	Rotational acceleration about y axis, $\dot{Q}$
QO	Initial angular velocity about y axis, Q_o
R	Rotational velocity about z axis
RAD	Radius of cylinder, base of nose cone, hemisphere
RD	Rotational acceleration about z axis, $\dot{R}$
RO	Initial angular velocity about z axis, R_o
T	Time

TERM	$1-U/U_o$
TH	Euler angle θ
THD	Euler angular velocity, $\dot{\theta}$
THO	Initial Euler angle, θ_o
U	Velocity relative to x axis
UD	Acceleration relative to x axis, $\dot{U}$
UO	Initial velocity relative to x axis, U_o
V	Velocity relative to y axis
VD	Acceleration relative to y axis, $\dot{V}$
VO	Initial velocity relative to y axis, V_o
W	Velocity relative to z axis
WD	Acceleration relative to z axis, $\dot{W}$
WO	Initial velocity relative to z axis, W_o
XP	x' axis
XPD	Velocity relative to x' axis
YP	y' axis
YPD	Velocity relative to y' axis
ZP	z' axis
ZPD	Velocity relative to z' axis

2. INTRODUCTION

The necessary format and language for programming is contained in Control Data Corp. reference manual entitled Control Data MIMIC and only the details for datainput are included here. All input data either constants (CON) or parameters (PAR) are placed at the end of the program and correspond exactly to the manner in which they are called for by the CON and PAR cards preceding the program. Details of input data are shown for Computer Program II.

In the first case shown, Computer Program I, the force coefficients A_x through C_z are assumed to be independent of the velocity terms, therefore all these values are shown as parameters. However, in the second case, Computer Program II, the value of C_x is then given a variable status included in the body of the program.

Parameters K1 through K6 are used to select forces and moments depending on type of nose cone used as well as the option not to use the forces and moments on the after body. These parameters take on values of zero or unity and are defined as follows:

Configuration 1	K1	K2	K3	K4	K5	K6
Cylinder only, all moments and forces	1	0	0	1	0	0
Cylinder plus cone, all moments and forces	1	1	0	1	1	0
Cylinder plus cone, only nose moments and forces	0	1	0	1	0	0
Cylinder plus hemisphere, all moments and forces	1	0	1	0	0	1
Cylinder plus hemisphere, only nose moment and forces	0	0	1	0	0	1

3. COMPUTER PROGRAM I

```
                 CON(D.,DTMIN,DTMAX)
                 PAR(AX,BX,CX,AY,BY,CY)
                 PAR(AZ,BZ,CZ)
                 PAR(MAS,IXX,IYY,CMX,CMY,CMZ)
                 PAR(LNCY,LNCO,RAD )
                 PAR(UO,VO,WO,PO,QO,RO)
                 PAR(PHIO,THO,PSIO,XPO,YPO,ZPO)
                 PAR(K1,K2,K3,K4,K5,K6)
 SOIL PENETRATION -- COMPLETELY SUBMERGED

 FORCE TERMS
   PI            3.14159
   PRESU         -(AX+BX*ABS(U)+CX*U*U)*U/ABS(U)
   PRESV         -(AY+BY*ABS(V)+CY*V*V)*V/ABS(V)
   PRESW         -(AZ+BZ*ABS(W)+CZ*W*W)*W/ABS(W)
   FX            PI*RAD*RAD*PRESU
   FYCY          2.*RAD*LNCY*PRESV
   FZCY          2.*RAD*LNCY*PRESW
   FYCO          RAD*LNCO*PRESV
   FZCO          RAD*LNCO*PRESW
   FYHE          PI*RAD*RAD*PRESV/2.
   FZHE          PI*RAD*RAD*PRESW/2.
   FY            K1*FYCY+K2*FYCO+K3*FYHE
   FZ            K1*FZCY+K2*FZCO+K3*FZHE
 MOMENT TERMS
   LCY           K4*(FZCY*CMY-FYCY*CMZ)
   LCO           K5*(FZCO*CMY-FYCO*CMZ)
   LHE           K6*(FZHE*CMY-FYHE*CMZ)
   MCY           -K4*FZCY*(CMX-LNCY/2.)
   MCO           -K5*FZCO*(CMX-2.*LNCO/3.)
   MHE           -K6*FZHE*(CMX-5.*RAD/8.)
   NCY           K4*FYCY*(CMX-LNCY/2.)
   NCO           K5*FYCO*(CMX-2.*LNCO/3.)
   NHE           K6*FYHE*(CMX-5.*RAD/8.)
   L             LCY+LCO+LHE
   M             MCY+MCO+MHE-FX*CMZ
   N             NCY+NCO+NHE-FX*CMY
```

```
FORCE EQUATIONS
  UO          FX/MAS-Q*W+R*V
  U           INT(UO,UO)
  VO          FY/MAS-R*U+P*W
  V           INT(VO,VO)
  WO          FZ/MAS-P*V+Q*U
  W           INT(WO,WO)
MOMENT EQUATIONS
  PO          L/IXX
  P           INT(PO,PO)
  QO          M/IYY-R*P*(IXX-IYY)/IYY
  Q           INT(QO,QO)
  RO          N/IYY+Q*P*(IXX-IYY)/IYY
  R           INT(RO,RO)
EULER ANGLE EQUATIONS
  PHIO1       P+Q*SIN(PHI)*SIN(TH)/COS(TH)
  PHIO2       R*COS(PHI)*SIN(TH)/COS(TH)
  PHIO        PHIO1+PHIO2
  PHI         INT(PHIO,PHIO)
  THO         Q*COS(PHI)-R*SIN(PHI)
  TH          INT(THO,THO)
  PSIO        Q*SIN(PHI)/COS(TH)+R*COS(PHI)/COS(TH)
  PSI         INT(PSIO,PSIO)
INERTIAL FRAME EQUATIONS
  XPO1        U*COS(PSI)*COS(TH)
  XPO2        V*(COS(PSI)*SIN(TH)*SIN(PHI)-SIN(PSI)*COS(PHI))
  XPO3        W*(COS(PSI)*SIN(TH)*COS(PHI)+SIN(PSI)*SIN(PHI))
  XPO         XPO1+XPO2+XPO3
  XP          INT(XPO,XPO)
  YPO1        U*(SIN(PSI)*COS(TH))
  YPO2        V*(SIN(PSI)*SIN(TH)*SIN(PHI)+COS(PSI)*COS(PHI))
  YPO3          W*(SIN(PSI)*SIN(TH)*COS(PHI)-COS(PSI)*SIN(PHI))
  YPO         YPO1+YPO2+YPO3
  YP          INT(YPO,YPO)
  ZPO         -U*SIN(TH)+V*(COS(TH)*SIN(PHI))+W*(COS(TH)*COS(PHI))
  ZP          INT(ZPO,ZPO)

              HDR(T,XPO,XP)
              OUT(T,XPO,XP)
              FIN(T,.03)
              END
```

4. COMPUTER PROGRAM II

```
              CON(CT,DTMIN,DTMAX)
              PAR(AX,BX,AY,BY,CY)
              PAR(AZ,BZ,CZ)
              PAR(MAS,IXX,IYY,CMX,CMY,CMZ)
              PAR(LNCY,LNCO,RAD )
              PAR(UO,VO,WO,PO,QO,RO)
              PAR(PHIO,THO,PSIO,XPO,YPO,ZPO)
              PAR(K1,K2,K3,K4,K5,K6)
SOIL PENETRATION -- COMPLETELY SUBMERGED
```

```
FORCE TERMS
  PI        3.14159
  LCX       1.41-.1*LOG(U)
  CX        EXP(LCX)
  CO        1.25*CX
  PRESU     -(AX+BX*ABS(U)+CX*U*U)*U/ABS(U)
  PRESV     -(AY+BY*ABS(V)+CY*V*V)*V/ABS(V)
  PRESW     -(AZ+BZ*ABS(W)+CZ*W*W)*W/ABS(W)
  FX        FI*RAD*RAD*PRESU
  FYCY      2.*RAD*LNCY*PRESV
  FZCY      2.*RAD*LNCY*PRESW
  FYCO      RAD*LNCO*PRESV
  FZCO      RAD*LNCO*PRESW
  FYHE      FI*RAD*RAD*PRESV/2.
  FZHE      FI*RAD*RAD*PRESW/2.
  FY        K1*FYCY+K2*FYCO+K3*FYHE
  FZ        K1*FZCY+K2*FZCO+K3*FZHE
MOMENT TERMS
  LCY       K4*(FZGY*CMY-FYCY*CMZ)
  LCO       K5*(FZCO*CMY-FYCO*CMZ)
  LHE       K6*(FZHE*CMY-FYHE*CMZ)
  MCY       -K4*FZCY*(CMX-LNCY/2.)
  MCO       -K5*FZCO*(CMX-2.*LNCO/3.)
  MHE       -K6*FZHE*(CMX-5.*RAD/8.)
  NCY       K4*FYCY*(CMX-LNCY/2.)
  NCO       K5*FYCO*(CMX-2.*LNCO/3.)
  NHE       KE*FYHE*(CMX-5.*RAD/8.)
  L         LCY+LCO+LHE
  M         MCY+MCO+MHE-FX*CMZ
  N         NCY+NCO+NHE-FX*CMY
FORCE EQUATIONS
  UD        FX/MAS-Q*W+R*V
  U         INT(LO,UO)
  VD        FY/MAS-R*U+P*W
  V         INT(VD,VO)
  WD        FZ/MAS-P*V+Q*U
  W         INT(WD,WO)
MOMENT EQUATIONS
  PD        L/IXX
  P         INT(PD,PO)
  QD        M/IYY-R*P*(IXX-IYY)/IYY
  Q         INT(QD,QO)
  RD        N/IYY+Q*P*(IXX-IYY)/IYY
  R         INT(RD,RO)
EULER ANGLE EQUATIONS
  PHID1     P+Q*SIN(PHI)*SIN(TH)/COS(TH)
  PHID2     R*COS(PHI)*SIN(TH)/COS(TH)
  PHID      PHID1+PHID2
  PHI       INT(PHID,PHIO)
  THD       Q*COS(PHI)-R*SIN(PHI)
  TH        INT(THD,THO)
  PSID      Q*SIN(PHI)/COS(TH)+R*COS(PHI)/COS(TH)
  PSI       INT(PSID,PSIO)
```

```
INERTIAL FRAME EQUATIONS
   XPD1       U*COS(PSI)*COS(TH)
   XPD2       V*(COS(PSI)*SIN(TH)*SIN(PHI)-SIN(PSI)*COS(PHI))
   XPD3       W*(COS(PSI)*SIN(TH)*COS(PHI)+SIN(PSI)*SIN(PHI))
   XPD        XPD1+XPD2+XPD3
   XP         INT(XPD,XPO)
   YPD1       U*(SIN(PSI)*COS(TH))
   YPD2       V*(SIN(PSI)*SIN(TH)*SIN(PHI)+COS(PSI)*COS(PHI))
   YPD3         W*(SIN(PSI)*SIN(TH)*COS(PHI)-COS(PSI)*SIN(PHI))
   YPD        YPD1+YPD2+YPD3
   YP         INT(YPD,YPO)
   ZPD        -U*SIN(TH)+V*(COS(TH)*SIN(PHI))+W*(COS(TH)*COS(PHI))
   ZP         INT(ZPD,ZPO)
   TERM       1.-U/UO

              HCR(T,XPD,XP,CD)
              OLT(T,XPD,XP,CD)
              FIN(TERM,.98)
              FIN(T,.03)
              END
```

5. INPUT DATA FOR COMPUTER PROGRAM II

DT = 5.0×10^{-4}

DTMIN 1.0×10^{-5}

DTMAX 1.0×10^{-3}

AX 0.0

BX 0.0

AY 0.0

BY 0.0

CY 0.0

AZ 0.0

BZ 0.0

CZ 0.0

MAS 5.44×10^{2}

IXX 2.687×10^{2}

IYY 2.317×10^{4}

CMX 1.127×10^{1}

CMY 0.0

CMZ 0.0

LNCY 2.254×10^{1}

LNCO 0.0

RAD 0.992

U_0 4.06×10^{4}

V_0 0.0

W_0 0.0

P_0 0.0

Q_0 0.0

R_0 0.0

PHIO 0.0

THO 0.0

PSIO 0.0

XPO 0.0

YPO 0.0

ZPO 0.0

K1 1.0

K2 0.0

K3 0.0

K4 1.0

K5 0.0

K6 0.0

INITIAL DISTRIBUTION

Hq USAF/RDQ	1
Hq USAF/SAMI	1
DIA/DB-4C3	1
AUL (AUL/LSE-70-239)	1
Hq SAC/NRI/STINFO Library	1
NWC/Code 3269	1
NWC/Code 603	1
NWC/Code 533/Tech Lib	1
NWC/Code 407	1
AFSC Liaison Office/Code 143	2
Ogden LAC/MMWM	2
AFATL/DLODL	9
AFATL/DL	1
AFATL/DLJK	1
AFATL/DLJW	1
AFATL/DLD	1
AFATL/DLY	1
ADTC/XR	1
ADTC/SD	2
SAC Project Office	1
USAFTAWC/OA	1
AFATL/DLYV	10
AFATL/DLYW	1
Southwest Rsch Inst	1
Orlando Tech Inc	1
Sundstrand Data Control, Inc	1
Texas Tech Univ	2
Univ of Fla Graduate Ctr	3
Univ of Florida	7
US Army Engineer Waterways Exp Stn	2
Defense Nuclear Agcy	3
Goodyear Aerospace Corp	1
Sandia Labs	2
Lawrence Livermore Lab	1
Martin Marietta Aerospace	1
Georgia Inst of Technology	1
Univ of New Mexico	2
USAMSAA/DRXSY-S	1
DDC	2
Okalhoma State Univ	1
Lockheed Missiles & Space Co	1
ASD/NEFEA	1
TAWC/TRADOCLO	1
AFIS/INTA	1
Terra Tek	1
Picatinny Ars/SARP-AD-F-D	2
US Army Ballistic Rsch Labs DRXBR-TE	1
US Army Ballistic Rsch Labs DRXBR-TE	1
US Army Ballistic Rsch Labs AMXBR-VL	1
US Army Ballistic Rsch Labs Technical Library	1
AVCO Corp	2
Univ of California	1
Honeywell Inc	1
ARRADCOM/DRDAR-LCU-TM	1
Hq TAC/DRA	1
Hq USAFE/DOQ	1
Hq PACAF/DOO	1
TAC/INA	1
ASD/XRP	1

(The reverse of this page is blank)